EFFECT OF CATALYST SUPPORT PROPERTIES

ON HYDRODENITROGENATION OF A

COAL LIQUID

By

RAJASUNDARAM SIVASUBRAMANIAN

Bachelor of Technology
University of Madras
Madras, India
1969

Master of Technology
University of Madras
Madras, India
1971

Submitted to the Faculty of the Graduate College
of the Oklahoma State University
in partial fulfillment of the requirements
for the Degree of
DOCTOR OF PHILOSOPHY
May, 1977

EFFECT OF CATALYST SUPPORT PROPERTIES

ON HYDRODENITROGENATION OF A

COAL LIQUID

Thesis Approved:

Billy L. Gynes
Thesis Adviser

John Herban

Robert E. Robinson Jr.

E. Harris

Norman N. Durham
Dean of the Graduate College

ii

ACKNOWLEDGEMENTS

I am deeply indebted to my major adviser, Dr. Billy L. Crynes for his valuable suggestions and keen interest during the course of this work. His advice on the preparation of this thesis has been of great help to me.

I would like to express my sincere appreciation for the other members of my examining committee, Dr. R. L. Robinson, Jr., Dr. J. H. Erbar and Dr. G. J. Mains. A special thanks is due Dr. Mains for agreeing to serve as a committee member at the last moment.

I would like to thank Dr. S. D. Hottman, M. Ahmed and Gil Greenwood for their interest in this study and their valuable suggestions. I would like to thank fellow graduate students, D. C. Mehta and Jan Wells for their help in completing this work. I am very grateful to Dorsey Payne, Vaikuntam Raghavan, Paul Madison, Kerry Scott, Anthony Jones, Susan Phillips, D. Soni, Nitin Mehta and Ken Dillard for their long hours of patient operation of the equipment. I would like to thank Jan Keasling for her understanding and perserverance in typing this thesis.

I shall always be indebted to my parents without whose encouragement and personal sacrifices this graduate study would not have been possible.

Finally I would like to thank my wife, Anantharani, for her understanding attitude in my moments of frustration.

TABLE OF CONTENTS

LIST OF TABLES

LIST OF FIGURES

CHAPTER I

INTRODUCTION

In 1975 the United States used 71.08 quadrillion Btus of energy in all forms (1) and by the year 2000, the energy consumption is expected to rise to 163 quadrillion Btus per year (2). With ever-increasing demands on fossil fuels as a source of energy and ever-decreasing supplies of petroleum within the United States, this country must turn more and more to the use of coal.

The U. S. coal reserves are estimated at 83,000 quadrillion Btus, enough to meet all U. S. energy requirements for hundreds of years (3). Of this total only about 3600 quadrillion Btus are open to development under conditions of current technology, economics and environmental controls (3). However, this total is still a sufficient supply for many years, and coal in all probability represents the best hope for expansion of U. S. energy production.

The limitations of using coal as a fuel are related to the physical and chemical properties. Since coal is a solid which contains considerable ash content, it is inconvenient and expensive to transport and utilize on a Btu basis. Also, sulfur and nitrogen compounds are present in coal and these lead to air pollution problems when the coal is burned. Coal can be converted to the fluid forms which we like to use (gasification and liquefaction). The basic problems involved in affecting these conversions are removing the ash and increasing the

hydrogen/carbon ratio of the product. In addition, it is necessary to reduce the amount of sulfur and nitrogen compounds for environmental reasons as well as to increase the quality of the product.

This study concerns itself with reducing the nitrogen content of certain liquids derived from coal. Liquid fuels from coal can be produced by single stage catalytic hydroprocessing or by two stage processes involving liquefaction followed by catalytic hydroprocessing. Figures 1 and 2 show nitrogen content of liquids produced from different types of coal as a function of the average boiling point. Surprisingly little difference is evident between the nitrogen contents of particular product fractions from catalytic and non-catalytic systems. The nitrogen content of the liquid fuels can be further reduced by catalytically treating them with hydrogen. This process is known as hydrodenitrogenation. Most of the nitrogen compounds in coal liquids are in the form of heterocyclic nitrogen compounds. Some characteristic nitrogen compounds found normally in coal-derived liquids are shown in Figure 3. Hydrodenitrogenation of these substances is believed to proceed via saturation of the heterocyclic ring followed by ring fracture and subsequent removal of nitrogen as ammonia.

Coal liquefaction is likely to be commercialized within the next decade. In view of time constraints, first generation coal liquefaction processes are likely to be based on existing catalyst technology, which is largely an outgrowth of petroleum processes. Much effort has been given to catalyst development for hydrotreating of petroleum stocks, whereas relatively little has been directed toward those for coal liquids. Problems and limitations may surface when the existing catalyst technology is applied to coal liquefaction. To surmount
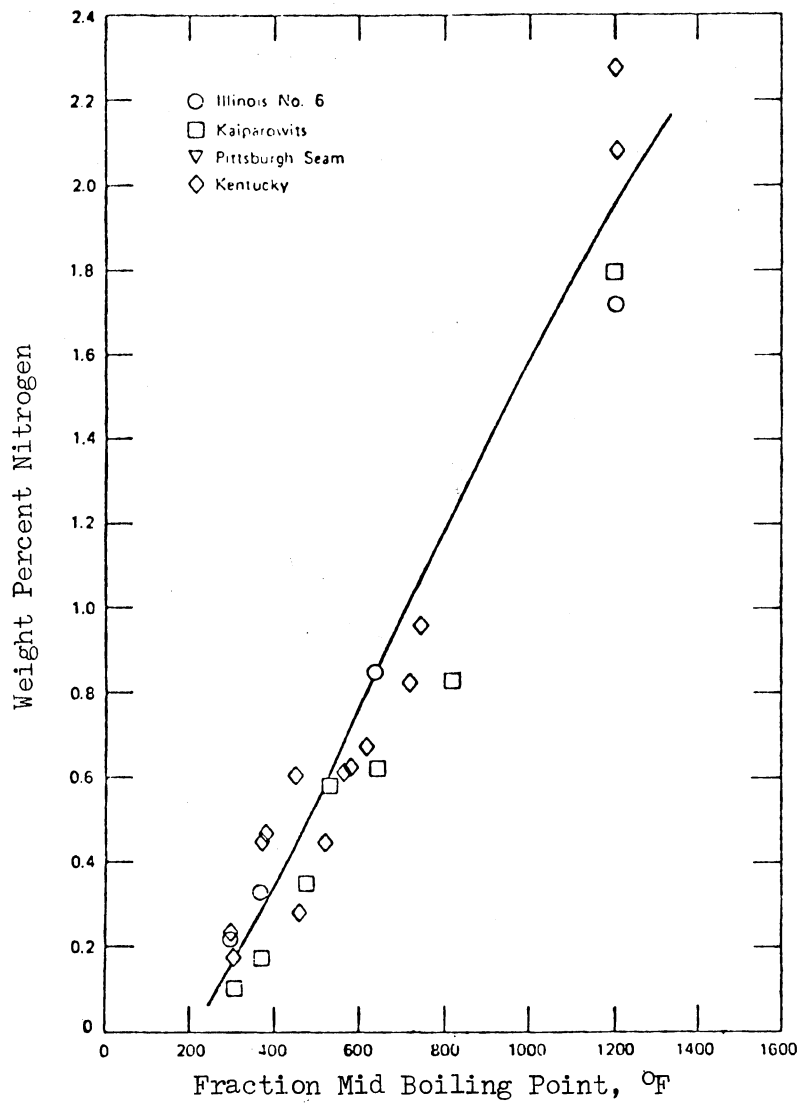
Figure 1. Nitrogen Content of Coal Liquids
from Noncatalytic Operations (4)
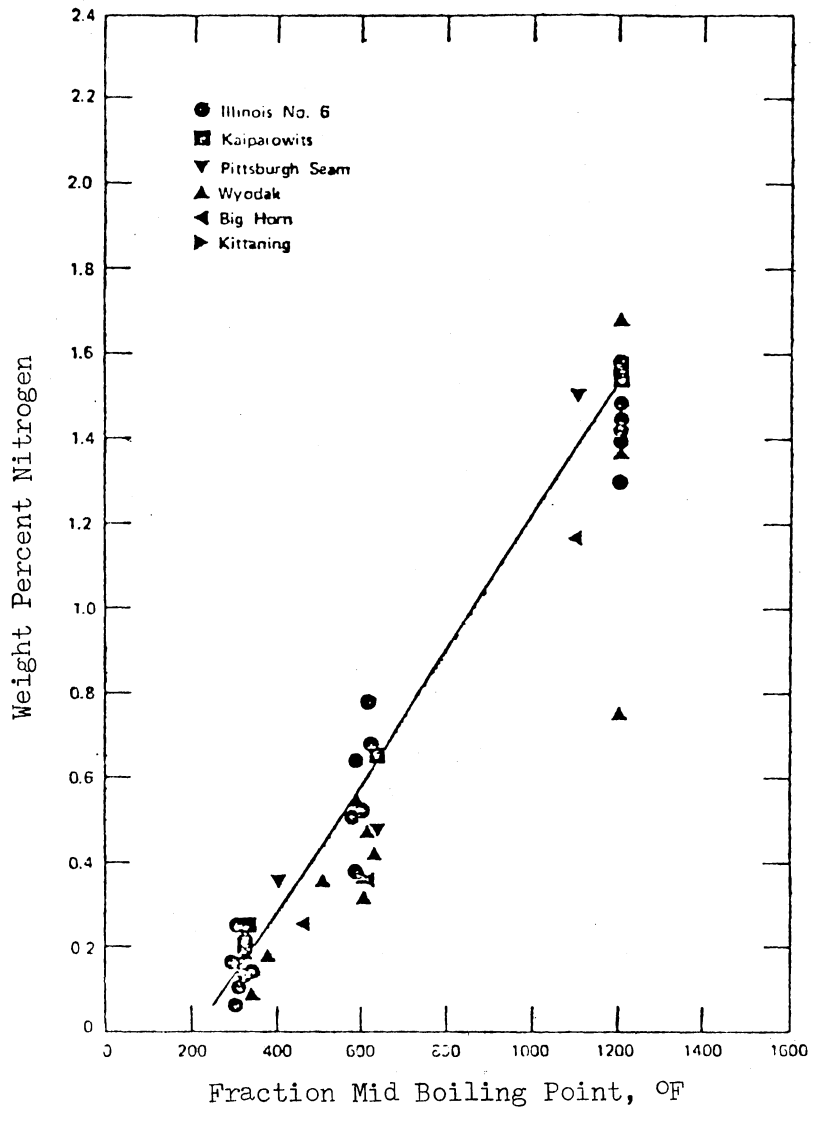
Figure 2. Nitrogen Content of Coal Liquids
from Catalytic Operations (4)
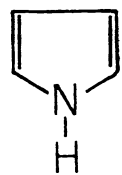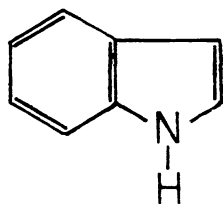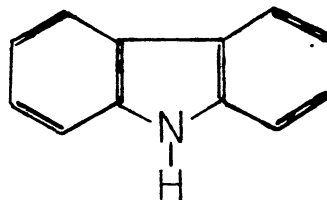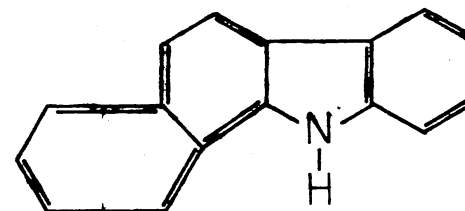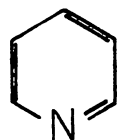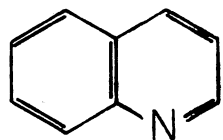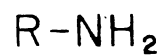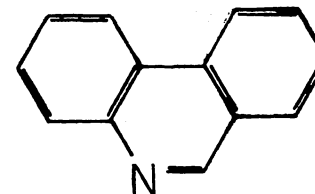
Figure 3. Nitrogen Compounds Found in Coal Derived Liquids

these difficulties, second generation processes will require new and improved catalytic materials and concepts.

This study is part of a larger program at the Oklahoma State University, given to tailoring hydrotreating catalysts especially for coal derived liquids. Hydrodenitrogenation of raw anthracene oil, a coal derived liquid has been studied in a trickle bed reactor using several Co-Mo-Alumina catalysts. In addition to using raw anthracene oil, the same feedstock was doctored with quinoline (a coal type nitrogen containing compound) and hydrotreated over the same Co-Mo-Alumina catalysts. Both feedstocks and selected product samples were separated into several fractions, using an ASTM vacuum distillation technique, to assess nitrogen removal throughout the feedstock boiling range.

The objectives of the present study were as follows:

1. In the long term, to provide useful information towards tailoring catalysts specifically for hydrotreating coal derived liquids.

2. To determine the effects of reactor operating conditions on hydrodenitrogenation of raw anthracene oil using certain chosen catalysts.

3. To determine the effect of catalyst support properties on hydrodenitrogenation of raw anthracene oil, a coal derived liquid.

4. To assess whether doctoring a complex feedstock such as raw anthracene oil with quinoline (a coal type nitrogen containing compound) and hydrotreating the doctored feedstock could provide significant information towards catalyst tailoring.

CHAPTER II

LITERATURE REVIEW

Hydrodenitrogenation will become increasingly important in the future to lower the organonitrogen content of synthetic crudes extracted from oil shale and coal, which contain relatively large amounts of sulfur and nitrogen. Hydrodesulfurization and hydrodenitrogenation of petroleum feedstocks are practiced commercially in most of the cases in trickle bed reactors. In trickle bed reactors, the liquid phase flows down through a fixed catalyst bed while the gaseous phase flows either co-current or countercurrent to it. Earlier in the research program at Oklahoma State University a decision was made to use the trickle bed reactor design in the hydrodesulfurization and hydrodenitrogenation studies of coal-derived liquids. The success of Wan (5) and Satchell (6) in using a trickle bed reactor in their denitrogenation studies has been encouraging. Hence, for direct comparison of the results, a trickle bed reactor has been chosen for this study.

In previous studies (5-9) conducted in our laboratory, the catalysts used were obtained from commercial vendors. However in the present study, catalyst supports were obtained from commercial vendors and were impregnated with active metals. Larger variations in support properties and their effect on denitrogenation can be studied this way. An attempt was also made to change the pore size

7

distribution of a catalyst support using steam treating techniques reported by Schlaffer, et al. (10).

The observed performance of a catalyst and the effect of its physical properties such as surface area, pore volume and pore size distribution are determined by the severity of the hydrotreating conditions as well as the hydrodynamics of fluid flow in the trickle bed reactor. Hence this literature survey is divided into three sections. The first section will present some of the pertinent literature concerned with the hydrodynamics of fluid flow in trickle bed reactors. The second section will deal with the effect of reactor operating conditions on hydrodenitrogenation. The final section will deal with the effect of catalyst support properties on denitrogenation.

Trickle Bed Reactors

Analysis of constant pressure, isothermal kinetic hydrotreating data for various petroleum feedstocks obtained in standard small scale pilot plant trickle bed units indicates that the following four effects may be of importance: reactor backmixing, liquid hold up, incomplete catalyst wetting and internal diffusion within the catalyst. Backmixing is solely a mass transfer phenomenon, whereas liquid hold up and incomplete catalyst wetting are caused by maldistribution and by passing of the liquid over the porous catalyst pellets. Internal diffusion within the catalyst is normally characterized by the effectiveness factor. Backmixing and incomplete catalyst wetting reduce the overall efficiency of the trickle bed reactor. A discussion of the effects of backmixing, hold up, incomplete catalyst wetting and pore diffusion limitations follows.

Axial Dispersion and Backmixing in

Trickle Bed Reactors

Plug flow is normally assumed in evaluating kinetic data from trickle bed reactors. However, deviations from plug flow can occur in experimental reactors due to axial eddy dispersion. Since axial dispersion effects tend to reduce conversion, it is important to understand and account for the effects of axial dispersion. Lapidus (11) concluded that for a first order reaction, deviations from plug flow become important only at reactant conversions of 95% or greater. However, Murphree, et al. (12) from their work on commercial reactors, showed that plug flow could become important at reactant conversions much lower than those suggested by Lapidus. Under these conditions it becomes important to have adequate models for predicting the extent of liquid-phase backmixing in trickle bed reactors.

Mears (13) reported a criterion for predicting axial dispersion effects in laboratory trickle bed reactors. He reported that the minimum reactor length for freedom from significant axial dispersion effects is given by

$$\frac{L}{d_s} > \frac{20 \, n}{B_o} \, \ell n \, \frac{C_o}{C_f}$$

where

L - length of reactor bed, cm

d_s - equivalent spherical diameter of catalyst particle, cm

n - order of reaction

C_o - initial concentration of reactant, $moles/cm^3$

C_f - final concentration of reactant, $moles/cm^3$

B_o - Peclet number based on particle diameter

$$(\bar{v}\, d_s/D_a)$$

$\bar{v}$ - superficial velocity, cm/hr

D_a - axial eddy diffusivity, cm^2/hr.

This model, known as the dispersion model, requires only one parameter, the Peclet number, to characterize backmixing. Mears showed that the behavior of a laboratory trickle bed reactor was well described by this model using values of P_{e_L} estimated from the correlation of Sater and Levenspiel (14) and Hochman and Effron (15).

More recent studies of liquid flow in trickle beds suggest that the dispersion model may not provide an adequate description of the details of backmixing. Three of the models that have been developed to supersede the dispersion model, specifically the "modified mixing cell" model (16), the cross flow model (17) and the time delay model (18) require two adjustable parameters to describe liquid backmixing in contrast to the one adjustable parameter involved in the dispersion model. Although correlations of the axial Peclet number are readily available (14, 15, 19), only one attempt has been made to develop general parameter correlation for a two parameter model (15). However, Schwartz and Roberts (20) reviewed these models in detail and found that the three models are mathematically equivalent in that they all lead to the same expression for the residence time distribution. Schwartz and Roberts made a detailed comparison of the effect on predicted reactor performance of various residence time distribution data correlated in terms of the dispersion model versus the cross flow model. Taking the residence time distribution data of Hochman and Effron (15) for representative reactor cases corresponding to Reynolds

numbers of 8 and 66, the ratio of required catalyst volume calculated by the dispersion model to that calculated by the cross flow model was 1.03 to 1.09 at 80% conversion and 1.11 to 1.22 at 90% conversion. This suggests that the axial dispersion model may be the more conservative in general. Schwartz and Roberts also concluded that deviations from plug flow become significant only for short reactors and high fractional conversions of reactant. For cases where it is desirable to account for liquid backmixing, Schwartz and Roberts concluded that the dispersion model is adequate.

Most other studies reported in the literature are generally for air water systems, almost invariably with ring or saddle packing and sometimes for flow conditions outside the range of interest in trickle bed reactors. A summary listing is given by Michell and Furzer (21). Satterfield (22) in his recent review article states that gas-phase dispersion is not ordinarily of concern in trickle-bed-processing. Shah and Paraskos (23) extended Mean's analysis of isothermal trickle bed reactors to obtain criteria for significant axial dispersion effects in adiabatic trickle bed hydroprocessing reactors. Their criteria indicated that at high conversions, an adiabatic operation produces a larger axial dispersion effect than the isothermal operation. At low conversion, opposite results were obtained. Schwartz, et al. (24) found that the available correlations for particle Peclet numbers, obtained for beds packed with larger particles, fit the dispersion data for beds packed with small particles as well. In addition to backmixing, the kinetic data obtained in a trickle bed reactor may be affected by hold up, incomplete catalyst wetting and maldistribution of the liquid.

Liquid Holdup and Catalyst Wetting

Liquid hold up is a measure, although approximate and incomplete, of the effectiveness of contacting between liquid and solid catalyst. The liquid hold up is generally expressed as fractional bed volume, that is as the volume of liquid present per volume of empty reactor. It comprises liquid held internally in the pores of the catalyst plus that outside the catalyst pellets, normally referred to as internal and external hold up. The external holdup can be further divided into dynamic (free draining) hold up and static (residual) hold up.

Volumetric, gravimetric and tracer methods are used most frequently in hold up measurements. A large amount of information on hold up has been published for packing of rings and saddles because of their use in absorption towers. Because of their different shapes, the high void fraction of the beds, and the operating conditions utilized; the applicability of most of these studies to trickle bed reactors is uncertain. The design variable affecting hold up is primarily the liquid flow rate. Satterfield (22) listed the following factors as those that could be of considerable importance:

1. The liquid inlet distributor (in large columns)

2. Shape and size of catalyst particles

3. Catalyst bed height

4. Wetting characteristics of packing and fluid

5. Gas flow rate.

Only hold up studies concerning trickle bed reactors will be discussed in this section.

The only hold up data on commercial reactors appear to be those of Ross (25) who studied 5.1 cm and 10.2 cm diameter columns - a 5.1 cm pilot hydrotreater reactor and a 2 meter diameter commercial desulfurization reactor. He observed that under similar operating conditions the commercial reactor hold up was only about 2/3 that of the pilot reactor and the poorer performance of the commercial unit was attributed entirely to this difference.

The external hold up is generally correlated as proportional to

$$L^n \quad \text{or} \quad R_{e_L}^n \quad ,$$

where
$$L = \text{length of the catalyst bed, and}$$
$$R_{e_L} = \text{Reynolds number.}$$

However, different investigators report substantially different values for n. Satterfield and Way (26) proposed that the dynamic hold up in a trickle bed reactor was a function of the superficial velocity and viscosity of the liquid:

$$H_d = A(U_L)^{1/3}(100\mu)^{1/4}$$

$$H_d = \text{dynamic hold up}$$
$$A = \text{proportionality constant}$$
$$U_L = \text{superficial velocity}$$
$$\mu = \text{viscosity}$$

with the dimensional parameter A is to be determined from hold up data for each type of particle. Goto and Smith (27) obtained hold up data for glass beads (0.431cm), porous CuO-ZnO catalyst particle (0.291cm) and for non-porous granular β-naphthol particles (0.241cm) in a trickle bed reactor. Both dynamic and static hold ups were measured.

They found that Satterfield and Way's correlation to be adequate for the porous or solid particles so long as d_p is less than 0.3 to 0.4 cm. Goto and Smith concluded that the effect of particle size on hold up changes at a particle diameter of 0.3 to 0.4 cm. Charpentier and Favier (28) presented experimental data on hold up concerning twenty gas-hydrocarbon systems with three types of cobalt/molybdenum/aluminum oxide catalyst (0.3cm) and with glass spheres (0.3cm). Charpentier and Favier observed several distinct flow patterns when the liquid flow rate was kept constant while the gas flow rate was increased. They tested the correlations for liquid hold up by Larkins, et al. (29) and Sato, et al. (30) and found that Larkins' correlation does not fit the data while the fit was better with Sato's correlation. Charpentier and Favier attributed this to the fact that Larkins' correlation does not concern results reported from experimental measurements with hydrocarbons and stated that predicting correlations relative to water as the liquid phase may be somewhat questionable when applied to hydrocarbons. Charpentier and Favier also presented a correlation of their own, and concluded that either Sato's correlation or theirs may be used to determine hold up data for foaming and non-foaming hydrocarbons and for any flow regime with catalyst packings.

Schwartz, et al. (24) presented results on liquid hold up and dispersion in a trickle bed packed with either nonporous or porous alumina of equal size and compared them with data of other investigators and predictions of various correlations. Their study confirmed the previous observations that under trickle flow conditions and co-current downward flow, liquid hold up increases with liquid flow rate and is almost independent of gas flow rate if the latter is changed over a

moderate range. However, they found that most available correlations underestimate the hold up in trickle beds packed with small particles by more than 40%.

Henry and Gilbert (31) presented a model which was used to evaluate kinetic data from trickle bed reactors assuming that hold up effects were controlling with negligible backmixing. Their model related reactor performance to superficial mass velocity, liquid space velocity, liquid viscosity, catalyst bed length and catalyst size. Part of Mears (13) data were satisfactorily correlated by the hold up model of Henry and Gilbert. They suggested that, for first order reactions, the effect of catalyst bed length on conversion can be accounted for by the relationship $\ln(C_{A_i}/C_{A_0}) \propto L^{1/3}$ where C_{A_i} and C_{A_0} are the reactor inlet and outlet concentrations of the reactant and L is the length of the catalyst bed. However, Mears (32) later questioned the Henry-Gilbert correlation and suggested that it is more realistic to assume that the reaction rate is proportional to the fraction of the outside catalyst surface which is effectively wetted by the flowing fluid. Mears also showed that his data with diluted bed cannot be evaluated with the model of Henry and Gilbert and proposed an almost identical relationship between $\ln(C_{A_i}/C_{A_0})$ and L based on incomplete catalyst wetting effects. This shows that kinetic data obtained in small scale trickle bed reactors can be influenced by liquid hold up and axial dispersion effects as well as incomplete catalyst wetting effects.

Satterfield (22) found that prewetting of the bed can cause substantially different behavior than that encountered if an initially dry bed is used. In this as in other studies, it was found that the

time required to reach steady state with an initially dry bed may be several hours (33, 34). Sedricks and Kenney (34) found that surrounding catalyst pellets with finer mass material improved wetting. Mears (32) found the same to substantially improve conversion at constant liquid flow rate. Wijffels, et al. (35) studied wetting of catalyst particles under trickle flow conditions and found that the wetted fraction increases with the liquid flow rate. Wijffels, et al., also developed a model that can predict the wetting of packings in which liquid descends by gravity and the flow pattern is independent of height. Schwartz, et al. (36) had developed a new tracer technique for simultaneous evaluation of liquid-solid contacting and hold up. Their technique relies on the measurement of mean residence times for adsorbable and nonadsorbable tracers. Their comparison of experimental results with available correlations for hold up and contacting indicated that correlations obtained for adsorbants on nonporous packing of large sizes and various shapes may not be applicable to trickle bed reactors.

The axial dispersion model of Mears, the hold up model of Henry and Gilbert and the catalyst wetting model of Mears all suggest that at constant liquid hourly space velocity, bed length will not affect the reactor performance provided it exceeds a minimum value. Montagna and Shah (37) evaluated the applicability of the above model to explain catalyst bed length effects on the removal rates of nitrogen, sulfur, metals and asphaltene from 36% reduced Kuwait atmoshperic crude oil and 53% reduced Kuwait crude oil. A 36% reduced crude means that the 36 volume % of the original crude is obtained as the distillate bottoms. Montagna and Shah used an 8 x 14 mesh catalyst for the 36% reduced

crude and a 20 x 30 mesh catalyst to hydrotreat the 56% reduced crude. Results from 20 x 30 mesh catalyst studies indicated that the axial dispersion, hold up and catalyst wetting effects were not important in these experiments. Results from the 36% reduced crude indicated that all three models explain the data equally well. Paraskos, et al. (38) on their study of hydrotreating 53% reduced Kuwait residue oil found that the kinetics in trickle bed reactors are best modelled by considering either the hold up model or incomplete catalyst wetting model. They found backmixing to be negligible in their study in accordance with Mears (13).

There exists close agreements as well as contradictions in the literature reviewed above. However, it is clear that kinetic data obtained in small trickle bed reactors may be affected by possible backmixing, hold up and incomplete catalyst wetting. Mears' (13) correlation has been shown to be the most conservative in predicting backmixing effects, and hence is adequate for making initial estimates as to whether or not deviation from plug flow will be significant. Montagna and Shah's (37) study shows that backmixing, liquid hold up and effective catalyst wetting all appear to be strongly dependent on the catalyst particle size or the viscosity of the feedstock. They concluded that liquid hold up, effective catalyst wetting and back-mixing effects all should be less important at smaller particle size.

Mass Transfer and Pore Diffusion
Limitations

Mass transfer is a combination of two processes, a diffusional process predominating in the direction normal to flow, and a convective

process predominating in the direction of flow. Very little information is available regarding mass transfer limitations in trickle-beds. Satterfield, et al. (39) concluded that mass transfer from the gas phase to the outer surface of the catalyst pellets will not be significant unless the inequality of the following equation holds.

$$\frac{(10\ d_p)}{C^*}\ r\ (1 - \varepsilon) > k_{\ell_s}$$

where

d_p = catalyst particle diameter, cm

C^* = equilibrium concentration of gas, $gmole/cm^3$

r = rate of reaction, $gmole/(s)(cm^3\ reactor\ volume)$

ε = void fraction in catalyst bed

k_{ℓ_s} = mass transfer coefficient for overall transfer through the liquid.

In his recent review of trickle bed reactors, Satterfield (22) reported that mass transfer through the liquid film does not seem to be a significant resistance under typical hydrodesulfurization conditions. He stated that the average film thickness is so much less than the radius of the usual catalyst particle that film thickness will not ordinarily be a significant resistance unless the effectiveness factor of the catalyst pellets themselves is quite low.

This brings up the question of internal pore diffusion limitations. Internal diffusion limitations are commonly expressed in terms of the catalyst effectiveness factor, η, defined as the ratio of the observed rate of reaction to that which would be observed in the absence of any internal concentration or temperature gradients (22). For a first order reaction, Satterfield (22) reports that internal diffusion will be insignificant if the following relationship holds:

$$\frac{(d_p/2)^2 \, r \, (1 - \varepsilon)}{D_{eff} \, C_s} < 1$$

where

d_p = particle diameter, cm

r = rate of reaction (gmole)/(s) (cm^3 of reactor volume)

D_{eff} = effective diffusivity, cm^2/s

C_s = concentration at liquid solid interface, $gmole/cm^3$

ε = void fraction of the catalyst bed.

The catalyst activity (the rate of heterogeneous reaction at a specified set of operating conditions) without pore diffusion resistances can be determined experimentally by extrapolating a plot of catalyst activity as a function of the catalyst particle diameter to zero diameter. Then the effectiveness factor is the ratio of the catalyst activity at any diameter of interest to the extrapolated activity at zero diameter. This method is limited in trickle bed reactors by the large pressure drop across the catalyst bed encountered when very small particles are used and by the time and effort required to perform successful experiments. However, the effectiveness factor can be estimated using the catalyst activity at a given set of operating conditions and only two catalyst particle diameters (40). Van Deemter (41) in the hydrodesulfurization studies with straight run gas oil at 707F, 735 psig and weight hourly space velocity of 2.0 hours^{-1} calculated an effectiveness factor of 0.99 for 0.0138 inches diameter Co-Mo-Alumina catalysts and an effectiveness factor of 0.36 for 0.197 inches diameter catalyst particles. Van Zoonen and Douwes (42)

hydrotreated a straight-run-gas oil over a cobalt-molybdenum-alumina catalyst with dimensions of 3x3 millimeter and 25-50 mesh. The greater than four fold reduction in the catalyst particle did not result in an increase in the conversion of organonitrogen species. This indicates that the effectiveness factor was near one for the system studied. Addington and Thomas (43) in the hydrodesulfurization of gas oils at 780 F and 500 psig reported an effectiveness factor of 0.6 using a Co-Mo-Alumina catalyst.

Sooter (7) in his hydrodesulfurization studies with raw anthracene oil, a coal derived feedstock, estimated an effectiveness factor of about one. Satchell (6) also found the effectiveness factor for denitrogenation over a Co-Mo-Alumina catalyst to be nearly one with reactor operating temperatures of 650 and 700 F and 1000 psig, when the catalyst particle size was varied from 8-10 mesh to 40-48 mesh.

To summarize, mass transfer in the liquid phase can be considered negligible except for low effectiveness factors. However, pore diffusion limitations depend on the reaction conditions and the type of feedstock used. Hence, effectiveness factors should be established before analyzing the kinetic data from trickle bed reactors.

Denitrogenation Studies

The removal of nitrogen compounds from petroleum and synthetic crudes derived from coal or oil shale is best achieved by catalytic hydrodenitrogenation. In this section, a review of the denitrogenation studies present in the literature will be reviewed. Denitrogenation studies on pure compounds, petroleum compounds and coal liquids will be presented first. This will be followed by the effect of reactor

operational characteristics on denitrogenation.

Pure Compounds

McIlvried (44) studied hydrodenitrification of pyridine in a
bench scale fixed bed reactor, using a nickel-cobalt-molybdenum
supported on alumina catalyst. The catalyst was presulfided with
hydrogen sulfide before use. Their work indicated that the path by
which pyridine denitrification proceeds is a rapid hydrogenation of
pyridine to piperidine followed by slow ring ruptures to form
n-pentylamine and rapid denitrification of n-pentylamine to ammonia.

$$\text{(pyridine)} \rightleftharpoons \text{(piperidine)} \longrightarrow C_5H_{11}NH_2 \longrightarrow C_5H_{12} + NH_3$$
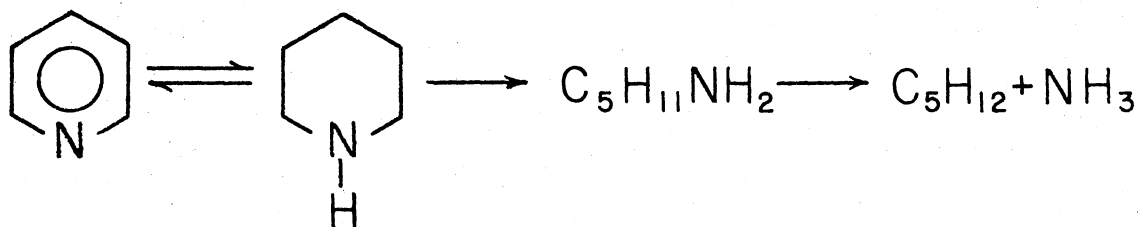
Only ammonia appears to be strongly adsorbed on hydrogenation sites,
but all the nitrogen compounds involved appear to be about equally
adsorbed on denitrification sites or else are present in too small
a concentration to have a significant inhibition effect on kinetics.
These two facts explain why apparent first order kinetics can be
obtained for what is basically a complex system. It may also help
explain why first order kinetics can fit the data for refinery feeds
which are known to contain a number of different nitrogen compounds.

Satterfield and Cocchetto (45) studied the hydrodenitrogenation
pyridine and piperidine, its hydrogenated analogue in a continuous flow
isothermal micro reactor over $NiMo/Al_2O_3$ and $CoMo/Al_2O_3$ commercial
catalysts. An ideal catalyst for hydrodenitrogenation reactions should
have good hydrogenation functionality to cause the hydrogenation step

to proceed with dispatch but also good hydrogenolysis functionality to cause the rupture of the C-N bond in the next step. Satterfield and Cocchetto (45) found that a $NiMo/Al_2O_3$ commercial catalyst appeared to have greater hydrogenation-dehydrogenation activity than a $CoMo/Al_2O_3$ catalyst, but the $CoMo/Al_2O_3$ catalyst appeared to have greater hydrogenolysis activity at least at $300^{\circ}C$ and below.

In order to determine the effect of organosulfur compounds on hydrodenitrogenation, Satterfield, et al. (46) studied the interactions between catalytic hydrodesulfurization of thiophene and hydrodenitrogenation of pyridine. They presented information on previous studies which had indicated that during simultaneous hydrodesulfurization/- hydrodenitrogenation, nitrogen compounds inhibit the hydrodesulfurization process. However, effects of sulfur compounds on hydrodenitrogenation are only poorly understood. Hence they explored these two groups of effects using thiophene and pyridine as model compounds which represent some of the less reactive organosulfur and organonitrogen compounds respectively. Studies were made with a flow microreactor at temperatures of $200^{\circ}C$ to $500^{\circ}C$, 4.4 and 11.2 bars pressure, on commercial catalysts consisting of $CoMo/Al_2O_3$, $NiMo/Al_2O_3$, NiW/Al_2O_3 and $NiW/S_1O_2-Al_2O_3$. They found that sulfur compounds have a twofold effect on hydrodenitrogenation. At low temperatures they are postulated to compete with pyridine for hydrogenation sites on the catalyst, thereby inhibiting the rate of the hydrogenation step in the pyridine decomposition mechanism. At high temperatures the hydrodesulfurization product, H_2S, interacts with the catalyst to improve the hydrogenolysis activity. This increases the rate of piperidine hydrogenolysis, which is the rate limiting step at high

temperatures and results in the entrancement of the hydrodenitrogenation rate.

Flinn, et al. (47) added samples of pure nitrogen compounds to a nitrogen-free straight run furnace oil and hydrodenitrogenated the resulting mixture over an Ni-W on Al_2O_3 catalyst at 600F. They found that amines and anilines reacted readily to form ammonia, but indole was much less reactive and quinoline was the most difficult to denitrogenate.

Doleman and Vlughter (48) studied the denitrogenation of quinoline in the temperature range of 300F to 840F over a Co-Mo on Al_2O_3 catalyst. Their results suggest that the mechanism by which quinoline type compounds are converted to hydrocarbons and ammonia is first an aromatic ring saturation step followed by the opening of the saturated ring to form aryl amines. The aryl amines then decompose to form ammonia. Doleman found that at reaction temperatures below 600F tetrahydroquinoline accumulated in the reactor product. As the temperature was increased still further to about 840F, the tetrahydroquinoline ring opened to form aryl amines which then decomposed to ammonia and hydrocarbon. These results show the importance of both aromatic hydrogenation and saturated ring opening reactions on the overall observed rate of quinoline denitrogenation.

Gheit (49) studied the kinetics of quinoline hydrodenitrogenation in the presence of Co-Mo-alumina catalyst. He presented the following mechanism:

Step 1
Hydrogenation

Step 2
Hydrocracking

Step 3
Hydrocracking
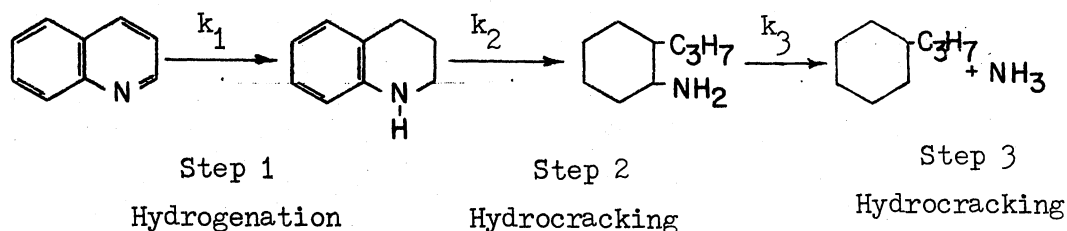
Gheit found that the first step was too fast to measure whereas the second step is the slowest. The ratio of the rate constants of the second to the third step ranges between 0.33 and 0.62 at reaction temperatures between 350 and $400^\circ C$.

Gheit and Abdou (50) dissolved representative petroleum nitrogen compounds such as pyridine, quinoline, aniline, pyrrole and indole in paraffin oil and hydrogenated them in a batch autoclave using a Co-Mo-Alumina catalyst. They presented the kinetic parameters under conditions of 20 atm hydrogen pressure, reaction temperatures between 300 and 400F and reaction periods up to six hours. They found the hydrodenitrogenation of both basic and nonbasic compounds to be pseudo first order. However, their integral approach is confusing since according to their definition of the variables used (a and x , where a is the original concentration of the nitrogen compound and x is the concentration after the measured reaction period) a plot of $\log a/a-x$ versus reaction period should provide a straight line with a negative slope whereas in their plots they get a positive slope. They also used a differential approach and arrived at the same conclusion. This leads one to believe that their definition of x could be wrong.

Another interesing study of quinoline hydrodenitrogenation was done by Madkour, et al. (51). They studied catalytic hydrodenitrogenation of quinoline in the presence of chlorides and found that

$Co-Mo-Al_2O_3-HCl$ catalytic system was extremely active. Dichloroethane was added to the feedstock. Fractional conversion of quinoline increased by a factor of two for Cl/N atomic ratios of 5 to 10 compared with that observed with no chloride in the feedstock. Since dichloroethane was completely converted to HCl, the improved hydrodenitrogenation activity was probably related to the presence of HCl in the reactor.

Almost all of the above studies concluded that denitrogenation is first order with respect to the concentration of nitrogen species. A discussion of the kinetics of denitrogenation becomes much more complicated when one considers industrially important feeds such as petroleum stocks, shale oil and coal derived liquids. These feedstocks typically contain a large number of unspecified organonitrogen species. A brief review of the hydrodenitrogenation studies on petroleum feedstocks, oil shale and coal derived liquids will be followed by a qualitative discussion of the effect of reactor operating conditions on the rate of denitrogenation of coal derived liquids.

Petroleum Feedstocks and Oil Shale

Flinn, et al. (47) found that the ease of denitrogenation tends to decrease with the increasing boiling point of a petroleum feed. Very high hydrogen pressures are required for complete removal of nitrogen substances from petroleum feeds. The reason it is so difficult to remove the last remnant of nitrogen compounds lies in the fact that secondary products of hydrodenitrogenation are nitrogen compounds which are considerably more resistant than the precursors. Moreover, the difficulty of nitrogen removal rises with the rising boiling point of the fraction refined, since the increasing size of the non-nitrogen part

of the molecule lowers the rate of denitrogenation, probably because the catalytic surface is less readily accessible to a large molecule. In addition, the higher content of very stable high-molecular weight aromatic heterocycles contributes to the increasing resistance of nitrogen compounds in high boiling fractions.

Hydrodesulfurization (HDS) studies had been carried out extensively on petroleum fractions and several excellent reviews are available in the literature (52, 53). Eventhough, hydrodesulfurization is always accompanied by some hydrodenitrogenation, studies on hydrodenitrogenation (HDN) have not been as extensive as HDS. Montagna and Shah (37) studied the denitrogenation of a 53% reduced Kuwait crude to test various models available in the literature and concluded that all the three (axial dispersion, holdup and catalyst wetting models) models explain the data equally well. Hydrodenitrogenation results for a lube distillate were presented by Gilbert and Katzmark (54). Mears (13) studied nitrogen removal from a West Coast gas oil and presented a criteria for predicting axial dispersion effects.

McCandless and Berg (55) investigated the hydrodenitrogenation of petroleum using a supported nickelous chloride-gaseous chloride catalyst system. Methylene chloride was used to maintain a high HCl partial pressure in the reactor and to keep the metal in the chloride form. The study was carried out in a continuous flow system and under identical operating conditions the system was more active for nitrogen removal than commercially available nickel tungsten sulfide and cobalt molybdenum hydrotreating catalysts. However, the sulfur removal was at a relatively low level. The authors concluded that the high hydro-denitrogenation activity may result from an interaction between the

acid catalyst system and the basic nitrogen compounds. This compares with an earlier cited study by Madkour, et al. (51) where they found that addition of dichloroethane improved the activity of Co-Mo-Alumina catalysts.

Koros, et al. (56) studied the change in concentration of various types of nitrogen compounds in shale oil at successive stages of hydro-denitrogenation over a cobalt-molybdate on alumina catalyst at 800 and 800 psig. In direct contrast to the results reported by Flinn (47), Koros reported that quinoline type compounds in shale gas oil denitro-genate more readily than indole-type compounds. He explained this apparent reversal in reactivity on the basis of competitive adsorbtion on the catalyst surface. However, Silver, et al. (57) studied hydrodenitrogenation of shale oil on a $Co-Mo/Al_2O_3$ catalyst at pressures on the order of 5000 psig and reported that at 5000 psig and temperatures of 750F and above, the denitrogenation rate constants for indole-type nitrogen compounds were greater than the denitrogenation rate constants for quinoline-type compounds.

Benson and Berg (58) investigated twelve different catalysts as potential denitrogenation catalysts for hydrotreating shale oil. They found that an HF-activated cobalt-molybdate catalyst was superior to all other catalysts investigated. These catalysts were tested at a pressure of 1000 psig and at two different temperatures, namely 440C and 510C.

Frost and Jensen (59) showed while using a $Co-Mo/Al_2O_3$ catalyst that hydrogen partial pressure had a significantly greater effect on the denitrogenation rate constants of indole-type compounds than on either the quinoline type compounds or total nitrogen pressure in shale oil.

Coal Liquids

Even fewer studies had been done on hydrodenitrogenation of coal derived liquids compared to petroleum fractions or pure compounds. White, et al. (60) studied hydrotreating of a coal derived oil from the COED process. Wolk, et al. (4) found that there is a steady increase in nitrogen content of coal liquids as average boiling point increases. Two other hydrodenitrogenation studies by Satchell (6) and Wan (5) using the same feedstock as used in this study, are also of interest. FMC Corporation, under an OCR contract had developed a process to convert high volatile bituminous coal to product oil, gas and char. Hydrotreating of the above oil was carried out by Atlantic Richfield Company (ARCO). The results of the above hydrotreating had been presented in a series of reports called "Char Oil Energy Development" (61-66). All of the above mentioned works will serve as a basis for the following discussion on the effects of reactor operating conditions on the rate of denitrogenation of coal derived liquids.

Effects of Reactor Operating Conditions

The effects of feedstock characteristics should be kept in mind while determining the effect of process variables in the hydrodenitrogenation processes.

Temperature

White, et al. (60) found experimental conditions that an Anhenius plot on nitrogen removal, showed a sharp break at about 752F giving two different activation energies. They found that the activation energy for denitrogenation assuming first order kinetics with

respect to organonitrogen species' content, was 48,500 Btu/lb mole

below 752F and 16,400 Btu/lb mole above 752F. No explanation for

the break in the activation energy was offered. Quader and Hill (67)

hydrotreated low temperature coal tar at 1500 psig over the temperature

range of 752 to 932F using a cobalt-molybdate catalyst. They observed

an activation energy of 15,900 Btu/lb mole for nitrogen removal.

Satchell (6) in his hydrodenitrogenation study on the same feed-

stock used in this study, raw anthracene oil, found activation energies

of 28,000, 31,000 and 32,700 Btu/lb mole for three different catalysts

(Co-Mo-Alumina) over the temperature of 600 to 750F using a second

order reaction model. He observed an activation energy of 12,300

Btu/lb mole for the temperature range of 750 to 800F.

These studies indicate that there is an abrupt decrease in the

apparent activation energy at about 750F, for cobalt-molybdenum

alumina catalysts. Information on a variety of feedstocks are required

before a valid conclusion can be drawn.

Pressure Effect

Scotti, et al. (65) studied the effects of reactor operating

pressure on the heteroatom removals and the hydrocracking reactions

using Utah and Western Kentucky oils derived from coal. They found

that the hydrogen consumption doubled for the Utah syncrude, by

increasing reactor pressure from 1800 psig to 2400 psig. For the

Western Kentucky syncrude, they found that the hydrogen consumption

leveled off to a constant value of about 3200 scf/bbl at pressures

above 2300 psig. The weight percent removal of nitrogen increased with

increasing reactor pressure in the range of 1400 to 2600 psig.

The effect of reactor operating pressure on the rate constant k, is often expressed by an equation of the following form:

$$k \propto P^b \quad .$$

Satchell (6) studied the effect of reactor operating pressure over the pressure range of 500 to 1500 psig at 650 and 700F using a cobalt-molybdenum-alumina catalyst and raw anthracene oil. He reported the values of b to be 0.76 and 0.84 at 650 and 700F, respectively.

Jones and Friedman (66) studied the effect of catalyst pressure on the rate of denitrogenation of a COED coal derived liquid and presented a plot of the percent nitrogen removed as a function of the reactor operating pressure. Satchell (6) reduced their data using least squares regression and found that the first order rate constant was proportional to the absolute pressure to the 1.1 power.

Space Time

Jones and Friedman (66) tested for the effect of space time on denitrogenation of a COED oil at 3000 psig and 725F over a nickel-cobalt-molybdenum on alumina catalyst. If the rate of denitrogenation could be described by a first order rate expression with respect to organonitrogen content, then a plot of the logarithm of the percent total nitrogen remaining as a function of space time should yield a straight line. Figure 4 is a plot of the logarithm of the percent of total nitrogen remaining as a function of 1.0/WHSV (reciprocal of weight hourly space velocity). The data in Figure 4 show that a first order rate expression is a reasonable representation of the kinetics of denitrogenation of the COED oil over the range of operating conditions
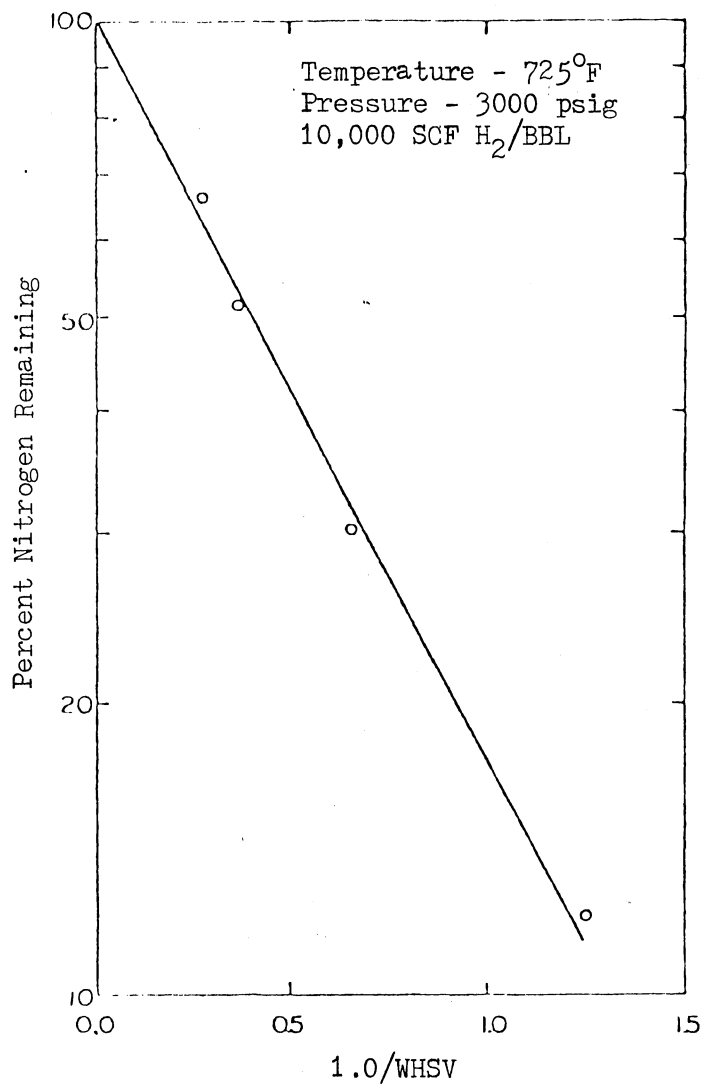
Figure 4. Effect of Weight Hourly Space
Time on Denitrogenation of
COED Oil (66)

studied.

Wan (5) and Satchell (6) in their work with raw anthracene oil
observed an increase in denitrogenation with increase in space time in
the range of 0.216 to 1.802 hours. However, the denitrogenation
increases markedly till one hour, beyond which the rate of increase is
relatively slow.

Hydrogen Flow Rate

Wan (5) with raw anthracene oil, found that increasing the
hydrogen rate from 3980 to 39,800 SCF/bbl resulted in an increase of
the percent nitrogen conversion from 61.2 to 69.2. The reactor was
operated at 800F, 1000 psig and a space time of 0.901 hours using a
cobalt-molybdenum on alumina catalyst.

Satchell (6) also tested the effect of hydrogen flow rate on raw
anthracene oil over the range of 1500 to 20,000 SCF/bbl using the
same feedstock and catalyst as Wan. The reactor was operated at 700F.
1000 psig and a space time of 1.5 hours. The conversion obtained was
found to be essentially independent of the hydrogen rate.

Pore Size Effects

Van Zoonen and Douwes (42) studied the effect of the volume average
pore radius in the range of 33 to 232 angstroms with a cobalt-molybdenum
of alumina catalyst on the rate of denitrogenation of a Middle East gas
oil at 707F and about 5000 psig. The study found that the volume
average pore radius had a negligible effect on the rate of denitrogena-
tion over the entire range studied.

Satchell (6) also concluded that pore size distribution probably had a negligible effect on the rate of denitrogenation of raw anthracene oil over Co-Mo-Alumina catalysts in the range from 25Å to 33Å.

Catalyst Particle Size and Bed Length

Van Zoonen and Douwes (42) hydrotreated a straight run gas oil over a cobalt-molybdenum-alumina catalyst with dimensions of 3x3 millimeter and 25-50 mesh. The greater than four fold reduction in the catalyst particle did not result in an increase in the conversion of organonitrogen species, suggesting that the effectiveness factor may have been closer to one.

Satchell (6) used two different particle sizes, 8-10 mesh and 40-48 mesh and found that the effectiveness factor was closer to one. Satchell used Co-Mo-Alumina catalysts at a pressure of 1000 psig and at 700F and used raw anthracene oil as feedstock.

Satchell (6) studied the effect of bed height by using 10 inch and 20 inch deep catalyst beds. He concluded that decreasing bed height resulted in a decrease in the apparent activity of the catalyst. This is in agreement with the earlier findings of Mears (13).

Metcalfe and Ruangteprat (68) pelletized solid cobalt-molybdenum catalyst into wafers of varying thickness to find the limiting diffusion path length of the catalyst. They found that a path length of 1/8" or less is necessary for full utilization of the catalyst.

Catalysts

In previous studies conducted in this laboratory (5-9), the catalysts used were obtained from commercial vendors. However in the

present study only the catalyst supports were obtained from commercial

vendors, and these were impregnated with active metals by the author.

This section will review the pertinent literature on catalyst supports,

choice of active metal types and method of manufacture of catalysts.

Catalyst Supports Material

Choice of support is very important since it constitutes about

one half the total cost of raw materials for the catalyst and its

properties largely determine the final characteristics of the catalyst.

The main functions of a carrier are to provide a structural framework

for the catalyst component and increase the surface area per unit

weight of metal above that of the unsupported metal. Other desirable

effects may include such factors as i) increased stability due to

small crystallites of metal being sufficiently separated to prevent

sintering and ii) a greater resistance to poisoning. The choice of a

carrier depends to a large extent upon the purpose for which the

catalyst is required.

The increase in knowledge concerning the function of the carrier

has triggered the development of a wide variety of those materials that

are now available in commercial quantities. Many suppliers sell

carriers having various ranges of pore characteristics, surface area

and chemical composition, which are designed to encompass those

properties that are considered as the most desirable in a support

material. Maio and Naglieri (69) listed some of the more common support

materials in a table, emphasizing the wide range of critical physical

and chemical properties. This table is presented on page 35.

TABLE I

TYPICAL PHYSICAL AND CHEMICAL PROPERTIES OF
CATALYST SUPPORT MATERIALS (69)

Chemical Composition	(1)	(1)	(2)	(1)	(2)	(1)	(2)	(2)	(1)	(3)	(4)	(5)
Al_2O_3	77.0	92.7	99.5	2.6	11.4	3.1	0.5	68.7	3.0	13.0	0.8	3.0
SiO_2	17.0	6.0		6.5	26.4	96.0	0.6	29.9	32.3	67.0	0.9	7.0
Fe_2O_3	1.2	0.2		0.2	0.3	0.3	0.2	0.3	0.2	4.0	0.3	2.0
TiO_2	2.5	0.2		0.1	0.3	0.3	0.3	0.3	0.2	0.6		
CaO	0.8	0.1		0.1	0.4		5.0	0.1	0.2	2.0	1.5	0.2
MgO	0.6	0.2		0.1		0.1	0.2		0.3	11.0	96.0	0.1
Na_2O	0.4	0.4	0.5	0.1	1.1	0.2		0.4		0.3		0.1
K_2O	1.0	0.1		0.2	1.0	0.1		0.2	0.1	0.6		0.1
SiC					90.0	59.1						
ZrO_2								93.2	63.8			
C												87.0
Physical Properties												
Porosity, % voids	36	10	58	45	41	37	43	44	6			
Pore dia. range-microns	2-30	1-3	.03-10	30-100	.3-88	1-5	.03-88	.3-100	2-10			
Pore dia. % of volume	80	90	100	100	100	90	100	100	85			
Surface area sq. m/g	1	1	5.6	1	0.3	1	0.2	0.2	1	120	230	1,100
Bulk density g/cc	2.0	3.1	1.6	1.7	1.6	1.4	3.1	1.9	3.9	0.5	0.1	0.4

(1) Norton Co., Worcester, Mass.
(2) Carborundum Co. Latrobe, Pa.
(3) Attapulgus Clay – Attapulgus Minerals & Chemical Corp.
(4) Magnesia – Westvaco Div. – Food Machinery & Chemical Corp.
(5) Pittsburgh Coke & Chemical, Neville Island, Pittsburgh, Pa.

Historically, hydrotreating catalysts' supports have been made with alumina. The most commonly used supports are gamma alumina and gamma alumina stabilized with minor amounts of silica.

Kawa, et al. (70) evaluated catalysts for hydrodesulfurization and liquefaction of coal. They selected various support materials so as to cover wide ranges of compositions. Alumina contents were 3.1 to 99.3 percent and silica contents were 0.1 to 96 percent. Three catalysts contained silicon carbide as the principal component. They concluded that the best catalyst tested in their study was a high-surface area silica promoted catalyst. The catalyst contained 5% SiO_2.

Grimm and Berg (71) studied alumina-silica catalyst supports for hydrodesulfurization properties. They concluded that the support should contain a high amount of gamma-alumina. They also noted that the physical characteristics and basic chemical composition of the catalyst supports appeared to have more effect on hydrodesulfuruzation than the amount of cobalt or molybdenum added. They reported that materials that have a pore size of $55\overset{o}{A}$ and greater can tolerate silica even when silica is the major component. The silica content varied from 0.24-74.7% in their catalysts.

Schlaffer, et al. (73) studied the effect of heat and steam on the structure of silica-alumina cracking catalysts. The temperatures were in the range of from 478 to 950°C and steam partial pressures were in the range from 0-7 atmospheres. They found that the decline in specific surface area can be described by an empirical equation of the form $-ds/dt = ks^n$ where s is the specific surface area, t is time and n and k are constants for any given set of conditions. These constants vary smoothly with changing temperature and partial

pressure of steam.

In a later article, Schlaffer, et al. (10) studied the aging of silica and alumina gels. They examined the physical changes that occur to silica and alumina gel upon exposure to steam at moderate to high temperatures and the aging of these supports were compared to that of silica-alumina cracking catalyst. The surface area and pore volume of silica gel were found to be less stable toward prolonged steaming than those of silica-alumina cracking catalysts. In the case of alumina, prolonged steaming produced a considerable decline in surface area accompanied by little or no loss of pore volume.

Type and Concentration of Active Metals

Commercial experience over the years has pretty well shown that essentially all hydrotreating requirements can be accomplished by combinations of cobalt and molybdenum (CoMo) or nickel and molybdenum (NiMo). Some manufacturers suggest (75) improved performance with trimetallic NiCoMo formulations, but others express doubt that these offer any real advantages (75).

The concentration of the active metals is usually determined by cost and competitive factors, although there is an optimum concentration and ratio for each type of application. The optimum concentration is a function of the catalyst or best porosity, and therefore, the available catalytic surface of the substrate. As the concentration of active metals is increased, the activity goes up, but at a decreasing rate. Eventually, the concentration reaches a point where the active metals start significantly reducing the active surface resulting in a decrease in activity. Also, as the active metals concentration increases, the

bulk density of the finished catalyst goes up which pushes the costs up even further.

The preferred industrial catalysts for hydrotreating contain 2-4% Co as CoO and 8-15% Mo as MoO_3. Beuther, et al. (74) reported that commercial preparations consist of cobalt and molybdenum in atomic ratios of 0.1:1.0 to 1.0:1.0 and the maximum activity was observed for ratios around 0.3:1.0. In the case of Ni-Mo catalysts they observed a maximum activity for an atomic ratio of about 0.6:1.0. The addition of cobalt or nickel to catalysts containing Co and Mo in atomic ratios of 0.2:1.0 to 0.5:1.0 had insignificant effect on the activity of the catalyst. However, for ratios less than 0.2:1.0, the addition of Ni to give an atomic ratio of 0.5Ni:1.0Mo was observed to increase the activity of the catalyst significantly.

Ahuja, et al. (72) studied the activity and selectivity of hydro-treating catalysts and evaluated many combinations of metals and supports. They concluded that most hydrotreating catalysts are bi-functional - i.e., hydrogenating-dehydrogenating activity is produced by nickel or cobalt sulfides with sulfurized molybdenum or tungsten compounds and acidic activity is generally due to the carrier and for each type of hydrotreatment both functions must be optimized. They also concluded that nickel promoted catalysts are better for hydro-denitrogenation than cobalt promoted catalysts since nickel tends to reinforce the hydrogenating function of the catalyst.

Livingston (75) found that NiMo catalysts are no better than CoMo ones for sulfur removal from petroleum liquids as long as their physical properties and method of manufacture are similar. Kawa, et al. (70) reported that in Co-Mo-Alumina catalysts, increasing the concentration

of Mo beyond 14% had no significant effect in increasing the activity

of the catalyst for hydrodesulfurization. They suggested that for

concentrations more than 14%, the carrier surface can be assumed to

be completely covered with a monolayer of MoS_2 and there exists a

possibility of loss in catalyst activity.

Method of Manufacture

It is in this area that the manufacturer has the greatest number

of options. Livingston (75) divided the manufacturing of catalysts into

three general procedures:

    i)   Precipitation or coprecipitation

    ii)   Impregnation

    iii)   Comixing or compounding.

Since, impregnation was used as a method of manufacture of catalysts

used in this study, it will be discussed briefly.

In impregnation, the support is preformed and then impregnated

with the metals solution. The impregnation methods can vary widely as

well as the nature of the solution. This provides additional flexi-

bilities in determining how the active metals are dispersed on or within

the support. Also, it is possible to put all active metals on in a

single step, separately or in various combinations. Costwise, this

procedure is better than co-precipitation and in some cases it produces

a more active catalyst (71).

Higginson (76) presented a review of the techniques and principles

involved in making catalysts. He also outlined the pros and cons of

making a catalyst inhouse rather than through an established manufact-

urer. The procedure used in preparing catalysts for this study will

be described in the experimental procedure section. Since the catalysts used in this study were the Co-Mo-Alumina type, some of the pertinent literature on Co-Mo catalysts will be reviewed in the next section.

Co-Mo Catalysts

Richardson (77) used magnetic susceptibility measurements to determine the nature and composition of active and inactive components in cobalt-molybdate-alumina catalysts containing 10% MoO_3 with initial Co:Mo ratios from 0.1 to 1.0 and then heat treated in the range of 538 to 816C. He found that below an initial Co:Mo ratio of 0.3, the fresh catalyst contains no $CoAl_2O_4$ and less than 10% of the cobalt exists as CoO, the remainder forming an active complex with molybdena. Above an initial ratio of 0.3, the final composition depends on both heat treatment and cobalt content. In the desulfurization of West Texas gas oil, he found that the intrinsic rate constant correlated with the active Co:Mo ratios passing through a maximum at an active Co:Mo ratio of 0.18.

Lipsch and Schuit (78) also studied the structure and properties of the catalyst "cobalt molybdate" on alumina. Infra red spectra showed that the molybdenum is present as MoO_3. Radiation spectra led to the conclusions that cobalt is distributed throughout the bulk of the alumina as $CoAl_2O_4$, whereas MoO_3 is spread over the carrier surface, probably as a monomolecular layer. They used magnetic measurements to confirm the conclusion that cobalt is present as $CoAl_2O_4$.

The above mentioned studies have been done on the oxidic form of the catalyst. Friedman, et al. (79) undertook an electron spectroscopy study to monitor five commercial cobalt-molybdenum-alumina

catalysts subjected to five different preparation conditions.
They interpreted their results to note that only part of the total
dispersed cobalt actually is an aluminate. The remainder of the cobalt
in the oxidic form of the catalyst is located in an environment similar
to the aluminate, but nevertheless reactive. They also concluded that
from their limited sampling, there is no obvious correlation between
the activity and Co:Mo ratio.

Although originally in the form of cobalt and molybdenum oxides,
the usual hydrotreating catalysts undergo extensive reduction and
sulfiding before and during hydrotreating. Hence, the effect of
presulfiding will be discussed next.

Presulfiding

Mitchell and Trifiro (80) studied the effect of sulfiding on the
structure of a cobalt-molybdenum-alumina catalyst. They suggested that
the catalyst contains linked molybdenum and cobalt tetrahedra and
octahedra. They found the atomic ratios of the sulfided catalysts
are Co:Mo:S = 1:1.77:4.18, and concluded that the sulfur content was
less than that required for complete sulfiding, which is about 4.43
atoms per atom of cobalt.

Ahmed (9) in his hydrodesulfurization study of FMC oil, a coal
derived liquid, found that the extent of catalyst presulfiding by
H_2S in H_2 had an effect on the activity of the catalyst. Tantarov,
et al. (81) investigated the effect of sulfiding of an alumina-cobalt-
molybdenum catalyst on its activity, selectivity and deposition of
coke in the hydrorefining of thermally cracked gasoline. They found:

1) preliminary sulfiding is advantageous for hydrorefining;

2) deposition of coke on a previously sulfided catalyst during the same period was only one third of that on the oxide catalyst;

3) the mechanical strength of a catalyst is increased by a factor of 1.4 by sulfiding.

Goudriann, et al. (82) studied the effect of hydrogen sulfide on the hydrodenitrogenation of pyridine over a Co-Mo-Al$_2$O$_3$ catalyst. They concluded that the effect of hydrogen sulfide on the hydrodenitrogenation of pyridine is twofold. First, the pyridine ring hydrogenation activity of the sulfided catalyst is greater than that of the oxidic catalyst. Secondly, the presence of hydrogen sulfide has a beneficial effect on the hydrocracking activity of the catalyst.

It can be concluded that presulfiding improves the activity of the catalysts and the sulfided species are responsible for the activity of the hydrotreating catalysts.

Nitrogen Compounds in Petroleum and
Coal Liquids

A better knowledge of the nitrogen compounds present in coal derived liquids is important for the development of improved catalysts and processing techniques for their subsequent removal. Characterization of coal derived liquids are currently underway in chemistry laboratories at Oklahoma State University as well as other laboratories across the nation. Since nitrogen compounds present in coal derived liquids are similar to those present in petroleum liquids, a brief review of the nitrogen compounds present in petroleum and coal liquids
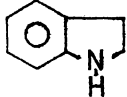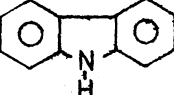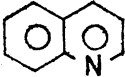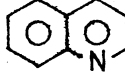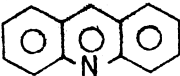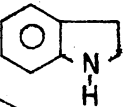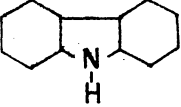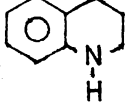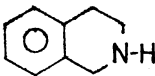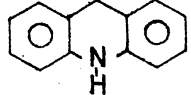
will be presented in this section. This section is by no means an exhaustive literature survey, but presents an overall picture of the nitrogen compounds present in petroleum as well as coal liquids.

Most of the nitrogen present in coal liquids are in the form of heterocyclic nitrogen compounds which are most resistant to hydro-denitrogenation (45). The small quantities of nonheterocyclic nitrogen compounds present in liquid fuels include anilines, aliphatic amines and nitriles. These compounds are generally easier to denitrogenate by catalytic hydrogenation than the relatively unreactive heterocyclic compounds, so they are not a serious problem.

The heterocyclic nitrogen compounds in petroleum and synthetic crudes can either be basic or nonbasic. Cochetto and Satterfield (83) presented some representative compounds in the form of a table. Table II presents these compounds.

Several studies have been made on the nature of the nitrogen compounds in petroleum. Snyder (84) reported the presence of indoles, pyridines and their higher benzologs in a California petroleum. Snyder also found that the nitrogen content increased with increasing boiling point of the petroleum fractions. One and two-ring heterocyclic compounds predominated (pyridines, quinolines) the lighter fractions while the large multi-ring structures accummulated in the heavier fractions. Bratton and Bailey (85) found several pyridines and quino-lines in a cracked gasoline. Nixon and Thorpe (86) found quinolines, pyridines and anilines in a catalytically cracked jet fuel. Jewell and Hartung (87) identified quinolines, benzoquinolines, hydroxy-benzoquinolines in a straight run heavy-gas oil. Brandenburg and Latham (88) characterized the classes of nitrogen compounds in the

TABLE II

REPRESENTATIVE HETEROCYCLIC NITROGEN
COMPOUNDS

Name	Formula	Structure
Pyrrole	C_4H_5N	
Indole	C_8H_7N	
Carbazole	$C_{12}H_9N$	
Pyridine	C_5H_5N	
Quinoline	C_9H_7N	
Isoquinoline	C_9H_7N	
Acridine	$C_{13}H_9N$	
Pyrrolidine	C_4H_9N	
Indoline	C_8H_9N	
Hexahydrocarbazole	$C_{12}H_{15}N$	
Piperidine	$C_5H_{11}N$	
1,2,3,4-Tetrahydroquinoline	$C_9H_{11}N$	
1,2,3,4-Tetrahydroisoquinoline	$C_9H_{11}N$	
9,10-Dihydroacridine	$C_{13}H_{11}N$	

130 to 350C distillate fraction of a Wilmington Petroleum. They separated and identified two individual compounds - an alkyl substituted cyclopentapyridan and an alkylcycloalkyl-substituted pyridine.

By comparison, little information is available on the nitrogen compounds in coal liquids. Quader, et al. (67) reported that pyridines, quinolines, pyrroles, indoles and carbazoles are the principal heterocyclic nitrogen structures present in low-temperature coal tars. Anderson and Wu (89) compiled the properties of 832 compounds that have been found in the physical properties data for quite a number of nitrogen compounds found in coal carbonization products. McNeil (90) presented a list of the compounds of boiling point above 300 identified in high temperature coal tars or pitches. A. G. Sharkey, Jr., and his associates at the Pittsburgh Energy Research Center are doing considerable amounts of work in high resolution mass spectrometric investigation of heteroatom species in coal-carbonization products (91-94). Scheppele and Greenwood (95) characterized raw anthracene oil, the feedstock used in this study. The acid and base fractions of raw anthracene oil were isolated by using nonaqueous cation-anion exchange chromotography using pentane as an eluent (96). Table III presents possible compound types present in the acid ractionn of raw anthracene oil and four reactor samples. For the base fraction from the raw anthracene oil, Scheppele and Greenwood (95) tabulated the molecular weights and associated empirical formulas and weight percents for each of the seven observed molecular weight series. Table IV presents this information. It is interesting to note that quinoline accounts for about 9 percent of the base fraction while carbazole accounts for about 5 percent of the base fraction of the feedstock

TABLE III

POSSIBLE COMPOUND TYPES PRESENT IN ACID
FRACTIONS OF RAW ANTHRACENE OIL AND
FOUR RELATED REACTOR SAMPLES

Nominal Mass of Parent Compound	Empirical Formula of Parent Compound	Example of Possible Structural Type	Maximum Number of of Alkyl Carbons Alkylated Homologues
94	C_6H_6O	phenol	6
134	$C_6H_{10}O$	indanol	5
158	$C_{11}H_{10}O$	methylnaphthol	3
170	$C_{12}H_{10}O$	acenaphthol	4
182	$C_{13}H_{10}O$	fluorenol	4
198	$C_{13}H_{10}O_2$	hydroxydibenzofuran, fluorenediol	4
194	$C_{14}H_{10}O$	phenanthrenol	2
210	$C_{14}H_{10}O$	phenanthrendiol	1
226	$C_{14}H_{10}O_3$	phenanthrentriol	1
218	$C_{16}H_{10}O$	fluoranthenol	2
220	$C_{16}H_{12}O$	dihydropyrenol	4
234	$C_{16}H_{10}O_2$	fluoranthendiol	2
117	C_8H_7N	indole	2
167	$C_{12}H_9N$	carbazole	3
207	$C_{15}H_{13}N$	indanylindanol	–
217	$C_{16}H_{11}N$	naphthlindanol	1
145	C_9H_7NO	hydroxyazanaphthalene	2
195	$C_{13}H_9NO$	hydroxyazaphenanthrene	1

TABLE IV

COMPOSITIONS AND WEIGHT PERCENTS FOR MOLECULAR
WEIGHT SERIES FOR BASE FRACTION
FROM ANTHRACENE OIL

	Series 1			Series 2			Series 3			Series 4	
MW	Comp.	wt.%	MW	Comp.	wt.%	MW	Comp.	wt.%	MW	Comp.	wt.%
79	C_5H_5N	–	117	C_8H_7N	0.034	119	C_8H_9N	0.010	129	C_9H_7N	0.852
93	–	–	131	–	–	133	$C_9H_{11}N$	0.020	143	$C_{10}H_9N$	0.600
107	–	–	145	–	–	147	$C_{10}H_{13}N$	0.064	157	$C_{11}H_{11}N$	0.413
121	$C_8H_{11}N$	0.035	159	–	–	161	$C_{11}H_{15}N$	0.059	171	$C_{12}H_{13}N$	0.177
135	$C_9H_{13}N$	0.019	173	$C_{12}H_{15}N$	0.018		$C_{10}H_{11}NO$		185	$C_{13}H_{15}N$	0.105
149	–	–	187	$C_{13}H_{17}N$	0.020	175	$C_{12}H_{17}N$	0.019	199	$C_{14}H_{17}N$	0.046
163	–	–	201	–	–	189	–	–	213	$C_{15}H_{19}N$	0.022
177	–	–	215	–	–	203	$C_{15}H_9N$	0.885	227	$C_{16}H_{21}N$	0.008
191	$C_{14}C_9N$	0.094	229	$C_{17}H_{11}N$	0.278	217	$C_{16}H_{11}N$	0.318	241	–	–
205	$C_{15}H_{11}N$	0.182	243	$C_{18}H_{13}N$	0.066	231	$C_{17}H_{13}N$	0.142	255		0.010
219	$C_{16}H_{13}N$	0.192	257	$C_{19}H_{15}N$	0.018	245	$C_{18}H_{15}N$	0.052			
	$C_{15}H_9NO$					259	$C_{19}H_{17}N$	0.012			

TABLE IV (Continued)

| | Series 1 | | | Series 2 | | | Series 3 | | | Series 4 | |
MW	Comp.	wt.%	MW	Comp.	wt.%	MW	Comp.	wt.%	MW	Comp.	wt.%
233	$C_{17}H_{15}N$ $C_{16}H_{11}NO$	0.125									
247	$C_{18}H_{17}N$	0.044									
261		0.011									
TOTAL wt.%		0.702			0.434			1.581			2.233

| | Series 5 | | | Series 6 | | | Series 7 | |
MW	Comp.	wt.%	MW	Comp.	wt.%	MW	Comp.	wt.%
155	$C_{11}H_9N$	0.118	167	$C_{12}H_9N$	0.427	179	$C_{13}H_9N$	1.462
169	$C_{12}H_{11}N$ $C_{11}H_7NO$	0.186	181	$C_{13}H_{11}N$	0.294	193	$C_{14}H_{11}N$	0.774
183	$C_{13}H_{13}N$ $C_{12}H_9NO$	0.304	195	$C_{14}H_{13}N$ $C_{13}H_9NO$	0.128	207	$C_{15}H_{13}N$	0.337
			209	$C_{15}H_{15}N$ $C_{14}H_{11}NO$	0.061	221	$C_{16}H_{15}N$	0.114
						235	$C_{17}H_{17}N$	0.039
						249	$C_{18}H_{19}N$	0.010

TABLE IV (continued)

Series 5			Series 6			Series 7		
Comp.	wt.%	MW	Comp.	wt.%	MW	Comp.	wt.%	
$C_{16}H_{17}N$	0.029							
$C_{15}H_{13}NO$								
$C_{17}H_{19}N$	0.012							
$C_{16}H_{15}NO$								
-	-							
	0.841			0.951			2.736	

used in this study.

Wolk, et al. (4) presented the nitrogen content of coal liquids as a function of the average boiling points of product fractions. Their results indicated that there was a steady increase in nitrogen content as average boiling point increased. This compares with the evidence found by Snyder (84) for petroleum fractions.

The nitrogen compounds found in petroleum liquids and coal liquids seem to be similar type of compounds. However, coal liquids have not been studied as exhaustively as petroleum feedstocks. For the present, it is reasonable to assume that raw anthracene oil contains quinoline, carbazole and phenanthridine type compounds.

Summary

The literature reviewed above for this study can be summarized as follows:

1. Knowledge of the effects of backmixing, liquid holdup and incomplete catalyst wetting in trickle bed reactors is important in evaluating the kinetic data from these reactors. Mears' correlation (13) for backmixing effects seems to be the most conservative in predicting backmixing effects and hence is adequate for making initial estimates.

2. Backmixing, liquid holdup and efective catalyst wetting effects all should be less important on smaller particle sizes.

3. Mass transfer effects in the liquid phase can be considered negligible except for low effectiveness factors.

4. Hydrodenitrogenation is a step series process involving hydrogenation and hydrocracking reactions. Most of the

nitrogen in coal liquids is in the form of heterocyclic compounds and hydrodenitrogenation proceeds via saturation of the heterocyclic ring, followed by ring fracture and subsequent removal of the nitrogen as ammonia. Most of the studies indicate that denitrogenation is first order with respect to the concentration of the nitrogen species.

5. Studies on hydrodenitrogenation of coal derived liquids (6, 59, 66) indicate that there is an abrupt decrease in the activation energy at about 750F.

6. The choice of operating pressures is markedly affected by the nature of the feedstock. In the case of raw anthracene oil pressure was observed to have a marked influence up to 1000 psig, beyond which the effect of an increase in pressure was less significant.

7. Higher space times can result in increased liquid holdup and hence increased denitrogenation due to more liquid-solid contacting.

8. Increase in H_2 flow rate beyond a hydrogen to oil feed ratio of 1500 SCF/bbl seems to have negligible effect on nitrogen removal.

9. Volume average pore radius seems to have negligible effect on the rate of denitrogenation in the range of 25 to 40Å for raw anthracene oil as feedstock.

10. Co-Mo-Alumina is the most commonly used catalyst for hydrodenitrogenation of petroleum as well as coal derived liquid feedstocks. The support properties appeared to have more effect on hydrotreating than the amount of cobalt or

molybdenum added. Two studies reported improvement in the catalyst activity in the presence of chlorides.

11. Presulfiding of the catalyst seems to improve the activity of the catalyst.

12. The nitrogen compounds present in petroleum and coal liquids seem to be similar type of compounds.

CHAPTER III

EXPERIMENTAL EQUIPMENT

The hydrodenitrogenation studies were conducted in a trickle bed
reactor system designed and constructed by Satchell and Sooter (6, 7).
The overall flow system, presented in Figure 5, was designed to fulfill
the following requirements:

1. The reactor should be capable of operating up to 800F with
   an isothermal profile along the length of the reactor.

2. The reactor should be able to operate up to 2000 psig and
   pressure control at a desirable level must be maintained.

3. Continuous operation should be feasible. In order to ensure
   continuous operation, back up valves must be provided wherever
   necessary so that when one valve fails the other could be
   used without shutting down the reactor.

4. No voids for undesirable liquid accummulation should be
   present in the system.

5. Replacement of parts must be made as easy as possible.

6. Ample hydrogen supply must be available and changing hydrogen
   cylinders should be made with minimum interruptions.

7. Flow rates of oil and hydrogen must be measured and controlled
   accurately.

8. The feed oil pump should be capable of delivering very low
   flow rates (10-100 ml/hr) accurately.

9. Sampling of liquid products should be possible without disturbing normal operation.

10. Provisions should be made to read the temperature profiles along the reactor length.

11. Adequate safety procedures should be incorporated into the system.

A schematic diagram of the equipment is shown in Figure 6. The feed oil was pumped and metered into the reactor with a Ruska positive displacement pump, and hydrogen flow was used from the bottles on a once-through basis. The liquid and hydrogen streams were combined in a tee at the reactor top and passed cocurrently down across the reactor bed. The reactor was packed with catalyst and the two ends of the reactor were packed with inert material to serve as pre- and post-heat zones. This was done so that the axial temperature distribution will be stabilized and the catalyst bed will be at uniform temperatures throughout the length of the bed. A thermowell, positioned at the center of the reactor was used to monitor the temperature by sliding a thermocouple across the length of the reactor. Temperatures were measured at one inch intervals during reaction along the length of the reactor. Disengaging and sampling bombs at the bottom of the reactor provided for gas-liquid separation and liquid isolation for sample removal. The flow rate of reactor effluent gases was monitored on a bubble meter.

FEED TANK

PUMP

TO HOOD

H$_2$ DETECTOR

PI

TI

V

TC

V

V

V

REACTOR

PI

PI

TO HOOD

SAMPLE
BOMB 1

CAUSTIC
SOLUTION

SAMPLE
BOMB 2

PI

TO HOOD

HYDROGEN

N$_2$ or H$_2$S-H$_2$ MIXTURES

SYMBOLS

TI   TEMPERATURE INDICATOR

TC   TEMPERATURE CONTROLLER

⊗   PRESSURE CONTROLLER

PI   PRESSURE GAUGE

►►   CHECK VALVE

V   VARIAC

►◄   VALVE

►◄   RUPTURE DISK

PRODUCT
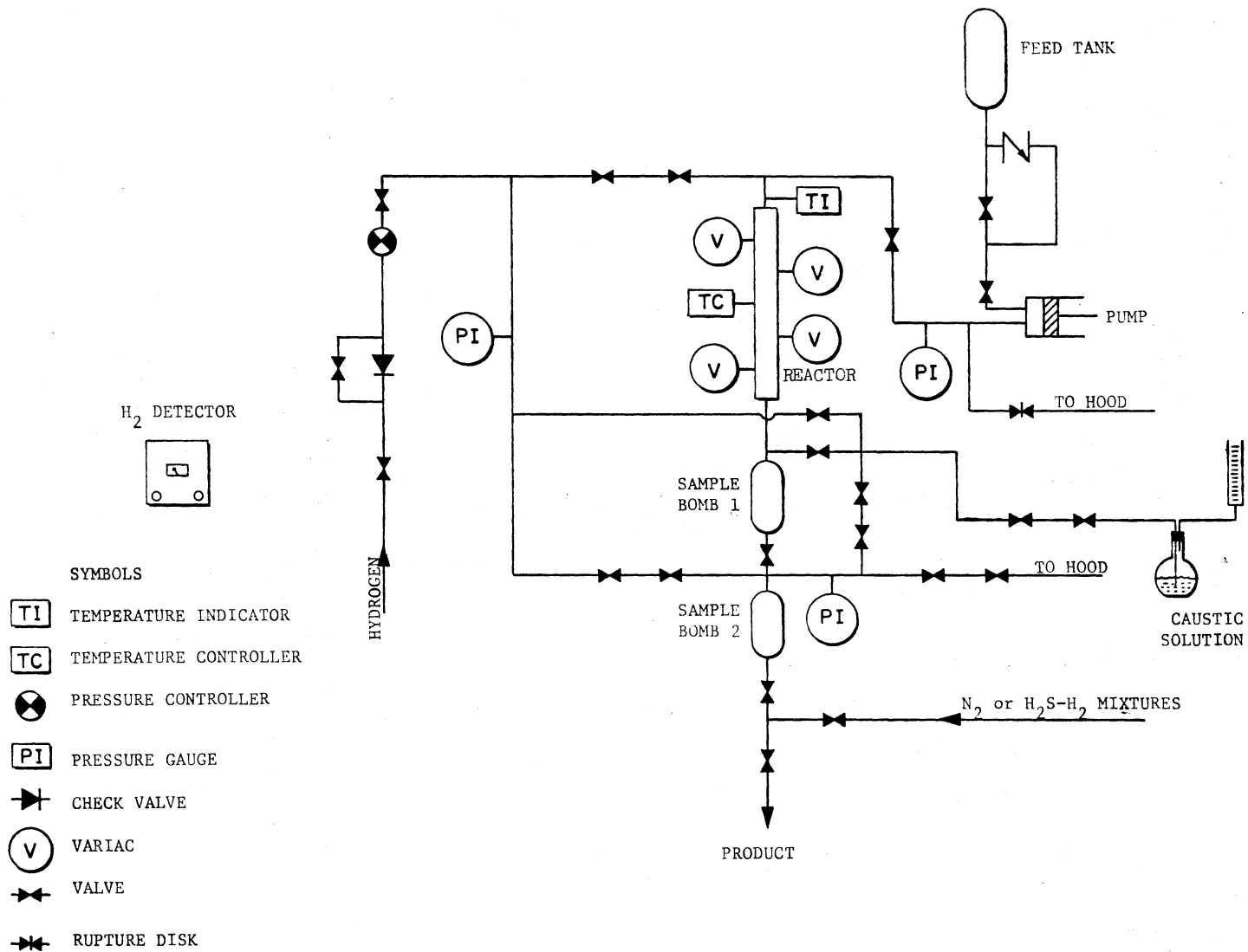
Figure 5. Schematic Flow Diagram of the Experimental System
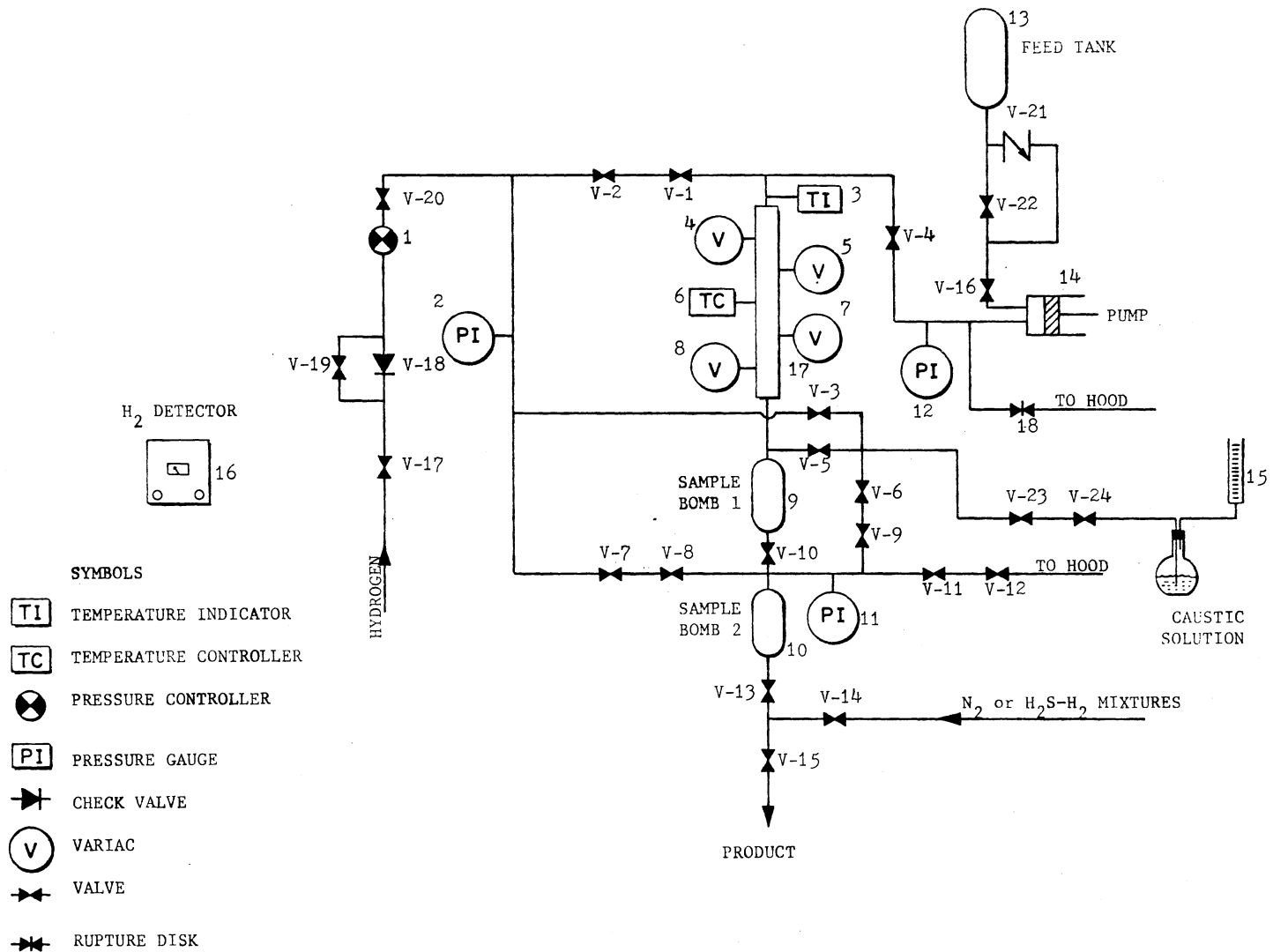
Figure 6. Numbered Experimental System

56

Description of Individual Units

Reactor

The reactor (17 in Figure 6) was made up of 1/2" stainless steel tubing with swagelok fittings at both ends. Figure 7 is a drawing of the reactor details. A 1/2" swagelok cross was connected to the top of the reactor and two 1/2" to 1/4" reducers were connected to the two sides of the cross. Hydrogen was allowed to flow from the left while oil flowed from the right. A 1/8" stainless steel tube was used as a thermowell. The thermowell was welded shut on the bottom and secured at the top of the reactor by another swagelok fitting. The 1/4 to 1/8 inch reducer through which the thermowell passed was drilled out to accommodate the thermowell. An iron constantan thermocouple was moved inside the thermowell to measure the temperature profile along the length of the reactor. 50 mesh stainless steel screens were used to hold the catalyst and inert in the reactor. The bottom of the reactor was fitted with a 1/2" union to enable it to be connected to the sample bombs.

Reactor Heaters

The heaters consist of five different aluminum blocks with a 1/2" diameter hole in the center. The blocks are split in the middle and hinged at one end for easy mounting and removal. A detailed drawing of the heaters are shown in Figure 8. The blocks were grooved with 3/8" wide by 5/8" deep slots, and beaded heaters were placed in these slots. The blocks were of different length in order to provide better temperature control. The final placement of the heaters are summarized

1/8" Thermowell

1/4" to 1/8" Reducer

1/2" to 1/4" Reducer

1/2" Cross

1/2" to 1/4" Reducer

Hydrogen

Oil

50 mesh Screen

Inert Packing 8-3/16"

Catalyst 19-5/8"

Inert Packing 5-1/2"

50 mesh Screen
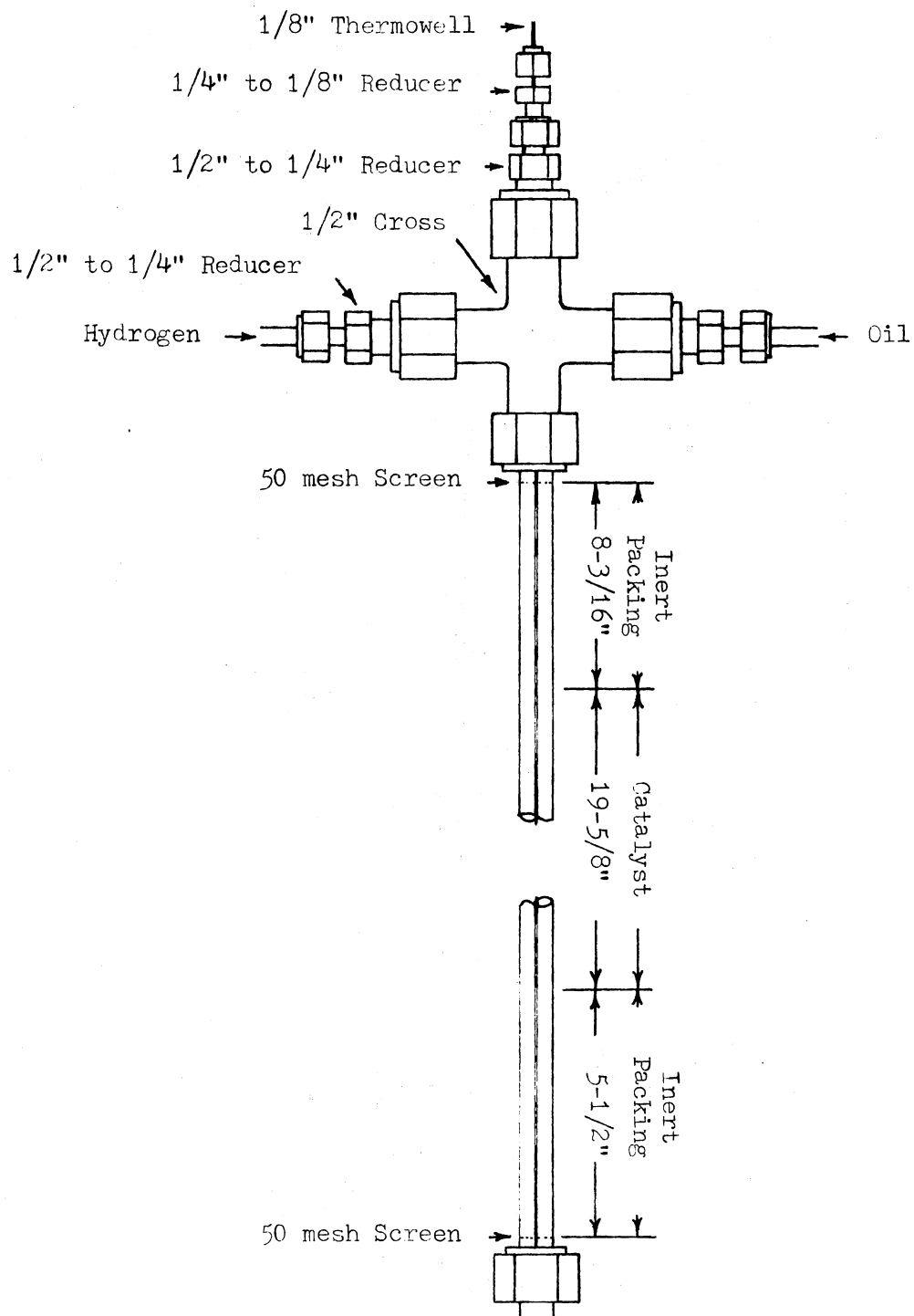
Figure 7. Reactor
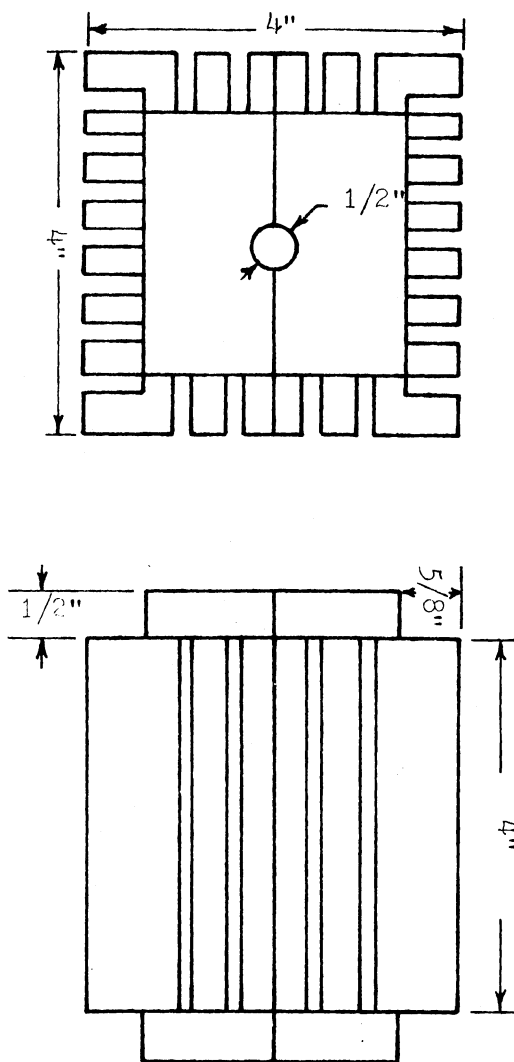
Figure 8. Heater Block Design

in Table V. The middle block, the longest one, was controlled by a
Hewlett-Packard temperature controller, whereas the others were
controlled normally by using powerstats. This arrangement provides a
manual override in case the temperature controller fails. Control with
powerstats was maintained by balancing heat input with loss by trial
and error to achieve the required temperature profile. The sensing
thermocouple for the controller was placed through a small hole drilled
into the middle heating block.

TABLE V

REACTOR HEATER CONFIGURATION

Block Number from Reactor Inlet	Aluminum Block Height, Inches	Control Type
1	4	Variac
2	5	Variac
3	10	Hewlett-Packard
4	5	Variac
5	4	Variac

Reactor Insulation

The aluminum blocks were wrapped first with a one inch layer of felt insulation tied together with asbestos tape. Then a two inch layer of fiber-glass was wrapped around the felt insulation and these were also held in place by using asbestos tape. Electrical connections for the heaters were made through the break in the insulation, while carefully packing the break with fiber-glass to avoid heat losses

Feed System

Oil was fed to the system from the top of the reactor. A Ruska positive displacement pump (14 in Figure 6) with a single barrel (1000ml capacity) was used to pump and meter the oil to the top of the reactor. The oil flow rate can be varied by changing the gear settings on the pump. A stainless steel bomb of 2 litres capacity was used as a feed tank from which the pump barrel was filled.

Hydrogen was fed to the system directly from cylinders on a once-through basis. A Mitey Mite double stage (1 in Figure 6) regulator was used to control pressure. The cylinders were connected to a manifold with three stations so that the changing of H_2 cylinders can be done with minimum interruptions. The discharge gas flow rate was measured at the discharge end using a bubble flow meter.

Sampling System

The sampling system was designed to provide continuous operation of the reactor. This was done using two stainless steel bombs (9 and 10 in Figure 6) of 1 litre capacity, rated at 1800 psig. Figure 9 is

Hydrogen + Oil

Hydrogen

Oil
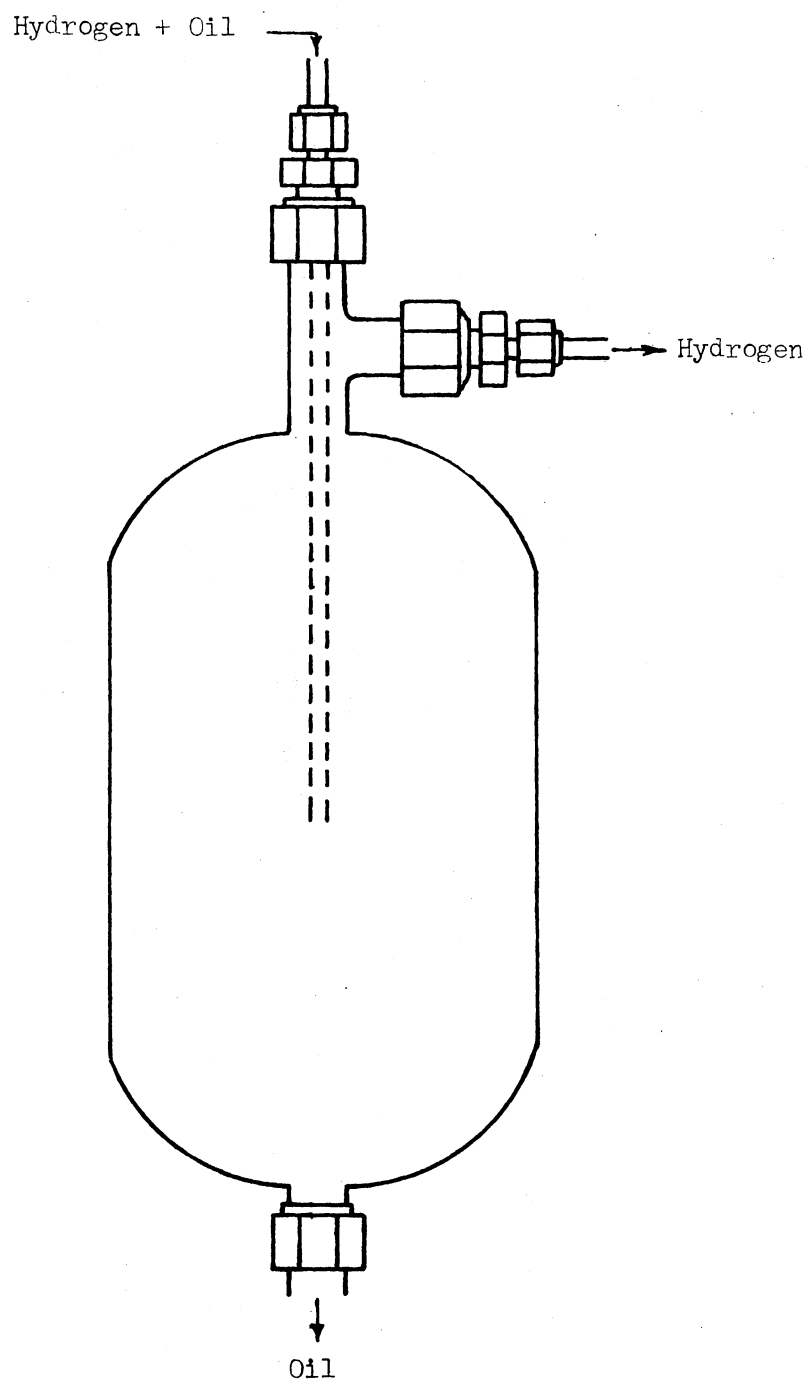
Figure 9. Sample Bomb Design

a drawing of the sample bomb design. The bottom of the reactor was attached to the first sample bomb using a 1/4" stainless steel tube. The entry of the 1/4" stainless steel tube into the bomb was made possible by drilling out the 1/2" to 1/4" swagelok reducer. The seal on the tube was made by a swagelok fitting on the 1/4" tube. Vapor and liquid separates within the bomb and the liquid collects at the bottom. A second bomb identical to the first one was placed directly below the first one. Sampling techniques will be described in the section on experimental procedure.

Temperature Measurement

The temperatures were measured by sliding an iron-constantan thermocouple inside the thermowell located at the center of the reactor. The thermocouple was connected to a Numatron digital thermometer (3 in Figure 6) which registered the temperature directly.

Pressure and Flow Control

The system pressure was monitored using a 0-5000 psig Heise gauge (12 in Figure 6). This gauge is located upstream from the reactor. The inlet pressure to the reactor was controlled using a Mitey-Mite pressure controller (1 in Figure 6). Pressure upstream from the Mitey-Mite controller was maintained with Matheson regulators connected to the manifold which in turn was connected to the hydrogen supply cylinders.

The gaseous flow control was maintained with two valves. The first valve (V-24) was an Autoclave vee tip valve designed to take a major portion of the pressure drop. The second valve (V-24) is a Whitey

needle valve designed for fine control of gas flow. The gas flow was monitored downstream from the control valve on a 0-25ml bubble flow meter.

Inert Gas Purging Facility

The liquid product samples were purged with an inert gas, nitrogen, before collection from the second sample bomb to remove the ammonia and hydrogen sulfide dissolved in the liquid sample.

Nitrogen was supplied to the second sample bomb directly from a supply cylinder. A Matheson regulator was used to regulate the pressure at the nitrogen supply cylinder. The nitrogen, after entering and purging the oil, was then vented to the hood directly.

Safety Devices

A combustible gas detector (16 in Figure 6) (Model 50), was installed with two detector hoods located over and near the reactor. The alarm light was set to come on when the hydrogen concentration in the room reached 50% of the lower explosive limit.

A rupture disc rated at 3000 psig (18 in Figure 6) was installed to eliminate possible pressure buildup due to clogged oil lines on the liquid delivery line close to the pump exit. A rupture disc was vented with a 1/2" stainless steel tubing to the hood. If a line rupture occurs while the system is operating, the rupture would allow hydrogen to pour into the room at the delivery pressure until the entire bottle was emptied if no check was provided. An excess flow check valve (V-18) was installed to prevent such an occurrence.

In order to prevent splashing of the oil in case V-16 was acciden-
tally opened while the pump was still under pressure, a one way valve
V-21 was installed which allowed the oil flow through in one direction
only. V-22 was kept closed at all times.

System Materials

Figure 6 is a schematic diagram of the system with numbers. The
numbers correspond to those listed within parantheses in Table III which
lists all materials. A list of chemicals used is presented in Table
in the next chapter.

TABLE VI

LIST OF EXPERIMENTAL EQUIPMENT

Equipment		Description
Manifold		with 3 stations - Matheson rated for 3000 psig
Mitey-Mite Pressure Regulator	(1)	Model 94 (Internally Loaded), inlet pressure 5000 psi, outlet pressure 3000 psi maximum, operating temperature 0-165°F, 1/4" inlet and outlet connections.
Pressure gauge	(2)	Heise-Bourdon tube gauge, maximum 3000 psig
Reactor	(17)	1/2" O.D., 0.049" thickness, 316 stainless steel tubing
Thermowell		1/8" O.D., 316 stainless steel tubing
Felt Insulation Fabric		McMaster-Carr No. 9326P5
Fiberglass Insulation		McMaster-Carr No. 9356M13
Thermocouple		Iron-constantan, 0.04 in an O.D., 304 stainless steel sheath, grounded sensor tip Conax No. J-SS4-G-T3-36"
Powerstats	(4, 5, 7, 8)	Input 120 volts, output 0-140 volts, 10 amperes and 1.4 KVA, Superior Electric type 116, Fisher No. 9-521
Temperature Controller	(6)	Hewlett-Packard temperature programmer, Model 240, 0-1500°C
Temperature Indicator	(3)	Leeds and Northrop digital readout, Model 900-001-003-1
Sample Bombs	(9, 10)	316 Stainless, 1000 cc, 1800 psig maximum, Matheson

TABLE VI (Continued)

Equipment		Description
Pressure Gauges	(11, 12)	0-3000 psig, Autoclave No. P-480
Feed Tank	(13)	2250 cc, 316 stainless, Matheson
Pump	(14)	Ruska positive displacement pump, variable drive
Bubble Meter	(15)	0-25 ml capacity
MSA – Hydrogen Detector	(16)	Model I-501 Wall Mount, dual diffusion head
Regulator		for hydrogen, Matheson Model 8
Regulator		for nitrogen, Air Products No. E11-F-N115G
Tubing		1/8 inch O.D., 316 stainless steel
		1/4 inch O.D., 316 stainless steel
		1/2 inch O.D., 316 stainless steel
Beaded Heaters		115 volt Marsh beaded heaters
Heating Blocks		Aluminum block heaters – specifically designed for heating the reactor (See Figure 8)
Rupture disk	(18)	3000 psig, Autoclave
Screens		Tyler standard screens used to screen 8-10 mesh particles

TABLE VI (Continued)

Equipment	Description
V-1	Vee-tip Valve - Autoclave number 10V-4071
V-2	Soft Seat Valve - Whitey SS-3TS4
V-3	Vee-tip Valve - Whitey SS-1VS4
V-4	Vee-tip Valve - Autoclave 10V-4071
V-5	Vee-tip Valve - Autoclave 10V-4071
V-6	Vee-tip Valve - Autoclave 10V-4071
V-7	Whitey - SS-1VS4
V-8	Vee-tip Valve - Autoclave 10V-4071
V-9	Whitey - SS-3TS4
V-10	Vee-tip Valve - Autoclave 10V-4071
V-11	Whitey - 21RS4
V-12	Needle Valve - Autoclave 10V-4071
V-13	Whitey - SS-1VS4
V-14	Whitey - SS-1VS4
V-15	Whitey - SS-1VS4

TABLE VI (Continued)

Equipment	Description
V-16	Vee-tip Valve - Autoclave 10V-4071
V-17	Ball Valve - Whitey SS-4152
V-18	Check Valve - Autoclave 10-6904-316-CW
V-19	Vee-tip Valve - Autoclave 10V-4071
V-20	Whitey - SS-1VS4
V-21	Whitey - One Way Valve
V-22	Whitey - SS-1VS4
V-23	Needle Valve - Autoclave 10V-4071
V-24	Needle Valve - Autoclave 10V-4071

CHAPTER IV

EXPERIMENTAL PROCEDURE

The experimental procedure consists of catalyst preparation and
loading, start up procedure, catalyst activation, normal operation,
sampling, shutdown and analysis. A detailed discussion of each follows.

Catalyst Preparation and Loading

In previous studies, the catalysts were obtained from commercial
vendors and the catalyst preparation consisted mainly of packing the
reactor and activating the catalyst. However, in the present study,
catalyst supports were obtained from commercial vendors and impregnated
in our laboratory. Ideally, in order to determine the influence of
catalyst support properties on hydrodenitrogenation we should have sets
of catalysts exactly similar in every respect except for the support
properties. It was not possible to achieve this in the past studies
(5-9), since different catalysts with varying physical properties were
obtained from vendors and used. Schlaffer, et al. (10, 73) studied
the physical changes that occur to support alumina upon exposure to
steam at moderate to high temperatures, and they found that there is
a considerable decline in surface area accompanied by little or no loss
of pore volume. Hence, one of the supports used in this study was
steam treated for ten hours at about 1000F in order to change the pore
structure, hopefully to obtain a "matched" pair of catalysts with only

pore distribution differences.

Three different catalyst supports were used in this study. The first support was used mainly to determine whether impregnation is feasible in our laboratories. Out of the two remaining supports, one was steam treated for ten hours and both the supports and steam treated support were impregnated and used as catalysts. A third support with a bimodal distribution was also impregnated giving a total of four different catalysts to be used in this study. Steam treating and impregnation are described in detail.

Steam Treating

Steam treating of the alumina support was done in a 3/4" steel pipe filled with inert and catalyst support. Figure 10 is a schematic representation of the steam treating system. Steam was prepared by allowing water to boil in a three liter standard flask. A thermowell similar to the one used in the reactor was passed through the center of the tube. The steel pipe containing the catalyst and inerts was heated by means of tubular furnaces. The temperatures were measured by sliding a thermocouple along the length of the thermowell and by noting the response of a Doric digital temperature readout. The supports were steam treated for periods of one hour and ten hours at a temperature of about 1000F and the samples were sent to be analyzed for pore size distribution. Based on these results it was decided to use the support material that was treated for 10 hrs. The temperature profiles along the length of the support bed are presented in Appendix G.
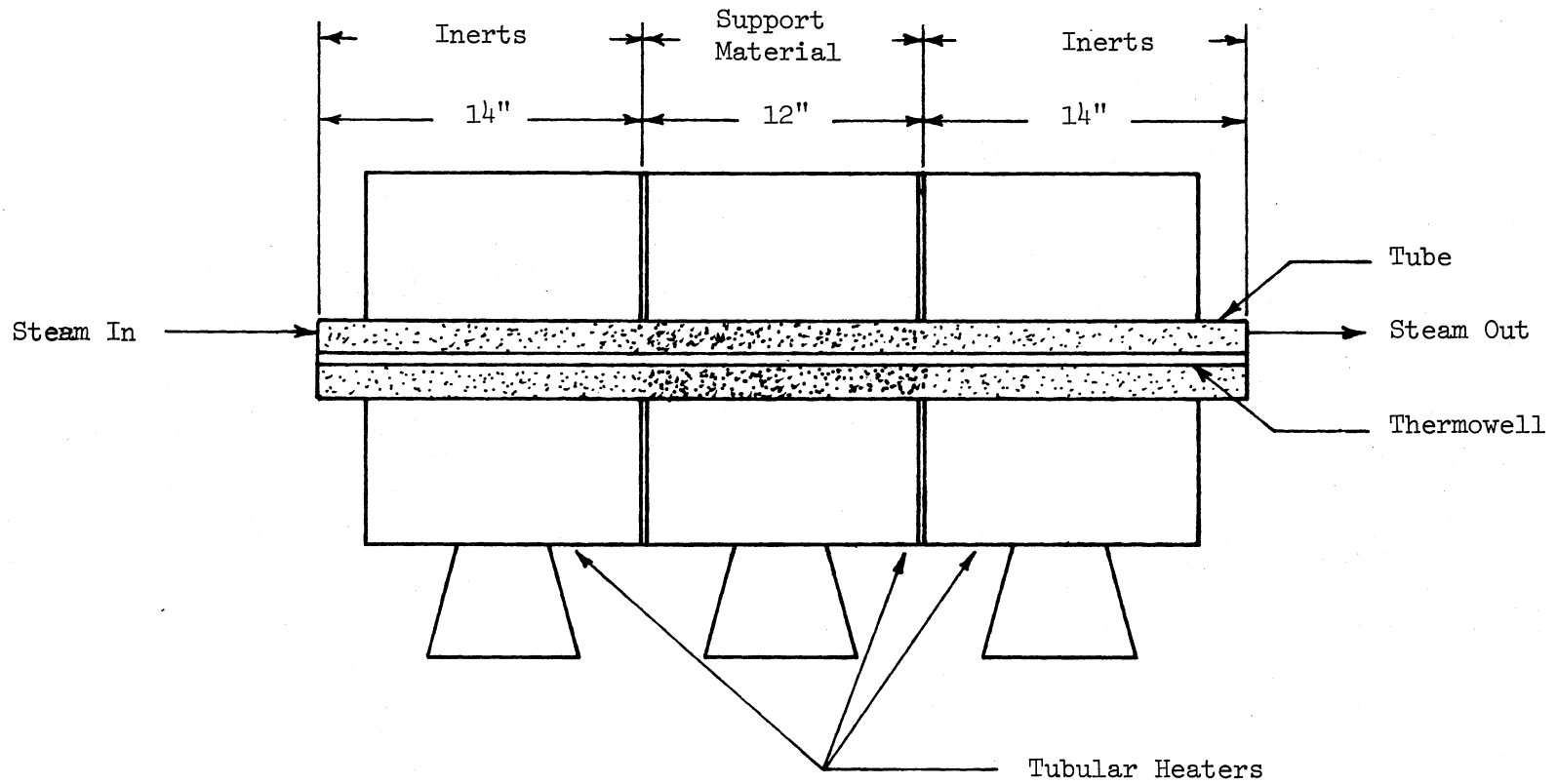
Figure 10. Schematic Diagram of the Steam Treating System

Impregnation

The impregnation was done following the method suggested by Leach (97). He described the procedure for 100 gm samples which was scaled down to suit a 25 gm sample of the support material. About 3.72 gm of MoO_3 was dissolved in 15 ml of water plus 5 ml of 30% aqueous ammonia. The mixture was heated since the solubility of MoO_3 in water is very small. This solution was cooled to room temperature and then neutralized to a pH of 5.5 using concentrated nitric acid. About 10 ml of water and about 4.06 gm of $Co(NO_3)_2 6H_2O$ were added. This solution was diluted to about 40 ml and poured over the alumina extrudate (about 25 gm) kept in a casserole. After setting overnight, the contents of the casserole were dried at 100C in a furnace. After the support completely dried, the casserole was placed in an electric furnace. The temperature was slowly raised to 900F and was held at 900F for one hour. The exact weights used in each catalyst preparation are given in the Appendix E.

Loading the Catalyst

Typical catalyst bed lengths of 0.498 to 0.505 meters (19.630 to 19.88 inches) were maintained in this study. The catalyst bed was placed in the middle of the reactor to minimize end effects. The two ends of the reactor were packed with inert material crushed to 8-10 mesh. The following procedure was used to pack the catalyst into the reactor:

1. A fifty mesh size screen was wedged between the top of the reactor and the 1/2" Swagelok cross.

2. The thermowell was held centrally in the reactor.

3. The 8-10 mesh size crushed Berl saddles were poured in the bottom of the reactor while tapping vigorously for uniform packing around the thermowell. For every experimental run the reactor was packed with fresh Berl saddles to a height of 0.208 meters (8.18 inches).

4. The catalyst was then poured in the bottom of the reactor following the procedure described above. For every experimental run except for the CAT series, the reactor was packed with fresh catalyst to a height of 0.498 meters (19.63 inches). For the CAT series, the reactor was packed to a height of 0.505 meters (19.88 inches) with catalyst.

5. The 8-10 mesh crushed Berl saddles were again added to fill the reactor.

6. Lastly, a fifty mesh screen was wedged between the bottom of the packed reactor and the 1/2 inch Swagelok union.

An antiseizing compound, Silver Goop, was used on all Swagelok threads to facilitate their tightening and loosening.

Startup Procedure

The packed reactor was secured in the system by connecting the 1/2 inch Swagelok cross at the top to the two feed lines and by connecting at the 1/2 inch Swagelok union at the bottom of the reactor to the product line. The system was pressure tested before installing the heating blocks. Each fitting and tubing in the entire system was checked for leaks. The pressure testing was normally done at 1500 psig, the normal operating pressure. Snoop leak detector solution was used

for detecting leaks. After pressurizing to 1500 psig, the system was isolated and the pressure readings were monitored for several hours to observe any fall in pressure. This was done in addition to using the leak detector solution so as to confirm that there are no leaks in the system.

Once the system was found to be free of leaks, the heating blocks were put in position. The heaters were connected to the controllers and the insulation was installed. The system was checked for any short circuits using a volt-ohm meter, and the thermocouple was placed in the thermowell. The next step in the experimental procedure is the activation of the catalyst.

Catalyst Activation

The catalyst activation consists of two steps, calcination and sulfiding as described below.

Calcination

The reactor was gradually heated to $232^{\circ}C$ ($450^{\circ}F$) and the temperature profile noted every half hour. When the temperature was $232 \pm 5^{\circ}C$ ($450 \pm 10^{\circ}F$) in the catalyst zone nitrogen was allowed to flow through the reactor for 12 hours at a flow rate of about 3 cc/second. This heating in a nitrogen atmosphere was done to remove water from the catalyst.

Sulfiding

The last step in catalyst activation was sulfiding. The nitrogen supply was cut off from the system after 12 hours. Before sulfiding

Mitey-Mite regulator and the Heise gauge were isolated from the system to prevent their contact with H_2S. Then a five percent H_2S in H_2 mixture was allowed to flow over the catalyst for 90 minutes at a flow rate of about 3 cc/second. The catalyst bed temperature was maintained at 232C (450F) throughout the sulfiding operation. Gases from sulfiding step were scrubbed with caustic solution to remove H_2S before venting. After the sulfiding operation the system was flushed with nitrogen before reconnecting the Mitey-Mite and the Heise gauge.

Normal Operation

A few more steps to be performed before the system was considered to be at normal operating conditions. After the Mitey-Mite and Heise gauge were reconnected, the reactor was heated gradually with no gases flowing through it. The pump was filled with the raw anthracene oil feed and the pump was pressurized to the operating pressure. When the temperature in the catalyst zone was within 27C (50F) of the desired value, the system was pressurized with hydrogen to the experimental pressure, 1500 psig. The hydrogen flow rate was adjusted and raw anthracene oil was then fed into the reactor at 1500 psig at a pre-determined rate. The temperature was then stabilized at the desired value.

The system was considered to be at normal operating conditions when the temperature and pressure had stabilized. A maximum deviation of 1.5C (3F) along reactor or with respect to the desired value in the temperature and a maximum deviation of ±20 psig were considered acceptable during normal operation. Typically, the temperature and pressure stabilized within four hours from the time both oil and

hydrogen were on stream. The temperature profile at 1 inch intervals, pressure gauge reading, temperature controllers' settings and flow rate of the gaseous products leaving the system were recorded every hour. Table VII gives the valve positions for normal operation. In some positions, two valves back to back were used to ensure continuous operation in case of failure of any one of the valves. Previous experience revealed the desirability of this type of redundancy.

Sampling Procedure

The main objective was to collect an oil sample without disturbing the normal operation. Liquid samples were collected at predetermined intervals after the reactor had stabilized at the desired operating conditions. The following procedure was used to obtain a sample.

The second sample bomb was isolated from the system by closing the valves, V-10 and V-6, and then depressurized by releasing the gases through the valve, V-12, to the hood. Valve V-5 was opened to allow the product gases to pass to the hood. When the pressure in the bomb was completely released, the liquid in the bomb was purged with nitrogen for 30 minutes. This was done to strip-off the NH_3 and H_2S present in the liquid.

Nitrogen entered into the bomb through valves, V-14 and V-13, and escaped to the hood along with the stripped gases to the hood through V-12 and V-11. After 30 minutes of purging, the nitrogen supply to the bomb was cut-off by closing valve V-14. The liquid sample was then collected in glass bottles by opening valve V-15. After collecting the sample, valves V-12, V-13 and V-15 were closed.

TABLE VII

VALVES POSITION SUMMARY DURING
NORMAL OPERATION

Valve	Position	Valve	Position
V-1	Open	V-13	Closed
V-2	Open	V-14	Closed
V-3	Closed	V-15	Closed
V-4	Open	V-16	Closed
V-5	Closed	V-17	Open
V-6	Open	V-18	Open
V-7	Closed	V-19	Closed
V-8	Open	V-20	Open
V-9	Open	V-21	Open
V-10	Open	V-22	Closed
V-11	Open	V-23	Open
V-12	Closed	V-24	Partially Open

The bomb was then pressurized to 1500 psig using hydrogen from the main supply. This was done by closing the valve, V-2, to cut off the H_2 supply to the system and then opening valves V-7 and V-19. Immediately after repressurization, valves V-7 and V-19 were closed and V-2 opened to resume normal supply of hydrogen to the system. The lower bomb was reconnected to the system by opening valves V-10 and V-6 and closing V-5, so that liquid products collected in the upper bomb could drain into the lower bomb.

Shutdown Procedure

First hydrogen supply from the cylinder was cut-off, the pump was stopped and the temperature controllers were switched off. The pressure was then allowed to bleed down to about 100 psig. When the reactor temperature reached ambient, the system pressure was further reduced to atmospheric pressure.

After the reactor reached room temperature, the insulation was removed, heating blocks were taken out and the reactor disconnected from the system. The spent catalyst samples were recovered and the reactor was cleaned with acetone.

Sample Analysis for Nitrogen Concentration

A total of eight experimental run series was made in this study. Except for the first series, namely the series ⌐AT, the analysis of samples for the others were performed using a Perkin-Elmer Model 240 elemental analyzer. The analysis for the CAT series was done using a modified Kjeldahl method developed by Satchell. Details of this Kjeldahl method of analysis are given in Satchell's thesis (6). A

description of the principles for the elemental and analytical procedure
used in the present study follows.

A flow schematic of the Perkin-Elmer elemental analyzer is given
in Figure 11. These following sequence of steps are fully automated.
The weighed sample is combusted in an oxygen atmosphere, aided by
silver tungstate and magnesium oxide located in the combustion tube.
The gaseous combustion products are flushed by a helium stream through
a reduction tube. Excess oxygen and unwanted combustion products are
removed, and the oxides of nitrogen are reduced to molecular nitrogen.
The remaining mixtures, consisting now only of water vapor, carbon
dioxide, nitrogen and helium diluent are gathered into a glass vessel
of 300 ml capacity, which is filled to a pressure of approximately
2 atmospheres and held at a constant temperature. After equilibration,
the sample mixture is expanded into an elongated sampling system,
then swept into a series of thermal conductivity (T. C.) cells.
Situated between the first pair of T. C. cells is an adsorption trap
containing a dehydrating material, magnesium perchlorate. As the gas
passes through, water is removed from the stream. The thermal
conductivity difference before and after the trap, as read on a
potentiometer recorder reflects the water concentration and therefore
the amount of hydrogen in the original sample. A similar measurement
is made of the signal output of a pair of conductivity cells between
which is a trap which removes carbon dioxide. The remaining gas now
consists of only helium and nitrogen. This gas passes through a
conductivity cell, the output of which is compared to that of a
reference cell through which flows pure helium from the gas cylinder
to give the nitrogen concentration.
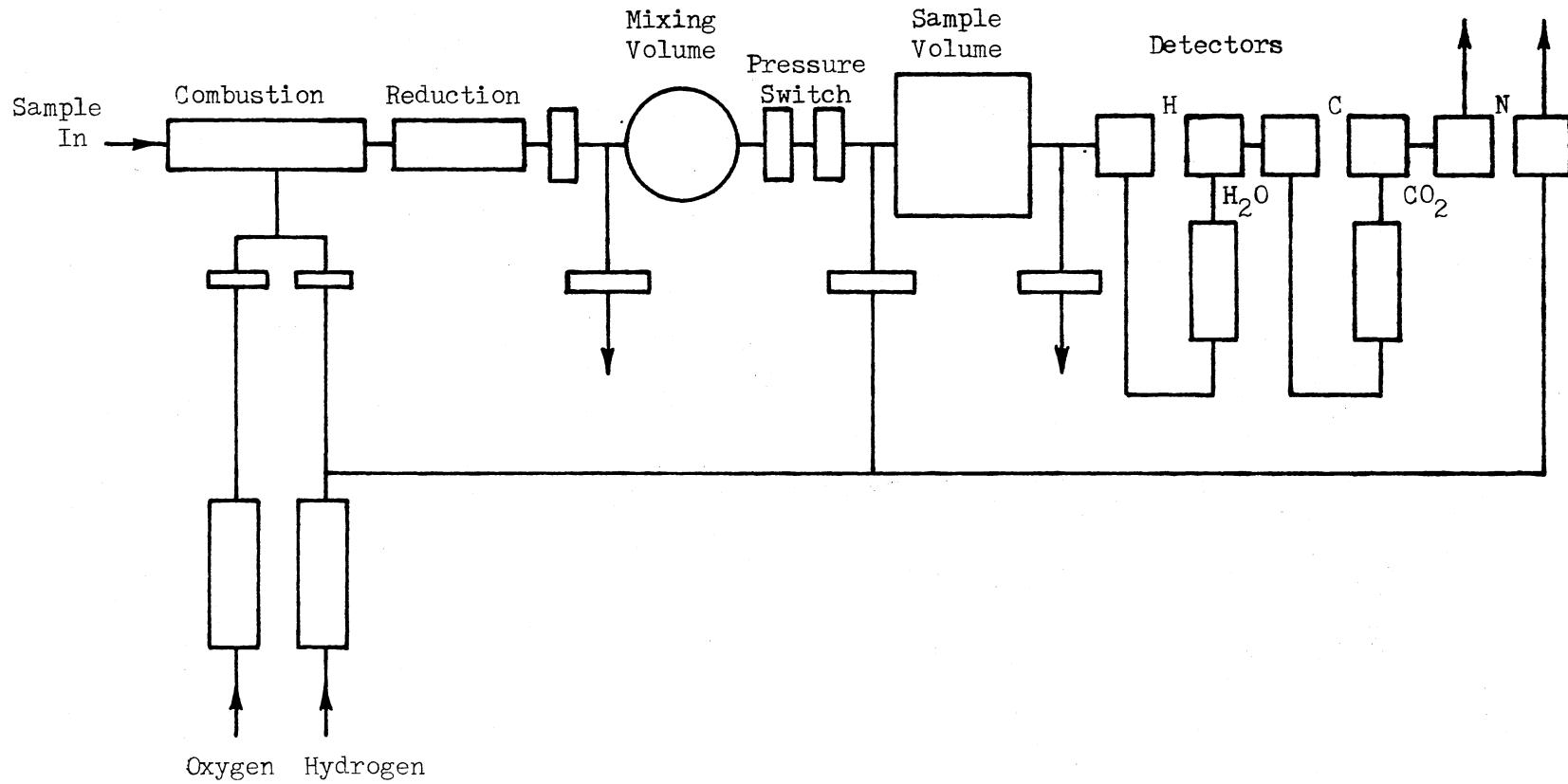
Figure 11. Flow Schematic of the Elemental Analyzer

The general procedure for analysis is described in the vendor instruction manual (98). The complete analytical system consists of a Model 240 Perkin-Elmer elemental analyzer, a Leeds and Northrop 1mv recorder, a Perkin-Elmer Autobalance model AD-2 and a volatile sample sealer from Perkin-Elmer.

A description of the analytical procedure is given below. This is the normal procedure used on a day to day when the instrument was in working condition. This assumes that the combustion tube, reduction tube, the traps and the scrubbers are all installed and none of them are exhausted. Detailed information on startup of the instrument and installation of tubes can be found in the instruction manual (98).

Before proceeding with the analysis of samples the instrument had to be calibrated. Combustion standards such as acetanilide and cyclohexanone were used for calibration as recommended by the vendor. First a few blanks were calculated. Blanks in which the instrument is run through a program cycle with a ladle and boat are required for measuring the background signal developed when only the sample is absent from the system. An empty platinum boat is placed in the ladle and the ladle is introduced in the combustion tube. The ladle is equipped with a magnet in the end. The start button is pressed after introducing the ladle in the combustion tube. When the inject lamp goes on, the ladle is moved into the furnace using an external magnetic manipulator. The combust button is pressed after this. The C, H, N readings that appear first are known as "zero" values and the second set of readings are known as the "read" values. The difference between the "read" values and the corresponding "zero" values, when no sample was used gives the blank values. After the blanks are extablished consistently, the

combustion standard is weighed out carefully in a clean platinum boat

and introduced into the combustion tube. The same procedure is

repeated, recording the "zero" and "read" values. The calibration

constants are calculated as given in the following example for deter-

mining the calibration constant for nitrogen, K_N.

Since the percentage of nitrogen in the standard is known, the

theoretical weight of nitrogen in the sample can be calculated. The

total signal from the instrument is given by subtracting the blank and

zero values from the read value. Dividing the total signal by the

theoretical weight gives the sensitivity or the calibration constant

in units of microvolts/microgram.

$$\text{theoretical weight} = \begin{array}{c} (\text{wt. of standard x \% of N in the standard}) \\ \text{in micrograms} \end{array}$$

$$\text{Total Signal (in } \mu V) = \text{Read} - \text{Blank} - \text{Zero}$$

$$K_N = \frac{\text{Total Signal}}{\text{Theoretical Weight}} \frac{(\mu V)}{(\mu g)}$$

Now this K_N can be used to calculate the nitrogen content of

unknown samples once the weight of the sample and the "read", "zero"

and blank values are known by following a reverse calculation such as

this:

$$\text{Wt. of N in sample} = \frac{\text{Total Signal } (\mu V)}{K_N \quad \frac{(\mu V)}{(\mu g)}}$$

A sealer was used to analyze liquid samples. The samples were

placed in aluminum capsules and then were sealed using the sealer and

then placed in the ladle. The same procedure is followed. However, new

blank values were determined using empty sealed capsules to be used

in the calculations.

TABLE VIII

LIST OF GASES AND CHEMICALS USED

Materials used for the Run

Hydrogen	--	pre purified, 99.95%, 2200 psig (Air Products)
Nitrogen	--	purity 99.997, 3500 psig (Air Products)
H_2-H_2S Mixture	--	5.14% H_2S in H_2 mixture, 2000 psig (Matheson)
Inert Packing	--	Semiporcelain berl saddles

Materials used in Doctoring the Feedstock

| Quinoline | -- | Reagent Grade (Fisher Scientific Company) |

Chemicals and Gases used in Analytical Work

i) For Kjeldahl Method

Concentrated Sulfuric Acid	--	Baker reagent grade
Sodium Hydroxide	--	Baker reagent grade
Boric Acid	--	Baker reagent grade
Bromocresol Green	--	Allied Chemical
Methyl Red	--	Allied Chemical
Hydrochloric Acid	--	Fisher Certified
Ethyl Alcohol	--	Baker reagent grade

ii) For Model 240 Elemental Analyzer

Helium	--	Ultrahigh purity, 2500 psig (Air Products)
Oxygen	--	Ultrahigh purity, 2500 psig (Air Products)
Magnesium Perchlorate	--	Reagent grade (Fisher Scientific Company)
Colorcarb	--	Perkin-Elmer
Copper	--	60-100 mesh (Perkin-Elmer)

TABLE VIII (Continued)

ii) For Model 240 Elemental Analyzer (continued)

Silver Gauze	--	(Perkin-Elmer)
Platinum Gauze	--	(Perkin-Elmer)
Silver Vanadate	--	Reagent grade (Coleman Instruments)
Silver Oxide + Silver Tungstate on Chromosorb	--	(Perkin-Elmer)
Silver Tungstate on Magnesium Oxide	--	(Arthur H. Thomas Company)
Tungstic Anhydride	--	purified (Fisher Scientific Company)
Aluminum Capsules	--	(Perkin-Elmer)
Acetanilide	--	combustion standard (BDH Chemicals, Ltd., England)
Cyclohexanone-2,4-dinitro phenylhydrazone	--	Analytical standard (BDH Chemicals, Ltd., England)
Acetone		

CHAPTER V

FEEDSTOCK AND CATALYST CHARACTERIZATION

Feedstock

The feedstock used in this study, raw anthracene oil, was obtained
from the Reilly Tar and Chemical Corporation and served as a liquid
analogous to a solvent fraction produced from a solvent refined coal
process. This is a process stream that may require rehydrogenation
and clean up in some processes. The properties of the raw anthracene
oil are shown in Table IX. The nitrogen concentration in the
feedstock was 1.06 weight percent with essentially no ash contents.
The feedstock had an ASTM distillation range of 193C (380F)
(Initial Boiling Point) to over 435C (815F) (90% point).

Scheppele and Greenwood (95) characterized the feedstock used
in this study by high resolution electron impact and field ionization
mass spectrometry. Their approach to separating raw anthracene oil
according to compound class is shown in the separation scheme,
Figure 12. The weight percent of the various fractions obtained from
the separation of the four fractions are shown in Table X. Note
that nearly three-fourths of the feed is classified as the hydrocarbon+-
ether fraction. The second largest class of compounds are the acid
fraction which comprises about 15% of the feed followed by the basic
fraction consisting of about 10% of the feed. For all fractions high
resolution mass spectra were recorded on photoplates using a CEC

87

TABLE IX

RAW ANTHRACENE OIL FEED PROPERTIES

Carbon	90.65
Hydrogen	5.76
Sulfur	0.48
Nitrogen	1.06
Oxygen*	2.05
Ash	Nil
API gravity @ 60°F	-7
Initial**	193°C (380°F)
10 vol%	232°C (450°F)
30	297°C (570°F)
50	343°C (650°F0
70	371°C (700°F)
90	435°C (815°F)

* By difference
** Normal boiling point determined from ASTM D1160 data

SEPARATION SCHEME[a]

Sample

↓

Amberlyst A-29   2) benzene / 3) methanol saturated with CO_2 ———→ acidic components

↓

1) Pentane

↓

Amberlyst 15   2) benzene / 3) 90% methanol, 10% tripropylamine ———→ basic components

↓

1) Pentane

↓

FeCl$_3$ supported on aluminum silicate-Amberlyst A-29 dual column   2) 1,2-dichloroethane ———→ neutral nitrogen containing components

↓

1) Pentane

↓

Mercuric acetate supported on aluminum silicate   2) boiling benzene / 3) Treatment with 10% aq. HCl sat. with H_2S ———→ neutral sulfur containing components

↓

1) Pentane

Hydrocarbon plus ethers

[a] In each step the numbers indicate the sequence of solvents used in elution except as noted.

Figure 12. Method of Separation (96)

TABLE X

WEIGHT PERCENTS OF VARIOUS FRACTIONS
OBTAINED FROM SEPARATION OF RAW
ANTHRACENE OIL

Component	Weight Percent
Acid	14.9
Base	9.5
Neutral Nitrogens	1.7
Hydrocarbons+ethers	73.9

21-110B double focusing mass spectrometer. Elemental compositions were then assigned consistent with these exact masses.

For the acid fraction from the feedstock raw anthracene oil, Table XI tabulates the molecular weights, and associated empirical formulas and weight percents for each of the thirteen observed molecular-weight series. Convergence of compound classes at various molecular weights in a given series complicates the interpretation. Table XII presents similar information for the hydrocarbon+ ether fraction. The compound classed for the base fraction was presented earlier in the literature review section in Table IV. No detailed information is available at present on the neutral nitrogen fraction which is only 1.7% of the feed oil. However, Scheppele and Greenwood (108) concluded that about 50% of the neutral nitrogen fraction consists of carbazoles and the rest consist of methyl carbazoles and other carbazole type compounds. The weight percents in these tables

TABLE XI

COMPOSITIONS AND WEIGHT PERCENTS FOR MOLECULAR
WEIGHT SERIES FOR ACID FRACTION FROM
RAW ANTHRACENE OIL

	Series 1			Series 2			Series 3	
MW	Comp.	wt.%	MW	Comp.	wt.%	MW	Comp.	wt.%
94	C_6H_6O	0.912	134	$C_9H_{10}O$	0.161	144	$C_{10}H_8O$	0.305
108	C_7H_8O	1.455	148	$C_{10}H_{12}O$	0.137	158	$C_{11}H_{10}O$	0.340
122	$C_8H_{10}O$	1.059	162	$C_{11}H_{14}O$	0.067	172	$C_{12}H_{12}O$	0.181
136	$C_9H_{12}O$	0.327	176	$C_{12}H_{16}O$	0.059	186	$C_{13}H_{14}O$	0.100
150	$C_{10}H_{14}O$	0.153	190	$C_{13}H_{18}O$	-	200	-	0.098
164	$C_9H_8O_3$	0.082	204	$C_{14}H_{20}O$	0.024			
	$C_{11}H_{16}O$	0.024	218	$C_{16}H_{10}O$	0.078			
178	$C_{12}H_{18}O$	0.057		$C_{13}H_{14}O_3$	-			
192	$C_{11}H_{12}O_3$	0.036	232	$C_{17}H_{12}O$	0.029			
				$C_{14}H_{16}O_3$	-			
			246	$C_{18}H_{14}O$	0.030			
Total		4.105			0.586			1.024

TABLE XI (Continued)

| Series 4 | | | Series 5 | | | Series 6 | | |
MW	Comp.	wt.%	MW	Comp.	wt.%	MW	Comp.	wt.%
170	$C_{12}H_{10}O$	0.345	182	$C_{13}H_{10}O$	0.526	194	$C_{14}H_{10}O$	0.133
184	$C_{12}H_8O_2$	1.107	196	$C_{14}H_{12}O$	0.309	208	$C_{15}H_{12}O$	0.089
	$C_{13}H_{12}O$	0.481	210	$C_{14}H_{10}O_2$	–	222	$C_{16}H_{14}O$	0.055
198	$C_{13}H_{10}O_2$	1.002		$C_{15}H_{14}O$	0.197	236	–	0.030
	$C_{14}H_{14}O$	0.354	224	$C_{15}H_{12}O_2$	0.029			
212	$C_{13}H_8O_3$	0.045		$C_{16}H_{16}O$	0.088			
	$C_{14}H_{12}O_2$	0.457	238	$C_{17}H_{18}O$	0.063			
	$C_{15}H_{16}O$	0.196	252	$C_{18}H_{20}O$	0.023			
226	$C_{14}H_{10}O_3$	0.055						
	$C_{15}H_{14}O_2$	0.162						
	$C_{16}H_{18}O$	0.076						
	$C_{15}H_{12}O_3$	0.022						
240	$C_{16}H_{16}O_2$	0.059						
	–	0.022						
Total		4.383			1.235			0.307

TABLE XI (Continued)

MW	Series 7 Comp.	wt.%	MW	Series 8 Comp.	wt.%	MW	Series 9 Comp.	wt.%
220	$C_{16}H_{12}O$	0.180	117	C_8H_7N	0.106	167	$C_{12}H_9N$	0.674
234	$C_{16}H_{10}O_2$	0.016	131	C_9H_9N	–	181	$C_{13}H_{11}N$	0.146
	$C_{17}H_{14}O$	0.122	145	C_9H_7NO	0.209	195	$C_{13}H_9NO$	0.056
248	$C_{17}H_{12}O_2$	0.075	159	$C_{10}H_9NO$	0.266		$C_{14}H_{13}N$[a]	0.062
	$C_{18}H_{16}O$		173	$C_{11}H_{11}NO$	–	209	$C_{14}H_{11}NO$	0.063
262	$C_{19}H_{18}O$	0.031						
Total		0.424			0.581			1.001

TABLE XI (Continued)

	Series 10			Series 11			Series 12	
MW	Comp.	wt.%	MW	Comp.	wt.%	MW	Comp.	wt.%
191	$C_{14}H_9N$	0.161	193	$C_{14}H_{11}N$	0.075	217	$C_{16}H_{11}N$	0.250
205	$C_{15}H_{11}N$	0.022	207	$C_{14}H_9NO$	0.034	231	$C_{17}H_{13}N$	0.050
				$C_{15}H_{13}N$				
Total		0.183			0.109			0.300

TABLE XI (Continued)

| MW | Series 13 | |
	Comp.	wt.%
243	$C_{18}H_{13}N$	0.014

TABLE XII

COMPOSITIONS AND WEIGHT PERCENTS FOR MOLECULAR WEIGHT SERIES FOR HYDROCARBON + ETHER FRACTION FROM RAW ANTHRACENE OIL

	Series 1			Series 2			Series 3	
MW	Comp.	wt.%	MW	Comp.	wt.%	MW	Comp.	wt.%
118	C_9H_{10}	0.202	120	C_9H_{12}	0.046	128	$C_{10}H_8$	4.828
132	$C_{10}H_{12}$	0.135	134	C_8H_6S	0.157	142	$C_{11}H_{10}$	2.312
	$C_{16}H_{10}S_2$	0.024		$C_{10}H_{14}$	0.035	156	$C_{12}H_{12}$	1.304
146	$C_{14}H_{14}$	0.081	148	C_9H_8S	0.100	170	$C_{13}H_{14}$	0.638
160	$C_{12}H_{16}$	0.037	162	$C_{13}H_6$	–		$C_{12}H_8S$	0.823
174	$C_{13}H_{18}$	–	176	–	–	184	$C_{14}H_{16}$	0.232
188	–	–	190	$C_{15}H_{10}$	1.393	198	$C_{13}H_{10}S$	0.236
202	$C_{16}H_{10}$	12.130	204	$C_{16}H_{12}$	2.365		$C_{15}H_{18}$	0.032
216	$C_{17}H_{12}$	2.663	218	$C_{16}H_{10}O$	1.302		$C_{14}H_{12}S$	0.078
230	$C_{18}H_{14}$	1.630		$C_{17}H_{14}$	0.905	212	$C_{16}H_{20}$	–
	$C_{18}H_{12}O$	0.109	232	$C_{18}H_{16}$	0.338	226	$C_{18}H_{10}$	0.125
244	$C_{19}H_{16}$	0.266	246	$C_{19}H_{18}$	0.334	240	$C_{19}H_{12}$	0.116
258	$C_{20}H_{18}$	0.160				254	$C_{20}H_{14}$	0.145
Total		17.437			7.727			10.869

TABLE XII (Continued)

MW	Series 4 Comp.	wt.%	MW	Series 5 Comp.	wt.%	MW	Series 6 Comp.	wt.%
154	$C_{12}H_8$	5.262	158	$C_{12}H_{14}$	0.043	168	$C_{12}H_8O$	2.064
166	$C_{13}H_{10}$	2.586	172	$C_{13}H_{16}$	–		$C_{13}H_{12}$	1.831
180	$C_{14}H_{12}$	1.849	186	$C_{14}H_{18}$	–	182	$C_{13}H_{10}O$	1.352
194	$C_{15}H_{14}$	0.737	200	$C_{15}H_{20}$	–		$C_{14}H_{14}O$	1.353
	$C_{11}H_{12}S_2$	0.126	214	$C_{16}H_{22}$	–	196	$C_{14}H_{12}$	0.857
208	$C_{15}H_{12}O$	0.121	228	$C_{18}H_{12}$	1.626		$C_{15}H_{16}O$	0.368
	$C_{16}H_{16}$	0.258	242	$C_{19}H_{14}$	0.383	210	$C_{15}H_{14}$	0.266
222	$C_{16}H_{14}O$	0.142	256	$C_{20}H_{16}$	0.161		$C_{16}H_{18}$	0.266
	$C_{17}H_{18}$	0.095				224	$C_{17}H_{20}$	0.139
236	$C_{17}H_{16}O$	–				238	–	0.044
	$C_{18}H_{20}$	0.051				252	$C_{20}H_{12}$	0.334
Total		11.227			2.213			8.874

TABLE XII   (Continued)

MW	Series 7 Comp.	wt.%
178	$C_{14}H_{10}$	10.406
192	$C_{15}H_{12}$	3.183
206	$C_{16}H_{14}$	1.322
220	$C_{17}H_{16}$	0.405
234	$C_{16}H_{10}S$	0.155
	$C_{18}H_{18}$	0.107
Total		15.578

refer to weight percents of individual compounds in the original raw anthracene oil feedstock and not to weight percent within the individual component fraction.

A brief explanation of Tables IV, XI and XII is presented below. Scheppele and Greenwood will be publishing characterization data on raw anthracene oil in detail. The information is presented in the form of molecular weiight series tables since it is quite common in petroleum chemistry to present characterization data in the form of molecular weight series.

Table XI reveals that series 1 and 4 comprise more than one half of the acid fraction. Series 1 consists of phenols and alkylated homologs of phenol. Series 4 consists of acenaphthenols and acenaphthylendiols. It is also interesting to note that nitrogen compounds such as carbazoles and dihydro azapyrene appear in the acid fraction whereas they are normally expected to appear in the base fraction. Table IV reveals that the second most abundant series in the base fraction is series 4, which consists of quinoline and its homologs. Series 7 of the base fraction represents the most abundant series in the base fraction. The empirical formulas and molecular weights are consistent with the presence of 3-ring nitrogen containing compounds. It can also be seen that the base fraction consists of essentially nitrogen compounds.

Table XII reveals that series 1 of the hydrocarbon+ether fraction accounts for nearly 17% of the total feedstock. The hydrocarbons and ethers account for nearly three fourths of the total feedstock. Series 7 which comprises of phenthrene type compounds is the second most abundant series in the hydrocarbon+ether fraction. Naphthalenes

are present in series 3 and acenaphthene and fluorene are present in series 4.

A complete explanation of every individual series and an interpretation of compounds present in each series is beyond the scope of this thesis. The data was presented in this section only to give an idea of the sort of compounds expected to be present in the feedstock used in this study.

Catalyst Supports and Catalysts

The catalysts used in this study were prepared from commercial alumina supports supplied by catalyst vendors. These supports were then impregnated with active metals in our laboratories, and the impregnation procedure was described earlier (p. 73). Three different supports (CONOCO CATAPAL HP-20, Ketjen 007-1.5E, Ketjen 000-3P) were used in this study. One of the supports (Ketjen 007-1.5E) was steam treated for 10 hours at $1000^{\circ}F$ to change the pore structure of the support. Table XIII presents the chemical composition of the three supports used in this study as supplied by the vendor.

The supports were sent out to an independent analytical laboratory (American Instrument Company) to determine the physical properties such as surface area, pore volume and pore size distribution. Table XLIV (Appendix B) presents this information along with the vendor supplied data, where available. Note that the Ketjen 007-1.5E has the highest surface area. Also note that the CONOCO support and the Ketjen 000-3P have bimodal pore distributions. The CONOCO support has the highest pore volume of the supports used in this study. Results from mercury penetration were used to plot pore frequency curves, which are presented

TABLE **XIII**

CHEMICAL COMPOSITION OF SUPPORT
MATERIALS

	CONOCO CATAPAL HP-20	Ketjen 000-3P	Ketjen 007-1.5E
Alumina	86.2% (α aluminum monohydrate)	(γ alumina)	(γ alumina)
SiO_2	0.008%	0.88%	–
Fe	50 ppm	0.028%	–
Na	40 ppm		–
TiO_2	0.12%		–
Na_2O	–	0.033%	0.03%
SO_4	–	0.6%	0.5%
Carbon	0.35%	–	–

in Figures 13, 14 and 15 for the supports. Most frequent pore radius, as used in this study, is the pore radius corresponding to the peak when $dv/d(\ln r)$ is plotted against pore radius, where V is the cumulative pore volume in cc/gm, and r is the pore radius in $\overset{\circ}{A}$.

The CONOCO CATAPAL HP-20 support material was prepared using a special method developed by the Continental Oil Company (101-104) by contacting an aqueous alumina slurry with an effective amount of an organic solvent. At present, no information is available on the method of preparation of the Ketjen catalysts.
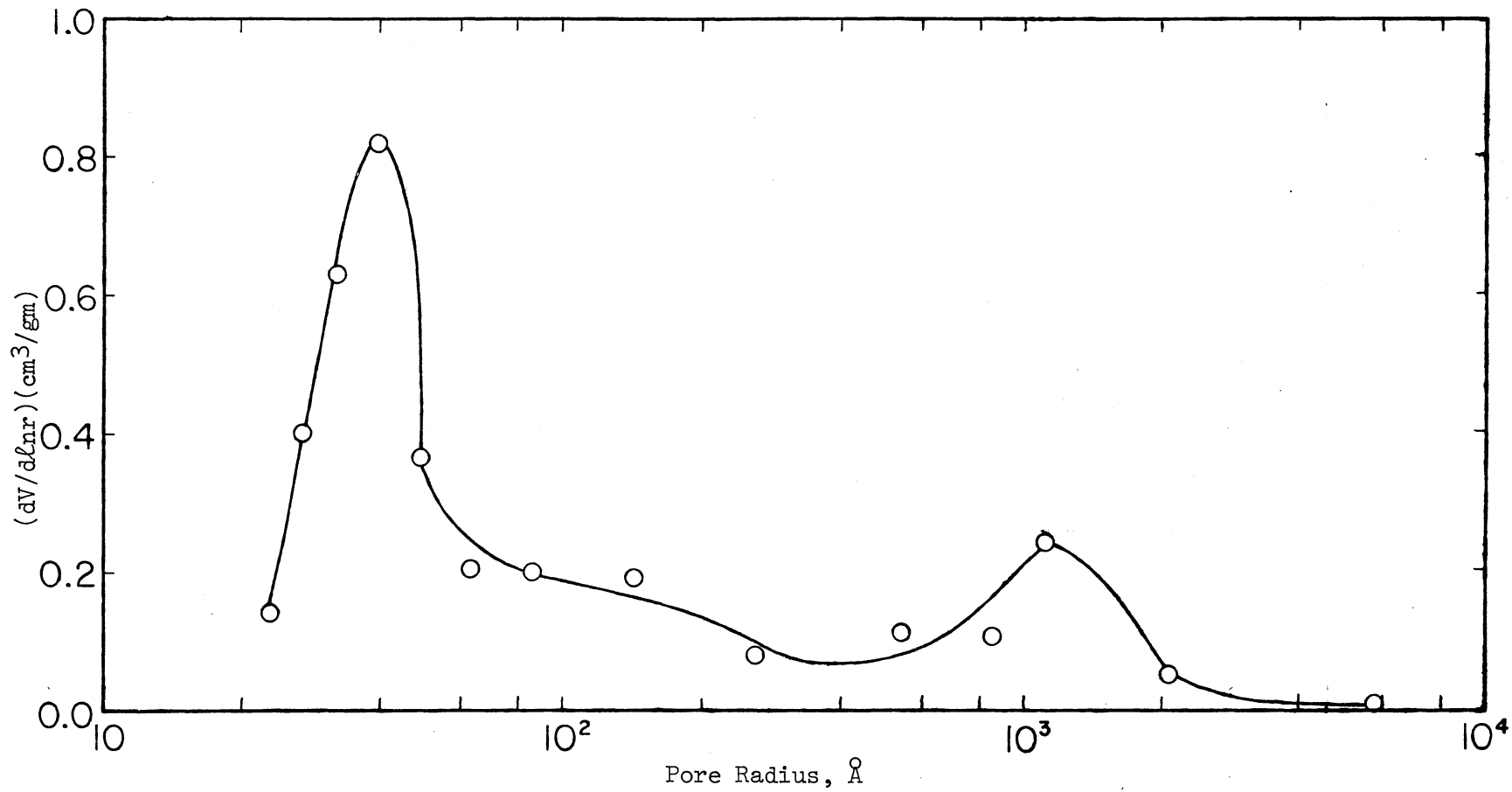
Figure 13.   Pore Size Distribution for CONOCO CATAPAL HP-20 Support Material
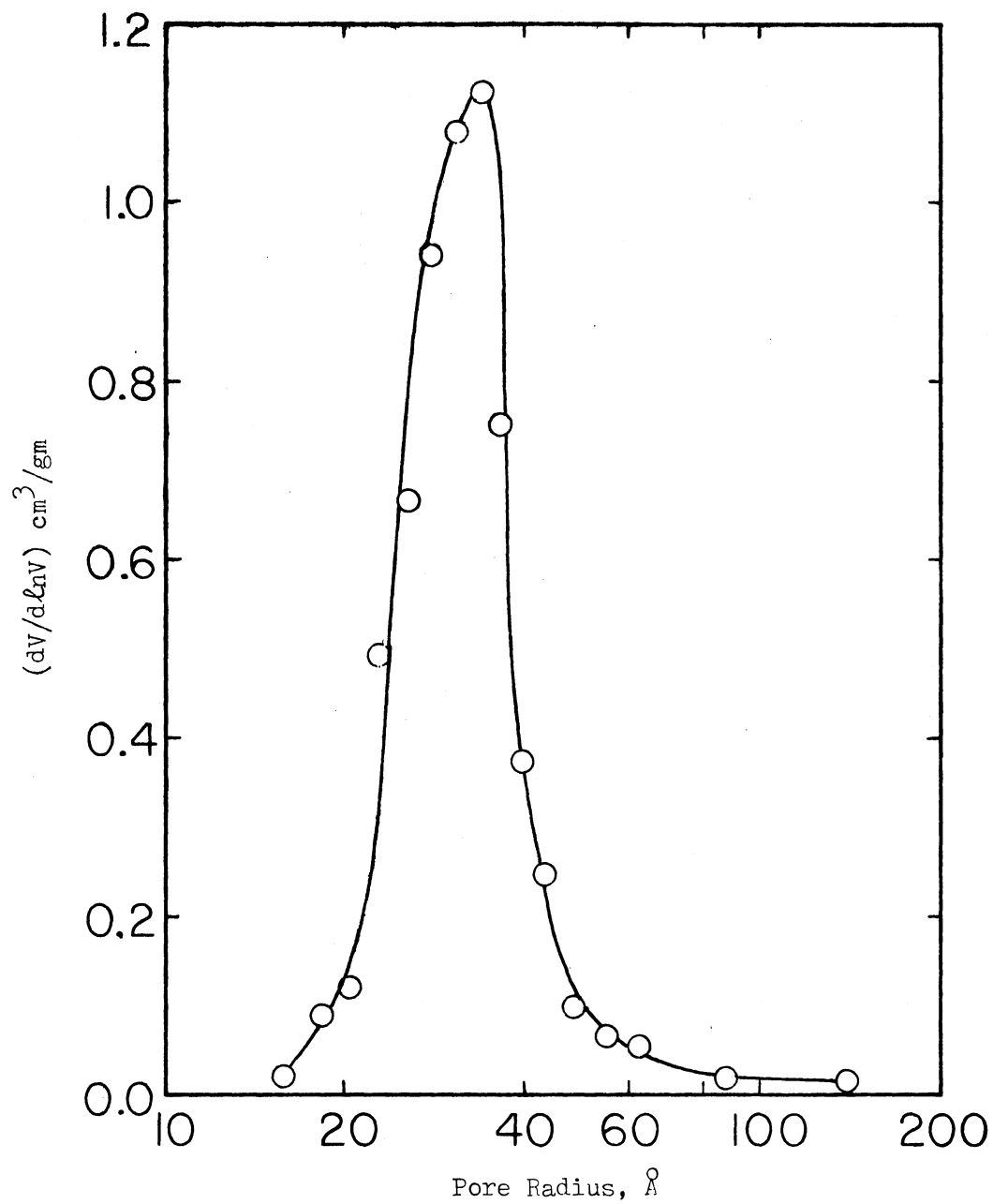
Figure 14. Pore Size Distribution for Ketjen 007-1.5E
Support Material
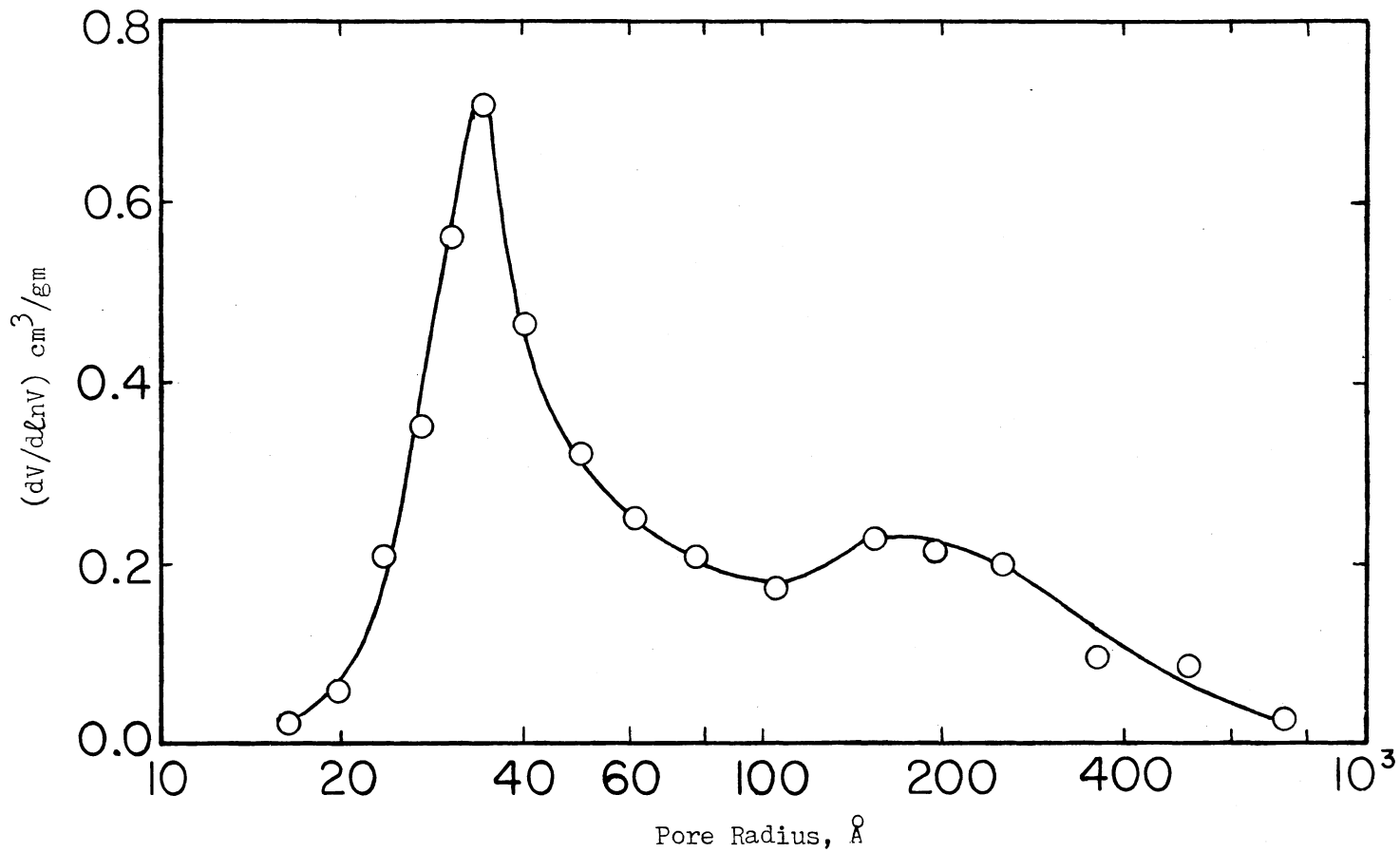
Figure 15. Pore Size Distribution for Ketjen 000-3P Support Material

In addition to the supports, impregnated supports were also sent out for physical property determinations. The properties of the individual catalysts used in each run are presented in Table XVII of the results section and the mercury penetration data for each catalyst used in this study are presented in Appendix B.

CHAPTER VI

RESULTS

The experiments were designed to gather kinetic data on hydrodenitrogenation of raw anthracene oil, a coal derived liquid. Catalyst supports consisting primarily of alumina were impregnated with oxides of cobalt and molybdenum in our laboratories and were used as catalysts. The supports and impregnated catalysts were sent to an independent commercial analytical laboratory for determining pore-size distribution, pore volume and surface area. The catalysts were presulfided in the reactor as part of the catalyst activation procedure. Three different supports (CONOCO CATAPAL HP-20, Ketjen 007-1.5E, Ketjen 000-3P) with varying physical properties were used in this study. Two different feedstocks, raw anthracene oil and raw anthracene oil doctored with quinoline were used. Table XIV presents the operating conditions for each run series as well as the catalyst and feedstock used for each series.

Experimental runs were conducted in a trickle bed reactor packed with fresh catalyst particles. All the runs were made at 1.03×10^7 pascals (1500 psig), varying temperature and space time. A total of eight experimental runs were made for this study. One of them was a reproducibility test using the same catalyst and feedstock under identical conditions. Three of the runs used quinoline doctored raw anthracene oil as feedstock. Product samples were analyzed for their

TABLE XIV

OPERATING CONDITIONS AND CATALYSTS

Run Series	Feedstock Used	Catalyst Support Used	Operating Conditions				
			Pressure psig	Temperature, $^\circ$F	Volume hourly Space time, $\dfrac{\text{cc of catalyst bed}}{\text{cc/hr of feed}}$	Bed Length Inches	Particle Size
CAT	Raw Anthracene Oil	CONOCO CATAPAL HP-20	1500	650, 700	0.465, 0.93, 1.86	19.875	-8 + 10 mesh
KEC	Raw Anthracene Oil	Ketjen 007-1.5E	1500	650, 700, 750	0.46, 0.92, 1.84	19.625	1/1/6" extrudate
KET	Raw Anthracene Oil	Steam treated (10 hrs) Ketjen 007-1.5E	1500	650, 700, 750	0.46, 0.92, 1.84	19.625	1/16" extrudate
KEP	Raw Anthracene Oil	Ketjen 000-3P	1500	650, 700, 750	0.46, 0.92, 1.84	19.625	-8 + 10 mesh
KER	Raw Anthracene Oil	Ketjen 007-1.5E	1500	650, 700, 750	0.46, 0.92, 1.84	19.625	1/16" extrudate
KDC	Doctored Raw Anthracene Oil	Ketjen 007-1.5E	1500	700	0.46, 0.92, 1.84	19.625	1/16" extrudate
KDT	Doctored Raw Anthracene Oil	Steam Treated (10 hrs) Ketjen 007-1.5E	1500	700	0.46, 0.92, 1.84	19.625	1/16" extrudate
KDP	Doctored Raw Anthracene Oil	Ketjen 000-3P	1500	700	0.46, 0.92, 1.84	19.625	-8 + 10 mesh

nitrogen content. In addition, selected samples were separated into different boiling fractions and these were analyzed for their nitrogen content.

The primary objective of this chapter is to present the results obtained from the experiments. A detailed discussion of the results will follow in the next chapter.

Effect of Impregnation on Support Properties

In order to estimate the effects of impregnation on support properties such as surface area, pore volume and most frequent pore radius, samples were sent out to an independent analytical laboratory (American Instrument Company) before and after impregnation. Impregnation of the supports were performed individually for each run series. In order to estimate the reproducibility of the laboratory, duplicate samples were sent to the laboratory under different names on different occasions. Table XV presents the results reported by the laboratory for two sets of duplicate samples.

TABLE XV

ANALYTICAL REPRODUCIBILITY OF
SUPPORT PROPERTIES

Support	Surface Area m^2/gm	Pore Volume cc/gm	Most Frequent Pore Radius, Å
Ketjen	306	0.671	34
007-1.5E	316	0.622	34
Steam treated			
Ketjen	230	0.551	38
007-1.5E	229	0.530	38

Table XVI presents the results from two sets of duplicate samples sent to another independent commercial laboratory (Micrometrics Corporation) as part of a special student project to assess the effects of activation procedure on Co-Mo/Alumina catalysts (105).

TABLE XVI

REPRODUCIBILITY OF SURFACE AREA
DETERMINATION

Support Material	Surface Area, m^2/gm
Ketjen 007-1.5E	303 303
Ketjen 000-3P	244 247

Tables XV and XVI reveal that the laboratories did not have any problems reproducing the most frequent pore radius. However, the surface area determinations varied by about three percent. This information should be considered while assessing the changes in surface area due to impregnation.

Table XVII presents the support properties before and after impregnation for each run series. Impregnation does not seem to change the most frequent micro-pore size whereas there is an increase in the most frequent macro-pore size. The surface area and the pore volume decrease after impregnation. The percent changes in surface area varied

TABLE XVII

EFFECT OF IMPREGNATION ON
ALUMINA SUPPORTS

Run Series	Support Used	Support Properties							
		Before Impregnation			After Impregnation				
		Surface Area m^2/gm	Pore Volume cc/gm	Most Frequent Pore Radius, $\overset{o}{A}$	Surface Area m^2/gm	%Change in Surface Area	Pore Volume cc/gm	%Change in Pore Volume	Most Frequent Pore Radius, $\overset{o}{A}$
CAT	CONOCO CATAPAL HP-20	244	1.01	40, 1100	218	11	0.875	13	40, 1900
KEC	Ketjen 007-1.5E	311	0.647	33	291	7	0.503	22	31
KET	Steam Treated (10 hrs) Ketjen 007-1.5E	271	0.686	38	230	15	0.540	21	38
KEP	Ketjen 000-3P	254	0.834	34, 150	199	21	0.625	25	36, 160
KER	Ketjen 007-1.5E	311	0.647	33	243	22	0.452	30	33
KDC	Ketjen 007-1.5E	311	0.647	33	252	19	0.467	28	31
KDT	Steam Treated (10 hrs) Ketjen 007-1.5E	271	0.686	38	221	18	0.499	27	39
KDP	Ketjen 000-3P	254	0.834	34, 150	220	14	0.448	46	33, 180

from 7 to 22 percent and the percent changes in pore volume varied
from 13 to 46 percent. The CONOCO CATAPAL HP-20 showed a tremendous
increase in the size of the macro-pores (1100 to 1900 Å) where as the
change in the macro-pore size of the KEP catalyst was only about 20
percent (150 to 180 Å). Yen, et al. (106) found that the surface area
decreased and the average pore radius increased as a result of impregna-
tion in their studies of catalytic hydrodesulfurization of coal using
Co-Mo-Alumina catalysts. Mamidi (105) studied the effect of impregna-
tion and the activation procedure (calcination and sulfiding) on the
physical properties of two of the supports used in this study. He
impregnated Ketjen 007-1.5E and Ketjen 000-3P supports with oxides of
cobalt and molybdenum. Impregnation was done following the same
procedure used in this study. This was considered as the first step.
Then these impregnated supports were packed in a 316 stainless steel
tube of $\frac{1}{2}$ inch I.D. (similar to the reactor used in this study) and
were calcined. Calcination was done at $232^{\circ}C$ ($450^{\circ}F$) for twelve hours
with prepurified nitrogen flowing through the catalyst bed. Mamidi
essentially tried to reproduce the exact procedure used for activating
the catalysts used in this study. Calcination was considered as the
second step. The calcined support was then sulfided with a 5% mixture
of hydrogen sulfide in hydrogen. Sulfiding was considered as the third
and final step. Samples were taken at the end of each of these steps
and were sent out to two independent commercial analytical laboratories
(American Instrument Company, Micrometrics Instrument Corporation) for
physical property determinations. Mamidi concluded that the surface
area and pore volume decreased as a result of calcination whereas the
activation procedure had negligible effect on pore size distribution.

Analytical Precision

The analysis of nitrogen in product oil was performed by two different methods for this study. Except for the CAT series, all the other samples were analyzed on a Perkin-Elmer Model 240 elemental analyzer. The CAT series samples were analyzed by a modified Kjeldahl technique developed by Satchell (6). The accuracy and precision of the Kjeldahl method can be found in Satchell's thesis (6). The precision of the analytical results obtained from the Perkin-Elmer Model 240 elemental analyzer is presented here.

Great care was taken while performing these analyses to maintain a very high precision. Raw anthracene oil was analyzed every day to check the consistency of the equipment. Also, the K_N values were determined every day to check whether variations in the K_N values remain within the manufacturer's specifications. 9-10 mg. samples were used in this study as recommended by Culmo (99) and Smith, et al. (100) to determine the weight percent nitrogen accurately at low levels (0.1 weight percent).

Unbiased estimate of the standard deviations were calculated at various levels of nitrogen, and are presented in Table XVIII. Table also includes results from the analysis of Baja crude performed by Smith, et al. (100) using a Perkin-Elmer Model 240 elemental analyzer.

As can be seen from the Table XVIII, the ability to determine the amount of nitrogen present in the samples deteriorate, when the weight percent nitrogen decreases below 0.05 weight percent. Smith, et al. also established the same conclusion in an independent study (100). However, in order to obtain a 0.05 weight percent sample, the catalyst

TABLE XVIII

PRECISION OF THE ANALYTICAL TECHNIQUE

% Nitrogen	Standard Deviation	Percent Deviation
1.055	0.025	± 2.39
0.681	0.007	± 1.03
0.571	0.014	± 2.45
0.482	0.021	± 4.29
0.328*	0.018	± 5.5
0.095	0.007	± 7.5
0.026	0.019	± 73.0

* from the study by Smith, et al. (100)

has to be extremely active since that corresponds to a 95% nitrogen removal. Only one sample in this study had such a low nitrogen content. Hence, the analytical technique is not a limiting factor within the scope of this study.

Overall Reproducibility

An experimental run consists of the following five steps.

1. Catalyst preparation from support materials.

2. Catalyst activation.

3. Startup of the reactor.

4. Normal operation of the reactor.

5. Sample analysis.

Hence, overall reproducibility consists of successfully reproducing all the steps mentioned above.

All of the experimental runs were conducted at a pressure of 1500 psig. The operating conditions were predetermined in such a way that the same space time existed at the beginning and end of a series of isothermal runs. Also before shutting down the reactor, the reactor was always brought to the same operating conditions that existed at the beginning of the run. One of the reasons for following this procedure was to check the reproducibility within the individual run and another was to find out whether any deactivation of the catalyst had taken place. The total hours of oil-on catalyst in this study never exceeded 130 hours. Mehta (8) made several runs on Co-Mo-Alumina catalysts using the same feedstock and observed no deactivation in sulfur removal up to 200 hours of oil contacting catalysts. Satchell (6) and Wan (5) found no appreciable deactivation in nitrogen removal for several Co-Mo-Alumina catalysts for the same feedstock used in this study up to 200 hours of operation. Table XIX presents results from the present study.

Table XIX reveals that there was no deactivation of the catalyst in all these runs. Other experimental runs conducted for this study are shorter than those shown and hence one can reasonably conclude that there was no deactivation in any of the runs in this study. Since catalyst deactivation was not evident the results from Table XIX can be used to check reproducibility of the experimental equipment within an individual run. Table XIX indicates that the maximum deviation in weight percent nitrogen in the product oil under identical conditions for the same catalyst is within ± 0.03 weight percent nitrogen.

Satchell (6) tested for overall reproducibility by conducting two identical runs using the same catalysts at the same operating

TABLE XIX

COMPARISON OF RESULTS FOR DEACTIVATION
AND REPRODUCIBILITY

Run Series	Hours On Oil	Operating Conditions P = 1500 psig		Weight Percent N_2 in Product Oil
		Temperature °F	Space Time hrs	
KET	48	650	1.84	0.502
	64	650	1.84	0.485
	121	650	1.84	0.490
	70	700	1.84	0.324
	87.5	700	1.84	0.326
	95.5	750	1.84	0.202
	112.5	750	1.84	0.207
KEP	44	650	1.84	0.598
	62.5	650	1.84	0.569
	128.5	650	1.84	0.588
	75.75	700	1.84	0.402
	92.25	700	1.84	0.428
	102.75	750	1.84	0.207
	120.5	750	1.84	0.222
KEC	48	650	1.84	0.437
	63	650	1.84	0.455
	124	650	1.84	0.418
	73	700	1.84	0.247
	88	700	1.84	0.220
	98	750	1.84	0.147
	111	750	1.84	0.176

conditions. He used vendor supplied Co-Mo-Alumina catalysts in his studies, and concluded that the weight percent in product oil varied in a ± 0.03 weight percent nitrogen range for both catalyst loadings. However, in the present study, the supports were impregnated with oxides of cobalt and molybdenum and the impregnated supports were used as catalysts. Hence, in order to assess overall reproducibility, from catalyst preparation through reactor operation and through product sample analyses, an experimental run series was repeated. Figure 16 presents the results from both series. The open points in the figure are for results from the KER series; whereas, the solid points are taken from the KEC series. A comparison of catalyst property duplication for these two data sets is presented in Table XX.

TABLE XX

COMPARISON OF SUPPORT PROPERTIES FOR
KEC AND KER SERIES

	KER Series	KEC Series
Surface Area, m^2/gm	243	291
Pore Volume, cc/gm	0.452	0.503
Most Frequent Pore Radius, $\overset{\circ}{A}$	33	31

Figure 16 shows nitrogen in product oil as a function of space time at different temperatures. This figure and figures 17 through 24 were

obtained by drawing a smooth curve across the data points and serve the sole purpose of comparing the performance of different catalysts. Figure 16 reveals that the catalyst used in the KER series is somewhat less active than the catalyst used in the KEC series. However, Table XX shows that the surface area of the KER catalyst was lower than that of the KEC catalyst. The lower activity of the KER catalyst can be attributed to the lower surface area and it will be shown later that the nitrogen removal is more sensitive to changes in surface area than to changes in pore radius.

This brings up the question of the ability of catalyst property duplication, since the catalysts were prepared in our own laboratories. The catalysts were prepared independently for each series, and Table XXI presents a comparison of catalyst property duplication for the supports used in this study.

TABLE XXI

CATALYST PROPERTY DUPLICATION

Support	Run Series	Surface Area m^2/gm	Pore Volume cc/gm	Most Frequent Pore Radius, $\overset{\circ}{A}$
Ketjen 007-1.5E	KEC	291	0.503	31
	KER	243	0.452	33
	KDC	252	0.467	31
Steam Treated Ketjen 007-1.5E	KET	230	0.540	38
	KDT	221	0.499	38
Ketjen 000-3P	KEP	200	0.625	36,160
	KDP	219	0.448	33,180
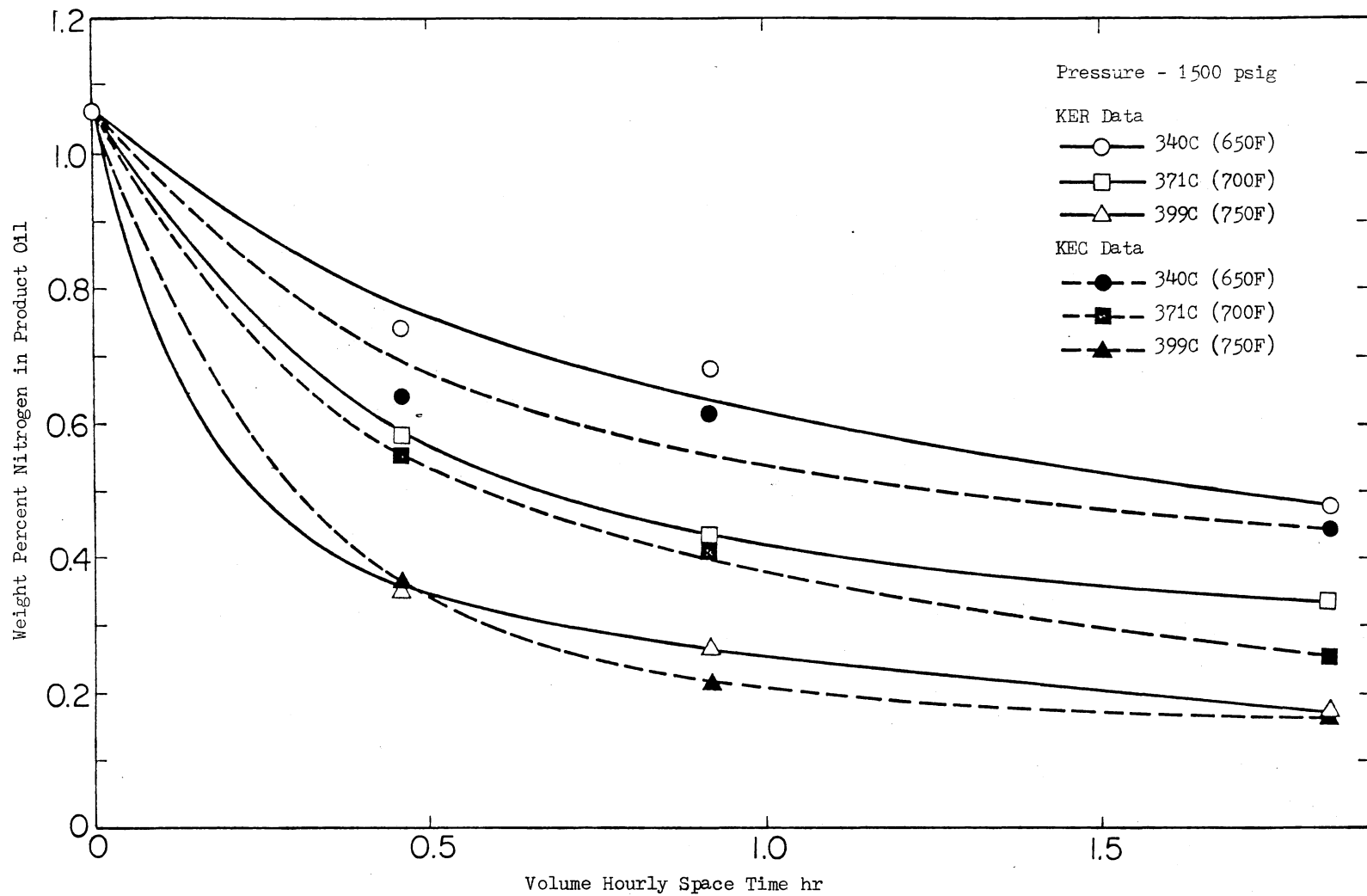
Figure 16.   Comparison of KEC and KER Series

Table XXI reveals that except for KEC and KER, the surface area changes for the others were within the precision of measurement of the analytical laboratories ($\pm$ 10 m^2/gm). At this point, no possible explanation can be offered for the poor reproducibility of surface areas in the KEC and KER series. However, taking into account that the reproducibility within an individual run was within 0.03 weight percent nitrogen and the fact that Satchell (6) was able to obtain a reproducibility within 0.03 weight percent when two identical runs were made using the same equipment and the feedstock used in this study, the lower activity of the KER series can be attributed to poor reproducibility of the physical properties of catalyst supports or in impregnation procedure. Further studies should be made by impregnating several samples of the same supports to establish a precision value.

Effect of Steam Treating on
Support Properties

Catalyst support properties such as surface area and pore size distribution play a major role in determining the performance of hydrotreating catalysts. However, the problem normally encountered in trying to compare two catalysts with varying support properties is that the supports have different chemical compositions. Ideally, in order to determine the influence of support properties, one should have sets of catalysts exactly similar in every respect except for the support properties. This was not possible in the past studies (5-9) since different catalysts with varying support compositions were obtained from vendors. Schlaffer, et al. (10, 73) studied the physical changes that occur with alumina supports upon exposure to steam at moderate to high

temperatures, and they found that there is considerable decline in sur-
face area accompanied by little or no loss of pore volume. Hence one
of the supports used in this study (Ketjen 007-1.5E) was steam treated
at about 538°C (1000°F) in order to change the pore structure, hopefully
to obtain a "matched" pair of catalysts with the only differences being
in the support properties. The steam treating procedure was described
earlier. Two different sets of experiments were conducted. The
supports were steam treated for periods of one hour and ten hours. The
steam treated supports were then submitted to a commercial laboratory
(American Instrument Company) for analysis. Table XXII presents the
results.

TABLE XXII

EFFECT OF STEAM TREATING ON
SUPPORT PROPERTIES

	Ketjen 007-1.5E	Steam Treated Ketjen 007-1.5E	
		One Hour	Ten Hours
Surface Area, m^2/gm	311	281	271
Pore Volume, cc/gm	0.647	0.674	0.686
Most Frequent Pore Radius, Å	33	37	38

Table XXII reveals that some modest changes resulted in surface

area and pore radius. As already established, these changes are outside the ranges of precision of the instrumentation used for support property analyses ($\pm$ 10 m^2/gm for surface area determination and $\pm$ 1 Å for most frequent pore radius). Since the changes were more profound in the ten hours sample than the one hour sample, the ten hours steam treated sample and the base support were used to prepare matched pair of catalysts. The hydrodenitrogenation results using the base and the ten hours steam treated support are presented in the next section.

<div align="center">

Comparison of Steam Treated

and Base Supports

</div>

Catalysts were prepared from the Ketjen 007-1.5E support and the ten hour steam treated Ketjen 007-1.5E. Two different runs were made using the two catalysts under identical operating conditions. Ketjen 007-1.5E was used in the KEC series and the steam treated support was used in the KET series. The properties of the supports themselves were presented in the previous section. However, impregnation changes these properties moderately. The properties of the two catalysts are presented in Table XXIII.

Figures 17, 18 and 19 compare the results from both series for the three temperatures for which the data were taken. The catalyst used in the KET series has a lower surface area and a higher pore radius than the catalyst used in the KEC series. Satchell (6) found that increasing the most frequent pore radius from 25Å to 33Å had no effect on nitrogen removal. However, figures 17, 18 and 19 show that the catalyst used in the KET series was less active than the catalyst used in the KEC series at all three temperatures. These two catalysts,
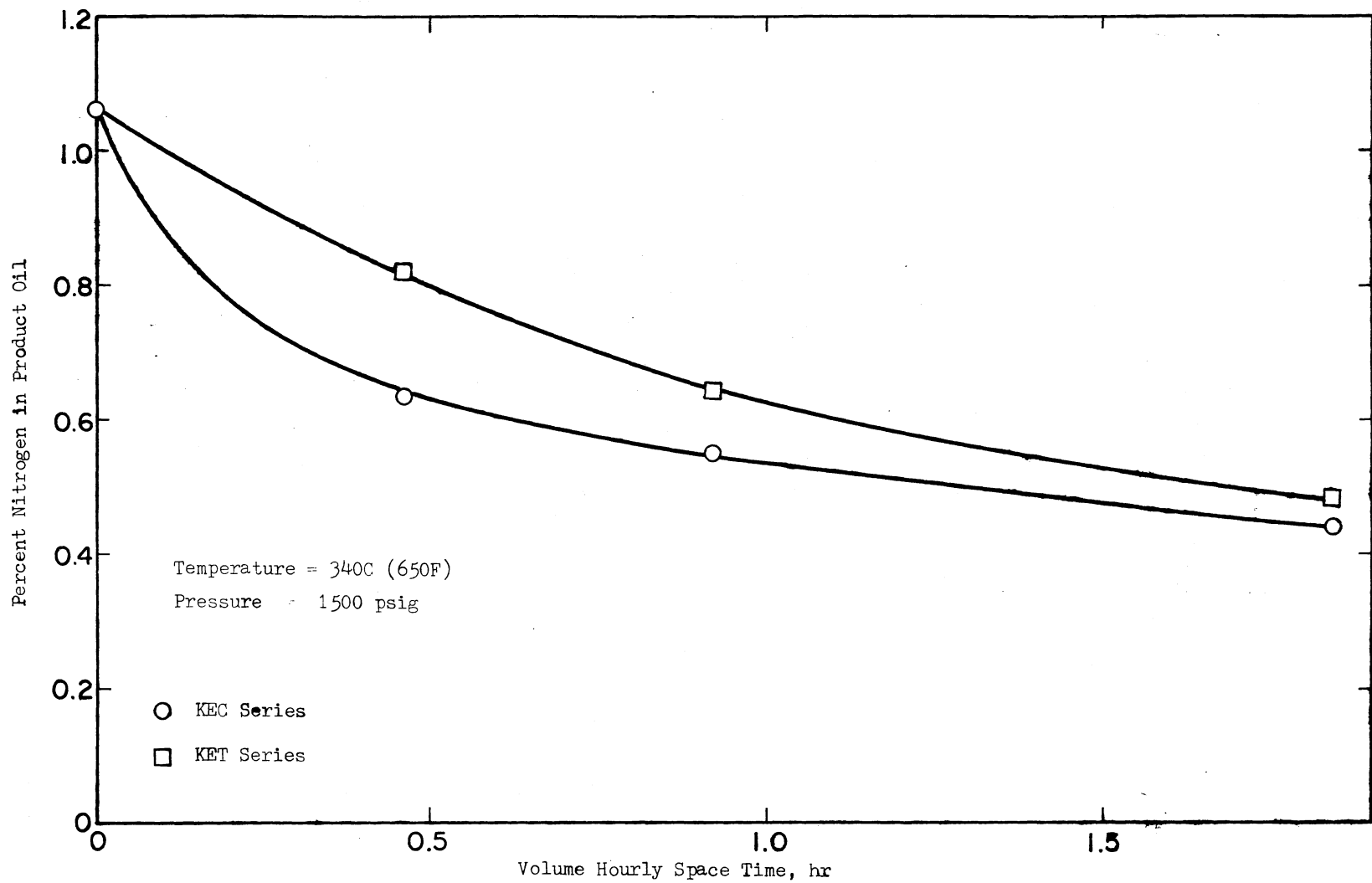
Figure 17. Effect of Steam Treating at Reactor Temperature of 650F
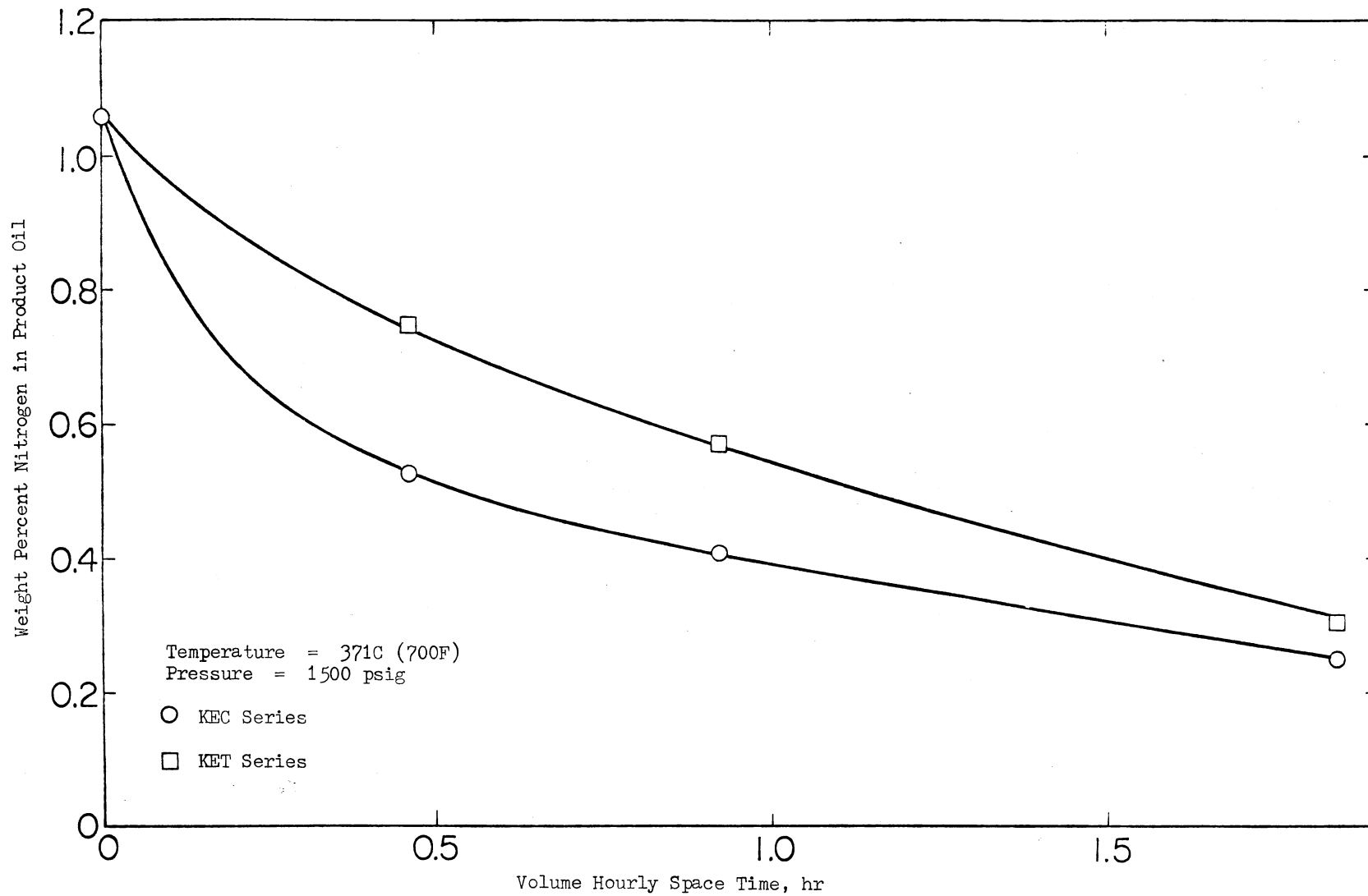
Figure 18. Effect of Steam Treating at Reactor Temperature of 700F
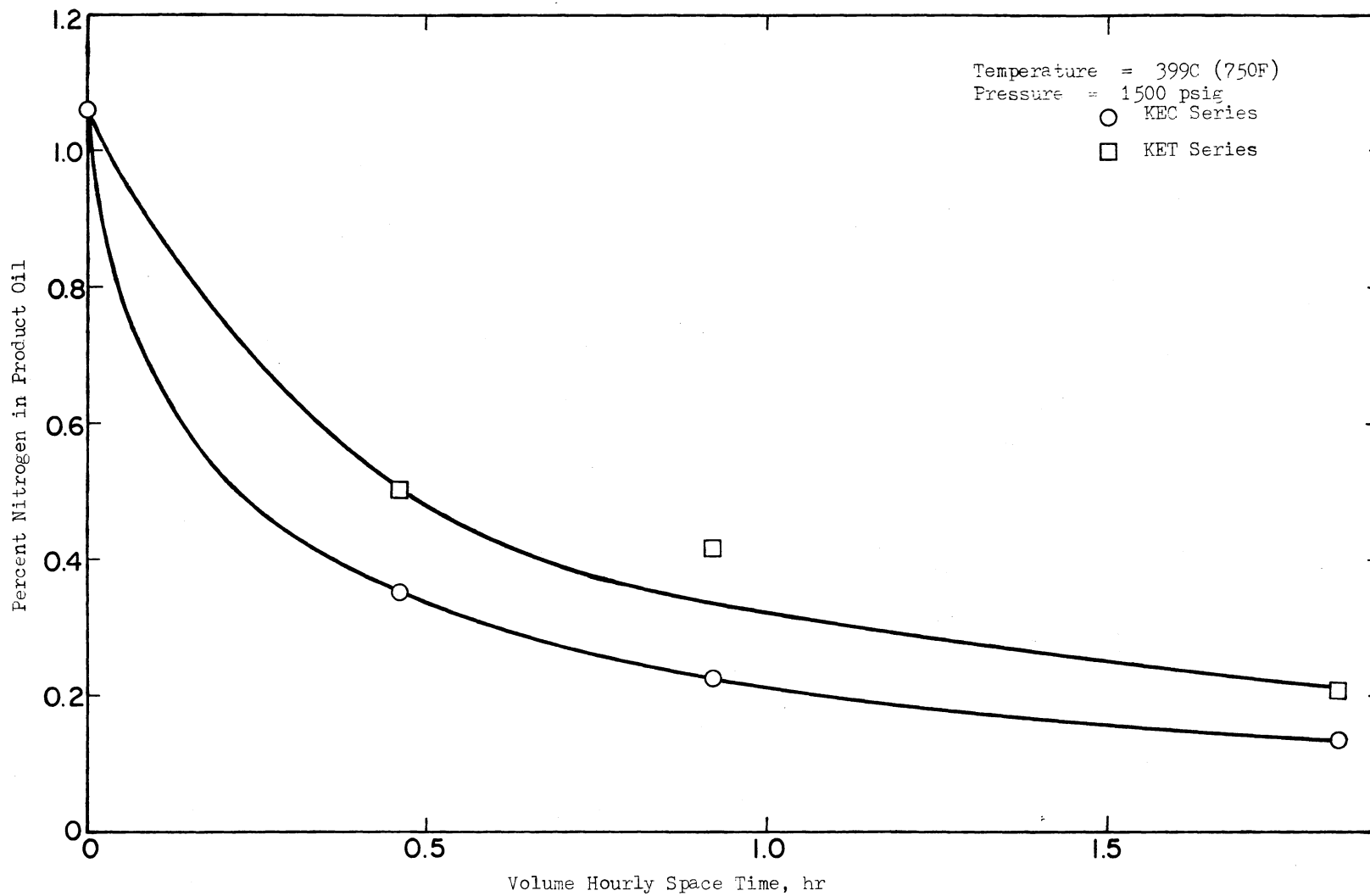
Figure 19. Effect of Steam Treating at Reactor Temperature of 750F

TABLE XXIII

PROPERTIES OF CATALYSTS USED IN
KEC AND KET SERIES

Property	KEC Series	KET Series
CoO, wt. %	3.5	3.5
MoO_3, wt. %	12.5	12.5
Support	Ketjen 007-1.5E	Ten hour steam treated Ketjen 007-1.5E
Surface Area, m^2/gm	291	230
Pore Volume, cc/gm	0.647	0.540
Most Frequent Pore Radius, $\overset{\circ}{A}$	33	38

as already pointed out were essentially a matched pair except for the differences in their support properties. Hence, the lower activity of the KET catalyst can be attributed to the lower surface area available for reaction. This will be discussed in the next chapter.

Comparison of Different Catalysts

In addition to the Ketjen 007-1.5E and the 10 hour steam treated support, another Ketjen support, 000-3P, was used in this study in order to compare the activities of different catalysts. Also, one of the long range objectives of the program at Oklahoma State University, of which this study is a part, is to tailor catalysts specifically for coal derived liquids. In order to meet this objective, the activities of different catalysts with respect to their hydrotreating capabilities should be compared. Hence, Ketjen 000-3P support was impregnated and

used as a catalyst in the KEP series. The properties of this catalyst and its support can be found in Table XVII. This support was different from the 007-1.5E support in the sense that this support had a bimodal pore distribution. The pore distribution curves were presented in Chapter V. A comparison can be made between mono- and bidispersed supports. Figures 20, 21 and 22 present a comparison between KEC (007-1.5E), KET (steam treated 007-1.5E) and KEP (000-3P) series for results obtained at 343, 371 and 399C (650, 700 and 750F) under a pressure of 1.03×10^7 pascals (1500 psig). The figures present the weight percent of nitrogen in product oil as a function of space time.

These three figures show that the catalyst used in the KEC (007-1.5E) series was more active than the other two catalysts. In other words, the bidispersed catalyst used in the KEP series has no obvious advantage over the monodispersed catalyst. However, the KEP catalyst (bidispersed support), was more active than the KET catalyst (steam treated support). Detailed discussions will be presented in the next chapter.

<div align="center">

Comparison of Two Catalysts with

Bimodal Dispersion

</div>

At the time the decision was made to use alumina supports and impregnate them with active metals in our laboratories instead of using catalysts supplied by vendors, an initial run was made using a catalyst support supplied by CONOCO (CATAPAL HP-20), to establish our capabilities for impregnating the supports and using them as catalysts. This support had a larger pore radius (40 vs. 33 $\overset{o}{A}$) than those we had tested previously and also had a significantly larger pore volume
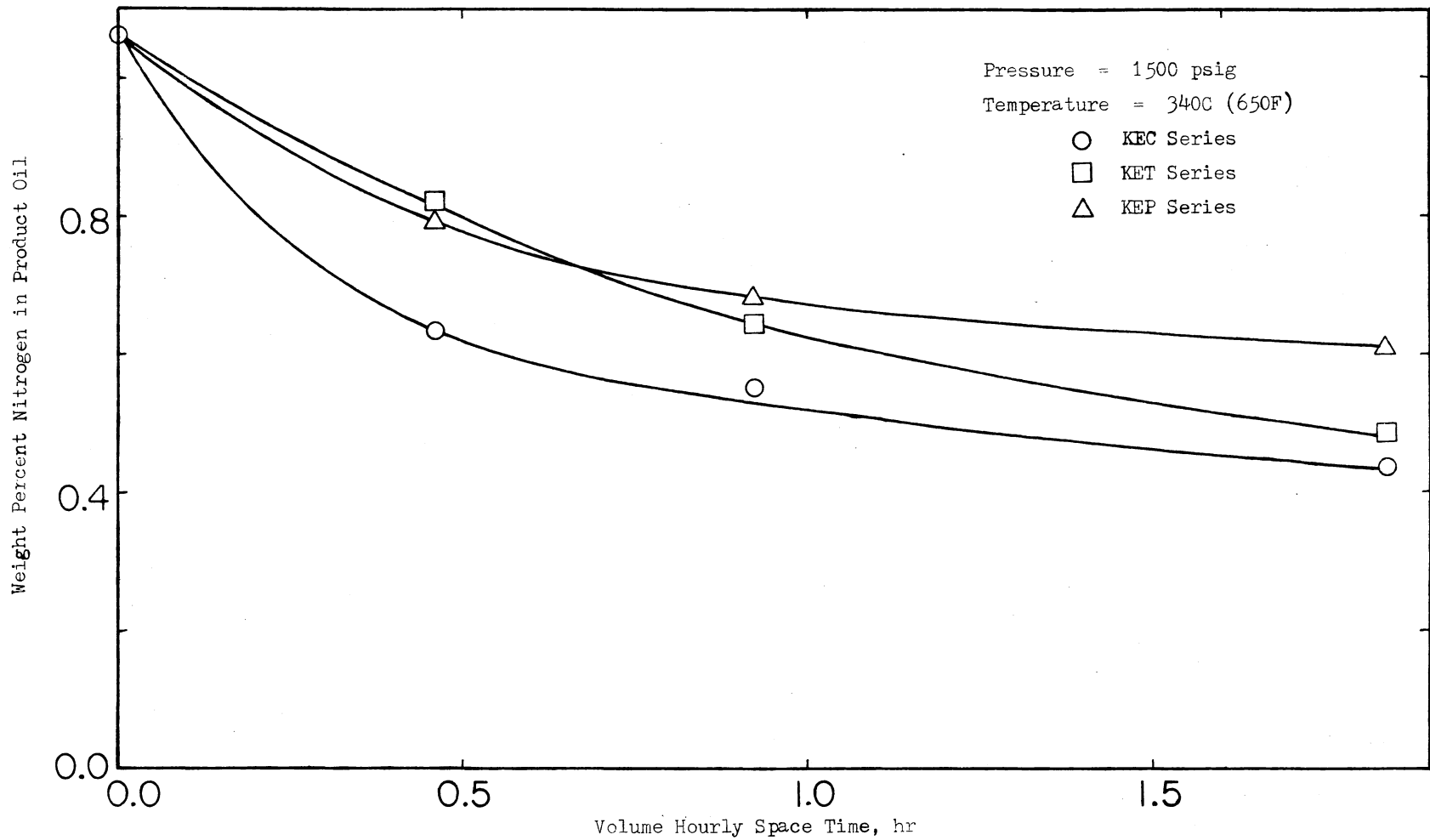
Figure 20. Comparison of Three Catalysts at 650F

The chart shows "Weight Percent Nitrogen in Product Oil" on the vertical axis (0.0, 0.4, 0.8) versus "Volume Hourly Space Time, hr" on the horizontal axis (0.0, 0.5, 1.0, 1.5).

Pressure = 1500 psig
Temperature = 340C (650F)
○ KEC Series
□ KET Series
△ KEP Series
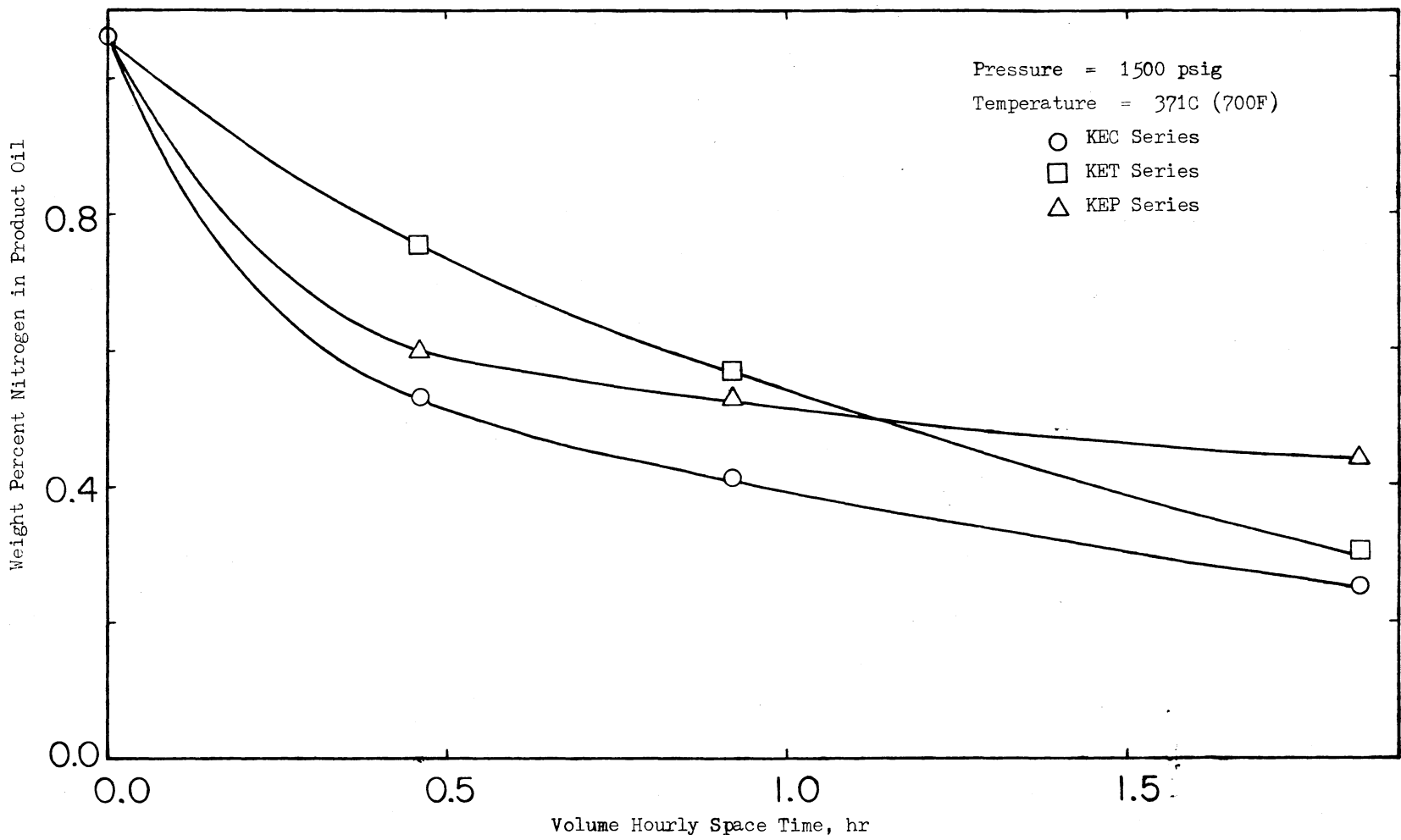
Figure 21. Comparison of Three Catalysts at 700F
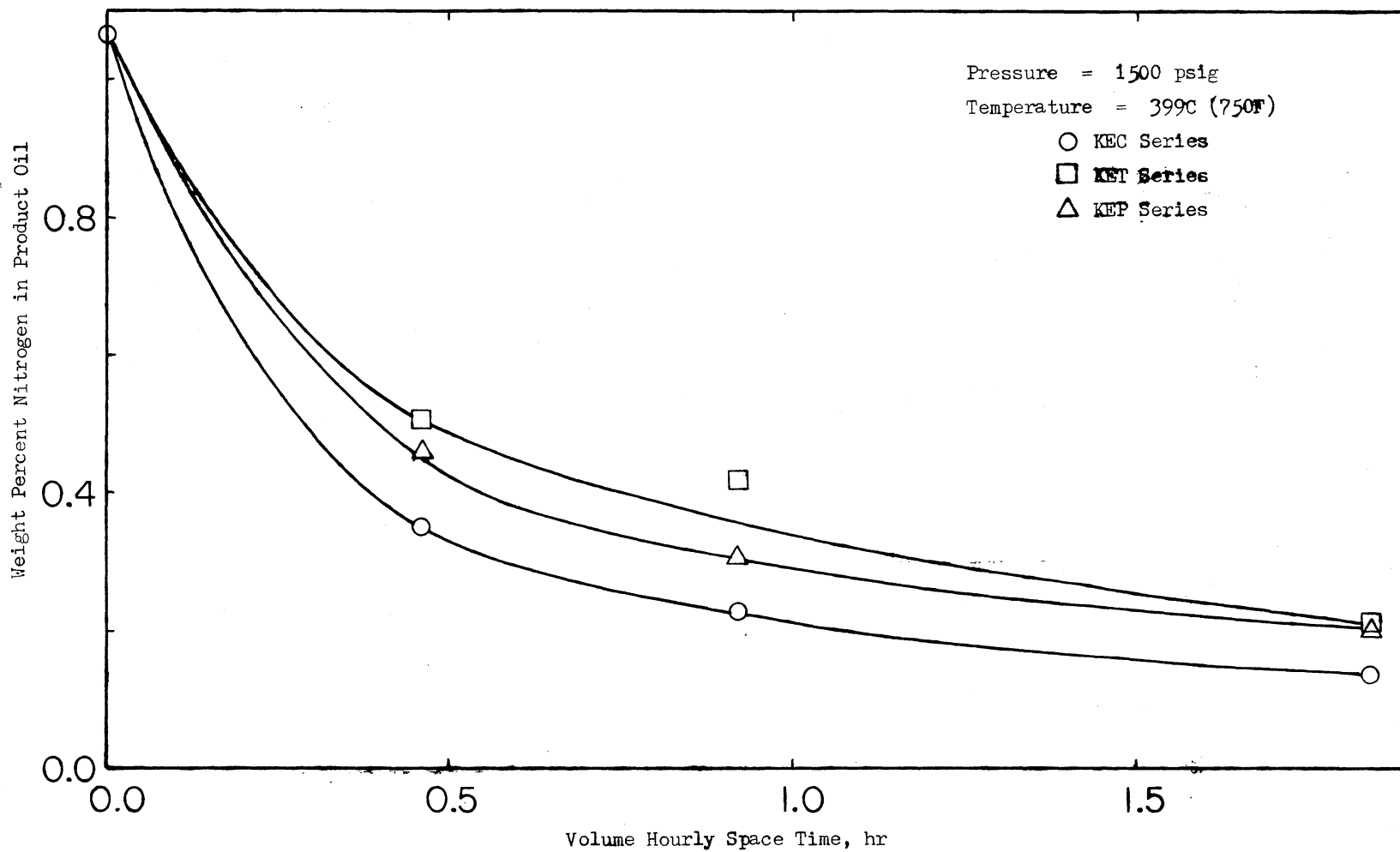
Figure 22.   Comparison of Three Catalysts at 750F

(1.01 vs. 0.647 cc/gm). CATAPAL HP-20 had a bimodal pore distribution. Hence, a comparison of CAT Series against the KEP series, which also used a catalyst with a bimodal pore distribution, would be interesting. The properties of the catalysts used are presented in Table XXIV. CATAPAL HP-20 was used in the CAT series. Note that the CAT catalyst has a significantly larger size macropores (1900 vs. 180 $\overset{\circ}{A}$) compared to the KEP catalyst as presented in Table XXIV.

TABLE XXIV

COMPARISON OF CATALYST PROPERTIES
FOR THE CAT AND KEP SERIES

Property	CAT Series (CATAPAL HP-20)	KEP Series (Ketjen 000-3P)
Surface Area, m^2/gm	218	200
Pore Volume, cc/gm	0.875	0.625
Most Frequent Pore Radius, $\overset{\circ}{A}$	40,1900	33,180

Figure 23 presents results from the two series. An examination of the figure indicates that at 343 C (650F), the CAT catalyst did not have any advantage over the KEP catalyst in spite of its larger pore size and pore volume. However, at 372 C (700F), the CAT catalyst was still less active than the catalyst used in the KEC series, (60% nitrogen removal vs. 76% nitrogen removal at a space time of 1.84 hrs),
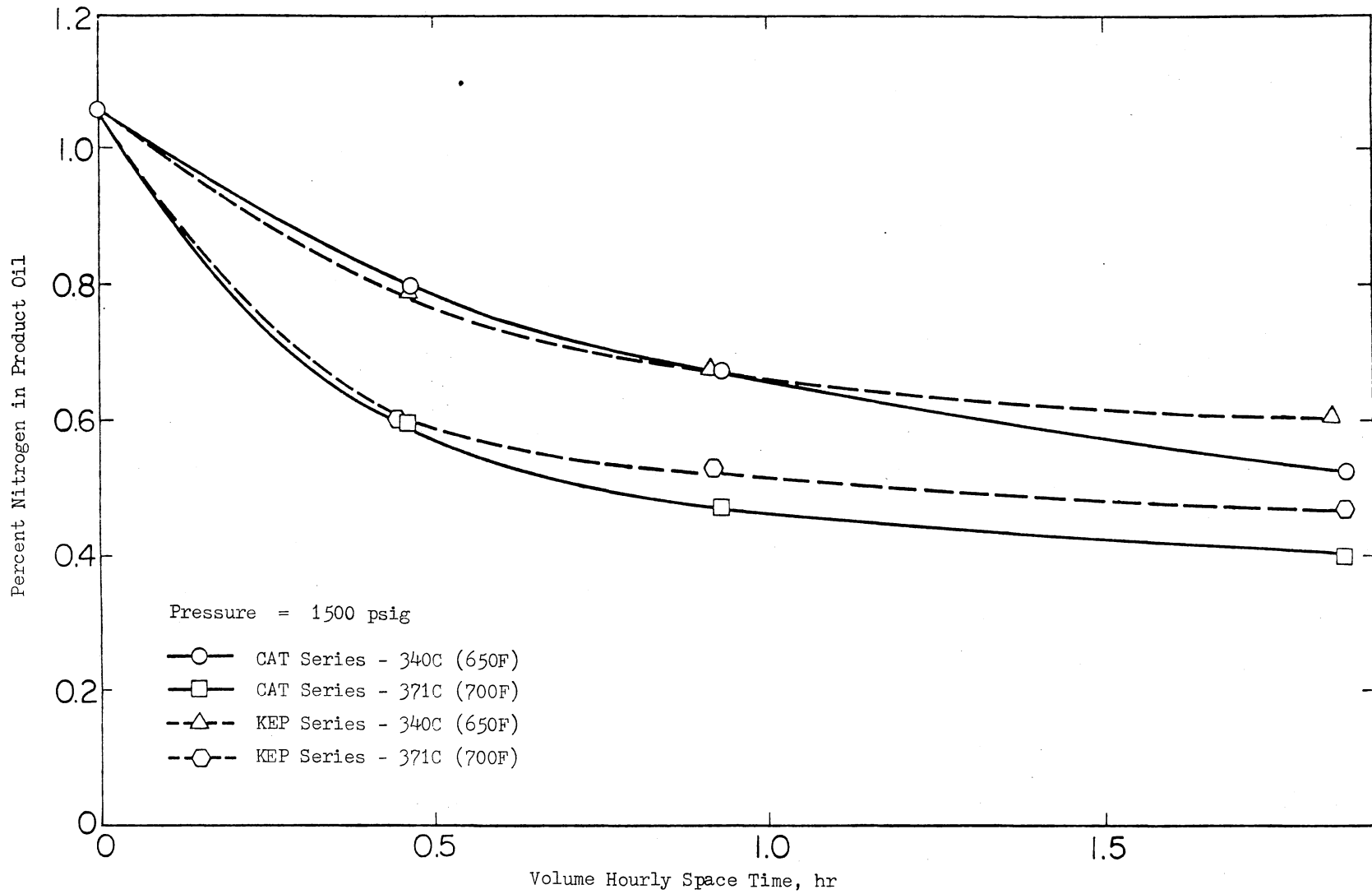
Figure 23. Comparison of Two Bidispersed Catalyst Supports

which was monodispersed but had a higher surface area. The surface area of the catalyst used in the CAT series was higher than the surface area of the catalyst used in the KEP series, (218 vs. 200 m^2/gm), which could account for the higher activity of the CAT series. Detailed discussions will be presented in the next chapter.

Feedstock Doctored with Quinoline

One of the major objectives of this study is to provide useful information towards tailoring hydrotreating catalysts specifically for coal derived liquids. In previous studies (5-9), the feedstock was hydrotreated over several catalysts and the activity of the catalysts were compared to a reference catalyst (Nalcomo 474). The characterization of feedstock and reactor products could provide useful information on tailoring in the long run. Characterization studies are currently underway in the Chemistry Department at Oklahoma State University. However, characterization studies are time consuming and activity tests provide only an overall picture of nitrogen removal. A test that is somewhere between the activity tests and characterization could provide more information in a short time. Also, a test is needed that could provide some information on the intrinsic activity of the different catalysts. The doctored runs in this study were performed to find out whether the doctored feedstocks could provide any information on the intrinsic activity and to find out whether this test can be used more effectively than simple activity tests towards tailoring of hydrotreating catalysts.

In order to have meaningful results, the doctoring compound should satisfy two conditions. First, it should be a model compound found in

coal derived liquids. Secondly, the doctoring compound should be relatively difficult to hydrotreat. Carbazole, which met both the requirements was tried first, but it did not dissolve in raw anthracene oil even when the temperature was raised to an appreciable extent. Also, problems were encountered in maintaining a homogeneous solution. Even though this information was not available at that time, characterization studies showed that raw anthracene oil contains about 1.10 weight percent of carbazole. This leads one to assume that maybe raw anthracene oil was saturated with carbazole. Quinoline, which is a two ring compound as compared to the three ring carbazole was tried next. Raw anthracene oil contains about 0.85 weight percent quinoline and with quinoline, maintaining a homogenous mixture was possible. Nitrogen analysis on the doctored feedstock confirmed that quinoline had mixed thoroughly in raw anthracene oil. This feedstock (which will be referred to as doctored raw anthracene oil, DRAO) was hydrotreated over three different catalysts and the products were analyzed for their nitrogen content.

Three experimental runs were made using raw anthracene oil doctored with quinoline to a total nitrogen content of 1.89 weight percent (raw anthracene oil has 1.06 weight percent of nitrogen initially). The catalyst type was varied amongst the three experimental runs. However, the catalyst supports used in these three experimental runs were the same supports that were used in the earlier runs using undoctored raw anthracene oil as feedstock. The experiments were conducted at one temperature (371C) while varying space time (0.46, 0.92 and 1.84 hours). Continuous 72 hours of oil-catalyst contact was achieved on each of the three catalysts. The catalyst properties are shown in Table XXV and

the results are presented in Figure 24.

TABLE XXV

PROPERTIES OF CATALYSTS USED
IN DOCTORED RUNS

Property	KDC Series	KDT Series	KDP Series
Catalyst Support	Ketjen 007-1.5E	Steam Treated (10 hrs.) Ketjen 007-1.5E	Ketjen 000-3P
CoO, wt. %	3.5	3.5	3.5
MoO_3, wt. %	12.5	12.5	12.5
Surface Area, m^2/gm	252	221	220
Pore Volume, cc/gm	0.467	0.499	0.448
Most Frequent Pore Radius, Å	31	39	33,180

Table XXV shows that the catalyst used in the KDC series has the highest surface area and that the catalyst used in the KDP series has a bimodal pore distribution. Figure 24 reveals very little difference between the three catalysts. However, the steam treated catalyst used in the KDT series was less active compared to the other two catalysts. At a space time of 1.84 hrs., the KDT catalyst had achieved a 51% removal of nitrogen while the KDC and KDP catalysts were able to remove 67 and 59 percent nitrogen, respectively. Detailed discussions will be presented in the next chapter.
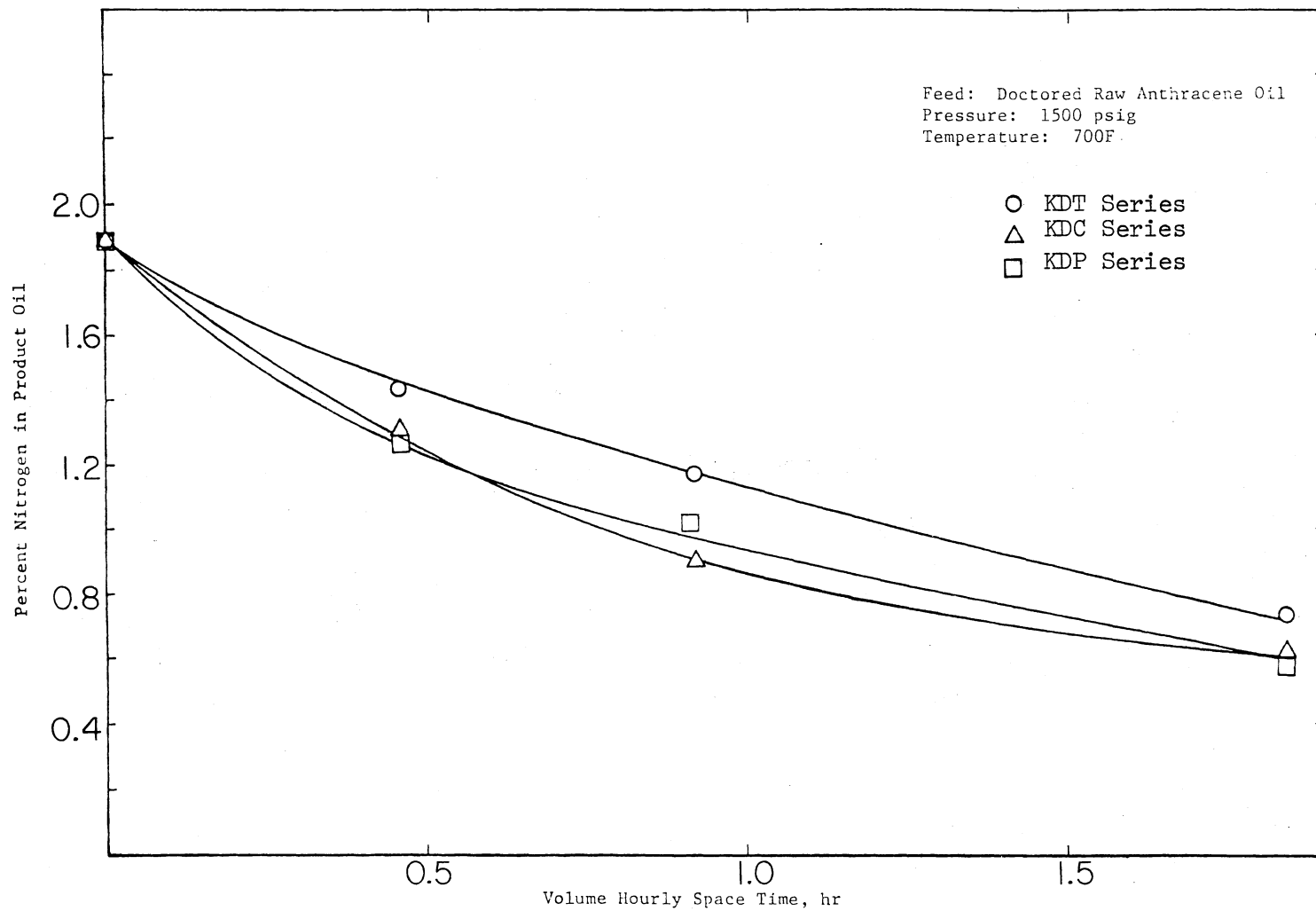
Figure 24. Nitrogen Response for Doctored Runs

ASTM Distillation Results

In order to assess nitrogen removal throughout the feedstock boiling range, the doctored feedstock, the original feedstock and selected product samples were fractionated using an ASTM distillation technique (107). In an earlier study, Satchell (6) had fractionated the same feedstock and some of his product samples. Hence, the temperature cuts used in this study correspond to Satchell's study so that comparisons can be made. These fractions were then analyzed for their nitrogen content.

Figure 25 presents the weight percent nitrogen in raw anthracene oil and doctored raw anthracene oil feedstock as a function of the boiling point measured at 50 millimeters of mercury pressure. These boiling points refer to the vapor temperature as determined using the ASTM technique (107). As can be expected, the addition of quinoline lowers the initial boiling temperature and most of the quinoline was found in the lower boiling ranges (less than $400^{\circ}F$). The higher boiling ranges ($400^{\circ}F+$) of both feedstocks are essentially identical. Hence, when the products are separated into fractions, the results of the nitrogen removal for higher boiling ranges can give us the same information from both feedstocks. A total of twelve samples were distilled into different fractions. Nine samples were from doctored runs, three for the three space times used in this study. Three representative samples were chosen from the runs using undoctored raw anthracene oil, one for each run. Raw distillation data are presented in Appendix C.

Figures 26, 27 and 28 present the nitrogen content of the different boiling fractions as a function of space time for KDC, KDT and KDP
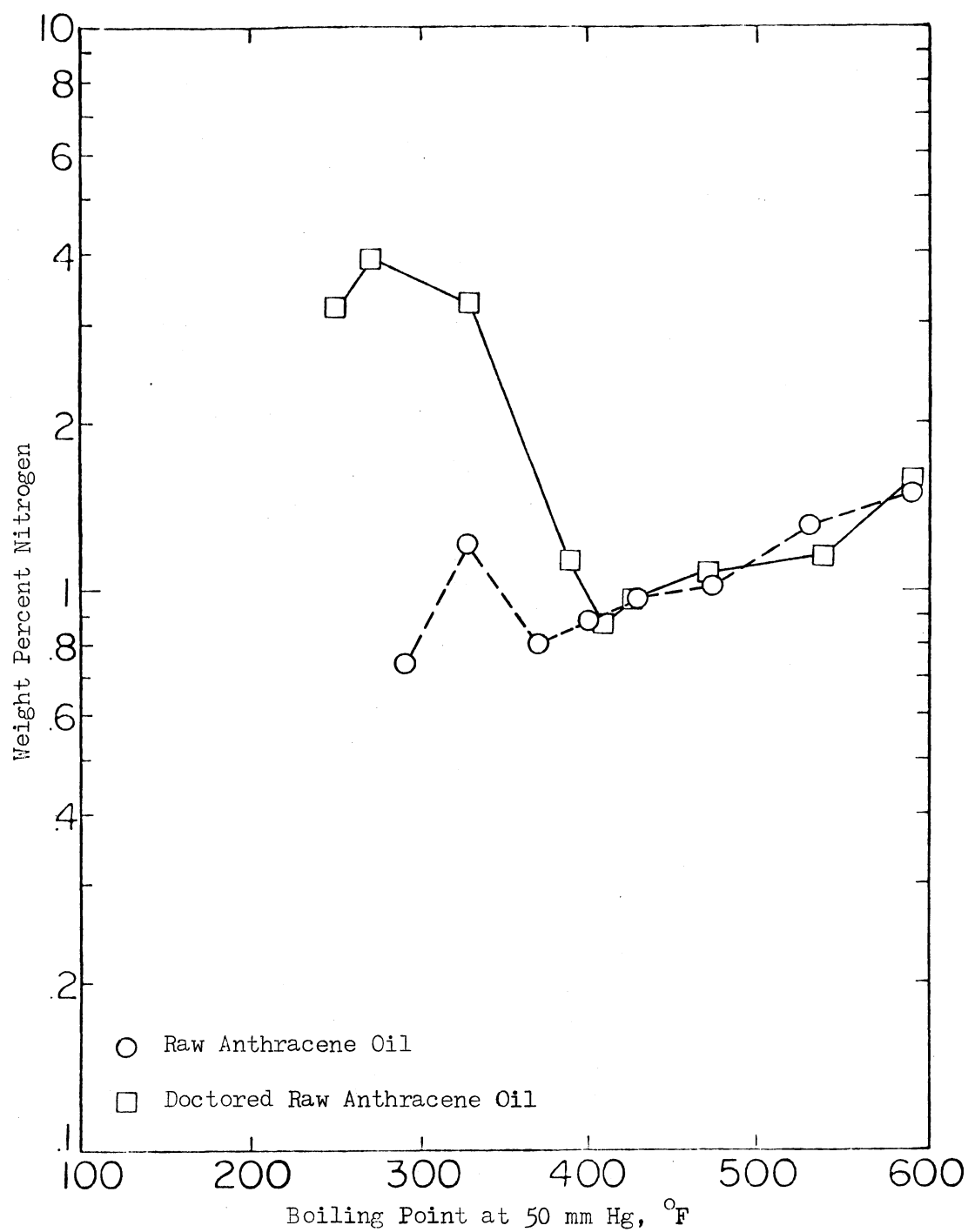
Figure 25. Feedstock Nitrogen Content as a Function of
Boiling Point
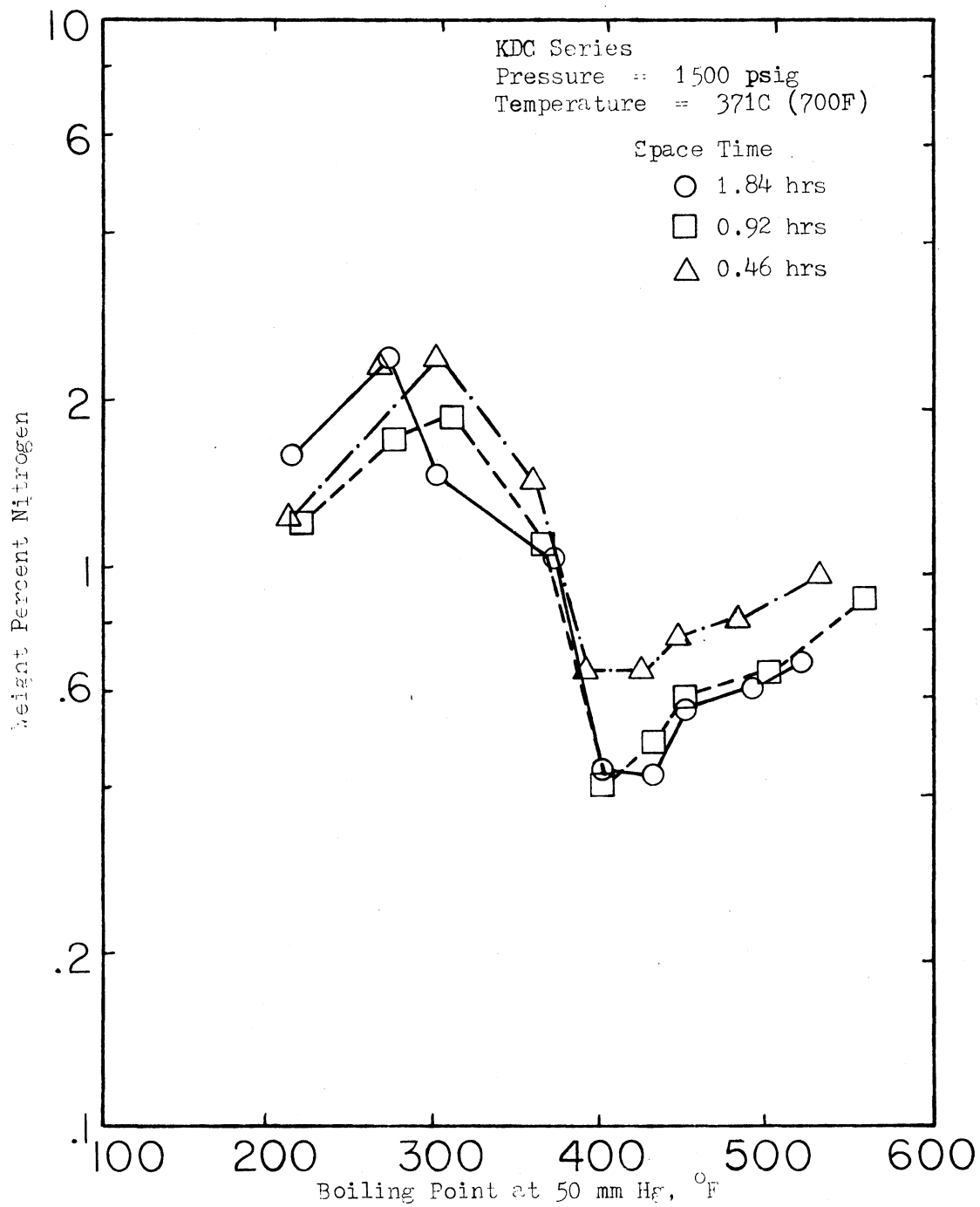
Figure 26. Product Oil Nitrogen Content as a Function of
Boiling Point for the KDC Series
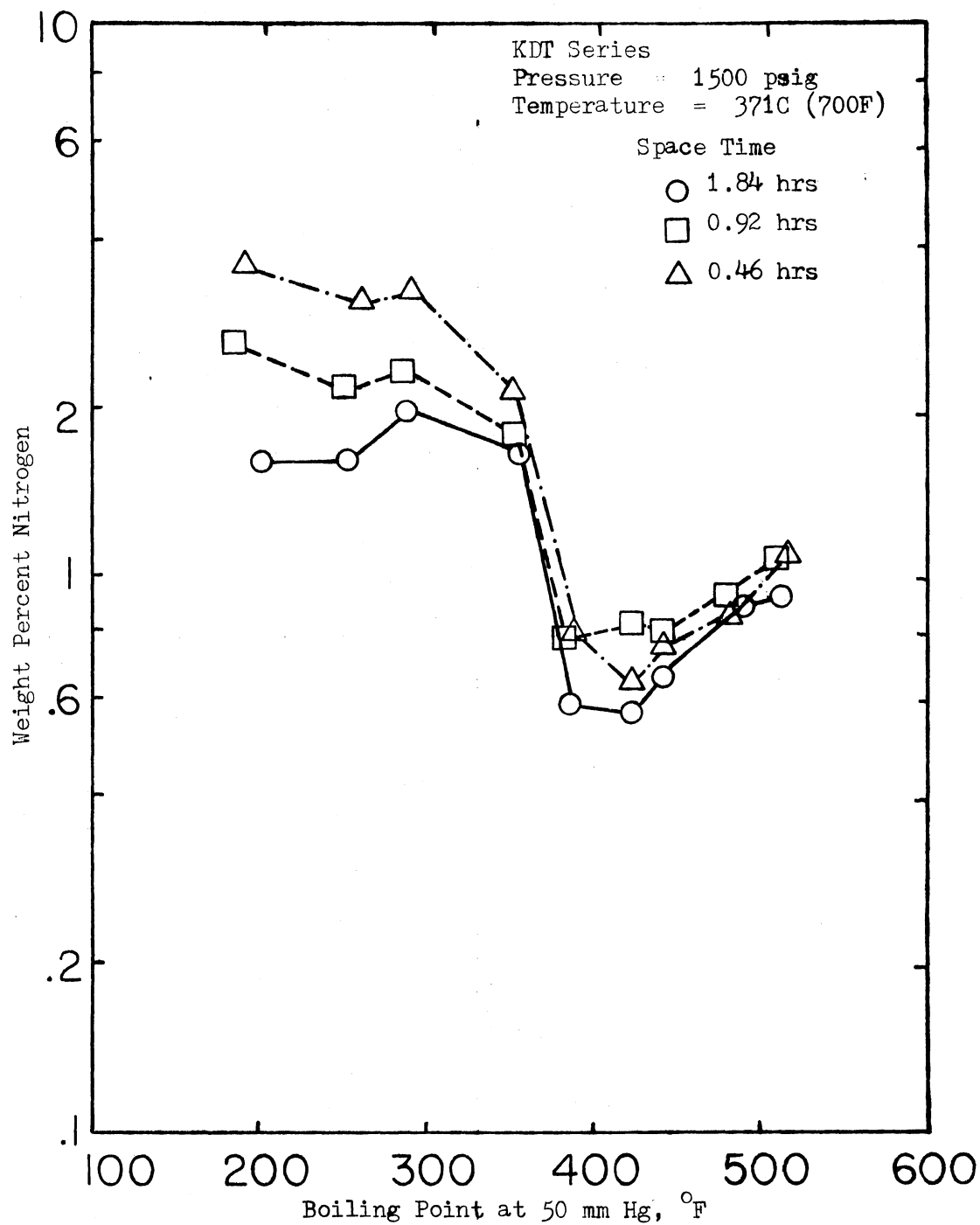
Figure 27. Product Oil Nitrogen Content as a Function of the Boiling Point for the KDT Series
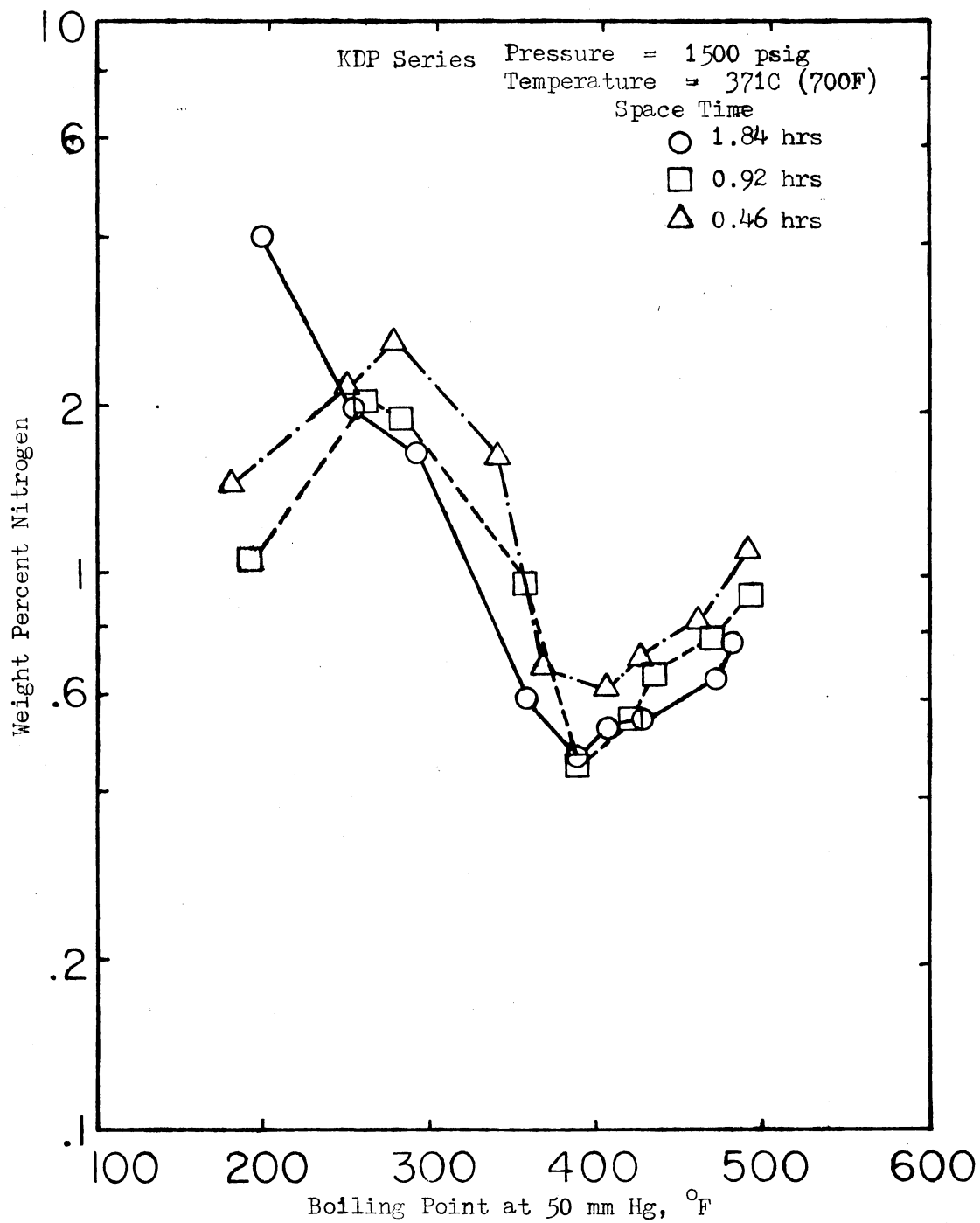
Figure 28. Product Oil Nitrogen Content as a Function of
Boiling Point for the KDP Series

series, respectively. For all three series, the higher the space time, the lower the nitrogen content in a particular fraction. Figures 29, 30 and 31 present the same data but comparing the three catalysts at a fixed space time. Figure 32 compares the three catalysts used in hydrotreating the undoctored raw anthracene oil by comparing the nitrogen content of different boiling fractions for the KEC, KET and KEP series at a space time of 0.46 hours.

Figures 33 through 38 present the ASTM distillation curves for the feedstocks and selected product samples. Figure 33 compares raw anthracene oil with doctored raw anthracene oil and shows that addition of quinoline suppresses the boiling point of individual fractions in the low boiling ranges and after about 390F, both curves essentially follow the same path. Figure 34 presents the distillation curves at a space time of 0.46 hours for the three catalysts used in this study when undoctored raw anthracene oil was used as the feedstock. Figure 35 presents similar results for doctored raw anthracene oil as the feedstock. The distillation curves are essentially the same for all three catalysts, thereby indicating that the cracking capabilities of the catalysts are almost identical. Figure 35, however, reveals that the KDP catalyst had a slightly higher cracking capacity than KDC or KDT. The presence of silica in the KDP catalyst could have contributed to the cracking capacity of the KDP catalyst. Figures 36 through 38 present ASTM curves for the three series as a function of space time for each catalyst when doctored raw anthracene oil was used as the feedstock. These figures reveal that the cracking capabilities of the catalysts studied do not increase with increase in space time. Detailed discussion on the distillation results will be presented in the next
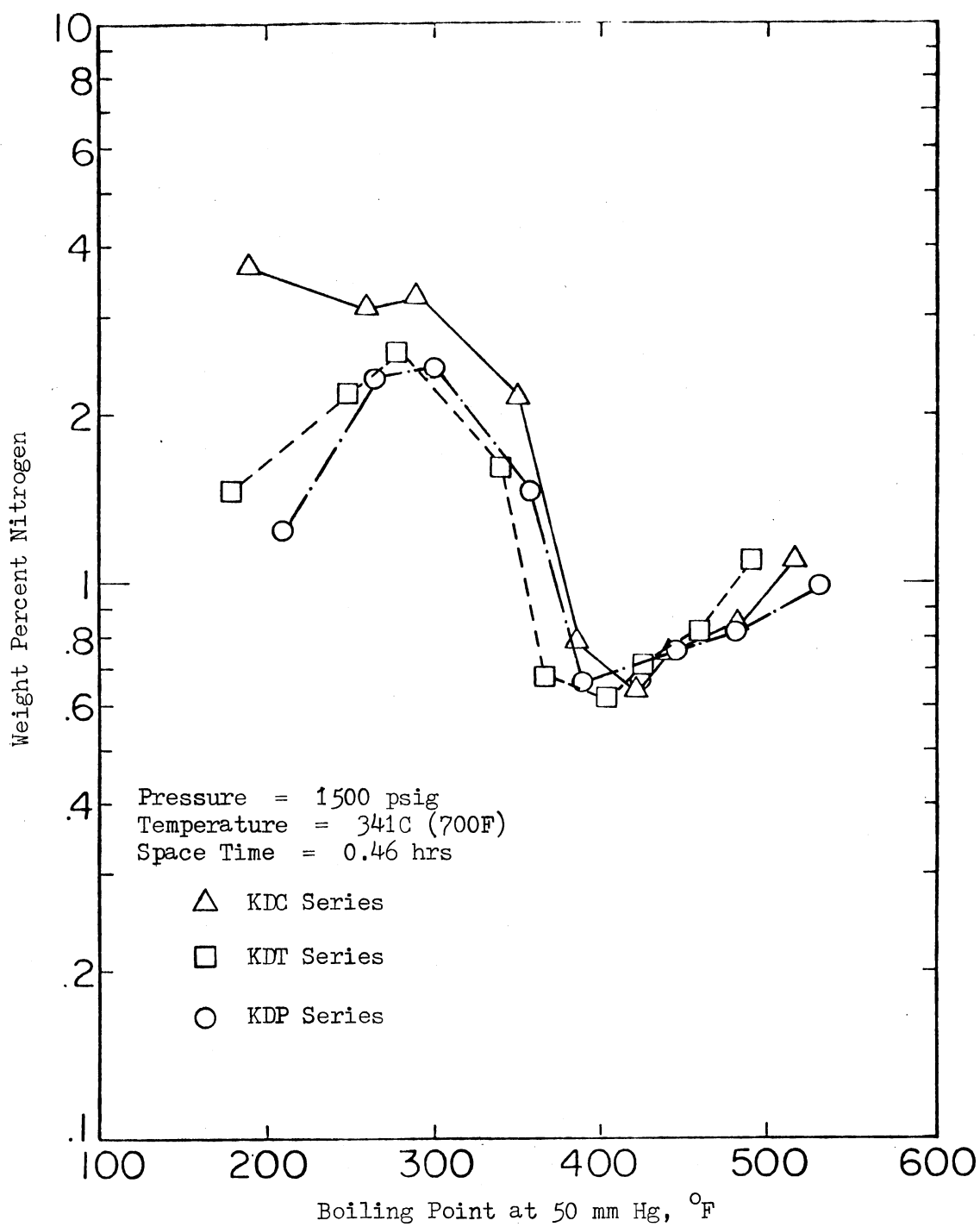
Figure 29. Comparison of Nitrogen Response as a Function of
Boiling Point for Three Catalysts at a Space
Time of 0.46 Hours Using Doctored Raw Anthra-
cene Oil as Feedstock
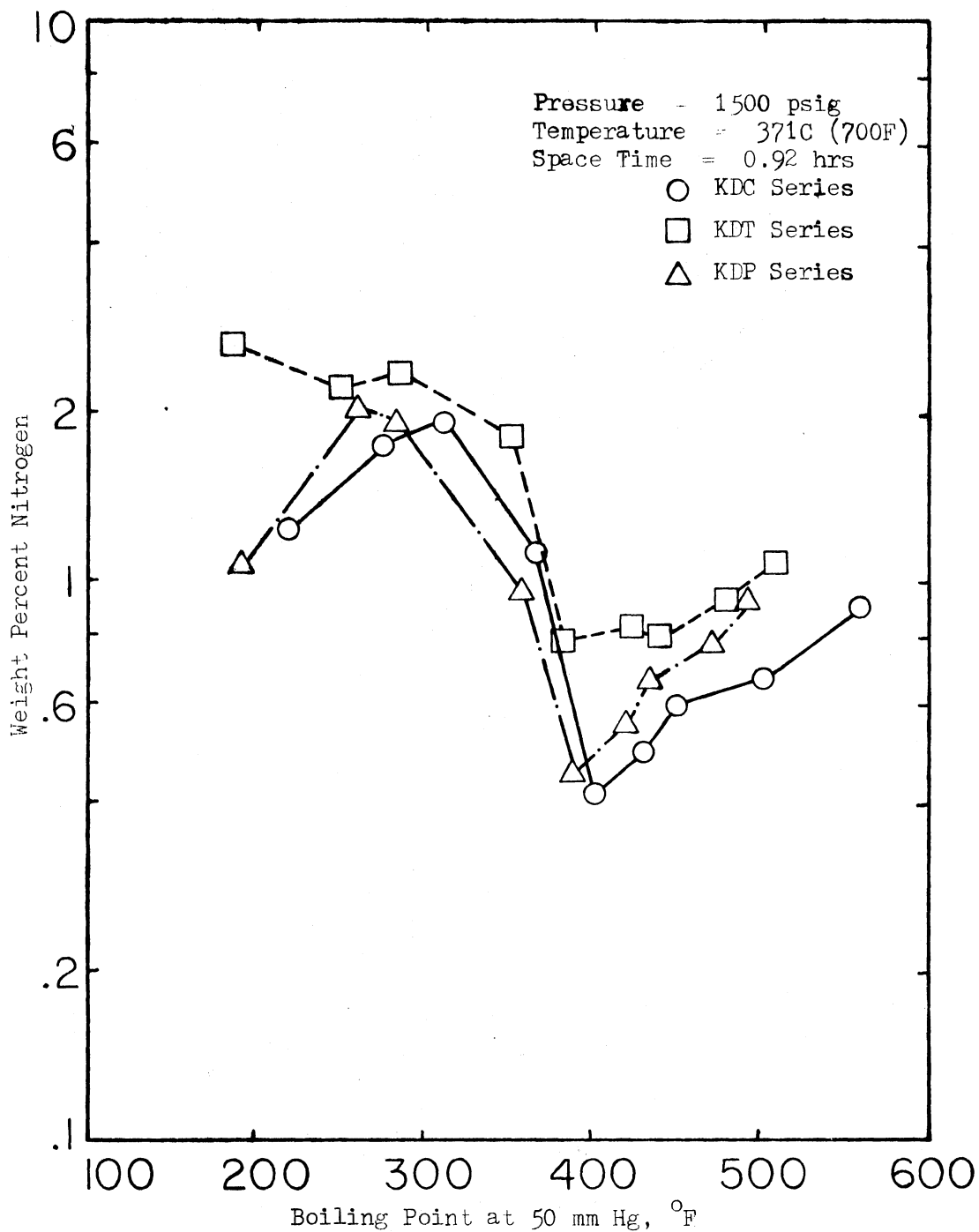
Figure 30. Comparison of Nitrogen Content as a Function of Boiling Point for Three Catalysts at a Space Time of 0.92 Hours Using Doctored Raw Anthracene Oil as Feedstock
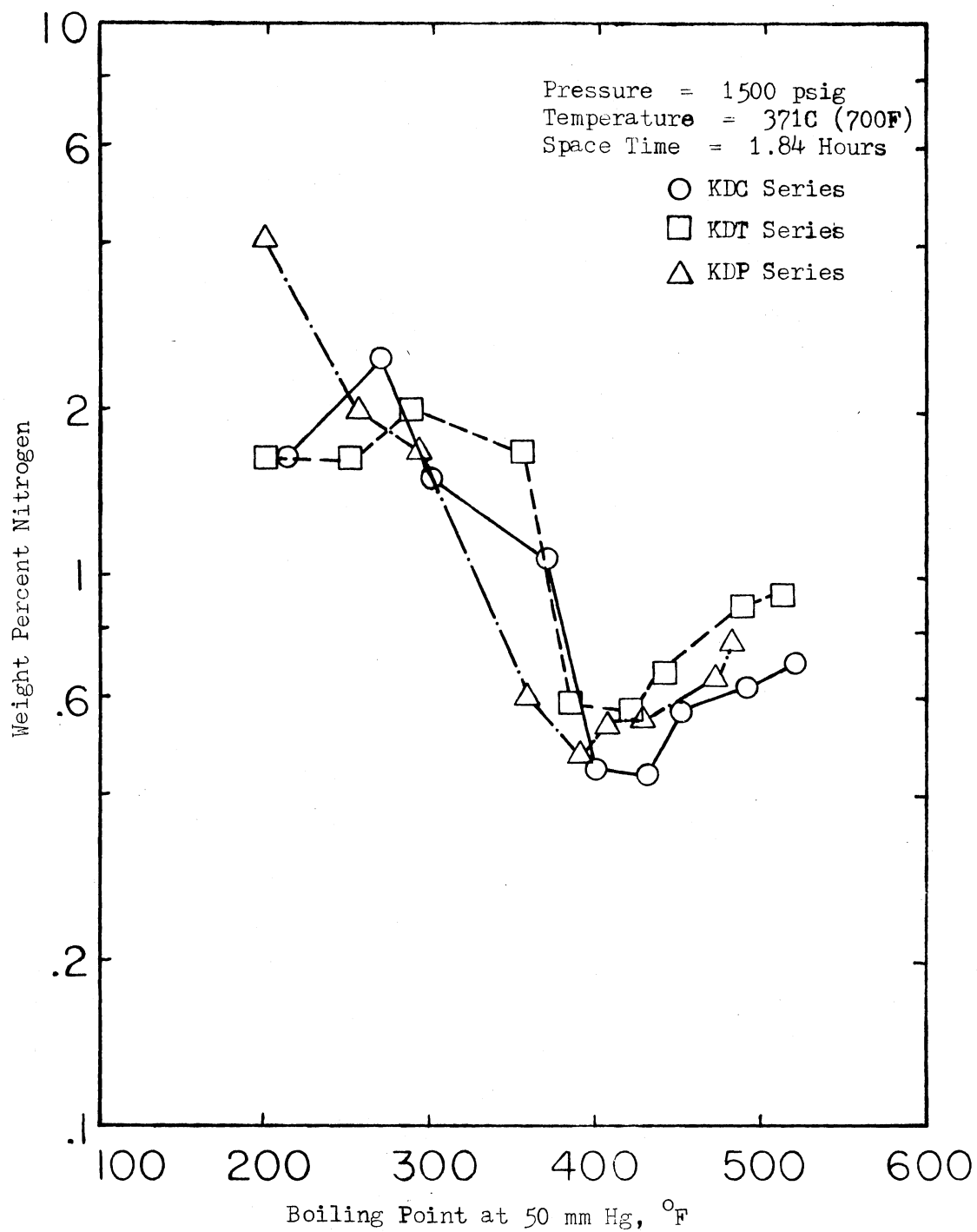
Figure 31. Comparison of Nitrogen Content as a Function of
Boiling Point for Three Catalysts at a Space
Time of 1.84 Hours Using Doctored Raw Anthra-
cene Oil as Feedstock
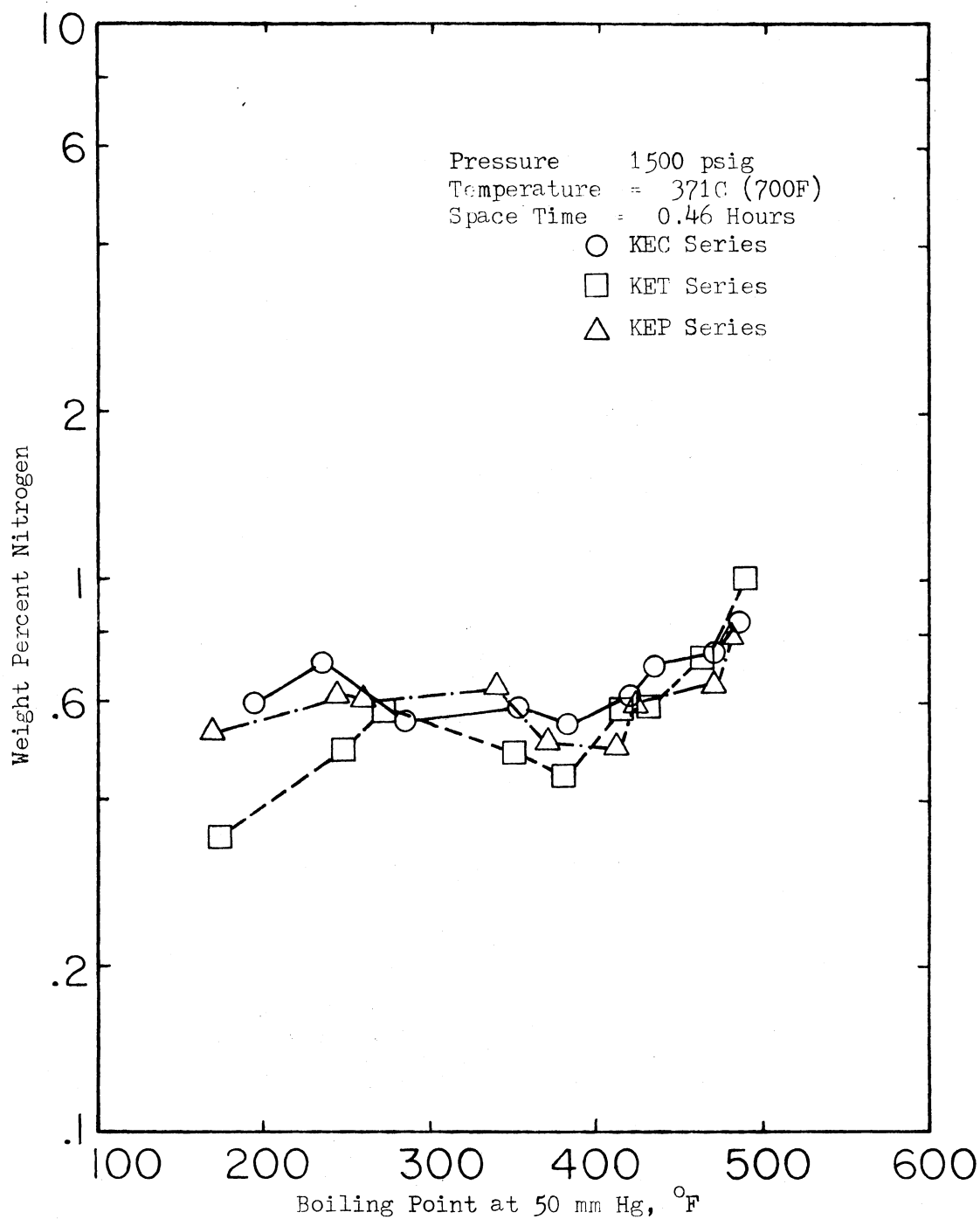
Figure 32. Comparison of Nitrogen Content as a Function of
Boiling Point for Three Catalysts at a Space
Time of 0.46 Hours Using Raw Anthracene Oil
as Feedstock
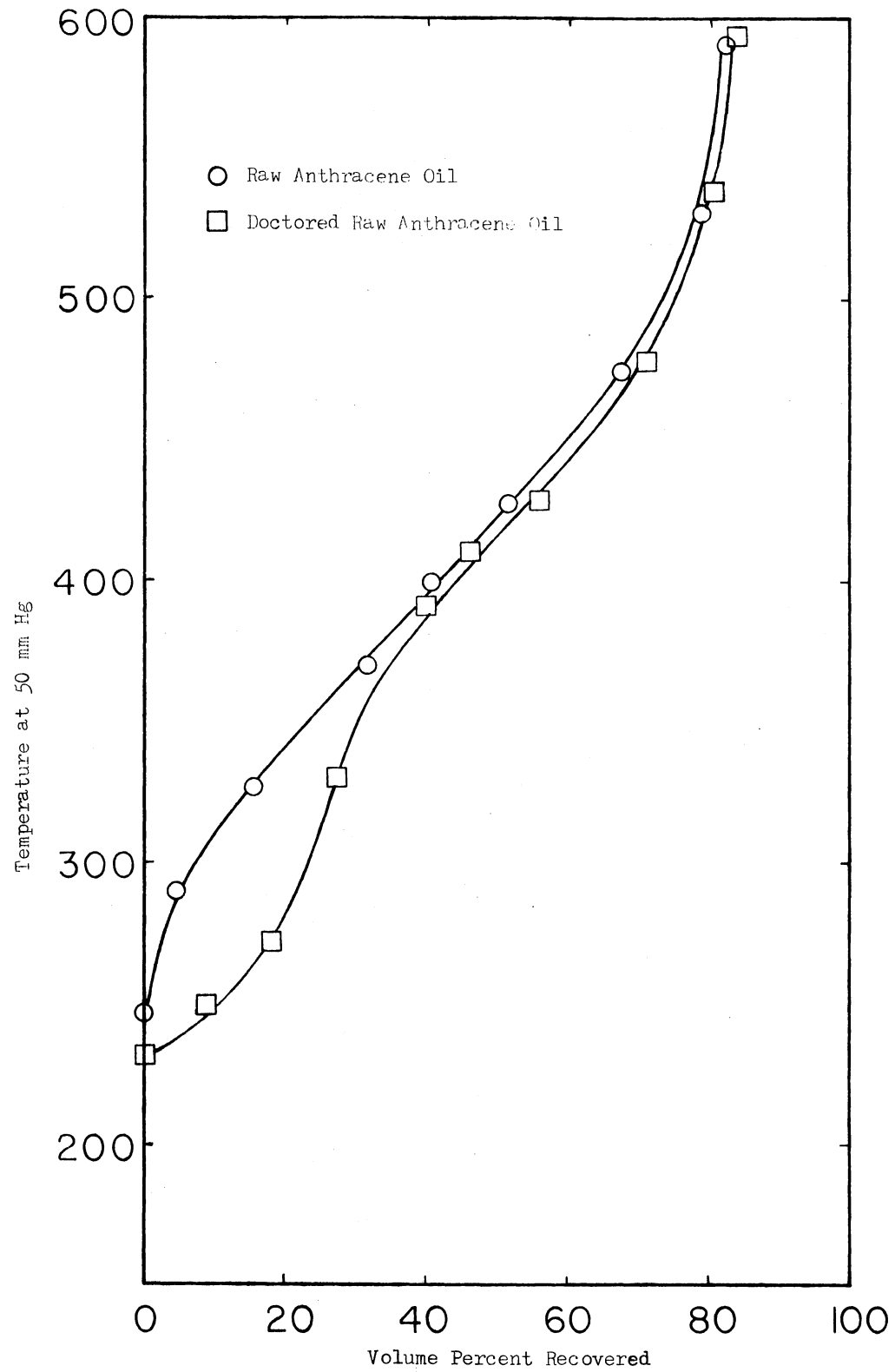
Figure 33. ASTM Distillation Results for the Feedstocks
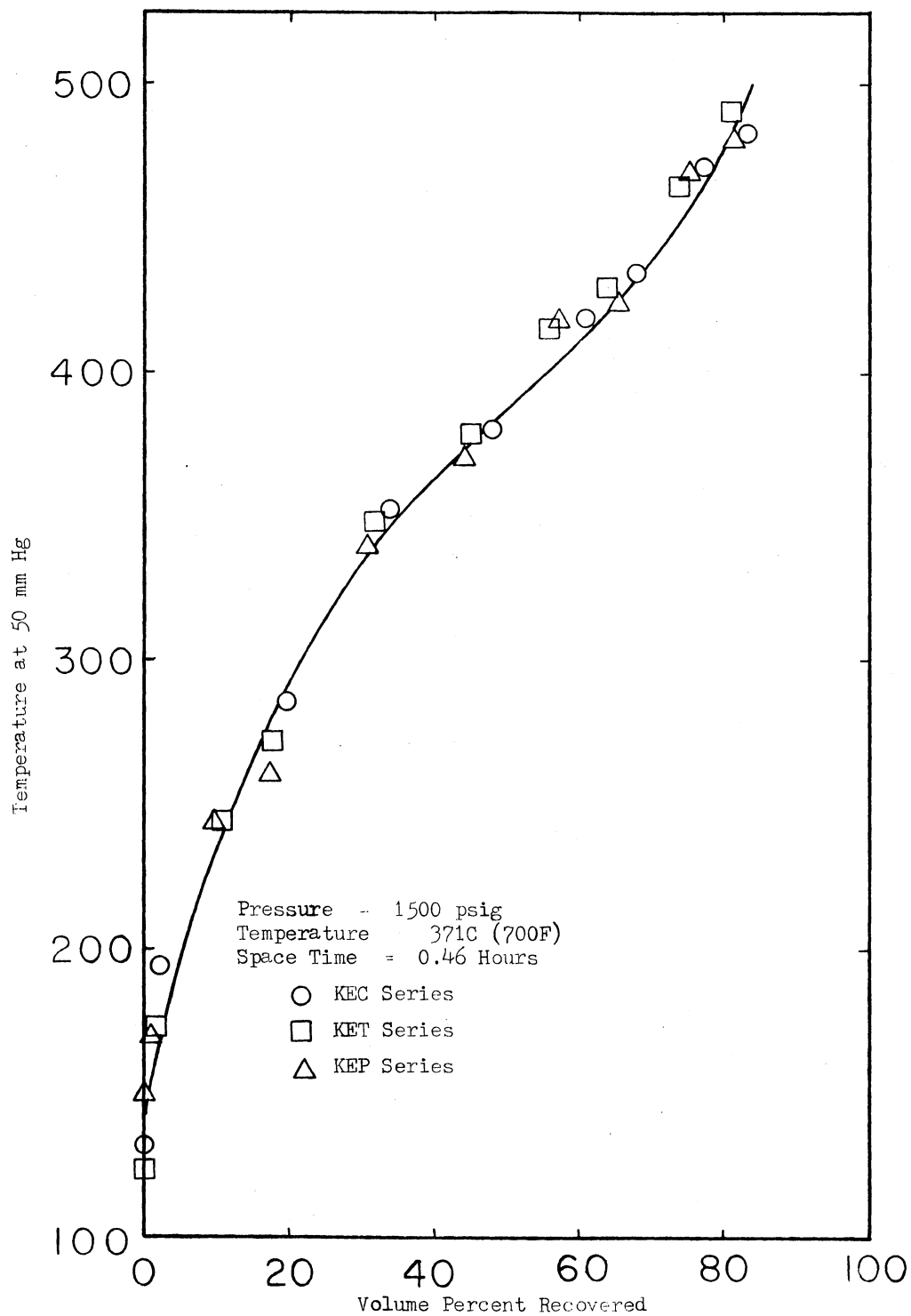
Figure 34. ASTM Distillation Results for Products
From Raw Anthracene Oil Runs
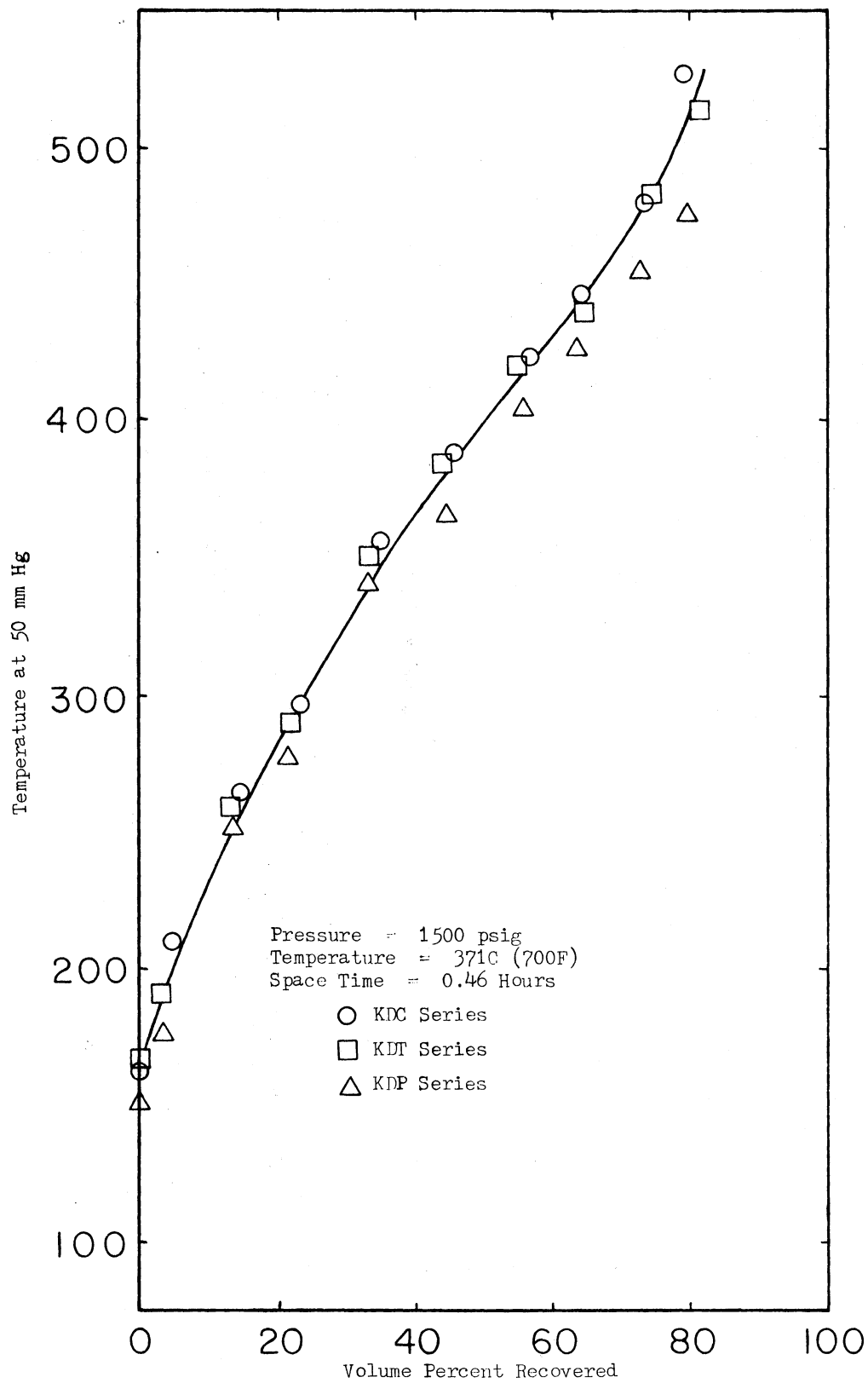
Figure 35. ASTM Distillation Results for Products from Doctored Raw Anthracene Oil Runs
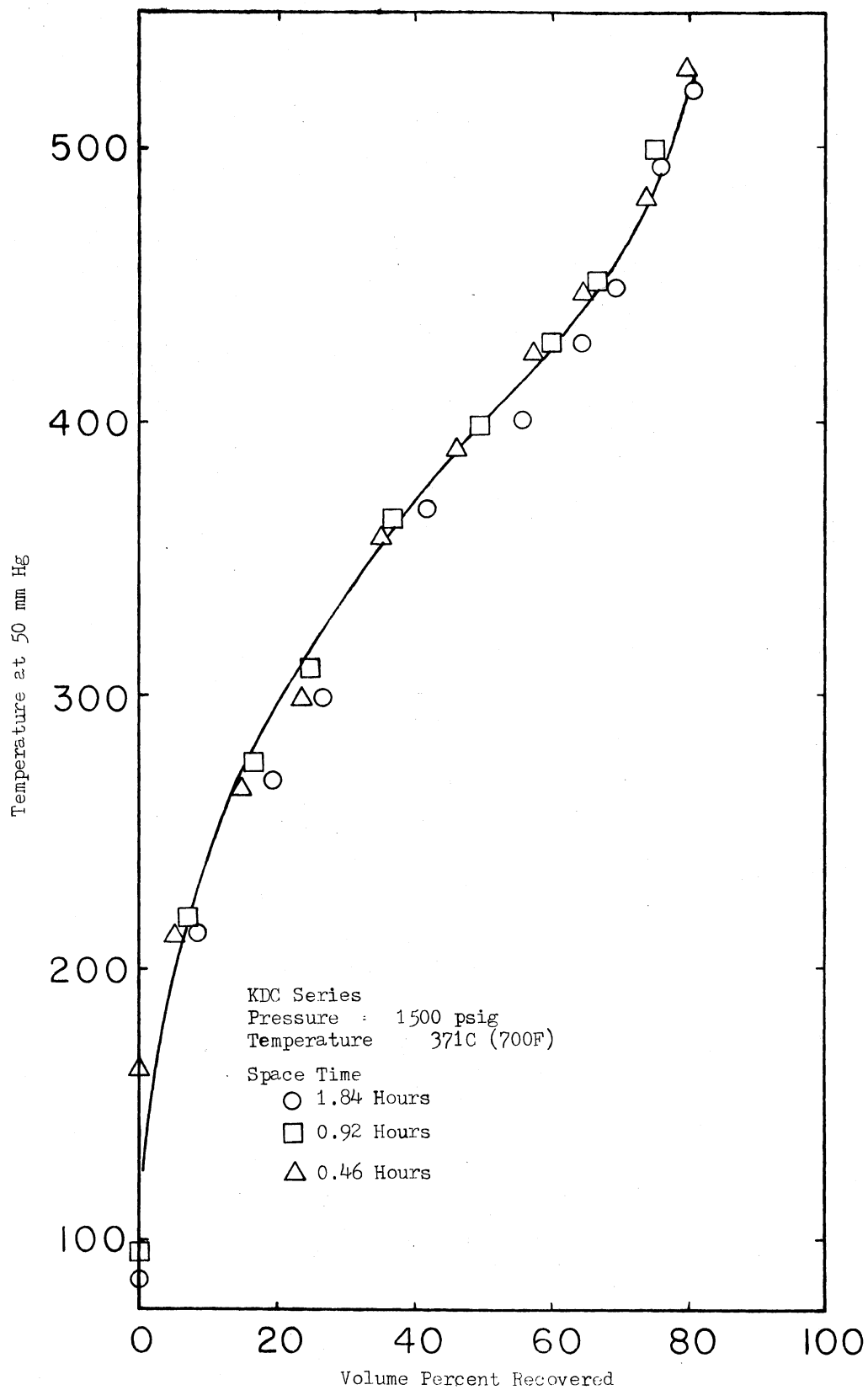
Figure 36. ASTM Distillation Results for the KDC Series
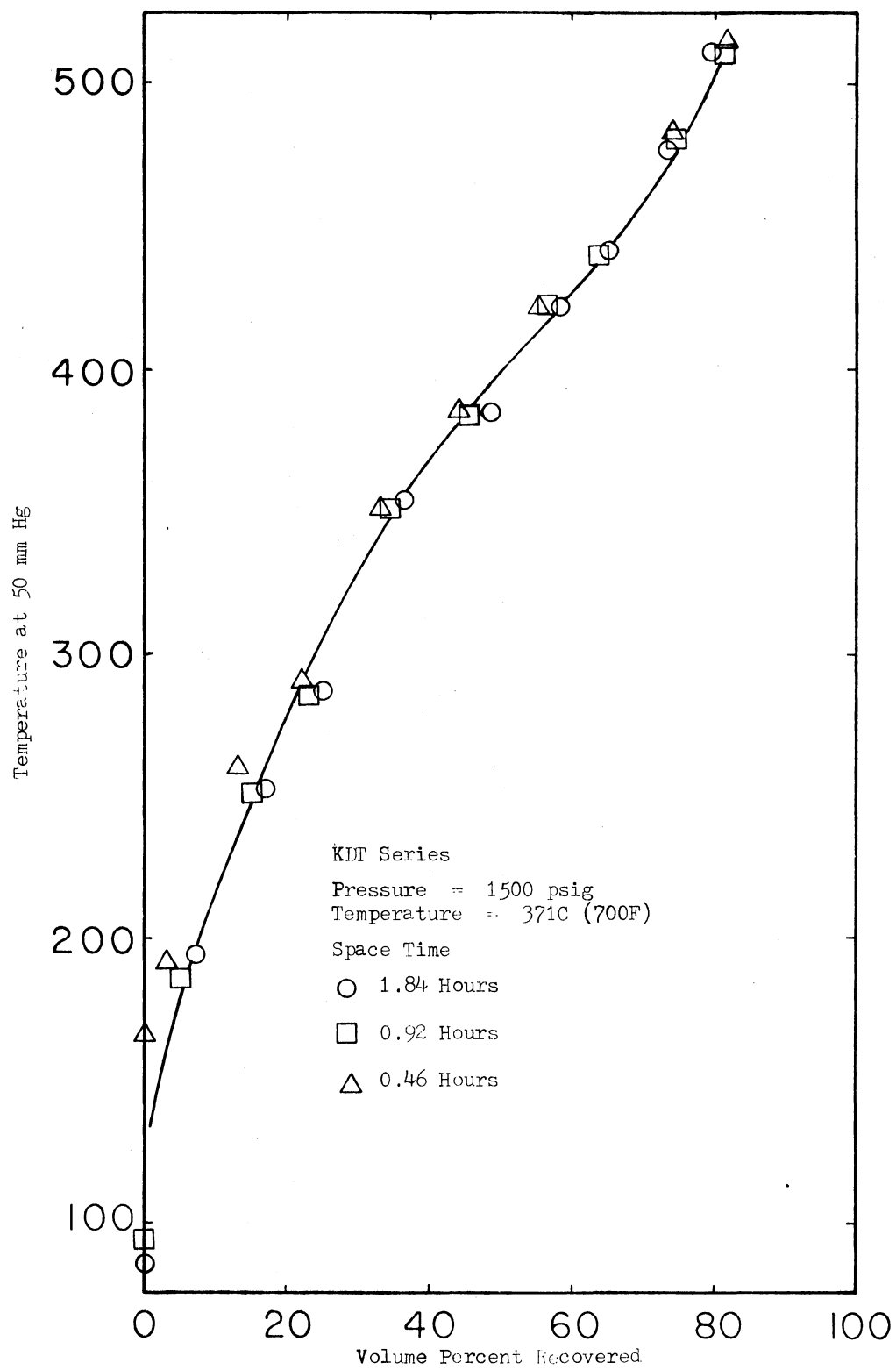
Figure 37. ASTM Distillation Results for the KDT Series
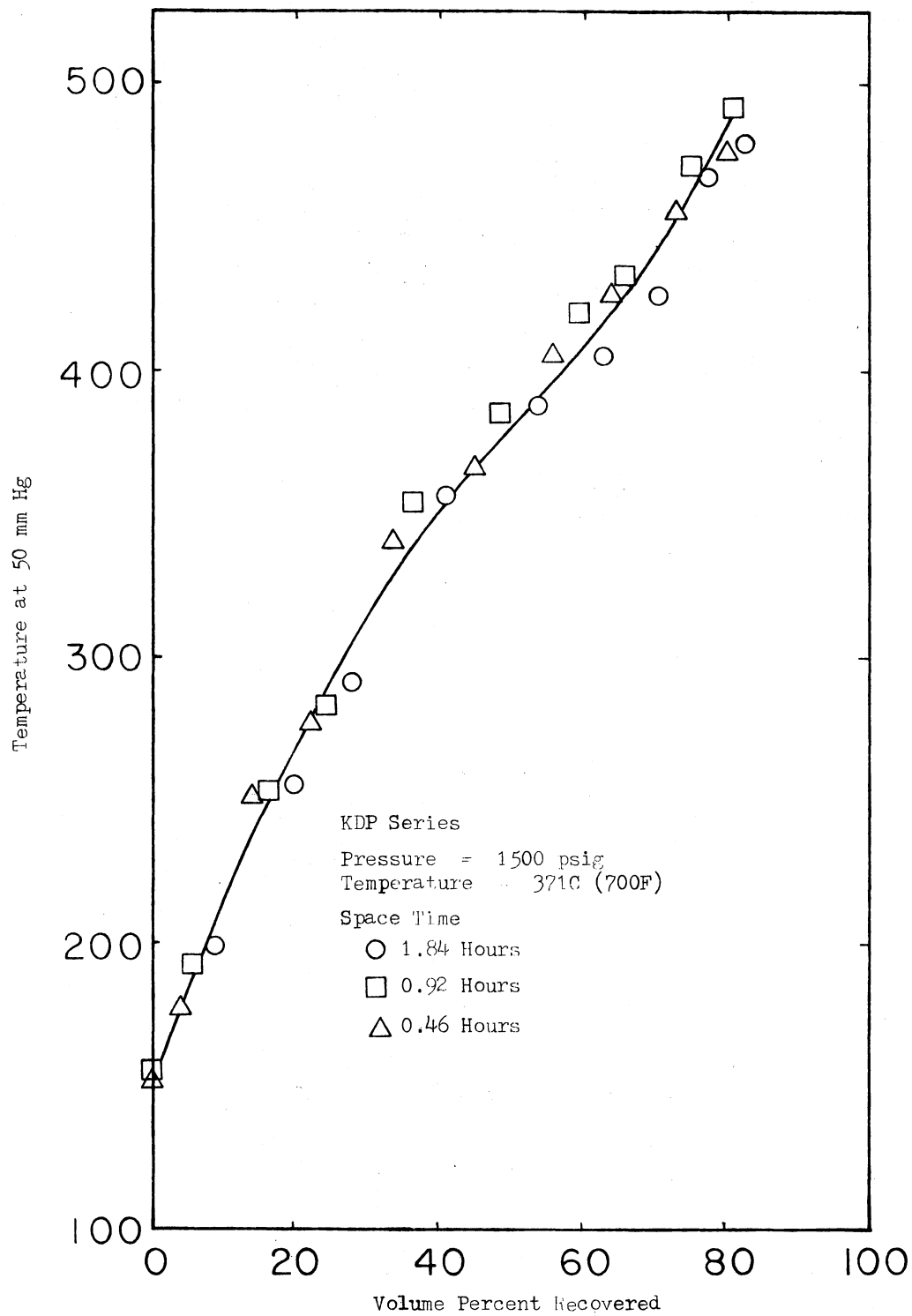
Figure 38. ASTM Distillation Results for the KDP Series

chapter.

The main objective of this chapter is to present the results gathered from experiments. Except for brief explanations, no attempt was made in this chapter to discuss the results. All results presented in this section will be discussed in detail in the next chapter. The raw data are presented in the Appendix section.

CHAPTER VII

DISCUSSION

The results presented in the previous chapter will be discussed in
detail in this chapter. An understanding of the operating conditions
and their fluctuations are vital in interpreting any experimental
work. Hence, some of the important aspects of the reactor operation
will be discussed first. Then the effects of backmixing and holdup
on the performance of the trickle bed reactor will be discussed
followed by the modelling studies on the overall kinetics of hydro-
denitrogenation. Then the effect of catalyst support properties on
hydrodenitrogenation of raw anthracene oil will be considered followed
by a discussion on the relative activity of difrerent catalysts. A
detailed discussion on the doctored runs and the distillation results
will be presented next. Questions often arise as to the molecular sizes
of the nitrogen compounds present in coal liquids and whether the
catalyst pores are completely filled with liquid or not. An attempt
will be made to answer some of these questions.

Reactor Operation

In trickle bed reactors, the exothermic reactions can result in
hot spots that can deactivate the catalyst and temperature control
can become a major operational problem for large diameter units.
However, the specially designed aluminum block heaters used in this

study were able to provide an isothermal temperature profile. Typical temperature profiles across the catalyst bed under steady state conditions during an experimental run were as shown in Figure 39, for the three temperatures used in this study. A maximum deviation of $\pm 1.5C$ (3F) was observed in the temperature profile across the catalyst bed at the highest temperature, and only $\pm 0.5C$ ($\pm 1F$) at the lowest temperatures. In addition to measuring the temperatures in the center of the reactor, the temperature at the external wall of the reactor was also measured using a hole drilled through the central heating block. A maximum radial ΔT of 1.5C (3F) was observed, and since the temperature was measured at the external wall, the ΔT across the catalyst bed would be smaller than 1.5C (3F).

All the experimental runs in this study were conducted at a pressure of 1500 psig, and pressure was controlled by using a Mitey-Mite regulator. In the present study, a maximum variation of ± 10 psi in the operating pressure was observed. This corresponds to a deviation of 0.7% from the desired value of 1500 psig.

A positive displacement pump was used for feeding the raw anthracene oil to the reactor. The pump can feed at a pre-set constant rate with little or no variation in liquid flow rate due to line voltage fluctuations. Hence, variations in the liquid flow rate were either absent or negligible in this study.

In all the runs in this study except the CAT series, the catalyst bed height was maintained at 0.498 meters (19.6 inches). The CAT series used a bed height of 0.505 meters (19.9 inches). The bed height was maintained within ± 0.002 meters (± 0.1 inch). This can cause a maximum of less than one percent error in the calculation of
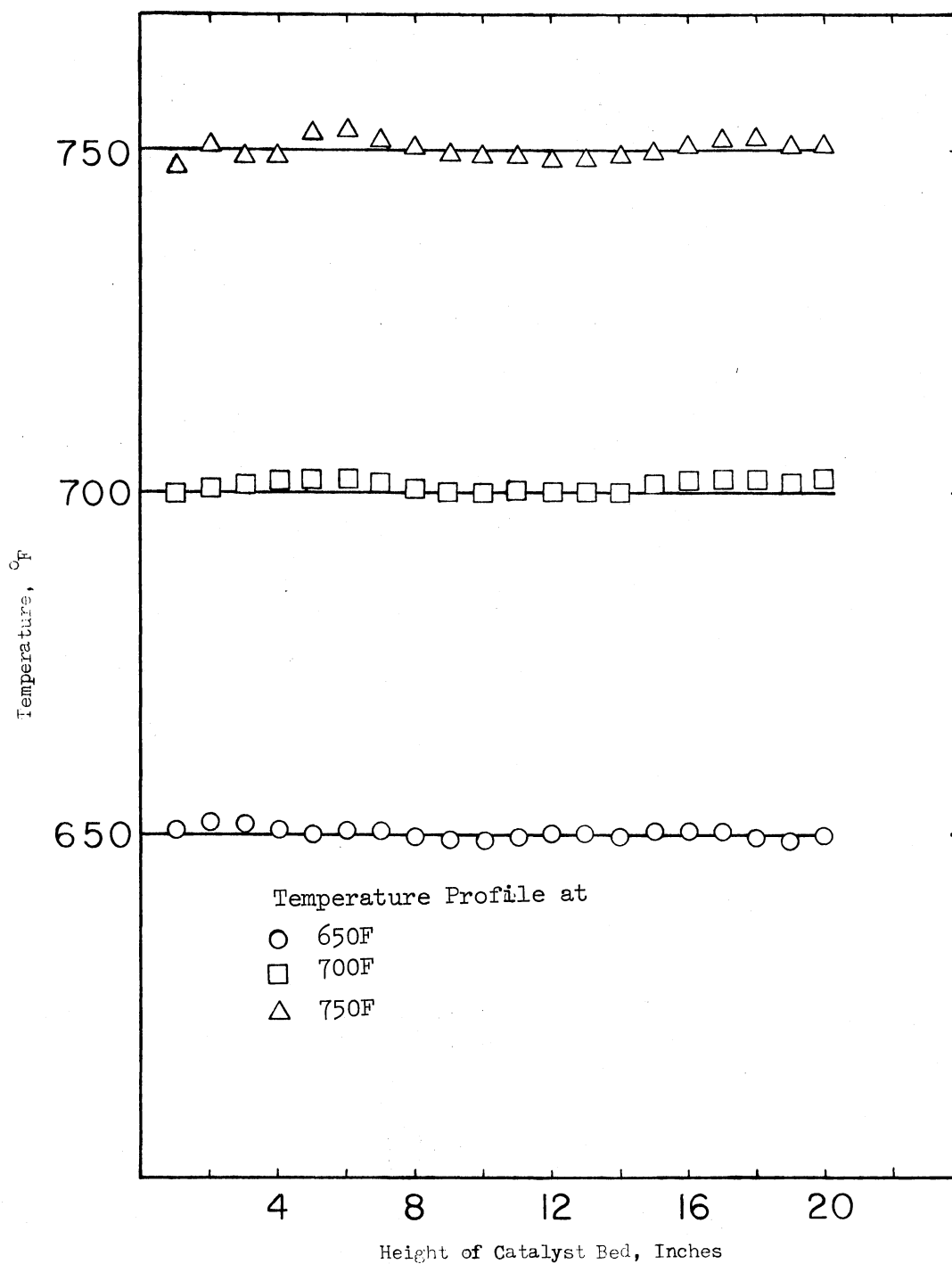
Figure 39. Typical Temperature Profiles

volume hourly space time. At the lowest flow rate (20 cc/hour), the fluctuations in the volume hourly space time due to changes in height of catalyst bed will be within $\pm$ 0.009 hours, while at the highest flow rate (80 cc/hour), these fluctuations will be within $\pm$ 0.002 hours. The volume hourly space time in this study is defined as the ratio of reactor volume based on catalyst bed length to the liquid volumetric flow rate.

Satchell (6) in his work on hydrodenitrogenation of raw anthracene oil using the same equipment as used in this study found that changing the hydrogen flow rate from 1500 to 20000 standard cubic feet/barrel (SCF/bbl) of oil had negligible effect on nitrogen removal. In the present work, the hydrogen flow rate was maintained at or above 1500 SCF/bbl of oil. The variations in this ratio were insignificant in affecting the results.

Hence, for reproducibility of results presented in this thesis work, the variations in temperature, space time, pressure and hydrogen/- oil feed ratio should be within the appropriate ranges mentioned above.

<div align="center">

Performance of the Trickle

Bed Reactor

</div>

The observed performance of a catalyst in a trickle bed reactor is determined by the severity of the hydrotreating conditions as well as the dynamics of fluid flow in the trickle bed. The complex fluid mechanics of the trickle bed reactor often interact with the chemical kinetics. Hence, an evaluation of the effects of flow distribution, holdup and backmixing are vital in order to use the kinetic information gathered from the experiments.

An experimental study of the effects of liquid distribution and backmixing were not performed as part of this investigation. This study is part of a broader project at Oklahoma State University to tailor hydrotreating catalysts for coal derived liquids, and previous studies (5-9) have established these effects under similar conditions. A brief explanation of these studies will be given here.

Satchell (6) considered the effect of liquid reactant mass flux over the range of 4.84 to 9.69 gallons per hour per square foot on the rate of denitrogenation. Satchell found that doubling the oil flux but holding the space time constant resulted in an eight percent increase in the observed denitrogenation rate constant. However, in order to keep the space time constant his catalyst bed height was increased from 0.254 meters (10 inches) to 0.508 meters (20 inches). Sooter (7), using the same equipment as used in Satchell's study, concluded that backmixing effects might have been present when the 0.254 meters catalyst bed was used. Hence, the change in reaction rate constant in Satchell's study cannot be attributed to changes in liquid mass flux alone.

The effect of liquid flux on hydrotreating a COED oil, a coal derived liquid was studied (66) over the range of 3.8 to 15.3 gallons per hour per square foot at a reactor temperature of 720 F and at a pressure of 3000 psig. The effect of liquid flux on the reactor per-formance was found to be small.

Experience in the petroleum industry indicates that the liquid flux will be in the range of 150 to 500 gallons per hour per square foot in industrial, hydrotreating, trickle bed reactors. Since the range of liquid fluxes in the above tests were much smaller than those

encountered in a commercial reactor, the assumption that the differences in the oil flux between a commercial reactor and these bench scale reactors will have a negligible effect on the rate of denitrogenation is not valid. However, in this study, the catalyst bed length was not varied and the changes in liquid flux as a result of the changes in space time were within the values reported in the above mentioned studies by Satchell and Jones, et al. Hence, for this study, effects of the changes in liquid mass flux on hydrodenitrogenation will be considered as negligible.

The question of how closely a reactor approaches ideal flow behavior must also be addressed. Mears (13) presented the following criterion for the minimum h/d_p ratio required to hold the reactor length within five percent of that needed for plug flow:

$$h/d_p > \frac{20\,n}{B_o} \ln \frac{C_{in}}{C_{out}} \qquad (7.1)$$

where

h = height of catalyst bed, inches

d_p = diameter of catalyst particle, inches

n = order of reaction

B_o = Bodenstein number, dimensionless

C_{in} = concentration of reactant in the feedstock, moles/cc

C_{out} = concentration of reactant in the product, moles/cc.

The minimum reactor height will increase with the order of reaction and is very sensitive to fractional conversion at high degrees of conversion. In order to be conservative, the calculations were done using the highest conversion achieved (87%) in this study. Detailed calculations

are presented in Appendix F. The calculations showed that h/d_p for these experiments is equal to 383 while the right hand side of the equation came out to be 274 for a first order reaction under the most severe conditions tested. This is well below 383 and hence it can be concluded that axial dispersion effects were absent from this study and ideal plug flow can safely be assumed, if denitrogenation is assumed to be a first order reaction. This assumption will be considered.

Kinetics of Hydrodenitrogenation

All of the experiments were designed to gather kinetic data on hydrodenitrogenation of raw anthracene oil. The experiments using raw anthracene oil as feedstock were conducted at 1500 psig, varying temperatures and space times. The experiments using doctored raw anthracene oil as feedstock were conducted at 1.03×10^7 pascals (1500 psig), 371C (700F) and with varying space times. Three samples were collected at every operating condition and an average nitrogen content of the three samples were taken as the nitrogen content of the product oil under those conditions. As pointed out in the previous chapter, no catalyst activity decay for denitrogenation was observed in the present study. The effectiveness factor, as will be explained later in this chapter, was taken as unity for this study.

A natural extension of determining space time and temperature effects is to determine appropriate kinetic models. A simple power rate law expression, Equation 7.2, was chosen initially to test the data since a power rate law tries to give an equivalent fit to experimental data with the fewest number of adjustable parameters.

$$dC_A/dt = kC_A^n \qquad (7.2)$$

where

$$dC_A/dt \quad = \quad \text{rate of change of concentration of total}$$

nitrogen with respect to time, moles/cc-hr

C_A = concentration of nitrogen in product oil,

moles/cc

n = order of reaction

k = reaction rate constant based on reactor volume,

$(hr)^{-1}$.

Most of the published information in the literature (47, 48), claim

denitrogenation to be a first order reaction. However, Satchell (6)

using the same feedstock as used in this study, found that a second

order model predicted his data better than a first order model. Hence,

reaction orders 1 through 3 were tried for this study. Equation 7.2

was integrated for reaction orders 1 through 3, and the data of this

study were tested for each reaction order using a least squares curve

fit. The sum of squares of the error, defined as the sum of the

squares of the difference between the weight percent nitrogen observed

and that obtained from the regression analysis, was determined for every

temperature studied for all of the experimental series. Table XXVI

presents the results from the regression analysis.

Table XXVI indicates that except for the KDT series at a temperature

of 371C (700F), for all the other conditions, the first order model

fits the data better by giving the smaller sum of squares of the error.

The difference between the sum of squares of error between the first

order and second order models are also relatively small in some cases.

Some interesting information is shown in Table XXVI. Even though

a first order reaction rate model fit the data very well, the reaction

rate constants do not agree with the observed performance of the differ-

ent catalysts used in this study. Note, for example, that the first

TABLE XXVI

RESULTS FROM LINEAR REGRESSION FOR
NTH ORDER MODEL TESTS

| Run Series | Temperature °C (°F) | Sum of Squres of Error for Reaction Order | | | Reaction Rate Constants | | |
		1	2	3	1st Order $(hr)^{-1}$	2nd Order $(Wt\%)^{-1}(hr)^{-1}$	3rd Order $(Wt\%)^{-2}(hr)^{-1}$
KEC	343 (650)	0.071	0.264	1.012	0.268	0.518	1.011
KEC	371 (700)	0.286	2.350	21.230	0.538	1.538	4.586
KEC	399 (750)	0.450	10.599	294.37	0.668	3.276	17.196
KET	343 (650)	0.138	0.359	0.988	1.038	0.602	1.000
KET	371 (700)	0.429	2.121	11.944	0.660	1.455	3.411
KET	399 (750)	0.431	4.585	54.84	0.655	2.111	7.222
KEP	343 (650)	0.034	0.072	0.153	0.181	0.263	0.386
KEP	371 (700)	0.046	0.179	0.704	0.216	0.426	0.844
KEP	399 (750)	0.319	3.660	47.41	0.560	1.921	6.925
KDC	371 (700)	0.278	0.366	0.537	0.520	0.607	0.737
KDT	371 (700)	0.092	0.072	0.057	0.305	0.269	0.241
KDP	371 (700)	0.134	0.138	0.151	0.842	0.374	0.391
CAT	343 (650)	0.079	0.191	0.476	0.279	0.435	0.686
CAT	371 (700)	0.084	0.358	1.574	0.279	0.584	1.235
KER	343 (650)	0.113	0.338	1.039	0.334	0.574	1.000
KER	371 (700)	0.147	0.762	4.178	0.374	0.865	2.04
KER	399 (750)	0.258	4.602	89.99	0.510	2.158	9.496

order reaction rate constants calculated for the KET series at temperatures of 340 and 371C (650 and 700F) are higher than the reaction rate constants for the KEC series at the same temperature. This is inconsistent with the observed facts since the catalyst used in the KEC series was more active than the catalyst used in the KET series at all temperature levels (Figures 17 and 18). Note also that the first order rate constants for the CAT series remain essentially the same when the temperature was raised from 340 to 371C (650 to 700F). Also, the first order reaction rate constant for the KET series decreases with increasing temperature. When the three series KEC, KET and KEP are compared, the reaction rate constants predict the KEP series to be lower in activity than the other two series at all temperature levels. However, Figures 20, 21 and 22 presented in the results section show this to be untrue.

Similar discrepancies exist in second and third order models too. Figure 24 presented on page 135, showed that the catalysts used in the KDC, KDT and KDP series to be essentially of the same activity with the catalyst used in the KDT series being slightly less active than the other two. However, the second and third order rate constants for the KDP series were about half that of the rate constants for the KDC series. Also, the second order reaction rate constant for the KDT series at a temperature of 343C (650F) is higher than the rate constant for the KEC series at the same temperature. Hence, even though the statistical analysis favored the power law expression for the first order model, the physical evidence suggests otherwise, and thereby dictates other model considerations.

Since the integral technique of data work up did not produce any convincing results, a differential approach was tried next to check

whether denitrogenation of the raw anthracene oil could behave as a
fractional order reaction. Values of the weight percent nitrogen in
the product oil were taken at 0.1 hour intervals between 0.5 and 1.8
hours from Figures 17, 18 and 19 for the KEC and KET series. These data
were then fitted to a second degree polynomial to get values of C_A in
terms of t, where C_A is the weight percent nitrogen in the product oil
and t is the volume hourly space time in hours. The polynomial was dif-
ferentiated to obtain values of dC_A/dt and these values of dC_A/dt with
the corresponding values of C_A were tested using a least squares method
to fit the following equation:

$$-dC_A/dt = kC_A^n \qquad (7.3)$$

Equation 7.3 was converted into a linear relationship and linear re-
gression analysis was used to determine k, the reaction rate constant
based on reactor volume and n, the order of reaction. The data used to
determine the polynomial equation along with the values of dC_A/dt are
presented in Appendix D for the KEC and KET series.

Table XXVII presents the values of k and n obtained for the two
series. Results from Table XXVII are even more confusing for the two
results in Table XXVI. Note that the order of reaction decreases
with increase in temperature for the KET series and for the KEC series,
the order of reaction decreases from 2.581 at 340C (650F) to 1.004 at
371C (700F). However, at 399C (750F) the differential method predicts
an improbable reaction order of 13.113. The reaction rate constants
cannot be compared directly since the units differ for each rate
constant. However, these results again indicate that a simple rate
expression cannot adequately fit the data. Hence, some complex models
were considered next.

TABLE XXVII

RESULTS FROM DIFFERENTIAL METHOD OF
DETERMINING THE ORDER OF REACTION

Series	Temperature C ($^\circ$F)	Order of Reaction	Reaction Rate Constant
KEC	343 (650)	2.581	0.737
KEC	371 (700)	1.004	0.501
KEC	399 (750)	13.113	3.018
KET	343 (650)	0.918	2.936
KET	371 (700)	0.452	0.589
KET	399 (750)	0.222	0.043

Flinn, et al. (47) showed that the ease of denitrogenation tends

to decrease with the increasing boiling point of a petroleum feed.

Satchell (6) estimated the reactivity of the organonitrogen species

in the feed used in this study by analyzing boiling point ranges of the

feed and product oils for organonitrogen level. He developed a model

to predict the nitrogen content of the product oil from the trickle bed

reactor assuming that the rate of denitrogenation is a linear function

of the boiling point of the individual fractions of the feed. However,

his reaction rate constants were calculated from data at a single space

time since he did not have sufficient data at other space times. Since

Satchell used the same feedstock that was used in this study, a fit

of his model to the data of this study would be interesting; however,

applying his model is not possible in the light of information gathered

from this study. Results from the present study (Appendix H) showed

that reaction rate constants calculated using data obtained from

different space times do not follow a definite trend with boiling points of the individual fractions. Hence, Satchell's model could not be used to test the data from this study. Appendix H gives a detailed description of Satchell's model and results from this study.

All the models tested so far were for completely ideal situations, where backmixing, holdup and incomplete catalyst wetting were negligible. The low flow rates used in this study, which are characteristic of bench scale operations, can magnify poor wetting of the catalyst and cause conversion rates that vary with liquid velocity. Due to the practical novolatility of the liquid phase reactants under reactor operating conditions, the reaction is often confined to the effectively wetted liquid-solid area. Several equations have been reported to account for holdup and incomplete catalyst wetting effects in trickle bed reactors (25, 31, 32).

In a completely ideal situation where backmixing and holdup or incomplete catalyst wetting effects are negligible, the governing equation for the reactor performance for a first order reaction may be expressed as:

$$\ell n \ (C_{A_0}/C_{A_f}) \ = \ \ell n \ (\frac{1}{1 \ - \ x}) \ = \ k_a/LHSV \qquad (7.4)$$

where C_{A_0} and C_{A_f} are the concentrations of a reactant at the reactor inlet and outlet respectively, and k_a is the apparent kinetic rate constant which includes the catalyst effectiveness factor and the void fraction of the catalyst bed and LHSV is the liquid volume hourly space velocity.

Ross (25) and Nakamura, et al. (109) proposed that k_a is proportional to $k_t H$, where k_t is the true reaction constant and H is the dynamic liquid holdup. Henry and Gilbert (31) extended this by

substituting the dynamic holdup correlation of Satterfield, et al. (39):

$$H = K R_e^{1/3} G_a^{-1/3} \qquad (7.5)$$

where

H = dynamic liquid holdup

K = proportionality constant

R_e = Reynold's number based on particle diameter

G_a = Galileo number based on particle diameter.

In the relationship $k_a \propto k_t H$. This substitution resulted in the simplified model:

$$\ell n \frac{C_{A_o}}{C_{A_f}} \propto (L)^{1/3}(\text{LHSV})^{-2/3}(d_p)^{-2/3}(\nu)^{1/3} \qquad (7.6)$$

where

L = length of reactor bed, ft

LHSV = liquid hourly space velocity, $ft^3/hr/ft^3$

d_p = characteristic diameter of catalyst particle, ft

ν = kinematic viscosity, ft^2/hr.

Part of Mears' data (13) in a laboratory were satisfactorily correlated by the holdup model of Henry and Gilbert. However, Mears (32) later showed that some of his data cannot be evaluated with the holdup model of Henry and Gilbert. He questioned the role of liquid holdup in trickle bed reactors, and noted that the empirical dependence of Henry and Gilbert conversion model on the 1/3 power of velocity does not agree with the exponent of 0.75 suggested by the literature for dynamic holdup in packed beds. Mears noted that the exponent, however, is

consistent with reported exponents of about 1/3 for the velocity dependence of the effectively wetted area. He hypothesized that the apparent reaction rate constant, k_a, is proportional to the true rate constant on a completely wetted catalyst. By substituting the wetted surface area correlation by Puranic and Vogelpohl (110), Mears arrived at the following relationship:

$$\ln \frac{C_{A_o}}{C_{A_f}} \ \alpha \ (L)^{0.32}(LHSV)^{-0.68}(d_p)^{.18} \ (\nu)^{-0.05}(\sigma_c/\sigma)^{0.21} \eta d_p$$

$$(7.7)$$

where

$$
\begin{aligned}
L \ &= \ \text{catalyst bed length, cm} \\
LHSV \ &= \ \text{liquid hourly space velocity, } cm^3/hr \ (cm^3 \ \text{catalyst}) \\
d_p \ &= \ \text{size of catalyst particle, cm} \\
\nu \ &= \ \text{kinematic viscosity, } cm^2/sec \\
\sigma_c \ &= \ \text{critical value of the surface tension for a given packing, } grams/sec^2 \\
\sigma \ &= \ \text{surface tension of the liquid, } grams/sec^2 \\
\eta d_p \ &= \ \text{effectiveness factor, dimensionless.}
\end{aligned}
$$

For a given catalyst and feedstock, both Mears' and Henry and Gilbert's correlations reduce to

$$\ln \frac{C_{A_o}}{C_{A_f}} \ = \ \frac{k(L)^y}{(LHSV)^{1-y}}$$

$$(7.8)$$

where the proportionality constant k includes the effect of catalyst particle size and physical properties of the feedstock, and y is equal to 0.32 for the Mears' correlation and 1/3 for the Henry and Gilbert correlation. If the catalyst bed length were held constant this equation reduces to

$$\ell n \, \frac{C_{A_o}}{C_{A_f}} \; = \; k(\text{LHSV})^{-x} \tag{7.9}$$

where $\quad$ $x = 1 - y.$

Values of k and x were calculated using a least square curve fit based on the data of this study and the results are presented in Table XXVIII. In addition, Table XXVIII also presents the sum of squares of the error using this model to predict the product oil nitrogen concentration.

A number of observations can be made from this table. The sum of squares of the error are comparable to that obtained using simple power law models. The values of the exponents varied from 0.306 to 0.932. Also, the reaction rate constants predicted from this model (Equation 7.9) seem to agree with the observed performance of the catalysts better than the simple model presented in Equation 7.2. The discrepancies that were pointed out earlier in the other model do not exist in the results obtained from the model presented by Equation 7.9. For example, the reaction rate constants for the KET series are lower than the reaction rate constants for the KEC series which agrees with the observed performance of the catalysts. The reaction rate constants for the CAT series and all other series increases with increase in temperature, which was not observed in the earlier model. The rate constants for the KDC, KDT and KDP series are close to each other confirming the experimental evidence. Summarizing, the exponential model (as this model will be called from now on) predicts the experimental data better than the earlier model.

TABLE XXVIII

RESULTS FROM REGRESSION ANALYSIS

Run Series	Temperature °F	Value of the exponent x	Error sum of squares	k first order reaction rate constant $(hr)^{-x}$
KEC	650	0.393	0.148	0.692
KEC	700	0.525	0.266	1.029
KEC	750	0.445	0.191	1.585
KET	650	0.803	0.628	0.497
KET	700	0.932	0.835	0.697
KET	750	0.563	0.324	1.089
KEP	650	0.463	0.212	0.433
KEP	700	0.306	0.090	0.720
KEP	750	0.481	0.223	1.246
KDC	700	0.797	0.625	0.721
KDT	700	0.674	0.438	0.473
KDP	700	0.626	0.377	0.618
CAT	650	0.627	0.379	0.467
CAT	700	0.391	0.150	0.787
KER	650	0.581	0.352	0.529
KER	700	0.466	0.213	0.223
KER	750	0.359	0.124	1.450

However, one may question the rate constants and the basis of the
model, since the value of the exponent varies from 0.306 to 0.932.
Paraskos, et al. (38) analyzed data derived from isothermal, isobaric
hydrotreating of 53% reduced Kuwait crude and various types of gas oils
in pilot plant trickle bed reactors on the basis of holdup and incomplete
catalyst wetting models. The slopes (x values) of log-log plots of
$\ln C_{A_o}/C_{A_f}$ vs. 1/LHSV varied from 0.532 to 0.922 for desulfurization
and demetallization reactions. For hydrodenitrogenation the slopes
were found to be approximately 0.766 at 393C (740F) and 0.747 at
416C (780F). Their results confirm the results from this study that
the values of the exponent vary with reaction conditions. Paraskos,
et al. concluded that in a reacting system, the power law coefficient
in the holdup or effective catalyst wetting-LHSV relationship may be
dependent on the reaction conditions. Neither their study nor the
results from this study could establish a definite correlation between
the power-law coefficients and the operating conditions. However,
some considerations can be addressed to explain the reasons for the
wide variations in the values of the exponents.

The correlation of Puranik and Vogelpohl (110) used by Mears to
arrive at his final equation, was empirical in nature and was developed
for incomplete contacting in adsorbers packed with different packing
size and shape. The packing sizes ranged from 0.8 cm to 3.5 cm.
Puranik and Vogelpohl claim that the wetted surface area can be
correlated by their equation within a maximum error of ± 20 percent.
They presented a plot comparing predicted vs. experimental data. An
examination of the plot indicates that for particle sizes of 0.8 cm, the
deviation from experimental value is close to 20 percent. Even the

particle size of 0.8 cm is still much larger than the particle sizes used in this study (0.22 cm). Puranik and Vogelpohl's correlation is expressed as:

$$\frac{a_w}{a_t} = 1.05 \ (R_e)^{0.047} (W_e)^{0.135} (\sigma_c/\sigma)^{-0.206} \tag{7.10}$$

where
R_e = Reynold's number based on particle size

W_e = Weber number based on particle size

σ_c = critical value of surface tension for a given packing, $grams/sec^2$

σ = surface tension of the liquid, $grams/sec^2$.

If the maximum error is to be incorporated into this equation, and then substituted in Equation 7.8, then the value of the exponent will definitely change. However, it seems reasonable to assume that the wetted surface area will be some function of the space velocity, depending on reaction conditions.

The question about the validity of comparing the reaction rate constants still remains to be answered. The apparent reaction rate constants calculated based on the exponential model is a function of the true reaction rate constant and all the other variables like kinematic viscosity, surface tension, particle size, etc. In a mathematical form,

$$k_a = K' \ k_t \tag{7.11}$$

where
k_a = apparent reaction rate constant

k_t = true rate constant

K' = $f(\rho, \ \sigma, \ L, \ d_p, \ \nu, \ \sigma_c)$.

However, for a given feedstock and given particle size, K' should remain constant. The same feedstock was used in five runs in this

study. The other three used the same feedstock doctored with quinoline.
Two different particle sizes were used in this study. The effectiveness
factor will be shown to be one for this study. Taking these factors
into consideration, the value of K' should remain the same for this
study. Hence, the apparent reaction rate constants calculated based
on the exponential model are proportional to the true reaction rate
constants and in order to compare the relative activities of the differ-
ent catalysts, these reaction rate constants can be used. The fact
that these reaction rate constants agree very well with the observed
performance of the catalysts provides additional evidence towards
accepting these reaction rate constants as quantitative measures of
comparison.

An attempt was also made to fit the data to the wetting model based
on second order reaction such as

$$1/C_{A_o} - 1/C_{A_f} = k \, (LHSV)^{-x} \, . \tag{7.12}$$

Table XXIX presents the sum of squares of the error for the first and
second order models and shows that the sums of squares of the error
for the first order model were lower for every data set than the sums
of squares of the error for the second order model.

All of the above evidence suggest that if catalyst wetting effects
are taken into account, denitrogenation is first order and the model
presented in Equation 7.9 fit the data best out of the various models
tested. Hence, the reaction rate constants calculated using the above
model will be used for further discussion. Figure 40 presents a typical
plot comparing the experimental data and the predicted data by the
exponential model.

TABLE XXIX

COMPARISON OF FIRST AND SECOND ORDER MODELS

Series	Temperature °F	Error Sum of Squares	
		First Order Model	Second Order Model
KEC	650	0.148	0.285
	700	0.266	0.688
	750	0.190	0.732
KET	650	0.628	0.984
	700	0.885	1.642
	750	0.324	0.923
KEP	650	0.212	0.313
	700	0.090	0.177
	750	0.223	0.658
KDC	700	0.625	1.175
KDT	700	0.438	0.681
KDP	700	0.377	0.665
CAT	650	0.379	0.588
	700	0.150	0.303
KEP	650	0.352	0.605
	700	0.213	0.463
	750	0.124	0.445
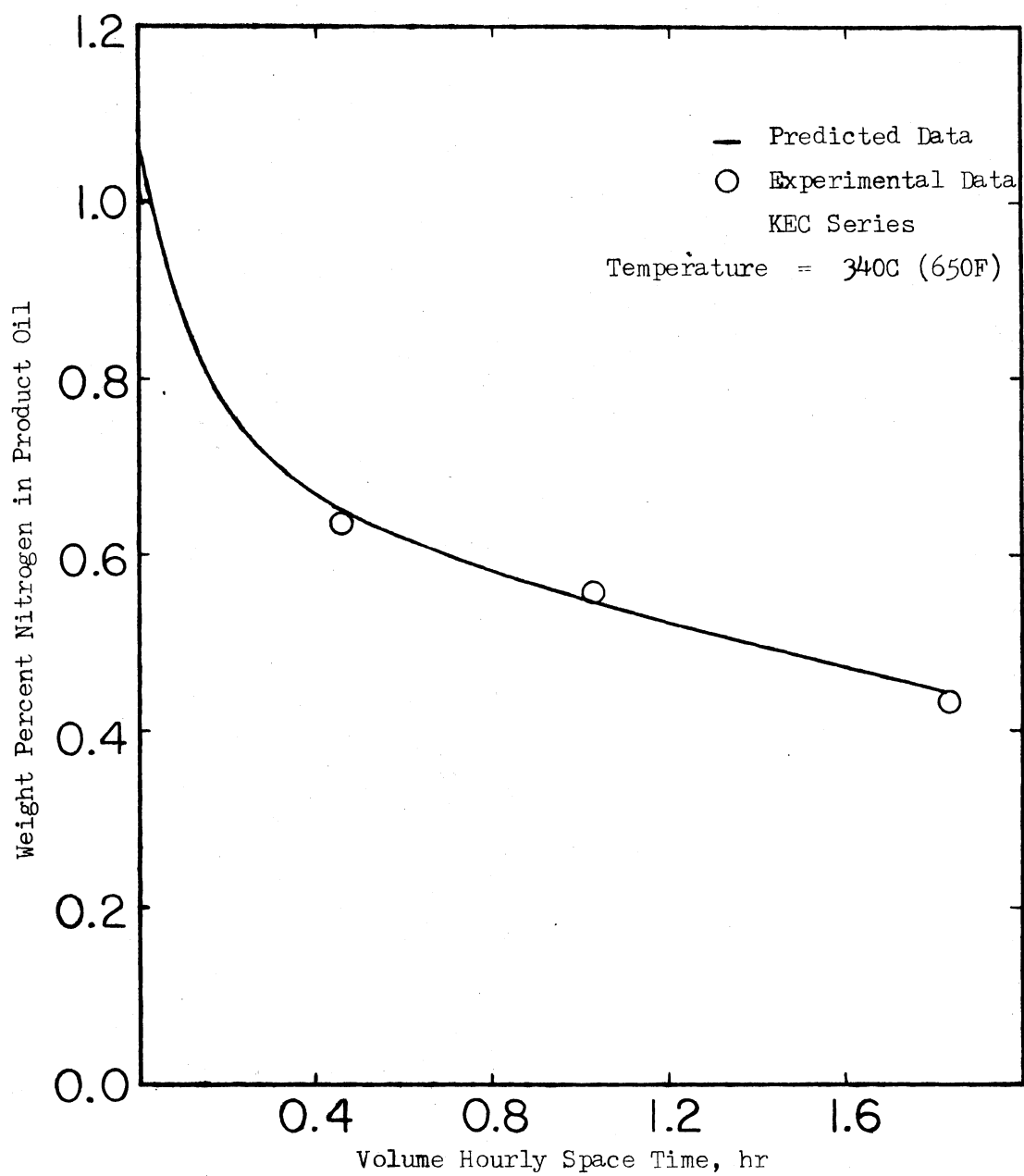
Figure 40. Comparison of Experimental Data to Predicted Data

The effect of reactor operating temperature on the rate constant is usually expressed by the Arrhenius equation:

$$k = A e^{-E/RT} \qquad (7.13)$$

where

k = rate constant

A = frequency factor

E = activation energy

R = universal gas constant

and T = absolute temperature.

Table XXX presents the activation energies calculated for the various catalysts used in this study.

TABLE XXX

ACTIVATION ENERGIES

Run Series	Support Used	Activation Energy BTU/lb mole	Temperature Range C (F)
CAT	CONOCO CATAPAL HP-20	26600	343-371 (650-700)
KEC	Ketjen 007-1.5E	21900	343-399 (650-750)
KET	Steam Treated Ketjen 007-1.5E	20900	343-399 (650-750)
KEP	Ketjen 000-3P	28000	343-399 (650-750)
KER	Ketjen 007-1.5E	26700	343-399 (650-750)

Table XXX reveals that the activation energies ranged from 21900 to 28000 Btu/lb mole for the catalysts used in this study. White, et al. (60) studied hydrotreating of COED oil using a nickel-molybdate catalyst. They used a first order rate expression to calculate activation energies and observed an activation energy of 48,500 Btu/lb mole at temperatures below 399C (750F). At temperatures above 399C (750F), an activation energy of 16,400 Btu/lb mole was observed. Satchell (6) using the same feedstock as used in this study, observed an activation energy of 31,000 Btu/lb mole for the commercial Nalcomo 474 Co-Mo catalyst in the temperature range of 316 to 399C (600-750F) and an activation energy of 12,300 Btu/lb mole in the temperature range of 399-427C (750-800F). Quader and Hill (67) studied the hydrotreating of low temperature coal tar over a Co-Mo catalyst and observed an activation energy of 15,900 Btu/lb mole in the temperature range of 401-500C (752-932F). The work of White (60), Satchell (6) and Quader and Hill (67) indicate that there is an abrupt decrease in the activation energy at about 399C (750F). Since no data were taken at temperatures beyond 399C (750F) in the present study, this observation cannot be confirmed for this study. The activation energies calculated in this work are lower than the other studies at temperatures below 399C (750F). The fact that different feeds and catalysts were used in each study could account for the difference in activation energies.

Effects of Catalyst Support
Properties

Experience in the petroleum industry suggests that the properties of the catalyst support material do affect performance of the

hydrotreating catalysts (75). One of the major objectives of this work was to study the effects of catalyst support properties such as surface area and pore size distribution on nitrogen removal from raw anthracene oil, a coal derived liquid. This section discusses such effects.

Pore Size and Pore Size Distribution

The main functions of the catalyst support are to provide a structural framework for the catalyst component and to increase the surface area per unit weight of metal above that of unsupported metal. The availability of the internal surface area can depend upon the size of the openings. This is because, in a given catalyst preparation, the distribution of pore sizes may be such that some of the catalyst is completely inaccessible to large reactant molecules and, furthermore, may restrict the rate of conversion of the reactants by impeding the diffusion of reactants in the internal pore structure. Hence, knowledge regarding detailed pore structure of the catalyst is desirable. Commercial catalysts and catalyst carriers do not have simple pore structures. Hence, a simplified model of the pore structure is necessary to be able to predict the effect of pore sizes on conversion. In all the widely used models the void spaces are simulated as cylindrical pores. Hence, the size of the void space is interpreted as radius r of a hypothetical cylindrical pore, and the distribution of pore volume is defined in terms of this variable. For this study, the cumulative pore volume as a function of the pore radius was determined by using mercury porosimetry performed by a commercial laboratory. The measurements of mercury intrusion per gram of catalyst as a function of applied pressure for all the supports used in this study are

presented in Appendix B.

Figures 13 and 14 presented in Chapter V are two typical results of mercury penetration porosity to 60,000 psia pressure performed by the American Instrument Company, Inc., on two of the supports used in this study. The curves obtained in Figures 13 and 14 are developed from the volume of mercury penetrated into the samples for different pressures, and are plots of $dV/d(\ell n\ r)$ against pore radius r, where the term dV is the change in cumulative volume for a definite change in pressure, and $d(\ell n\ r)$ is the differential of the natural log of the average pore radius corresponding to the same pressure change. Similar curves were obtained for all the supports and the impregnated supports (catalysts) used in this study. Appendix B contains the mercury penetration data used to prepare these curves. These curves are really frequency plots and indicate the pore size distribution of the catalysts and catalyst supports.

In the absence of pore distribution curves, average pore radius, defined by

$$\bar{r} = 2\ V_g/S_g \tag{7.14}$$

where
$\bar{r}$ = average pore radius, $\overset{\circ}{A}$

V_g = cumulative pore volume, cc/gm

S_g = surface area, m^2/gm

is normally employed to compare different catalysts. However, in this study, most frequent pore radii (defined in page 101) of the different catalysts will be used to compare them, since this variable presents a better evaluation of the pore distribution effects than the above average pore radius. Two more variables, the pore distribution factor

(PD) and most frequent pore diameter spread (ΔD_r) are calculated from these curves. The method of calculation of these variables are presented in Appendix M. The effect of the most frequent pore radius of catalyst supports on nitrogen removal will be discussed first followed by a discussion on the effects of pore size distribution on nitrogen removal.

Catalysts made from the Ketjen support 007-1.5E, untreated with steam (KEC series) and those made from the same support with 10 hours steam treating (KET series) provide a measure of comparison of pore size and distribution. Steam treating had shifted the most frequent pore radius from 33 Å to 38 Å, which is a change of 15% relative to the smaller size. However, the two catalysts used in these two series (KEC and KET series) were identical in every respect except for the support properties. Figures 16, 17 and 18 presented in the results section compare the two catalysts at the three temperatures used in this study. The steam treated catalyst used in the KET series was consistently less active than the catalyst used in the KEC series at all temperature levels as measured by the total nitrogen remaining in the product oil. The figures reveal this and the magnitude of the rate constants offer a quantitative measure.

Figure 23 shows a comparison of two bidispersed catalysts used in this study having about the same surface area (199 and 218 m^2/gm) but with varying pore radii, especially the macro pores (36 and 160 Å vs. 40 and 1900 Å). As can be seen from the figure, the differences in their activity was very small, with the higher surface area catalyst showing a slightly greater activity. Similar results were obtained when raw anthracene oil doctored with quinoline was used as a feedstock

over the catalysts prepared from the supports Ketjen 007-1.5E (KDC series) and the 10 hour steam treated Ketjen 007-1.5E (KDT series). Figure 24 presents a comparison of the results obtained from these two series. As noted with undoctored raw anthracene oil feedstock, the steam treated support used in the KDT series tends to be less active than the base support.

In hydrodesulfurization studies, using raw anthracene oil and similar catalysts, increasing the pore radius tends to increase sulfur removal (7). However, Satchell (6) found that increasing the pore radius from 25 to 33 Å had no effect on nitrogen removal from raw anthracene oil. Van Zoonen and Douwes (42) studied the effect of volume average pore radius with Co-Mo-Alumina catalysts on the rate of denitrogenation of a Middle East gas oil. Their study showed that for two catalysts with similar surface areas (190 and 204 m^2/gm), but with different average pore radii (33 and 73 Å), the average pore radius had a negligible effect on the rate of denitrogenation. However, for desulfurization, they found that pore sizes influence conversion.

With both sufrace area and pore radius changing, predicting the effects on nitrogen removal becomes difficult. However, from Figure 23, where two catalysts with varying pore properties produced almost similar nitrogen removal and taking Satchell's and Van Zoonen's study into consideration, nitrogen removal from this coal liquid, raw anthracene oil, was relatively insensitive to pore radius changes in the range between 25 and 40 Å. However, these results should be assessed for other coal derived liquids. One might expect that as the feedstock became more difficult to hydrotreat, and with higher boiling components, then the increasing pore sizes should begin to offer an

advantage. Also, with ash containing feeds, the large pores could offer an advantage in their ash tolerance while still maintaining activity.

Another possibility is that the entire pore structure of the catalysts was never filled with raw anthracene oil. If the outer surface area of the catalyst pellets or particles is soaked with raw anthracene oil and not the internal pores, then the reaction will take place only on the outer surface area. In that case, the pore structure of the catalyst would have no influence in the conversion of organo-nitrogen species. Also if the entire surface area available in a catalyst pellet can not be contacted by the liquid, the reactant conversion will be less than maximum. By assuming that the effectiveness factor was close to unity, one assumes that the entire surface area of the catalyst pellet is available for reaction. An attempt was made to determine whether raw anthracene oil does in fact fill the entire pore volume of the catalysts.

Simple calculations were performed based on the Kelvin equation for capillary condensation (111). Detailed calculations and the Kelvin equation are presented in Appendix L. The equation predicted that at a temperature of 391C (700F) and a pressure of 1500 psig all the pores up to 13 Å will be filled with raw anthracene oil. However, in this calculation the surface tension calculated at room temperature was used. Surface tension decreases with increasing temperature. Since, r , the pore radius up to which the pores will be filled is directly proportional to surface tension, with decreasing surface tension, the actual value of r will be lower than 13 Å. This means that raw anthracene oil will fill essentially all the pores at reaction conditions.

A simple experiment has been conducted by Ketkar (112), that provides additional evidence that raw anthracene oil does fill the pores of two of the catalyst supports used in this study by capillary condensation at room temperature. The experiment consisted of weighing single catalyst pellets, immersing them in raw anthracene oil for a period of time, removing them and weighing the pellets after wiping the oil that is sticking to the outer surface. Several samples were taken so as to check the reproducibility. Ketkar found that for both the supports (Ketjen 007-1.5E and Ketjen 000-3P), raw anthracene oil filled the entire pore volume of the supports within one hour. If raw anthracene oil can fill all the pores at room temperature and ambient pressure, it seems reasonable to assume that the pores were filled with liquid in this study at reaction conditions. Since raw anthracene oil can diffuse through the entire pore volume of the catalyst supports used in this study, the changes in pore sizes did not have any effect on nitrogen removal.

Pore size distribution, a measure of the pore volume as a function of the pore radius, is often neglected in the discussion of the effect of catalyst support properties on hydrotreating. One of the reasons may be that simple parameters such as most frequent pore radius cannot completely characterize a pore distribution curve. Sooter (7) gave several examples of various pore size distributions, which are presented in Figure 41. In this figure, if (a) represents the pore distribution of a base support which can be classified as a narrow distribution, then (b) shows broadening on both sides of the average, (c) shows broadening in the direction of smaller pores, (d) shows broadening in the direction of larger pores and (e) shows broadening by means of a bimodal type
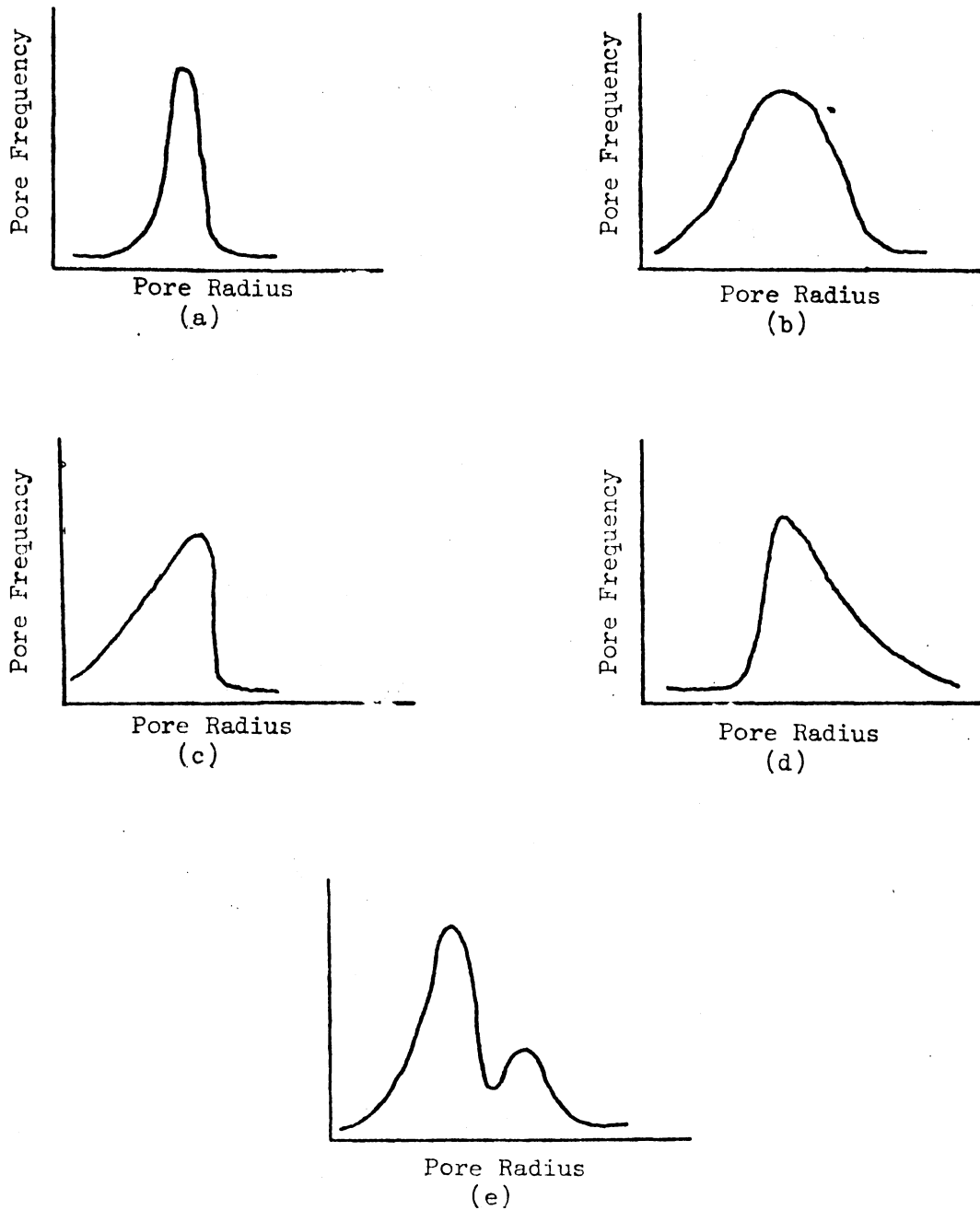
Figure 41. Examples of Various Pore Size Distributions

distribution. One patent (U.S. 2,890,162) presents some arbitrary methods of characterizing pore size distribution to quantify their effects on hydrotreating based on results obtained by hydrodesulfurization of gas oil feedstocks. Because of the absence of standard methods for characterizing pore size distribution, the methods recommended by the patent will be used for further discussion.

Briefly, the patent recommends a most frequent pore diameter (D_f) of above 60 Å and a spread of the range of the most frequent pore diameter (ΔD_r) of at least 10 Å for hydrodesulfurization. Also, a pore distribution factor (PD) of at least 5.0 is preferred by the patent. (The method of calculation of these variables are presented in Appendix M.) Table XXXI lists these variables for the catalysts used in this study. As can be seen from Table XXXI, all the catalysts used in this study met the specifications presented in the patent. Sooter (7) in his study on hydrodesulfurization of raw anthracene oil, found that two of his catalysts that were short of the necessary minimum ΔD_r and PD values described in the patent performed poorly compared to a catalyst that did meet the specifications. However, Satchell (6) using the same catalysts found no such effects for denitrogenation. In the present study, bimodal pore distribution did not offer any obvious advantages over monodispersed catalysts. Two of the catalyst supports used in this study had bimodal pore distribution (CAT, KEP and KDP series). CAT and KEP series used raw anthracene oil as feedstock while KDP series used doctored raw anthracene oil as feedstock. Both CAT and KEP catalysts were less active than the monodispersed catalyst used in the KEC series at all temperatures. For example, at 371C (700F) and at a space time of 1.84 hrs, the percent removal for the KEC, KEP and CAT were 77, 58

TABLE XXXI

PORE PROPERTIES OF CATALYSTS USED
IN THIS STUDY

Run Series	Support Used	D_f	ΔD_r	PD
KEC	Ketjen 007-1.5E	62	18	6.9
KET	Steam treated (10 hrs) Ketjen 007-1.5E	76	30	17.3
KEP	Ketjen 000-3P	72,320	44*	22.8
KER	Ketjen 007-1.5E	66	20	8.7
KDC	Ketjen 007-1.5E	62	16	6.2
KDT	Steam treated (10 hrs) Ketjen 007-1.5E	78	28	17.0
KDP	Ketjen 000-3P	66,360	52*	22.7
CAT	CONOCO CATAPAL HP-20	80,3800	44*	28.2

* Most frequent pore diameter spread for micropores.

and 63% respectively. When raw anthracene oil doctored with quinoline was used as the feedstock, the bidispersed catalyst used in the KDP series was comparable to the monodispersed catalyst used in the KDC series, but not more active. Hence, pore size distribution does not seem to affect nitrogen removal from raw anthracene oil over the range of parameters tested. However, it is possible that for nitrogen removal, the minimum values of the parameters used (ΔD_r and PD) may be different, possibly lower than those employed for sulfur removal. Also with heavier feedstocks, pore size distribution may begin to have an effect on nitrogen removal. Further studies should be made using

heavier feedstocks and with catalysts having smaller pore sizes and
narrow pore size distributions to find out whether there exists a
minimum value for these values, above which pore size and pore size
distribution cease to have an effect on nitrogen removal.

Surface Area

The total and active surface area available for reaction may be
an important parameter to be considered when comparing catalyst supports.
Catalysts made from the Ketjen support 007-1.5E, untreated with steam
(series KEC) and those made from the same support with 10 hours steam
treating (series KET) provide a measure of the effect of the change in
surface area on nitrogen removal. Steam treating the support consider-
ably reduced the total surface area available, while slightly increasing
the most frequent pore radius. The catalyst used in the KET series had
a surface area of 230 m^2/gm while the catalyst used in the KEC series
had a surface area of 291 m^2/gm, a 27% change relative to the lower
value. Referring back to Figures 20, 21 and 22 (pp. 127, 128 and 129),
if changes in pore radius had little or no effect on nitrogen removal
then the lower surface area of the catalyst used in the KET series can
possibly account for the lower activity of the catalyst. Similar
results were obtained when raw anthracene oil doctored with quinoline
was used as a feedstock over the catalysts prepared from the supports
Ketjen 007-1.5E untreated with steam (KDC series) and 10 hour steam
treated Ketjen 007-1.5E (KDT series). The KDC catalyst had a surface
area of 252 m^2/gm while the catalyst used in the KDT series had a surface
area of 220 m^2/gm. Figure 24 presents a comparison of the results
obtained from these two series. As noted with undoctored raw anthracene

oil feedstock, the steam treated support used in the KDT series tends to be less active than the base support.

Another possibility is that the intrinsic activity of the catalysts are different. However, this is not likely because a more conclusive proof of the effect of surface area on nitrogen removal can be found by examining Figure 16 which compares the two series KEC and KER. The catalysts used for the KEC and KER series were prepared from the same support (Ketjen 007-1.5E) and were designed to be replicates. However, the surface areas of the two catalysts were different (291 vs. 243 m^2/gm). This was discussed in the results section (p. 119) and Table XX in the results section presents the properties of the two catalysts.

The changes in pore volume and most frequent pore radius are negligible and within the precision of measurement of these variables. The change in surface area falls outside the range of precision in measuring the surface area ($\pm$ 10 m^2/gm). Figure 16 reveals that the catalyst used in the KER series was consistently less active than the catalyst used in the KEC series at all three temperature levels. The two catalysts were similar in every respect except for the change in surface area; this reduction of surface area resulted in lower conversion of organonitrogen species.

If the conclusion that average pore radius has a negligible effect on nitrogen removal is valid, then Figure 23 offers further evidence that reduction in nitrogen removal follows reduction in surface area. It shows that the catalyst used in the CAT series with a surface area of 218 m^2/gm was more active than the catalyst used in the KEP series which had a surface area of 200 m^2/gm. While the activity differences

are small, the greater activity is consistently favored by the greater

surface area.

Reaction rate constants based on unit surface area were calculated

in order to obtain further confirmation of the surface area effects on

denitrogenation. The reaction reate constant, k_s, based on unit

surface area was calculated from the reaction rate constants based on

reactor volume calculated earlier using the following relationship:

$$k_s = kV_r/S \qquad (7.15)$$

where $\quad k_s$ = reaction rate constant based on unit

surface area, $cm/(hr)^X$

k = reaction rate constant based on reactor

volume, $(hr)^{-X}$

V_r = Volume of the reactor catalyst bed, cc

S = total surface area, m^2.

Table XXXII presents the k_s values calculated for all the catalysts

used in this study. In order to compare the k_s values between different

catalysts, an uncertainty analysis (113) was made and the uncertainties

are presented in the table along with the k_s values. Details of the

undertainty analysis can be found in Appendix I.

If denitrogenation is sensitive to total available surface area

and if the intrinsic activities are the same and if changes in pore

sizes are unimportant, the k_s values should remain the same. The

catalysts used in the KEC and KET series were essentially the same

except for changes in the physical properties of the supports caused

by steam treating and the catalyst used in the KER series was a

replicate of the KEC series. A comparison of the k_s values for the KEC,

KET and KER series reveals that k_s values do remain constant within

TABLE XXXII

COMPARISON OF k_s VALUES

Temperature C (F)	$k_s \times 10^7$, cm/(hr)^X							
	KEC Series	KET Series	KER Series	KEP Series	CAT Series	KDC Series	KDT Series	KDP Series
340 (650)	3.41±0.28	3.52±0.36	3.06±0.29	3.71±0.39	3.71±0.39	--	--	--
371 (700)	5.09±0.41	4.93±0.47	5.11±0.43	6.17±0.58	6.26±0.57	4.17±0.30	3.48±0.28	5.06±0.40
399 (750)	7.83±0.67	7.72±0.68	8.41±0.72	10.68±0.99	--	--	--	--

experimental precision. These observations confirm that the lower
activity of the catalyst used in the KET series can be attributed to
the lower surface area of the KET catalyst ($230\ m^2/gm$) as compared to
the KEC catalyst ($290\ m^2/gm$). Same observation is true when KEC and
KER series are compared. The k_s values remain within experimental
uncertainty, for the KDC and KDT series which used doctored raw anthra-
cene oil as feedstock. The catalysts used in these two series were the
same except for the physical properties of the support. Hence, it can
be concluded that changes in surface area of the catalyst support
materials are more sensitive to nitrogen removal than changes in pore
radius over the range of variables tested and for these catalysts.

The k_s values for the other two supports used in this study, Ketjen
000-3P and CONOCO CATAPAL HP-20 are slightly higher than the k_s values
for the catalysts used in the KEC, KET and KER series, as can be seen
from Table XXXII. A discussion on these will be presented in the next
chapter. These two supports had lower surface areas (190 and $218\ m^2/gm$)
compared to the KEC ($290\ m^2/gm$) or the KET ($230\ m^2/gm$) catalysts. Still
the activities of these two catalysts seem to be higher on a per unit
surface area basis. This leads one to believe that the CAT catalyst
and the KEP catalyst could have been more active, if these catalyst
supports had been prepared with a larger surface area.

Another question that arises is the effect of active metal con-
centration per unit surface area. Since active metal concentration is
measured in terms of weight percents, the lower surface area catalysts
would have a higher active metal surface concentration if the same
weight percent of active metals are employed. However, the changes in
active metal concentration per surface area changes are relatively small

(0.00012 gm of MoO_3/m^2 for the KEC series vs. 0.00015 gm of MoO_3/m^2 for the KET series) and published information on the optimum concentration of active metals ranges from 2-4% Co as CoO and 8-15% Mo as MoO_3 (74). Also, increasing concentration of active metals beyond these optimum values has no significance in increasing the hydrotreating activity of catalysts (70). Hence, one can reasonably assume that the changes in active metal surface concentration did not have any effects on nitrogen removal in this study.

Comparison of Catalysts

The activity of a catalyst pellet at any time can be defined as (114)

$$a = \frac{\text{rate at which pellet converts reactant A}}{\text{rate of conversion of A with a fresh pellet}}$$

Hence, deactivation starts to occur when the rate of reaction with a used pellet starts to decrease. One of the major objectives of the program at Oklahoma State University of which this study is a part is to tailor hydrotreating catalysts specifically for coal derived liquids and this section will discuss the activities of the catalysts used in this study in an attempt to explain the reasons for the differences in activity.

Effect of Catalyst History

Even though a full assessment of catalyst deactivation was not a part of this study, the stability of the catalyst activity at any temperature was estimated by comparing the 1.84 hours space time results at the beginning and the end of a series of isothermal runs. Also, before shutting down, the reactor was always brought to the same

operating conditions that existed at the beginning of the run to check whether any deactivation had taken place. Table XIX in the results section presents the results from these check points, and reveals that very little or negligible nitrogen removal deactivation has taken place. This is not surprising since the total hours of oil on catalysts used in this study never exceeded 130 hours. Previous studies with raw anthracene oil and Co-Mo-Alumina catalysts (6) have indicated no catalyst deactivation up to 200 hours of operation. However, some coal liquids feedstocks have shown significant deactivation over the operational time interval (9).

Catalyst deactivation can also occur due to regular changes in operating conditions as a scheduled part of an experimental run. In all the runs in this study the pressure was held constant and the operational changes were only in temperature and space time. Satchell (6) studied catalyst deactivation as a function of the changes in operating conditions. He compared the catalyst activity when the reactor was previously operated at a higher or lower temperature with runs in which the catalyst was operated at only one temperature throughout its history. Satchell concluded that catalyst deactivation associated with a reduction in operating temperature was much greater than the deactivation resulting from isothermal operation or increase in reactor operating temperature. The only time the reactor operating temperature was decreased in this study was at the end of the run when the reactor was brought to the initial conditions that existed at the beginning of the run. In order to do this, the reactor temperature was brought down from 399C (750F) to 340C (650F). As can be seen from Table XIX, appreciable deactivation has taken place. Hence in this study,

deactivation is shown to be negligible under the conditions tested.

Effectiveness Factor

The utilization of a catalyst's total surface area can be quantified by the value of the effectiveness factor. The effectiveness factor is defined as the ratio of the actual measured reaction rate to that which would be observed if all of the entire surface of the catalyst pellet were exposed to the catalyst outer boundary reactant condition. One of the ways of estimating the effectiveness factor is to compare the catalyst performance of two or more catalyst particle sizes. If the effectiveness factor is unity, then the rate is independent of the particle diameter.

This study used two different particle sizes. Experimental series CAT, KEP and KDP used 8/10 mesh size. Experimental series KEC, KET, KER, KDC and KDT used 1/16 inch extrudates as supplied by the manufacturer. These extrudates were used as such because their diameter was smaller than the 8/10 mesh particle and would pass through a 8 mesh screen. Hence, in order to compare the results from these runs, the effect of particle size on conversion should be known. Satchell (6) using the same feedstock as used in the present study found the effectiveness factor to be close to one in his study. Satchell estimated the effectiveness factor using 8/10 mesh vs. 40/48 mesh to be one at temperatures of 340 and 371C (650 and 700F) and at a pressure of 1000 psig. The catalysts used in Satchell's study had pore sizes similar to the catalysts used in this study (most frequent pore radius of 33 $\overset{o}{A}$). Because of the similarities of operating conditions and the catalysts between Satchell's and this study, the effectiveness factor

was taken as unity for this study. The difference in particle sizes
of the extrudates and 8/10 mesh catalyst should have negligible effect
on the conversion of organonitrogen species.

Overall Activity of Catalysts

As pointed out earlier no catalyst denitrogenation deactivation
was observed in this study. Hence, the catalysts in this study will be
compared on a relative basis. If catalyst A removes more nitrogen than
catalyst B under identical operating conditions, then catalyst A is
considered as more active than catalyst B. One of the ways a comparison
between different catalysts can be made is to compare the reaction rate
constants for each series. Hence, in this section a comparison of the
catalysts tested in this study will be made based on reaction rate
constants. Since catalyst screening is one of the major objectives
of the program at Oklahoma State University, several catalysts that
were used to hydrotreat the feedstock used in this program by previous
investigators will be compared. But this comparison of catalysts
tested by others will be made based on percentage conversion at the
same operating conditions.

A total of eight experimental runs were made for this study;
however, only four different supports were used in this study.
Table XXXIII lists the reaction rate constants calculated using the
wetting model (Equation 7.9) for every series in this study. The
reaction rate constants based on reactor catalyst volume (k), total
surface area of the catalyst (k_s) and catalyst mass (k_w) will be used
to compare the relative activities of the catalysts. Table XXXIII
reveals that the catalyst prepared from untreated Ketjen 007-1.5E

TABLE XXXIII

COMPARISON OF CATALYSTS USED
IN THIS STUDY

Support Used	Series	Temp. ($^\circ$F)	k $(hr)^{-x}$	k_S $cm/(hr)^x \times 10^{-7}$	k_W $\dfrac{cc}{gm(hr)^x}$
Ketjen 007-1.5E	KEC	650	0.692	3.41	0.99
		700	1.029	5.09	1.48
		750	1.585	7.83	2.27
Steam treated Ketjen 007-1.5E	KET	650	0.497	3.52	0.81
		700	0.696	4.93	1.13
		750	1.096	7.72	1.77
Ketjen 000-3P	KEP	650	0.433	3.71	0.74
		700	0.720	6.17	1.23
		750	1.246	10.68	2.13
Ketjen 007-1.5E	KDC	700	0.721	4.168	1.05
Steam treated Ketjen 007-1.5E	KDT	700	0.473	3.477	0.77
Ketjen 000-3P	KDP	700	0.618	5.06	1.09
CONOCO CATAPAL HP-20	CAT	650	0.467	3.71	0.81
		700	0.787	6.26	1.37
Ketjen 007-1.5E	KER	650	0.529	3.06	0.75
		700	0.883	5.11	1.25
		750	1.450	8.41	2.05

support is the most active at all temperatures comparing k values. The
steam treated catalyst seems to be the least active catalyst at temper-
atures of 371C (700F) and 399C (750F). The catalyst prepared from
Ketjen 000-3P seems to be more active than the catalyst used in the
KET series even though the KEP catalyst had a lower surface area
(199 vs. 230 m^2/gm). This is also evident when the reaction rate
constants based on surface areas (k_s) are compared. Another interesting
observation is that the two bidispersed catalysts used in this study,
namely the CAT series catalyst and KEP series catalyst, have similar
activities based on unit surface area. However, earlier results showed
that bidispersed catalysts did not offer any advantage over mono-
dispersed catalysts. The same conclusion will be confirmed later when
results from the residue fraction of the distillation results are
compared. Hence, one had to conclude that the intrinsic activities of
these two catalysts had to be higher than the other catalysts.

In addition to bimodal dispersion, the other thing both these
catalysts had in common was the presence of silica. The presence of
silica is known to increase the cracking activity of the catalyst (72)
However, the CAT series catalyst had very little silica (0.0088 wt %)
whereas the KEP catalyst had nearly 1 percent silica. The CAT series
catalyst support material was prepared by a special method by contacting
aqueous alumina slurry with an effective amount of an organic solvent
(101-104). This could have contributed to the CAT catalyst's higher
intrinsic activity. However, no information is available on the method
of preparation of the Ketjen supports used in all other series. The
presence of silica in the KEP catalyst could have caused the higher
intrinsic activity of that catalyst.

The reaction rate constants based on unit weight follow the same trend as the rate constants based on reactor volume. Based on the above evidence, the KEC catalyst seems to be the most active catalyst for hydrodenitrogenation of raw anthracene oil under the conditions tested in this study. However, based on rate constants on a unit surface area basis, one can conclude that the CAT catalyst and KEP catalyst are more active.

A total of eleven different catalysts has been used to hydrotreat raw anthracene oil so far in the continuing program at Oklahoma State University. A brief comparison will be made here; however, detailed information on these catalysts can be found elsewhere (5-9).

Table XXXIV lists the properties of the eleven catalysts. Note that Harshaw HT-400 had a somewhat different active metals concentration than the other catalysts tested. Also, information on the chemical composition is not available from the vendors for three catalysts. Note that the surface areas of the catalysts tested varied from 199 to 303 m^2/gm and the pore volume ranged from 0.431 to 0.997 cc/gm. Three of the catalysts (Nalcomo Sphericat 474, CONOCO CATAPAL HP-20, Ketjen 000-3P) had a bimodal pore distribution. The most frequent pore radius in the micropores ranged from 26 to 50 $\overset{\circ}{A}$. Such wide variations in the properties present some problems in comparing these catalysts. In addition, since these catalysts were studied by different investigators at different times, the operating conditions also varied somewhat. In order to make a comparison some data were adjusted by interpolation to get percentage conversion at the same operating conditions.

TABLE XXXIV

CATALYST PROPERTIES

Properties	Catalyst from Vendors						Supports Impregnated in Our Laboratories				
	Nalcomo 474	Research Catalyst-A	Research Catalyst-B	Nalcomo Sphericat 474	Harshaw HT-400	Research Catalyst-C	Ketjen 007-1.5E	Steam Treated Ketjen 007-1.5E	Ketjen 000-3P	CONOCO CATAPAL HP-20	Norton SA 6175
Chemical Composition											
$\%$ MoO_3	12.5	12.5	12.5	12.5	15.0	12.5	12.5	12.5	12.5	12.5	12.5
$\%$ CoO	3.5	3.5	3.5	3.5	3.0	3.5	3.5	3.5	3.5	3.5	3.5
$\%Na_2O$	0.08	0.08	0.08				0.03	0.03	0.033	40ppm	0.02
$\%Fe$	0.03	0.03	0.03				-	-	-	50ppm	0.075
$\%SiO_2$	1.5	1.5	1.5				-	-	0.88	0.008	0.180
$\%SO_4$							0.5	0.5	0.028	-	
$\%TiO_2$										0.12	
Physical Properties											
Surface Area m^2/gm	240	298	303	287	234	242	291	230	199	219	220 ± 20*
Pore Volume cc/gm	0.463	0.441	0.556	0.997	0.431	0.525	0.503	0.540	0.625	0.875	0.75 ± 0.95*
Most frequent Pore Radius, Å	34	26	26	30,800	50	47	31	38	36, 160	40, 1900	100*

*Vendor Information

The percent nitrogen removal at a volume hourly space time of 0.82

hours was read from a plot of percent nitrogen removal vs. space time

at a temperature of 343C (650F). Information on all of the catalysts

was not available at the same pressure. Satchell (6), using raw anthra-

cene oil as feedstock, found that the rate constant is proportional

to the absolute pressure to the 0.76 and 0.84 power at 343C (650F) and

371C (700F), respectively. Using this relationship, at 343C (650F),

the rate constant at 1000 psig is 0.735 times the rate constant at

1500 psig. However, percent removal data need not necessarily follow

this relationship. Data were avialable for three catalysts (Nalcomo

474, Harshaw HT-400, Norton SA 6175) at both pressures. The ratios

between percent removal at 1000 psig and 1500 psig were calculated for

these three catalysts and were found to be 0.815, 0.859 and 0.853.

Hence, an average value of 0.842 was used to adjust the pressure param-

eter for catalysts for which data was not available at 1500 psig.

Table XXXV presents a comparison of the eleven catalysts used to hydro-

treat raw anthracene oil at one set of conditions.

Table XXXV reveals that except for Ketjen 007-1.5E and CONOCO

CATAPAL HP-20, little differences exist between the other catalysts.

Ketjen 007-1.5E is definitely superior to the other catalysts tested

while the CONOCO catalyst was the least active of those tested. Ketjen

007-1.5E had a surface area of 291 m^2/gm; while the CONOCO catalyst had

a surface area of 218 m^2/gm; which happens to be the second lowest

surface area among the catalysts tested. Also, one must remember

that these comparisons are made on a volume hourly space time basis.

Earlier results showed that the CONOCO catalyst had a higher activity

based on a unit surface area basis than Ketjen 007-1.5E. Hence,

caution must be taken before drawing any conclusions. A catalyst cannot

TABLE XXXV

COMPARISON OF ELEVEN CATALYSTS

Operating Conditions: 1500 psig, 0.82 hours, 343C (650F)

Catalyst	% Removal of Nitrogen
Nalcomo 474	38 ± 2
Harshaw HT-400	36 ± 2
Norton SA 6175	38 ± 2
Ketjen 007-1.5E	47 ± 2
Steam treated (10 hours) Ketjen 007-1.5E	36 ± 2
Ketjen 000-3P	34 ± 2
CONOCO CATAPAL HP-20	29 ± 2
Nalco Sphericat 474*	37 ± 2
Research Catalyst A*	42 ± 2
Research Catalyst B*	37 ± 2
Research Catalyst C*	39 ± 2

*Adjusted for pressure

be judged based on its performance at a single operating condition.
The trend shown in Table XXXV vary when the temperature is varied.
For example, Nalco Sphericat 474 which is comparable to other catalysts
at 343C (650F) was found to be the least active catalyst at 371C (700F).
Information from this study (Figures 20, 21 and 22) also suggests
that the relative activities of the catalysts do change with changes
in temperature. Pressure and space time do not seem to have any effects
on the relative activities of these catalysts.

Comparison of the relative activities of the catalysts should be
performed at different temperatures. Also, these comparisons should
be done on the basis of the volume of the catalyst, the weight of the
catalyst and the total surface area of the catalyst used. In addition,
further catalyst screening studies should be performed at similar
operating conditions so that comparisons can be made easily. However,
a few generalizations can be made based on the results from the runs
using these eleven catalysts.

Some of the conclusions derived from the present study which used
only four catalysts are supported when results from all the eleven
catalysts are taken into consideration. Increasing micropore sizes
in the range of 25 to 50 $\overset{o}{A}$ does not result in an increase in nitrogen
removal is evident from the fact that Harshaw HT-400 and Research
Catalyst B have the same denitrogenation activity even though most
frequent pore radius of Research Catalyst B was only 26 $\overset{o}{A}$, nearly half
that of the Harshaw Catalyst (50 $\overset{o}{A}$). A comparison of Nalco Sphericat
474 (bimodal pore distribution) with Nalcomo 474 (monodispersed)
supports the fact that bimodal pore distribution does not offer any
advantages over monodispersed catalysts. Also, rate constants based

on surface area presented earlier in this section, indicate that

hydrodenitrogenation of raw anthracene oil is more sensitive to changes

in surface area than to changes in pore radius.

Doctored Studies

Raw anthracene oil was doctored with quinoline to increase the

nitrogen content of the feed oil from 1.06 weight percent to 1.89

weight percent. This doctored feedstock was then hydrotreated over

three catalysts that were used in earlier studies using raw anthracene

oil under similar operating conditions. Selected product samples were

fractionated using an ASTM D1160 vacuum distillation technique (107).

The different fractions were then analyzed for their nitrogen content.

The doctored runs in this study were performed to find out whether

doctored feedstocks could provide any information on the intrinsic

activity and to find out whether this test can be used more effectively

than simple activity tests towards tailoring of hydrotreating catalysts.

This section will discuss results from doctored studies as well as

the results from distillation.

Three different catalysts were used in these doctored runs. The

properties of the catalysts were shown in Table XXV in the results

section (p. 134). Figure 24, in the results section, presents the

results from the three doctored runs. Figure 24 reveals that the

steam treated catalyst used in the KDT series was less active than the

other two catalysts.

Satterfield, et al. (46) showed that increasing nitrogen concentra-

tion had an effect on hydrodesulfurization of thiophene. In the present

study, the nitrogen concentration was increased from 1.06 weight percent

to 1.89 weight percent by the addition of quinoline, while the sulfur concentration remained the same at 0.47 weight percent. Since catalysts produced from the same supports were used over both the feedstocks (doctored and undoctored raw anthracene oil), the results can be compared to find out the effect of increasing nitrogen concentration on sulfur removal.

Figures 42, 43 and 44 compare the sulfur removal as a function of the nitrogen concentration for the three catalysts used in this study, catalysts prepared from the supports, Ketjen 007-1.5E, Steam treated (10 hrs) Ketjen 007-1.5E and Ketjen 000-3P. These figures reveal that sulfur removal is indeed affected by the increase in nitrogen concentration. However, the increase in nitrogen concentration seems to affect the steam treated catalyst more than the other two catalysts. Table XXXVI presents a comparison of the results from three catalysts at the same operating conditions. As can be seen from the Table XXXVI, the relative change in sulfur concentration when nitrogen concentration in the feedstock was increased was more than 100 percent for the steam treated catalyst.

Based on their studies concerning interactions between catalytic hydrodesulfurization of thiophene and hydrodenitrogenation of pyridine, Satterfield, et al. (46) concluded that there are two types of hydrodesulfurization sites involved. The first are postulated to be very active for hydrodesulfurization but very sensitive to nitrogen bases. Sufficient quantities of these bases will completely block these sites and render them inactive for hydrodesulfurization. The second type of sites are much less active for hydrodesulfurization, but they are also less susceptible to poisoning by nitrogen bases.
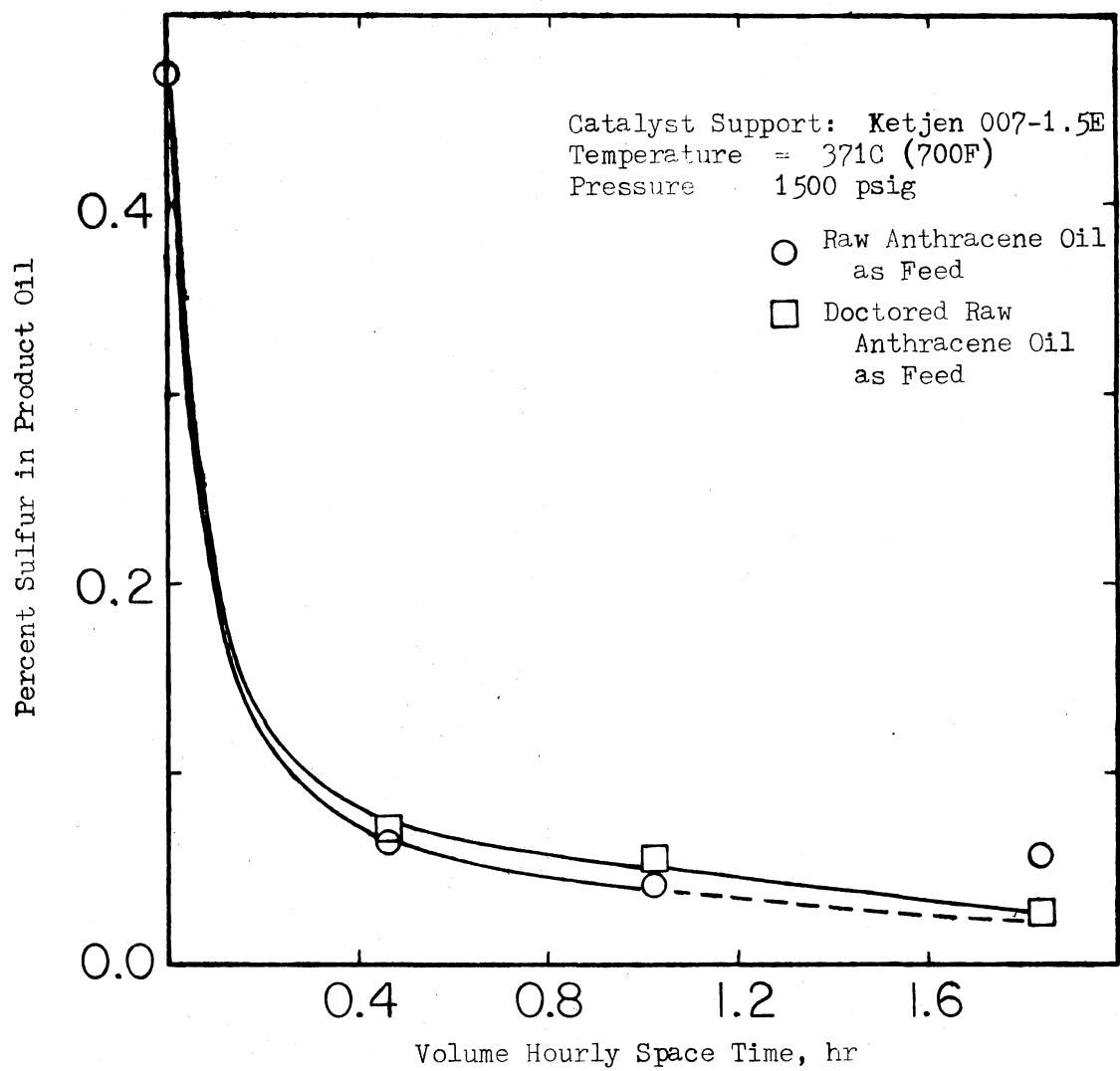
Figure 42. Effect of Nitrogen on Sulfur Removal Using
Catalyst Prepared from Ketjen 007-1.5E
Support
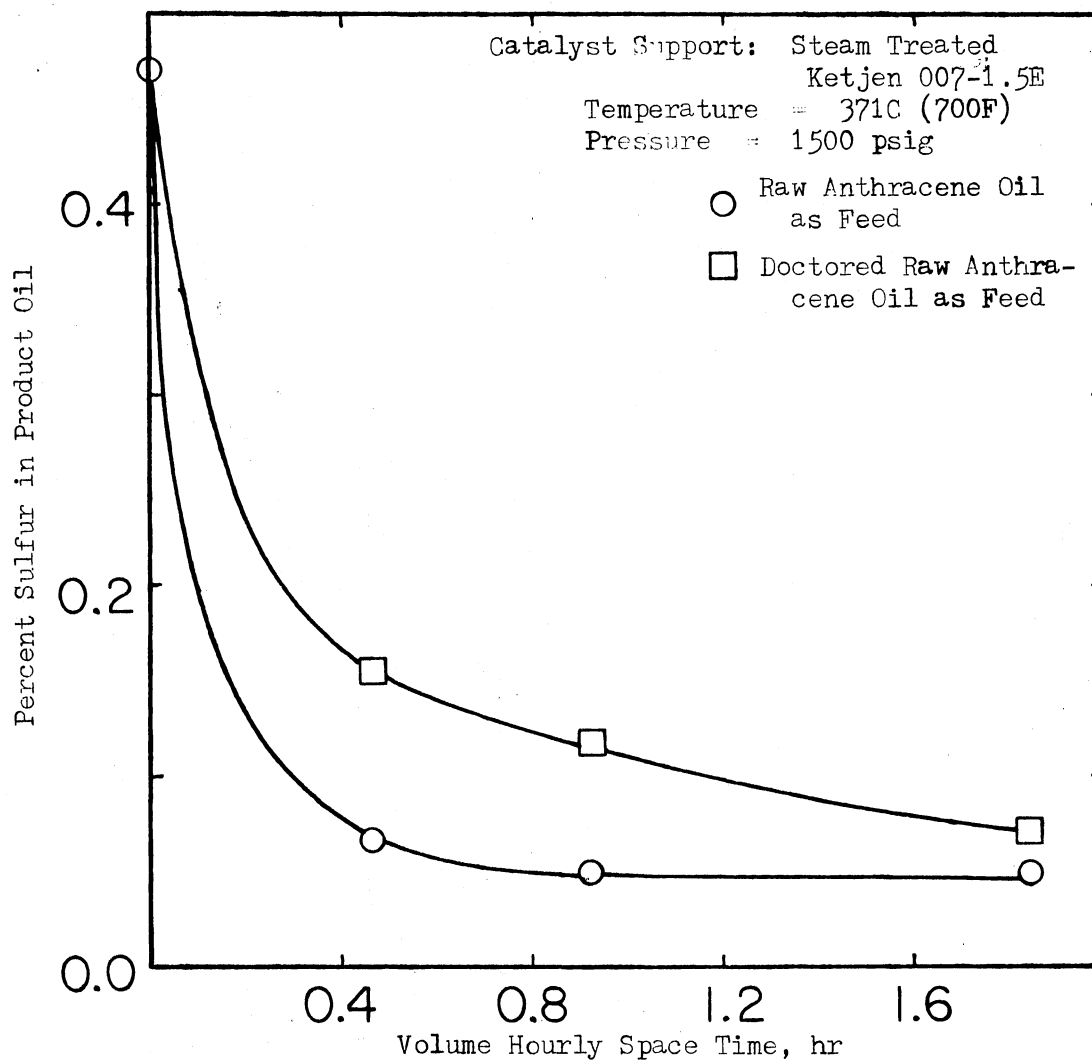
Figure 43. Effect of Nitrogen on Sulfur Removal Using
Catalyst Prepared from Steam Treated Ketjen
007-1.5E Support
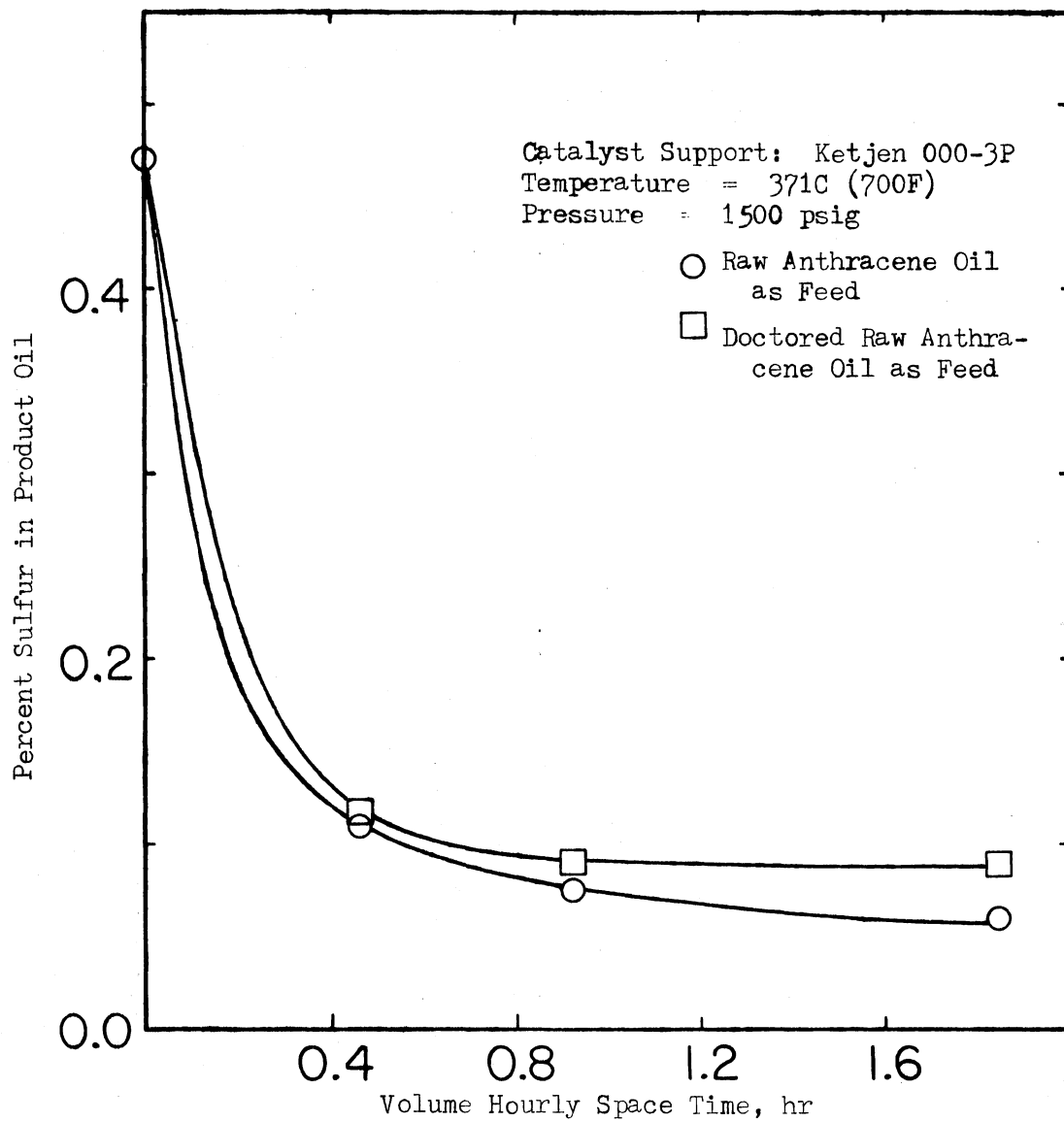
Figure 44. Effect of Nitrogen on Sulfur Removal Using
Catalyst Prepared from Ketjen 000-3P
Support

TABLE XXXVI

EFFECT OF NITROGEN CONCENTRATION
ON SULFUR REMOVAL

Operating Conditions: 1500 psig, 371C (700F), and 0.92 hours

Catalyst Support	Percent Sulfur in Product Oil		Percent Change Relative to Lower Value
	RAO as feed	DRAO as feed	
Ketjen 007-1.5E	0.042	0.055	31
Steam treated (10 hrs) Ketjen 007-1.5E	0.051	0.118	131
Ketjen 000-3P	0.076	0.09	18

RAO - Raw Anthracene Oil

DRAO - Doctored Raw Anthracene Oil

Satterfield, et al. (46) postulated that latter sites are responsible for hydrodesulfurization activity after first type of sites have been blocked. Their study used pure compounds namely thiophene and pyridine. However, results presented from this study using a complex feedstock such as raw anthracene oil provide additional evidence to support the theory that two types of hydrodesulfurization sites are present in Co-Mo-Alumina catalysts.

Table XXXVII presents a comparison of the reaction rate constants for hydrodenitrogenation based on reactor volume calculated using the model presented in Equation 7.9 for the same catalysts under identical operating conditions for the two feedstocks used.

TABLE XXXVII

COMPARISON OF REACTION RATE CONSTANTS
FOR DOCTORED AND REGULAR FEEDSTOCKS

Operating Conditions: 1500 psig, 371C (700F), 0.46, 0.92 and 1.84 hours

Catalyst Support	Reaction Rate Constants Based on Reactor Volume $(hr)^{-x}$	
	Raw Anthracene Oil as Feedstock	Doctored Raw Anthracene Oil as Feedstock
Ketjen 007-1.5E	1.029	0.721
Steam treated (10 hrs) Ketjen 007-1.5E	0.696	0.473
Ketjen 000-3P	0.720	0.618

Table XXXVII reveals that the activity of the catalysts tested remain in the same order for the two feedstocks used, even though the rate constants were lower in the case of doctored raw anthracene oil. The reaction rate constants presented in Table XXXVII are first order rate constants obtained from a model incorporating wetting effects. Theoretically, these constants should remain the same for both feedstocks if a single nitrogen containing species were present in each feed. However, Table XXXVII reveals that the rate constants were different for both feedstocks and this is due to the presence of different organo-nitrogen species with different reactivities.

Table XXXVIII presents reaction rate constants based on surface area, k_s (the method of calculation was presented earlier) for the catalysts under identical operating conditions for the two feedstocks.

TABLE XXXVIII

REACTION RATE CONSTANTS BASED
ON SURFACE AREA, $cm/(hr)^x$

Operating Conditions: 1500 psig, 371C (700F), 0.46, 0.92 and 1.84 hours

Catalyst Support	$k_s \times 10^7$	
	Raw Anthracene Oil as Feedstock	Doctored Raw Anthracene Oil as Feedstock
Ketjen 007-1.5E	5.09 ± 0.41	4.17 ± 0.30
Steam treated (10 hrs) Ketjen 007-1.5E	4.93 ± 0.47	3.48 ± 0.28
Ketjen 000-3P	6.17 ± 0.58	5.07 ± 0.40

The k_s values for the Ketjen 007-1.5E support and the steam treated Ketjen 007-1.5E support fall within the experimental uncertainty. These two catalysts had the same chemical composition, but different physical properties. The fact that k_s values do remain constant leads one to conclude that the lower activity of the steam treated catalyst was due to its lower surface area (252 vs. 222 m^2/gm). However, k_s values for the 000-3P support were higher compared to the other two supports, even though the overall activity of this catalyst was lower compared to the catalyst produced from the Ketjen 007-1.5E support. This means that the catalyst made from the 000-3P support was more active on a per unit surface area basis compared to the other catalysts. The 000-3P support had a bimodal pore distribution. However, the distillation results revealed (to be presented later in this chapter) that the macropores did not offer any advantage. The 000-3P support had a silica content of

nearly one percent. The chemical composition of 000-3P and 007-1.5E

supports were similar except for the presence of silica. Hence, the

presence of silica could have been responsible for the higher activity

of the 000-3P supported catalyst on a unit surface area basis, because

silica causes an increase in the hydrocracking activity of the catalyst.

As pointed out earlier, selected product samples from the doctored

runs were fractionated and analyzed for nitrogen to study the denitro-

genation activity throughout the entire boiling range of the feedstock.

The raw data are presented in Appendix C. Satchell (6) succeeded in

establishing a model assuming that the reaction rate constants for

the individual fractions follow a linear relationship with the boiling

point of the fraction. An attempt was made to establish a kinetic

model using the distillation results. Satchell (6) established his

kinetic model based on distillation results available for a single

space time. However, Appendix H shows that trying to establish a

kinetic model is confusing when one takes into account the results from

all three space times for each fraction of the entire feedstock. One

of the reasons for these confusing results is that the weight percent

nitrogen in an individual fraction does not adequately represent the

changes that are taking place. One of the inherent assumptions in

trying to calculate the rate constants of the individual fractions

was that the same organonitrogen species exist in both the feed and

product boiling within a certain range. This is not true if nitrogen

in higher molecular weight compounds in the feed are transferred to

lower boiling ranges in the product due to cracking and hydrogenation.

Since weight percent nitrogen in the individual fractions do not

adequately represent the changes that are taking place, the weights of

nitrogen present in the fractions were used for further calculations. The weights of nitrogen in individual fractions were calculated from the total weights of the fractions and the weight percent nitrogen present in each fraction. These total weights of individual fractions were determined by measuring the density of individual fractions and multiplying the measured volume collected during distillation for each fraction. The density measurements were made simply by weighing a known volume of the sample from each individual fraction. The nitrogen content of the residue left in the distillation flask was then calculated using a material balance. Some curious results were obtained when these material balances were completed. A total of nine samples from the doctored runs were distilled, consisting of three samples from each series representing the three space times used in this study. For two of these samples, the material balances were not satisfactory since the results from weight measurements showed more nitrogen in the fractions (excluding the nitrogen present in the residue) than originally present in the sample itself. Both of these samples (KDC #8 and KDP #8) were collected at the highest space time (1.84 hours) and nitrogen removal was about 67%. The possible source of error is the nitrogen gas which was used in the distillation apparatus to maintain an inert atmosphere. Some of this nitrogen could have dissolved in these two samples since the nitrogen content of these two samples were low compared to the other samples. Hence in the calculations to be discussed, these two samples and the other sample (KDT #8) collected at 1.84 hours were neglected.

Figure 45 presents the total mass of nitrogen and the weight percent nitrogen present in the individual fractions of the doctored
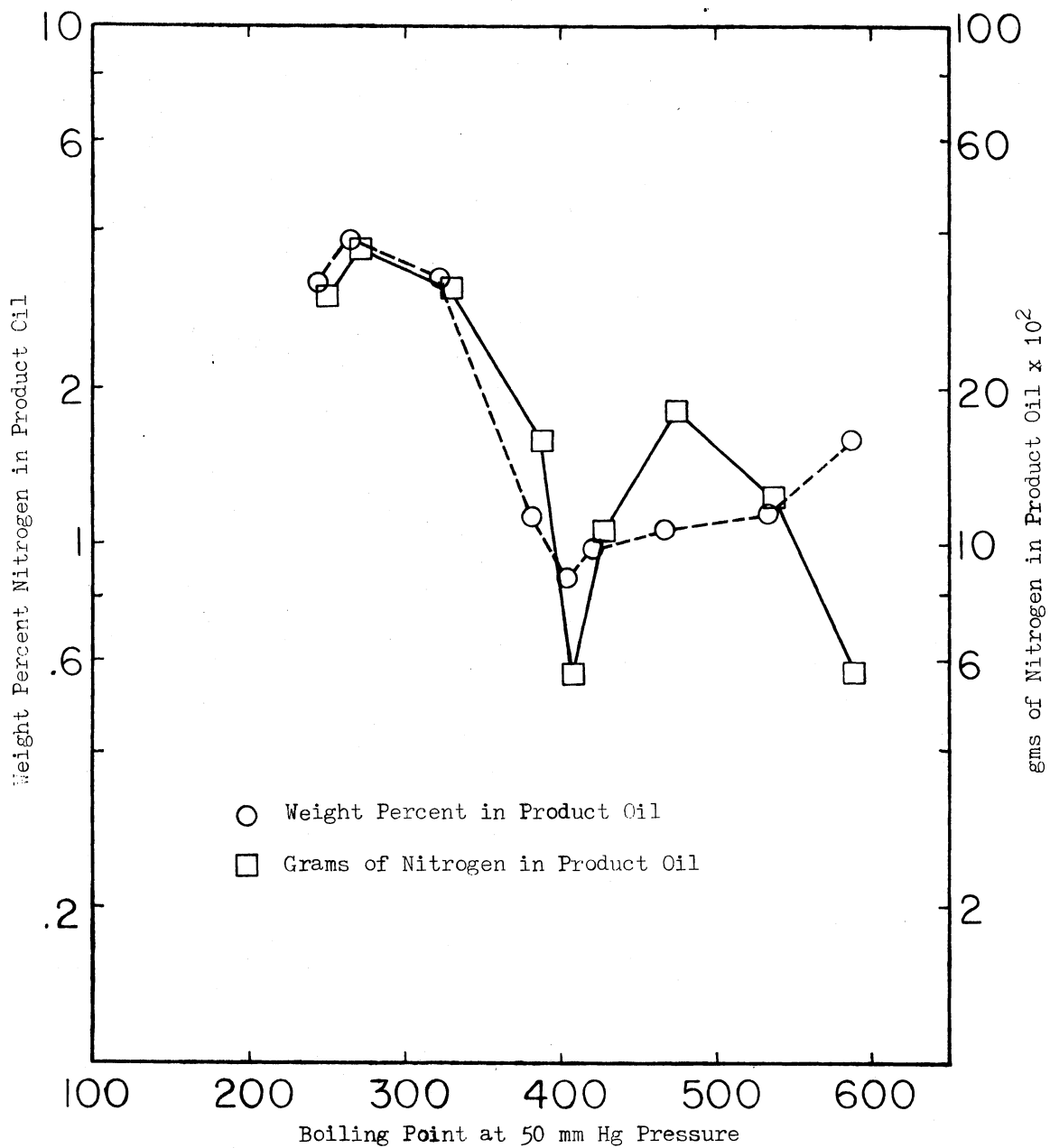
Figure 45. Weight Percent Nitrogen and Mass of Nitrogen in
            Doctored Raw Anthracene Oil as a Function of
            Boiling Point

feedstock as a function of the boiling point of these fractions. A curious thing to note is the differences in the shape of these two curves. The shape of the feedstock curve when plotted as the mass of nitrogen present in individual fractions is distinctly different than the shape resulting when the feedstock is plotted as weight percent nitrogen in the fractions. The weight percent nitrogen curve shows only one peak while the total mass curve shows two peaks. This observation confirms the earlier assumption that weight percent nitrogen in product oil does not adequately represent the changes taking place.

Figures 46 and 47 compare the three catalysts at two different space times as a function of the nitrogen present in individual fractions of product oils. The figures indicate that the KDT catalyst seems to be less active overall than the other two catalysts. The figures also indicate that the KDP and KDC catalyst have similar activities. However, the KDT catalyst, although less active overall, seems to be more active in removing the nitrogen from the residue left in the distillation flask. This is a qualitative observation and will be discussed later.

One question that arises is whether quinoline changes can be traced or followed somehow in these fractions of the product. Figure 25 showed that the higher boiling fractions ($> 400^\circ F$) of both doctored and regular feedstocks are essentially identical and all the quinoline that was added to the feedstock appears in the low boiling ($< 400^\circ F$) fractions. In addition to the figure, simple calculations were made which also confirmed that quinoline, in fact, can be identified in the feed and product fractions. These calculations are presented in Appendix J.
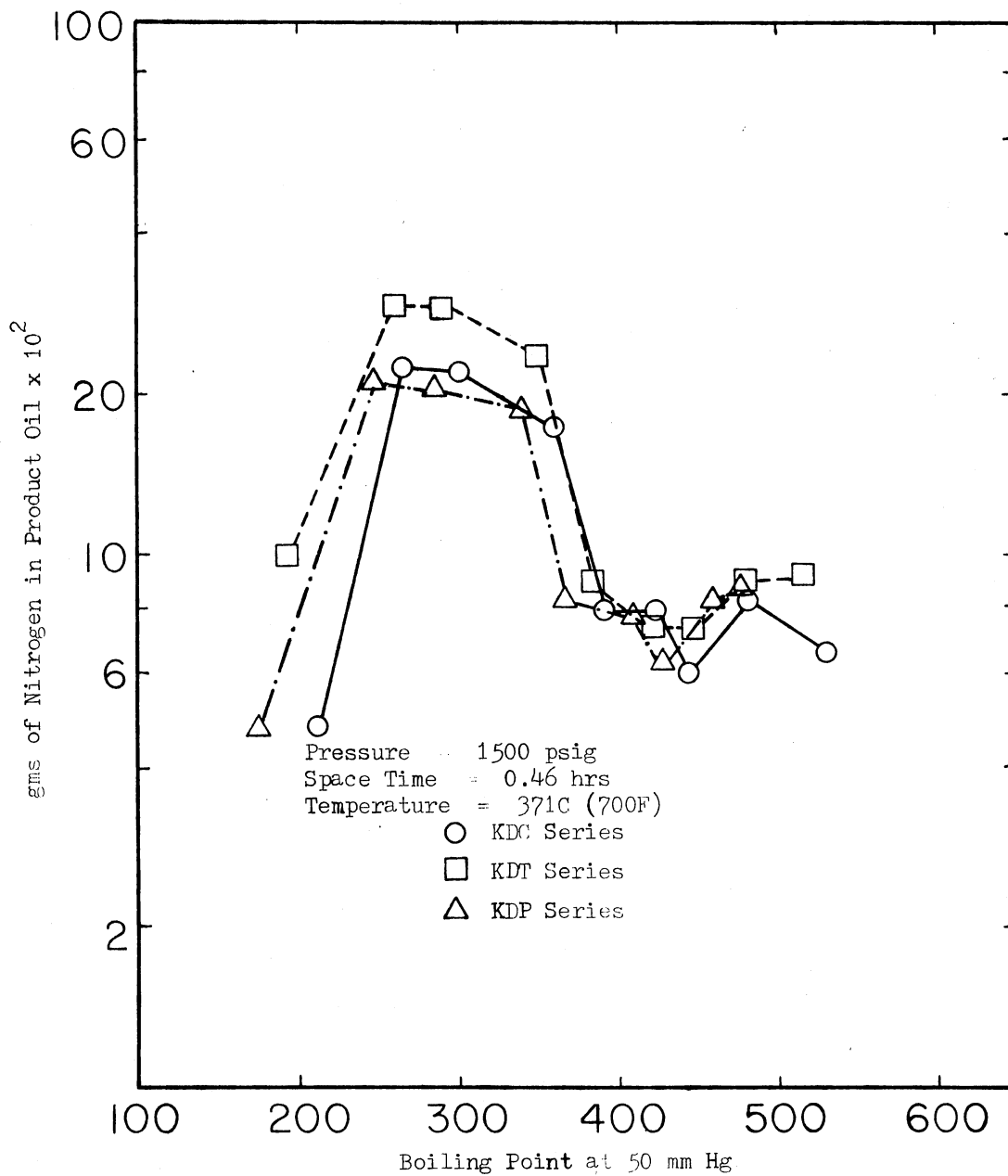
Figure 46. Mass of Nitrogen Present in Product Oils as a
Function of Boiling Point at a Space Time of
0.46 Hours
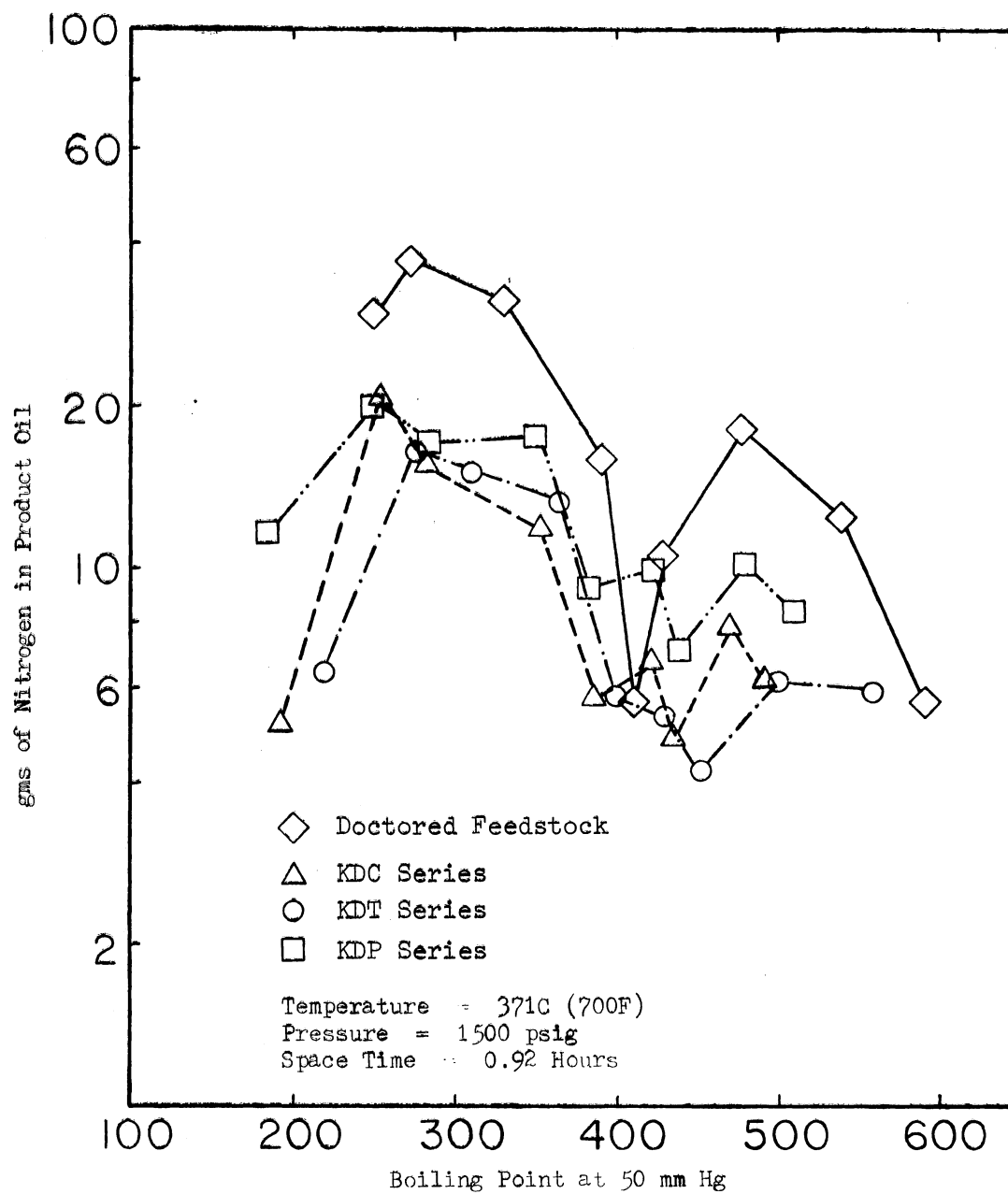
Figure 47. Mass of Nitrogen Present in Product Oils as a Function of Boiling Point at a Space Time of 0.92 Hours

Since the rate constants determined from all eight individual fractions of the product oils proved unsatisfactory, another method was considered where some fractions can be combined to form three major reaction zones. The plot of the mass of nitrogen in the product fractions as a function of the boiling points for the doctored feedstock suggests three such zones, namely the quinoline zone, the zone that boils above 204C (400F) and the residue zone corresponding to the residue left in the distillation flask. The distillation results will be discussed in terms of these three zones, designated as the quinoline, the middle and the residue zones.

Quinoline Zone

As pointed out earlier, the doctored studies were performed in an attempt to find out whether these methods could serve as an intermediate test to provide more information on catalyst tailoring than from simple overall activity tests and yet not requiring the time of full product characterization studies. In order for doctored studies to be effective, one should be able to trace the doctoring compound and the changes it undergoes. Hence, an attempt is made here to assess the rate of hydrodenitrogenation of the added quinoline.

At the outset, one should be aware that this is only psuedo-kinetic information since there are certain inherent assumptions involved. One assumption is that all of the quinoline that was added to the feedstock can be found in the zone boiling below 240C (400F) at 59 mm of mercury pressure as discussed earlier. This assumption is valid since we have two independent observations (Figure 25 and Appendix J) that confirm this.

Another assumption is that the changes in the nitrogen content
of the quinoline due to cracking of higher boiling compounds are
negligible compared to the high concentration of nitrogen in the
quinoline zone. Raw anthracene oil contains about 0.17 gram of nitro-
gen in the fractions boiling below 240C (400F) at 50 mm of mercury
pressure, while doctored raw anthracene oil contains about 1.14
grams of nitrogen in the fraction boiling below 240C (400F) at 50 mm
of mercury pressure. Because of this high concentration of nitrogen
in the quinoline zone, the small changes in the concentration due to
cracking can be considered negligible.

As pointed out earlier, the calculations will be made on the mass
of nitrogen present in the feed and the products in each zone. Since
constant amounts of the feed and product (100 ± 0.5 gm) were distilled
into fractions, this is equivalent to using weight percents. For
example, the mass of nitrogen present in the feed quinoline zone is
considered as the initial concentration and the mass of nitrogen found
in the quinoline zone of the products obtained from the reactor at
different space times will be considered as the final concentration
corresponding to the space time of the product. Table XXXIX lists
the data for the quinoline zone. Table XXXIX reveals that the steam
treated support used in the KDT series was the least active catalyst
for quinoline hydrodenitrogenation. Table XXXIX also reveals that
there is very little difference between the other two catalysts.

Reaction rate constants based on reactor volume and unit surface
area was calculated for hydrodenitrogenation of the quinoline zone
using Equations 7.9 and 7.15, and are presented in Table XL. Table XL
reveals that the k values agree with the observed performance of the

TABLE XXXIX

MASS OF NITROGEN IN THE
QUINOLINE ZONE

Run Series	Support Used	Space Time	Mass of Nitrogen in Quinoline Zone x 10^2 gms	Total Mass of Quinoline Zone gms
Doctored Feed			114.5	42.3
KDC	Ketjen 007-1.5E	0.92	56.9	47.6
		0.46	74.7	46.2
KDT	Steam Treated (10 hrs)	0.92	75.7	42.6
	Ketjen 007-1.5E	0.46	101.8	43.4
KDP	Ketjen 000-3P	0.92	58.6	47.7
		0.46	73.2	44.3

TABLE XL

REACTION RATE CONSTANTS FOR THE
QUINOLINE ZONE

First Order - Catalyst Wetting Model

Support Used	Run Series	k $(hr)^{-x}$ Rate Constant Based on Reactor Volume	k_s, $cm/(hr)^{-x}$ x 10^7 Rate Constant Based On Unit Surface Area
Ketjen 007-1.5E	KDC	0.742	4.29
Steam Treated (10 hrs) Ketjen 007-1.5E	KDT	0.482	3.54
Ketjen 000-3P	KDP	0.702	5.66

catalysts. The catalyst used in the KDT series has the lowest k value while the k values for the other two catalysts are about the same. The k_s values remain the same for the KDC and KDT series thereby confirming the earlier conclusion that reduction in surface area results in a reduction in nitrogen removal. The KDP catalyst, however, seems to be more active on a per unit surface area basis. The KDP catalyst was different from the other two catalysts in two respects. It had a bimodal pore distribution, and it contained almost 1 percent silica in the support. Bimodal pore distribution as a reason for the higher activity can be eliminated since the KDP catalyst was the least active catalyst in the residue zone where larger pores may offer an advantage over smaller pores. The presence of silica in Co-Mo-Alumina catalysts has been known to improve cracking and a possible reason for the KDP catalyst's higher activity could be due to its higher silica content compared to the other catalysts.

The information that a quinoline zone could in fact be followed through and pseudo-kinetics determined is useful. Hydrodenitrogenation of model compounds are being done in order to get a better understanding of the mechanisms involved. By doctoring the feedstock with a compound like quinoline one can obtain information about the hydrodenitrogenation of the feedstock as well as the performance of the catalysts used to hydrotreat model compounds instead of running two separate experiments. For example, in this study, the KDP catalyst was found to be comparable with the KDC catalyst in hydrotreating the quinoline zone. However, as will be shown, the KDP catalyst was the least active catalyst in the residue zone. Hence, the KDP catalyst may have more selectivity towards low boiling nitrogen containing compounds. Further, doctoring

studies are needed to test several compounds to determine the best doctoring compound and also to determine the optimum amount of the doctoring compound that should be added to the feedstock.

Middle Zone

Table XLI presents the results from the middle zone. Table XLI reveals that the middle zone shows essentially the same response for the three catalysts used in this study as theoverall kinetic data presented earlier in Table XXXVII. The KDC catalyst is the most active catalyst followed by the KDP catalyst with the steam treated KDT catalyst being the least active. One of the significant things to note is that the KDT catalyst shows no significant improvement in nitrogen removal when the space time is increased from 0.46 to 0.92 hours. A possible explanation for this could be that considerable cracking and hydrogenation take place resulting in compounds moving from residue zone into the middle zone, thereby making it difficult to determine the rate constants.

Cracking and hydrodenitrogenation take place simultaneously in this zone and unmasking the effects of cracking is not feasible without additional data. A comparison of Tables XXXIX and XLI reveals that the total mass of the quinoline zone has increased in the product oils while the total mass of the middle zone has decreased thereby indicating that some transfer occurs between the zones. While these changes may be negligible for the quinoline zone because of the higher concentration of nitrogen, the same may not be true in the case of the middle zone. Hence, the results from the middle zone and the residue zone will be discussed only on the basis of the mass of nitrogen remaining in the

TABLE XLI

MASS OF NITROGEN IN THE MIDDLE ZONE

Run Series	Support Used	Space Time	Mass of Nitrogen in Middle Zone x 10^2 gms	Total Mass of Residue Zone, gms
Doctored Feed			52.4	43.7
KDC	Ketjen 007-1.5E	0.92	21.7	36.6
		0.46	28.9	36.7
KDT	Steam treated (10 hrs)	0.92	33.9	39.4
	Ketjen 007-1.5E	0.46	28.9	40.1
KDP	Ketjen 000-3P	0.92	25.4	36.1
		0.46	30.9	38.9

zone instead of comparing on the basis of rate constants since these changes prevent the determination of the relative rate constants.

Residue Zone

Table XLII presents the mass of nitrogen present in the residue zone and reveals some interesting results. The percentage conversion varied from 46 to 77. This is interesting since this fraction should have been the most difficult to hydrotreat if Flinn's (47) conclusion that the rate of denitrogenation decreases with increasing boiling point of the feed. However, note that even the lowest conversion was about 50%. This coupled with the table presented in Appendix H confirm that the reactivities of the different organonitrogen species present in different zones or fractions do not necessarily follow a linear relationship with the boiling point of these zones or fractions.

TABLE XLII

MASS OF NITROGEN IN THE RESIDUE ZONE

Run Series	Support Used	Space Time	Mass of Nitrogen in Residue Zone x 10^2 gms	% Conversion	Total Mass of Residue Zone gms
Doctored Feed			43.6		20.5
KDC	Ketjen 007-1.5E	0.92	16.7	62	22.9
		0.46	21.9	50	22.8
KDT	Steam Treated (10 hrs) Ketjen 007-1.5E	0.92	9.9	77	20.8
		0.46	18.2	58	20.5
KDP	Ketjen 000-3P	0.92	18.7	57	19.1
		0.46	23.5	46	18.3

Another possibility is that the nitrogen compounds from this zone had been cracked and appear in the middle zone as products. The fact that increasing the space time did not produce significant improvement in the nitrogen removal from the middle zone for the KDT catalyst supports this theory. However, the results from the residue zone indicate KDP catalyst, with a silica content of nearly one percent, is the least active catalyst in this zone. Since the presence of silica is known to improve cracking, one would expect the KDP catalyst to be more active if only cracking is responsible for nitrogen removal from this zone.

Another interesting observation is that the KDT catalyst which was the least active catalyst in the other two zones and on a total nitrogen removal basis is the most active catalyst in the residue zone. The KDT

catalyst had a higher most frequent pore radius (38 Å) compared to the other two catalysts (31 Å for the KDC catalyst and 33 Å in the micropores for the KDP catalyst). The residue zone would probably have higher molecular weight compounds of the feed which in turn would have higher molecular diameters. When the size of a reactant molecule approaches the size of the pores then the surface area of the small pores becomes unavailable to the reactant molecule. Hence, increasing micropore sizes may offer an advantage with higher boiling compounds. From a catalyst tailoring point of view, information on the size of these molecules becomes important.

A discussion on the size of these molecules follows after a brief summary of the results from doctored runs.

Summary

The discussion presented so far indicate that the results from doctored runs can be discussed on the basis of three major zones, namely the quinoline zone, middle zone and the residue zone. This method revealed the selectivity of some catalysts. For example, Ketjen 000-3P catalyst was comparable to the untreated Ketjen 007-1.5E catalyst in the quinoline zone, while in the residue zone, Ketjen 000-3P catalyst was the least active catalyst. Hence, the Ketjen 000-3P catalyst may have more selectivity towards low boiling nitrogen containing compounds. The steam treated Ketjen 007-1.5E was found to be the most active catalyst in the residue zone even though this catalyst had the lowest surface area. The steam treated Ketjen 007-1.5E catalyst had a higher most frequent pore radius (38 Å) compared to the other two catalysts (33 Å), which may have been responsible for the

higher activity of this catalyst. Further doctoring studies are needed to test several compounds to determine the best doctoring compound and also to determine the optimum amount of the doctoring compound that should be added to the feedstock.

Molecular Sizes

Information on the molecular diameter of typical nitrogen compounds present in coal liquids are not available in the literature. In the absence of published information, simple methods were chosen to calculate these diameters. Two different procedures will be presented here.

The first procedure involves the assumption that the molecules are planar in configuration and calculating the longest length based on the structure of the compound and C-H bond lengths. Nonsaturated compounds are generally considered as planar in structure as compared to the saturated compounds. Using this approach, the longest length of a benzene ring (referred to as molecular diameter from now on) is calculated to be approximately 3.1 Å using a C-H bond length of 1.54 Å as shown below.
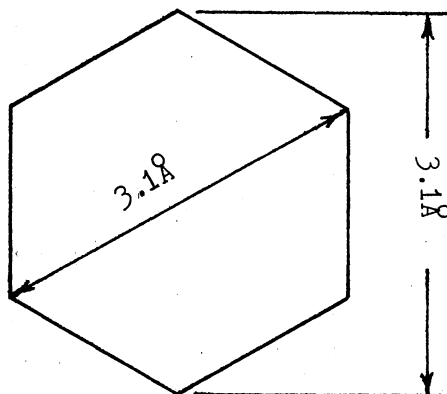
Some representative compounds and their molecular diameters are shown below.
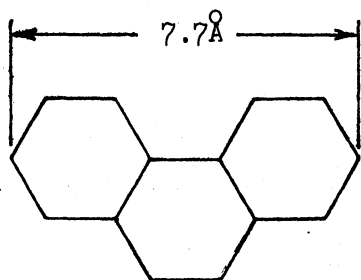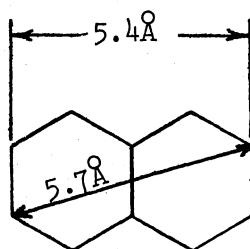
| Phenanthridine | Quinoline | Carbazole |
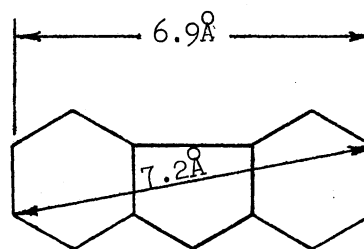
Assuming the diameter of a benzene ring to be 3.1 Å, a five ring compound would have a molecular diameter of about 15 Å.

Another approach is to use the expression developed by Taylor (115)

$$d = \sqrt[3]{M/D} \times 1.326$$

where

D = liquid density, gms/cc

M = molecular weight

d = diameter in Angstroms.

This expression assumes that the molecules are spherical and packed as closely as possible. For quinoline this equation predicts a molecular diameter of 6.5 Å, which is consistent with the value predicted by the other method. However, one of the disadvantages of this method is that it requires the knowledge of liquid densities which are not always available.

The characterization studies conducted on raw anthracene oil (95) show very few five ring compounds present. Even these will have a molecular diameter of less than 12 Å because of their structure. For example, dihydroazapyrene, a compound found in the acid fraction of the feed (p. 91) has the molecular structure shown below.
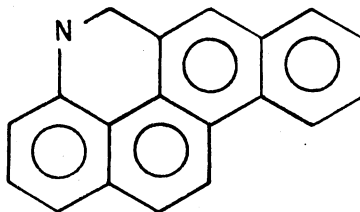
Results from mercury porosimetry indicated that very few or no pores
are present that have a pore radius less than 14 Å. Hence, all the
nitrogen compounds present in raw anthracene oil may have access to
the inner surface of the catalysts used in this study.

However, molecular diameters do not necessarily represent the best
way of characterizing molecules. Molecular sieves have been used for
selective adsorbtion of molecules based on their molecular dimensions.
The uniform pore openings of molecular sieves permit them to discrimi-
nate on the basis of the size and configuration of molecules in a
system. A quantity known as the critical diameter is used in the
molecular sieve industry. Benzene has a critical diameter of 6.7 Å.
This is more than twice the molecular diameter calculated by the method
presented earlier. Hence, higher molecular weight nitrogen compounds
with a molecular diameter of 12 Å may well have critical diameters
larger than 24 Å. In that case, the higher molecular weight nitrogen
compounds could not easily diffuse into the pores. The results observed
in the residue zone, where the catalyst with a 38 Å pore radius was
more active than a catalyst with a pore radius of 33 Å may be due to
this. However, exact critical diameters of nitrogen compounds present
in coal liquids are not available and the above discussion pertaining
to molecular series is merely a speculation based on the information

currently available. With catalyst tailoring becoming more important, further studies on critical diameters of large molecules could provide useful information.

CHAPTER VIII

CONCLUSIONS AND RECOMMENDATIONS

Conclusions

Hydrodenitrogenation of raw anthracene oil, a coal derived liquid
has been studied in a trickle bed reactor using Co-Mo-Alumina catalysts
at temperatures of 340, 371 and 399C (650, 700 and 750F), at 1.03×10^7
pascals pressure (1500 psig) and at liquid volume hourly space times
of 0.46, 0.92 and 1.84 hours. The physical properties of one of the
supports were varied using a steam treating technique, and the effects
of support properties on hydrodenitrogenation were studied. In
addition, raw anthracene oil was doctored with quinoline and hydro-
treated over the same Co-Mo-Alumina catalysts. Both feedstocks and
selected product samples were fractionated using an ASTM vacuum distill-
ation technique to assess nitrogen removal throughout the feedstock
boiling range. The following conclusions were drawn from this study.

1. The rates of denitrogenation of raw anthracene oil were sen-
   sitive to changes in the total catalyst surface area available
   for reaction. A reduction in surface area resulted in reduc-
   tion of nitrogen removal.

2. The rates of denitrogenation of raw anthracene oil were not
   sensitive to changes in the most frequent pore radius in the
   range of 25 to 40 Å for the Co-Mo-Alumina catalysts.

3. Bimodal pore distributions did not seem to offer any obvious advantages over monodispersed catalysts for removal of nitrogen from raw anthracene oil.

4. The data were satisfactorily correlated using a first order partial catalyst wetting model.

5. The exponent in the partial catalyst wetting model was found to vary from 0.306 to 0.932 in this study. In a reacting system, the exponent may depend on the reaction conditions as well as the nature of the reaction. Neither other studies nor the results from this study could establish a definite correlation between the exponents and the operating conditions.

6. Quinoline added to the feedstock could in fact be traced and its pseudo kinetics was studied. Quinoline hydrodenitrogenation was found to be a first order reaction. Doctoring studies could possibly be used as an intermediate test between activity tests and characterization studies.

7. The catalyst prepared from the Ketjen 007-1.5E support was found to be more active than the other three catalysts used in this study as well as seven other catalysts used by different investigators to hydrotreat raw anthracene oil. The larger surface area of the Ketjen 007-1.5E support material was responsible for this apparent higher catalyst activity. Steam treating reduced the surface area of the catalyst which resulted in a reduction of the catalyst activity.

8. Moderate changes in pore properties are observed when alumina supports were steam treated. Steam treating increases the most frequent pore radius and decreases the surface area.

Impregnation also changes pore properties, but does not seem to change the most frequent micro-pore radius whereas there is an increase in the most frequent macro-pore radius. The surface area and pore volume decreases after impregnation.

Recommendations

With increasing interest in coal conversion, research on hydrotreating catalysts will play a major role in the next decade. So many questions still remain unanswered with respect to hydrotreating of coal liquids. The following recommendations are made based on the results and experience gathered from this study.

1. The results from this study should be assessed for other coal derived liquids. One might expect that as the feedstock became more difficult to hydrotreat, and with higher boiling components, then the increasing pore sizes should begin to offer an advantage. Also, with ash containing feeds. the macro-pore system could offer an advantage in its ash tolerance while still maintaining activity.

2. Variations in the most frequent pore radius of the catalyst supports were small in this study. Hence, in order to study the effects of pore size distribution, catalyst supports with large variations in their most frequent pore radii and distributions should be studied. The catalyst supports with large variations can be obtained from commercial vendors or by increasing the steam treating time. In the present study, the support was steam treated only for a period of ten hours. Increasing this may result in larger variations in pore

structure.

3. The effect of support additives like Na_2O in small quantities on hydrodenitrogenation is still uncertain. Hence, the effect of the variations in the chemical composition of the supports on hydrodenitrogenation should be studied.

4. Silica-alumina supports have been shown to improve the performance of denitrogenation (70). The effect of varying the silica content in the support on hydrodenitrogenation should be studied.

5. In this study, the active metal concentration was not varied. Hence, in order to determine the optimum concentrations of metals, the cobalt and molybdenum concentrations should be varied. Ni-Co-Mo catalysts have been shown to be superior to Co-Mo catalysts in certain studies (72). Hence the effect of different active metals should be studied by using nickel or tungsten based catalysts in addition to Co-Mo catalysts.

6. Studies in the literature indicate that catalytic hydrodenitrogenation using Co-Mo catalysts in the presence of chlorides improves the activity of catalysts (57, 55). This aspect should be assessed.

7. Confusion still exists as to the rate limiting step in hydrodenitrogenation. Both cracking and hydrogenation play a major role. Hence, studies with mixed beds of catalysts with one layer of catalyst with a superior hydrogenation activity followed or preceded by another layer of catalyst with a superior hydrocracking activity should be conducted.

8. Characterization studies should be conducted on the different boiling fractions of the feedstock as well as the products. This will give an insight to the compounds present in a certain boiling range thereby making results from distillation studies more useful.

9. More doctoring studies should be performed to establish the best doctoring compound and the optimum amount of doctoring compound that should be added to the feedstock.

10. The fluid dynamics of trickle bed reactors are complex and have not been completely studied. Questions arise as to the degree of vaporization of the feed and about the number of phases present at reaction conditions. Independent studies should be performed to answer some of these questions.

BIBLIOGRAPHY

1. Bureau of Mines, Dept. of the Interior, News Release, April 5, 1976.

2. "United States Energy through the year 2000," Bureau of Mines, Dept. of the Interior, December 1975.

3. Coal Age, 79, No. 4, 72 (1974).

4. Wolk, R. H., N. C. Stewart, and H. F. Silver, American Chemical Society, Division of Fuel Chemistry Preprints, 20, No. 2, 116 (1975).

5. Wan, K. T., M. S. Thesis, Oklahoma State University, Stillwater, Oklahoma (1973).

6. Satchell, D., Ph.D. Thesis, Oklahoma State University, Stillwater, Oklahoma (1974).

7. Sooter, M., Ph.D. Thesis, Oklahoma State University, Stillwater, Oklahoma (1974).

8. Mehta, D. C., Ph.D. Thesis, In Preparation, Oklahoma State University, Stillwater, Oklahoma.

9. Ahmed, M. M., M. S. Thesis, Oklahoma State University, Stillwater, Oklahoma (1975).

10. Schlaffer, W. G., C. R. Adams and J. N. Wilson, J. Phys. Chem., 69, 1530 (1965).

11. Lapidus, L., Ind. Eng. Chem., 49, 1000 (1967).

12. Murphree, E. V., A. Voorhies, Jr., and F. X. Mayer, Ind. Eng. Chem. Process Design Develop., 3, 381 (1964).

13. Mears, D. E., Chem. Eng. Sci., 26, 1361 (1971).

14. Sater, V. E. and O. Levenspiel, Ind. Eng. Chem. Fundamentals, 5, 86 (1966).

15. Hochman, J. M. and E. Effron, Ind. Eng. Chem. Fundamentals, 8, 63 (1969).

16. Deans, H. A., Soc. Petrol. Eng. J., 3, 49 (1963).

17. Hoogendoorn, C. J. and J. Lips, Can. J. Chem. Eng., 43, 125 (1965).

18. Buffham, B. A., L. G. Gibilaro, and M. N. Rathor, AIChE J., 16, 218 (1970).

19. Furzer, I. A. and R. W. Mitchell, AIChE J., 16, 380 (1970).

20. Schwartz, J. G. and Roberts, "Analysis of Trickle Bed Reactors - Liquid backmixing and liquid-solid contacting." Presented at the 74th National Meeting, AIChE, New Orleans, (1973).

21. Mitchell, R. W. and I. A. Furzer, Chem. Eng. J., 4, 53 (1972).

22. Satterfield, C. N., AIChE J., 21, 209 (1975).

23. Shah, Y. T. and J. A. Paraskos, Chem. Eng. Sci., 30, 1169, (1975).

24. Schwartz, J. G., E. Weger and Dudukovic, "Liquid Holdup and Dispersion in Trickle Bed Reactors." Unpublished paper, Washington University, St. Louis, Missouri (1976).

25. Ross, L. D., Chem. Eng. Prog., 61, No. 10, 77 (1965).

26. Satterfield, C. N. and P. F. Way, AIChE J, 18, 305 (1972).

27. Goto, S. and J. M. Smith, AIChE J., 21, 706 (1975).

28. Charpentier, J. and M. Favier, AIChE J., 21, 1213 (1975).

29. Larkins, R. P., R. R. White and D. W. Jeffrey, AIChE J., 7, 231 (1961).

30. Sato, Y., T. Hirose, F. Takahashi and M. Toda, J. Chem. Eng. Japan, 6, 315 (1973).

31. Henry, H. C. and J. B. Gilbert, Ind. Eng. Chem. Process Des. Develop. 12, 328 (1973).

32. Mears, D. E., Adv. in Chem. Ser. No. 133, 218 (1974).

33. Satterfield, C. N. and F. Ozel, AIChE J. 19, 1259 (1973).

34. Sedricks, W. and C. N. Kenney, Chem. Eng. Sci., 28, 559 (1973).

35. Wijffels, J. B., J. Verloop and J. Zuiderweg, Adv. in Chem. Ser. No. 133, 151 (1974).

36. Schwartz, J. G., E. Weger and Dudukovic, "A new tracer method for determination of liquid-solid contacting efficiency in Trickle Bed Reactors," Unpublished paper, Washington University, St. Louis, Missouri (1976).

37. Montagna, A. A. and Y. T. Shah, Ind. Eng. Chem. Process Des. Develop. 14, 479 (1975).

38. Paraskos, J. A., J. A. Frayer and Y. T. Shah, Ind. Eng. Chem.
    Process Des. Develop. 14, 315 (1975).

39. Satterfield, C. N., A. A. Pelossof and T. K. Sherwood, AIChE J.,
    15, 226 (1969).

40. Satterfield, C. N. "Mass Transfer in Heterogeneous Catalysis,"
    M.I.T. Press, Cambridge, Massachusetts (1970).

41. Van Deemter, J. J. Third European Symposium on Chemical Reaction
    Engineering, 215 (1964).

42. Van Zoonen, D. and Douwes, J. Inst. Petroleum, 49, 385 (1963).

43. Addington, D. and E. Thompson, Third European Symposium on Chemical
    Reaction Engineering, 203 (1964).

44. McIlvried, H. G., Ind. Eng. Chem. Process Des. Develop. 10, 125
    (1971).

45. Satterfield, C. N. and J. F. Cochetto, AIChE J., 21, 1107 (1975).

46. Satterfield, C. N., M. Model and J. F. Mayer, AIChE J., 1100 (1975).

47. Flinn, R. A., O. A. Larson and H. Beuther, Hydrocarbon Processing,
    42, No. 9, 129 (1963).

48. Doleman, J. and J. C. Vlughter, Proc. Sixth World Pet. Cong.
    Section III, Paper 12-PD7, Frankfurt/Main, Germany, June 19-
    26, 1963.

49. Gheit, A. K., Can. J. Chem., 53, 2575 (1975).

50. Gheit, A. K. and I. K. Abdou, J. Inst. Petroleum, 59, 188 (1973).

51. Madkour, M. M., B. H. Mahmoud, I. K. Abdou and J. C. Vlughter,
    J. Indian Chem. Soc., 46, 720 (1969).

52. Schuman, S. C. and H. Shalit, Catal. Rev., 4, 245 (1970).

53. Schuit, G. C. A. and B. C. Gates, AIChE J., 19, 417 (1973).

54. Gilbert, J. B. and R. Kartzmark, Proc. Amer. Inst. Petroleum, 45,
    No. 3, 29 (1965).

55. McCandless, F. P. and L. Berg, Ind. Eng. Chem. Process Des.
    Develop., 9, 110 (1970).

56. Koros, R. M., S. Bank, J. E. Hoffman and M. I. Kay, Preprints,
    Div. of Petroleum Chemistry, ACS, 12, No. 4, B165 (1967).

57. Silver, H. F., N. H. Wang, H. B. Jensen and R. E. Poulson,
    Preprints, Div. of Petroleum Chemistry, ACS, 17, No. 4,
    G94 (1972).

58. Benson, D. B. and L. Berg, Chem. Eng. Prog., 62, No. 8, 61 (1966).

59. Frost, C. M. and H. B. Jensen, Preprints, Div. of Petroleum Chemistry, ACS, 18, No. 1, 119 (1973).

60. White, P. J., J. F. Jones and R. T. Eddinger, Hydrocarbon Processing, 47, No. 12, 97 (1968).

61. Jones, J. F., M. R. Schmid, M. E. Sacks, Y. Chen, C. A. Gray and R. T. Eddinger, "Char Oil Energy Development. Final Report," Office of Coal Research, Dept. of the Interior, 1966.

62. FMC Corporation, "Char Oil Energy Development," Office of Coal Research R & D Report No. 56, Interim Report No. 1, 1970.

63. Jones, J. F., F. H. Schoeman, J. A. Hamshar, B. D. McMunn, L. J. Scotti and R. T. Eddinger, "Char Oil Energy Development," Office of Coal Research, R & D Report No. 73, Interim Report No. 1, 1972.

64. Scotti, L. J., B. D. McMunn, M. I. Gveene, R. C. Merrill, F. H. Schoeman, H. D. Terzian, J. A. Hamshar, D. J. Domina and J. F. Jones, "Char Oil Energy Development," Office of Coal Research R & D Report No. 73, Interim Report No. 2, 1973.

65. Scotti, L. J., R. C. Merrill, B. D. McMunn, S. J. Romalczyk, D. J. Domina, L. Ford, H. D. Terzian and J. F. Jones, "Char Oil Energy Development," ERDA Interim Report No. 5, 1974.

66. Jones, J. F. and L. D. Friedman, "Char Oil Energy Development - Final Report," Office of Coal Research Report No. 56, (1970).

67. Quader, S. A. and G. R. Hill, Ind. Eng. Chem. Process Des. Develop., 8, 450 (1969).

68. Metcalfe, T. B. and A. Ruangteprat, AIChE Symposium Series, Vol. 70, No. 137, 252 (1974).

69. Maio, D. D. and A. Naglieri, Chem. Eng., 75, No. 16, 127 (1968).

70. Kawa, W., S. Friedman, W. R. K. Wu, L. V. Frank and P. M Yavorsky, Preprints, Div. Fuel Chemistry, ACS, 19, No. 1, 192 (1974).

71. Grimm, C. D. and L. Berg, "Hydrodesulfurization Support Materials," presented at 68th National Meeting, Houston AIChE, February 28 - March 4, 1971.

72. Ahuja, S. P., M. L. Derrien, and J. F. LePage, Ind. Eng. Chem. Prod. Res. Develop., 9, 272 (1970).

73. Schlaffer, W. G., C. Z. Morgan and J. N. Wilson, J. Phys. Chem., 61, 714 (1957).

74. Beuther, H., R. A. Flinn and J. B. McKinley, Ind. Eng. Chem., 51, 1349 (1959).

75. Livingston, J. Y., "Hydrotreating Catalyst Properties Do Affect Performance," presented at the 74th National Meeting, AIChE, New Orleans, Louisiana, March 11-15, 1973.

76. Higginson, G. W., Chemical Engineering, 81, No 20, 98 (1974).

77. Richardson, J. T., Ind. Eng. Chem. Fundamentals, 3, 154 (1964).

78. Lipsch, J. M. J. G. and G. C. A. Schuit, J. Catalysis, 15, 174 (1969).

79. Friedman, R. M., R. I. Declerk-Grimme and J. J. Fripiat, Journal of Electron Spectroscopy and Related Phenomena, 5, 437 (1974).

80. Mitchell, P. C. H. and F. Tripino, J. Catalysis, 33, 350 (1974).

81. Tantarov, M. A., R. A. Faskhutdinov, M. E. Levinter and I. G. Akhmetov, International Chemical Engineering, 12, No. 1, 85 (1972).

82. Goudriann, F., H. Gierman and J. C. Vlughter, J. Inst. of Petroleum, 59, 40 (1973).

83. Cochetto, J F. and C. N. Satterfield, Ind. Eng. Chem. Process Des. Dev., 15, 272 (1976).

84. Snyder, L. R., Am. Chem. Soc. Div. Petrol. Chem. Rep. 4 (2), C43 (1970).

85. Bratton, A. C. and J. R. Bailey, J. Am. Chem. Soc. 59, 175 (1937).

86. Nixon, A. C. and R. E. Thorpe, J. Chem. Eng. Data 7, 429 (1962).

87. Jewell, D. M. and G. K. Hartung, J. Chem. Eng. Data 2, 95 (1957).

88. Brandenburg, C. F. and D. R. Latham, J. Chem. Eng. Data 13, 391 (1968).

89. Anderson, H. C. and W. R. K. Wu, Bureau of Mines Bulletin 606, U. S. Dept. of the Interior, 1963.

90. McNeil, D., in Bituminous Materials: Asphalts, Tars and Pitches, ed. A. J. Hoiberg, Interscience Publishing Co., New York, N. Y., 1966, Vol. 3, pp. 139-216.

91. Shultz, J. L., R. A Friedel and A. G. Sharkey, Jr., Fuel, 44, 55 (1965).

92. Sharkey, A. G., Jr., G. Wood, J. L. Shultz, I. Wender and R. A. Friedel, Fuel, 30, 315 (1959).

93. Schultz, J. L., R. A. Friedel and A. G. Sharkey, Jr., "Mass
    Spectromatric Analyses of Coal Tar Distillates and Residues,"
    Bureau of Mines Report of Investigations No. 7000, U. S.
    Dept. of the Interior (1967).

94. Schultz, J. L., T. Kessler, R. A. Friedel and A. G. Sharkey, Jr.,
    Fuel, 52, 242 (1973).

95. Scheppele, S. E. and G. J. Greenwood, Quarterly Progress Report
    FE2011-4, prepared for the United States Energy Research and
    Development Administration by B. L. Crynes, Oklahoma State
    University, Stillwater, Oklahoma.

96. Jewell, D. M., J. H. Weber, J. W. Bunger, H. Planchor and D. R.
    Latham, Anal. Chem., 44, 1391 (1972).

97. Leach, B., Personal Communication to Dr. B. L. Crynes.

98. Perkin-Elmer Operating Manual for the Model 240 Elemental Analyzer.

99. Culmo, R., Perkin-Elmer Corporation, Personal Communications.

100. Smith, A. J., G. Myers, Jr., and W. C. Shaner, Jr., Michrochimica
     Acta, pp. 217-222 (1972).

101. U. S. Patent No. 3773691.

102. U. S. Patent No. 3907982.

103. U. S. Patent No. 3975231.

104. U. S. Patent No. 3975510.

105. Rajaram, Mamidi, Special Report submitted to Dr. B. L. Crynes,
     Oklahoma State University, 1976.

106. Yen, Y. K., D. E. Furlani and S. W. Weller, Ind. Eng. Chem. Prod.
     Res. Dev. 15, 24 (1976).

107. 1976 Annual Book of ASTM Standards, Part 23, p. 550, Standard
     Designation D1160.

108. Greenwood, G. J., Personal Communication, 1976.

109. Nakamura, H., et al., J. Jap. Petrol. Eng. Soc., 12, No. 10,
     26 (1969).

110. Puranik, S. S. and A. Vogelpohl, Chem. Eng. Sci., 29, 501 (1974).

111. Innes, W. B., Anal. Chem. 29, 1069 (1957).

112. Ketkar, R., Special Report Submitted to Dr. B. L. Crynes,
     Oklahoma State University, 1977.

113. Kline, S. J. and F. A. McClintock, Mech. Eng., 75, 3 (1953).

114. Levenspiel, O., Chemical Reaction Engineering, 2nd ed. Wiley, New York (1972).

115. Taylor, H. S., "A Treatise on Physical Chemistry", D. Van Nostrand Company, Inc., New York (1942).

116. _____, Engineering Data Book, 9th ed., Gas Processors Suppliers Association, Tulsa, Oklahoma, 1972.

117. Smith, J. M., Chemical Engineering Kinetics, 2nd ed., McGraw-Hill Book Company, New York, 1970.

118. U. S. Patent 2,890,162

APPENDIX A

RAW DATA

The data presented in Table XLIII are the corrected weight percent nitrogen in product oil for all the series except the CAT series. When these samples were analyzed using the Perkin-Elmer analyzer, the aluminum capsules that were used to transfer the samples to the combustion tube were sealed in air. The blank capsules were also sealed in air. However, this caused an error, because when the blank values are subtracted from the read values, the blank readings actually include the volume of the capsule occupied by the sample too. Even though this volume is quite small (8.5 μl), because of the low nitrogen content of the samples, this could cause an error of up to 8-10% in the analysis. Sealing the samples in helium could solve this problem. Since the samples in this study were sealed in air, they were corrected to the values that would have been obtained if these samples were sealed in helium.

The corrected values were calculated as follows. The volume of samples used for nitrogen analysis was 8.5 ± 0.2 microliters. Hence, the value of 8.5 microliters was used to calculate the correction factor. 8.5 microliters of air contains about 8.4 micrograms of nitrogen. So 8.4 micrograms were added to the micrograms of nitrogen determined from the analyzer and this total was divided by the weight of the sample to give the new weight percent nitrogen. Two samples

were chosen at random and analyzed by sealing them in helium to check the correction procedure and the results are presented below.

Sample No.	Weight Percent Nitrogen	
	Value Using Helium	Corrected Value
KEC 15	0.524	0.545
KEC 21	0.455	0.454

TABLE XLIII

RAW DATA

Sample Number	Temp[a] (°F)	Pressure (psig)	Space Time[b] (Vol. hrly)	Hydrogen (SCF/BBL)	Hours[c] on oil	%N[d]
CAT-1	650	1500	1.86	1500	8	0.574
CAT-2	650	1500	1.86	1500	11	0.627
CAT-3	650	1500	1.86	1500	13.5	0.534
CAT-4	650	1500	1.86	1500	16	0.576
CAT-5	650	1500	1.86	1500	20	0.616
CAT-6	650	1500	1.86	1500	24	0.537
CAT-7	650	1500	1.86	1500	28	0.559
CAT-8	650	1500	1.86	1500	32	0.548
CAT-9	650	1500	1.86	1500	36	0.544
CAT-10	650	1500	1.86	1500	40	0.504
CAT-11	650	1500	1.86	1500	44	0.539
CAT-12	650	1500	1.86	1500	48	0.531
CAT-13	650	1500	0.93	750	50.5	0.675
CAT-14	650	1500	0.93	750	52.5	0.675
CAT-15	650	1500	0.93	750	54.5	0.670
CAT-16	650	1500	0.465	375	56	0.804
CAT-17	650	1500	0.465	375	57	0.713
CAT-18	650	1500	0.465	375	58	0.788
CAT-19	650	1500	1.86	1500	60.5	0.586
CAT-20	650	1500	1.86	1500	62.5	0.499
CAT-21	650	1500	1.86	1500	64.5	0.484
CAT-22	700	1500	1.86	1500	71.5	0.404
CAT-23	700	1500	1.86	1500	73.5	0.304
CAT-24	700	1500	1.86	1500	75.5	0.391
CAT-25	700	1500	0.93	1500	78.5	0.379
CAT-26	700	1500	0.93	1500	80.5	0.497
CAT-27	700	1500	0.93	1500	82.5	0.456
CAT-28	700	1500	0.465	1500	84	0.608
CAT-29	700	1500	0.465	1500	85	0.708
CAT-30	700	1500	0.465	1500	86	0.591
CAT-31	700	1500	1.86	1500	88.5	0.529
CAT-32	700	1500	1.86	1500	90.5	0.350
CAT-33	700	1500	1.86	1500	92.5	0.353
KEC-1	650	1500	1.84	1500	10	0.429
KEC-2	650	1500	1.84	1500	12	0.432
KEC-3	650	1500	1.84	1500	14	0.435
KEC-4	650	1500	1.84	1500	16	0.443
KEC-5	650	1500	1.84	1500	20	0.457
KEC-6	650	1500	1.84	1500	24	0.406
KEC-7	650	1500	1.84	1500	28	0.435
KEC-8	650	1500	1.84	1500	32	0.423
KEC-9	650	1500	1.84	1500	36	0.457
KEC-10	650	1500	1.84	1500	40	0.427

TABLE XLIII (continued)

Sample Number	Temp[a] (°F)	Pressure (psig)	Space Time[b] (Vol. hrly)	Hydrogen (SCF/BBL)	Hours[c] on oil	%N[d]
KEC-11	650	1500	1.84	1500	44	0.444
KEC-12	650	1500	1.84	1500	48	0.437
KEC-13	650	1500	0.92	1500	50	0.538
KEC-14	650	1500	0.92	1500	52	0.570
KEC-15	650	1500	0.92	1500	54	0.546
KEC-16	650	1500	0.46	1500	55	0.614
KEC-17	650	1500	0.46	1500	56	0.617
KEC-18	650	1500	0.46	1500	57	0.667
KEC-19	650	1500	1.84	1500	59	0.463
KEC-20	650	1500	1.84	1500	61	0.492
KEC-21	650	1500	1.84	1500	63	0.455
KEC-22	700	1500	1.84	1500	69	0.283
KEC-23	700	1500	1.84	1500	71	0.223
KEC-24	700	1500	1.84	1500	73	0.247
KEC-25	700	1500	0.92	1500	75	0.325
KEC-26	700	1500	0.92	1500	77	0.516
KEC-27	700	1500	0.92	1500	78	0.386
KEC-28	700	1500	0.46	1500	80	0.600
KEC-29	700	1500	0.46	1500	81	0.496
KEC-30	700	1500	0.46	1500	82	0.524
KEC-31	700	1500	1.84	1500	84	0.219
KEC-32	700	1500	1.84	1500	86	0.302
KEC-33	700	1500	1.84	1500	88	0.220
KEC-34	750	1500	1.84	1500	94	0.126
KEC-35	750	1500	1.84	1500	96	0.132
KEC-36	750	1500	1.84	1500	98	0.147
KEC-37	750	1500	0.92	1500	100	0.195
KEC-38	750	1500	0.92	1500	102	0.216
KEC-39	750	1500	0.92	1500	104	0.233
KEC-40	750	1500	0.46	1500	105	0.349
KEC-41	750	1500	0.46	1500	106	0.348
KEC-42	750	1500	0.46	1500	107	0.417
KEC-43	750	1500	1.84	1500	109	0.261
KEC-44	750	1500	1.84	1500	111	0.176
KEC-45	750	1500	1.84	1500	113	0.206
KEC-46	650	1500	1.84	1500	120	0.427
KEC-47	650	1500	1.84	1500	122	0.423
KEC-48	650	1500	1.84	1500	124	0.418
KET-1	650	1500	1.84	1500	7	0.430
KET-2	650	1500	1.84	1500	9	0.581
KET-3	650	1500	1.84	1500	13	0.514
KET-4	650	1500	1.84	1500	16	0.614
KET-5	650	1500	1.84	1500	20	0.494
KET-6	650	1500	1.84	1500	24	0.583
KET-7	650	1500	1.84	1500	28	0.505

TABLE XLIII (continued)

Sample Number	Temp[a] (°F)	Pressure (psig)	Space Time[b] (Vol. hrly)	Hydrogen (SCF/BBL)	Hours[c] on oil	%N[d]
KET-8	650	1500	1.84	1500	32	0.602
KET-9	650	1500	1.84	1500	36	0.492
KET-10	650	1500	1.84	1500	40	0.592
KET-11	650	1500	1.84	1500	44	0.467
KET-12	650	1500	1.84	1500	48	0.502
KET-13	650	1500	0.92	1500	50.5	0.638
KET-14	650	1500	0.92	1500	52.5	0.665
KET-15	650	1500	0.92	1500	54.5	0.628
KET-16	650	1500	0.46	1500	56	0.809
KET-17	650	1500	0.46	1500	57	0.824
KET-18	650	1500	0.46	1500	58	0.828
KET-19	650	1500	1.84	1500	60.5	0.566
KET-20	650	1500	1.84	1500	62	0.503
KET-21	650	1500	1.84	1500	64	0.485
KET-22	700	1500	1.84	1500	68	0.422
KET-23	700	1500	1.84	1500	70	0.324
KET-24	700	1500	1.84	1500	72	0.284
KET-25	700	1500	0.92	1500	74.5	0.481
KET-26	700	1500	0.92	1500	76.5	0.523
KET-27	700	1500	0.92	1500	78.5	0.613
KET-28	700	1500	0.46	1500	79.5	0.702
KET-29	700	1500	0.46	1500	80.5	0.528
KET-30	700	1500	0.46	1500	81.5	0.802
KET-31	700	1500	1.84	1500	83.5	0.442
KET-32	700	1500	1.84	1500	85.5	0.314
KET-33	700	1500	1.84	1500	87.5	0.326
KET-34	750	1500	1.84	1500	91.5	0.326
KET-35	750	1500	1.84	1500	93.5	0.215
KET-36	750	1500	1.84	1500	95.5	0.202
KET-37	750	1500	0.92	1500	98	0.379
KET-38	750	1500	0.92	1500	100	0.436
KET-39	750	1500	0.92	1500	102	0.443
KET-40	750	1500	0.46	1500	103.5	0.394
KET-41	750	1500	0.46	1500	104.5	0.554
KET-42	750	1500	0.46	1500	105.5	0.412
KET-43	750	1500	1.84	1500	108.5	0.377
KET-44	750	1500	1.84	1500	110.5	0.207
KET-45	750	1500	1.84	1500	112.5	0.207
KET-46	650	1500	1.84	1500	117	0.471
KET-47	650	1500	1.84	1500	119	0.495
KET-48	650	1500	1.84	1500	121	0.490
KEP-1	650	1500	1.84	1500	8.5	0.846
KEP-2	650	1500	1.84	1500	11	0.785
KEP-3	650	1500	1.84	1500	14	0.709
KEP-4	650	1500	1.84	1500	17	0.706

TABLE XLIII (continued)

Sample Number	Temp[a] (°F)	Pressure (psig)	Space Time[b] (Vol. hrly)	Hydrogen (SCF/BBL)	Hours[c] on oil	%N[d]
KEP-5	650	1500	1.84	1500	20	0.547
KEP-6	650	1500	1.84	1500	24	0.591
KEP-7	650	1500	1.84	1500	28	0.547
KEP-8	650	1500	1.84	1500	32	0.565
KEP-9	650	1500	1.84	1500	36	0.627
KEP-10	650	1500	1.84	1500	40	0.618
KEP-11	650	1500	1.84	1500	44	0.598
KEP-12	650	1500	1.84	1500	48	0.608
KEP-13	650	1500	0.92	1500	50.5	0.683
KEP-14	650	1500	0.92	1500	52.5	0.693
KEP-15	650	1500	0.92	1500	54.5	0.662
KEP-16	650	1500	0.46	1500	56	0.783
KEP-17	650	1500	0.46	1500	57	0.782
KEP-18	650	1500	0.46	1500	58	0.807
KEP-19	650	1500	1.84	1500	60.5	0.644
KEP-20	650	1500	1.84	1500	62.5	0.569
KEP-21	650	1500	1.84	1500	64.5	0.553
KEP-22	700	1500	1.84	1500	71.75	0.487
KEP-23	700	1500	1.84	1500	73.75	0.439
KEP-24	700	1500	1.84	1500	75.75	0.402
KEP-25	700	1500	0.92	1500	78.25	0.543
KEP-26	700	1500	0.92	1500	80.25	0.538
KEP-27	700	1500	0.92	1500	82.25	0.516
KEP-28	700	1500	0.46	1500	83.75	0.515
KEP-29	700	1500	0.46	1500	84.75	0.583
KEP-30	700	1500	0.46	1500	85.75	0.613
KEP-31	700	1500	1.84	1500	88.25	0.507
KEP-32	700	1500	1.84	1500	90.25	0.403
KEP-33	700	1500	1.84	1500	92.25	0.428
KEP-34	750	1500	1.84	1500	98.75	0.177
KEP-35	750	1500	1.84	1500	100.75	0.233
KEP-36	750	1500	1.84	1500	102.75	0.207
KEP-37	750	1500	0.92	1500	105.5	0.308
KEP-38	750	1500	0.92	1500	108	0.257
KEP-39	750	1500	0.92	1500	110	0.308
KEP-40	750	1500	0.46	1500	111.5	0.424
KEP-41	750	1500	0.46	1500	112.5	0.451
KEP-42	750	1500	0.46	1500	113.5	0.492
KEP-43	750	1500	1.84	1500	116.5	0.197
KEP-44	750	1500	1.84	1500	118.5	0.197
KEP-45	750	1500	1.84	1500	120.5	0.222
KEP-46	650	1500	1.84	1500	124.5	0.628
KEP-47	650	1500	1.84	1500	126.5	0.648
KEP-48	650	1500	1.84	1500	128.5	0.588

TABLE XLIII (continued)

Sample Number	Temp[a] (°F)	Pressure (psig)	Space Time[b] (Vol. hrly)	Hydrogen (SCF/BBL)	Hours[c] on oil	%N[d]
KER-1	650	1500	1.84	1500	10	0.654
KER-2	650	1500	1.84	1500	12	0.409
KER-3	650	1500	1.84	1500	14	0.470
KER-4	650	1500	1.84	1500	16	0.493
KER-5	650	1500	1.84	1500	20	0.395
KER-6	650	1500	1.84	1500	24	0.372
KER-7	650	1500	1.84	1500	28	0.379
KER-8	650	1500	1.84	1500	32	0.437
KER-0	650	1500	1.84	1500	36	0.376
KER-10	650	1500	1.84	1500	40	0.478
KER-11	650	1500	1.84	1500	44	0.486
KER-12	650	1500	1.84	1500	48	0.455
KER-13	650	1500	0.92	1500	50	0.704
KER-14	650	1500	0.92	1500	52	0.667
KER-15	650	1500	0.92	1500	54	0.677
KER-16	650	1500	0.46	1500	55	0.647
KER-17	650	1500	0.46	1500	56	0.711
KER-18	650	1500	0.46	1500	57	0.767
KER-19	650	1500	1.84	1500	59	0.552
KER-20	650	1500	1.84	1500	61	0.465
KER-21	650	1500	1.84	1500	63	0.398
KER-22	700	1500	1.84	1500	68.5	0.371
KER-23	700	1500	1.84	1500	70.5	0.342
KER-24	700	1500	1.84	1500	72.5	0.305
KER-25	700	1500	0.92	1500	74.5	0.409
KER-26	700	1500	0.92	1500	76.5	0.437
KER-27	700	1500	0.92	1500	78.5	0.449
KER-28	700	1500	0.46	1500	79.5	0.551
KER-29	700	1500	0.46	1500	80.5	0.577
KER-30	700	1500	0.46	1500	81.5	0.621
KER-31	700	1500	1.84	1500	83.5	0.267
KER-32	700	1500	1.84	1500	85.5	0.263
KER-33	700	1500	1.84	1500	87.5	0.284
KER-34	750	1500	1.84	1500	94	0.189
KER-35	750	1500	1.84	1500	96	0.154
KER-36	750	1500	1.84	1500	98	0.174
KER-37	750	1500	0.92	1500	100	0.238
KER-38	750	1500	0.92	1500	102	0.407
KER-39	750	1500	0.92	1500	104	0.291
KER-40	750	1500	0.46	1500	105	0.391
KER-41	750	1500	0.46	1500	106	0.325
KER-42	750	1500	0.46	1500	107	0.336
KER-43	750	1500	1.84	1500	109	0.198
KER-44	750	1500	1.84	1500	111	0.160
KER-45	750	1500	1.84	1500	113	0.110
KER-46	650	1500	1.84	1500	119.5	0.359

TABLE XLIII (continued)

Sample Number	Temp[a] (°F)	Pressure (psig)	Space Time[b] (Vol. hrly)	Hydrogen (SCF/BBL)	Hours[c] on oil	%N[d]
KER-47	650	1500	1.84	1500	121.5	0.598
KER-48	650	1500	1.84	1500	123.5	0.645
KDC-1	700	1500	1.84	1500	14	0.614
KDC-2	700	1500	1.84	1500	18	0.612
KDC-3	700	1500	1.84	1500	21	0.623
KDC-4	700	1500	1.84	1500	24	0.616
KDC-5	700	1500	1.84	1500	30	0.565
KDC-6	700	1500	1.84	1500	36	0.578
KDC-7	700	1500	1.84	1500	42	0.610
KDC-8	700	1500	1.84	1500	48	0.626
KDC-9	700	1500	0.92	1500	52	0.884
KDC-10	700	1500	0.92	1500	55	0.906
KDC-11	700	1500	0.92	1500	57	0.910
KDC-12	700	1500	0.46	1500	61	1.364
KDC-13	700	1500	0.46	1500	63	1.187
KDC-14	700	1500	0.46	1500	65	1.363
KDC-15	700	1500	1.84	1500	68	0.830
KDC-16	700	1500	1.84	1500	70	0.640
KDC-17	700	1500	1.84	1500	72	0.693
KDT-1	700	1500	1.84	1500	11	1.146
KDT-2	700	1500	1.84	1500	12	0.882
KDT-3	700	1500	1.84	1500	18	1.037
KDT-4	700	1500	1.84	1500	24	0.805
KDT-5	700	1500	1.84	1500	30	1.072
KDT-6	700	1500	1.84	1500	36	0.799
KDT-7	700	1500	1.84	1500	42	0.942
KDT-8	700	1500	1.84	1500	48	0.917
KDT-9	700	1500	0.92	1500	52	1.224
KDT-10	700	1500	0.92	1500	55	1.545
KDT-11	700	1500	0.92	1500	58	1.162
KDT-12	700	1500	0.46	1500	61	1.392
KDT-13	700	1500	0.46	1500	63	1.468
KDT-14	700	1500	0.46	1500	65	1.430
KDT-15	700	1500	1.84	1500	68	0.968
KDT-16	700	1500	1.84	1500	70	0.832
KDT-17	700	1500	1.84	1500	72	0.888
KDP-1	700	1500	1.84	1500	11	1.059
KDP-2	700	1500	1.84	1500	14.5	0.803
KDP-3	700	1500	1.84	1500	18	0.993
KDP-4	700	1500	1.84	1500	24	0.910
KDP-5	700	1500	1.84	1500	30	1.104
KDP-6	700	1500	1.84	1500	36	0.773
KDP-7	700	1500	1.84	1500	42	0.813

TABLE XLIII (continued)

Sample Number	Temp[a] (°F)	Pressure (psig)	Space Time[b] (Vol. hrly)	Hydrogen (SCF/BBL)	Hours[c] on oil	%N[d]
KDP-8	700	1500	1.84	1500	48	0.737
KDP-9	700	1500	0.92	1500	52	1.040
KDP-10	700	1500	0.92	1500	55	1.056
KDP-11	700	1500	0.92	1500	58	0.998
KDP-12	700	1500	0.46	1500	61	1.280
KDP-13	700	1500	0.46	1500	63	1.257
KDP-14	700	1500	0.46	1500	65	1.269
KDP-15	700	1500	1.84	1500	68	0.844
KDP-16	700	1500	1.84	1500	70	0.770
KDP-17	700	1500	1.84	1500	72	0.830

a. Nominal Reactor Temperature

b. This is a volume hourly space time (volume of catalyst/volume of oil per hour).

c. Total hours which the catalyst has been contacted with oil.

d. Percent nitrogen in liquid product.

APPENDIX B

MERCURY PENETRATION DATA

The alumina supports and the supports impregnated with active metals were sent out to an independent analytical laboratory (American Instrument Company) to determine the physical properties such as surface area, pore volume and pore size distribution. Table XLIV presents this information along with vendor supplied data, where available, for the supports. The pore size distribution figures for the supports were presented in Chapter V. The mercury penetration data used to calculate the pore size distributions for all the supports and catalysts used in this study are presented in Tables XLV and XLVI. Procedures for obtaining pore size distribution curves from mercury penetration data are standard and can be found elsewhere (117).

TABLE XLIV

SUPPORT PROPERTIES

Property	CONOCO CATAPAL HP-20		Ketjen 007-1.5E		Ketjen 000-3P	
	Vendor Supplied Data	From AIC*	Vendor Supplied Data	From AIC*	Vendor Supplied Data	From AIC*
Surface Area m^2/gm	250	244	300	311	244	254
Pore Volume cc/gm	1.19	1.01	0.65	0.647	0.84	0.834
Most frequent pore radius, Å		40, 1100		33		34, 150

* American Instrument Company

TABLE XLV

MERCURY PENETRATION DATA FOR THE CATALYST
SUPPORTS USED IN THIS STUDY

CONOCO CATAPAL HP-20		Ketjen 007-1.5E		Steam Treated (10 hrs) Ketjen 007-1.5E		Ketjen 000-3P	
Absolute Pressure, psia	Intrusion, cc/gm	Absolute Pressure, psia	Intrusion, cc/gm	Absolute Pressure, psia	Intrusion, cc/gm	Absolute Pressure, psia	Intrusion, cc/gm
1.8	0.00	1.8	0.000	1.8	0.000	1.8	0.000
3.5	0.02	9.9	0.010	9.9	0.006	9.9	0.004
10.0	0.03	250	0.015	99.9	0.010	250	0.004
100	0.03	1000	0.020	400	0.013	1000	0.004
300	0.04	2500	0.020	1000	0.013	1500	0.013
700	0.08	5000	0.020	2000	0.016	2000	0.036
900	0.14	8000	0.030	4000	0.022	3000	0.084
1200	0.19	13000	0.040	6000	0.029	4000	0.142
2500	0.25	15000	0.050	10000	0.035	5000	0.191
5000	0.31	17000	0.060	12000	0.048	7000	0.266
8000	0.40	19000	0.070	16000	0.070	10000	0.328
12000	0.48	21000	0.095	19000	0.118	13000	0.382
16000	0.54	23000	0.129	20000	0.149	16000	0.435
20000	0.62	25000	0.189	21000	0.197	20000	0.506
25000	0.80	27000	0.279	22000	0.254	24000	0.590
30000	0.92	30000	0.398	24000	0.349	27000	0.675
35000	0.98	33000	0.483	26000	0.442	30000	0.737
40000	1.00	36000	0.543	28000	0.518	35000	0.790
50000	1.00	40000	0.592	30000	0.575	40000	0.817
60000	1.01	45000	0.607	35000	0.645	50000	0.830
		50000	0.617	40000	0.670	60000	0.834
		60000	0.622	50000	0.680		

TABLE XLVI

MERCURY PENETRATION DATA FOR THE CATALYSTS
USED IN THIS STUDY

Catalyst Used in:							
KEC Series		CAT Series		KET Series		KEP Series	
Absolute Pressure, psia	Intrusion, cc/gm	Absolute Pressure, psia	Intrusion, cc/gm	Absolute Pressure, psia	Intrusion, cc/gm	Absolute Pressure, psia	Intrusion, cc/gm
1.8	0.000	1.8	0.000	1.8	0.000	1.8	0.000
9.9	0.005	5.2	0.015	9.9	0.009	9.8	0.010
1000	0.005	10	0.020	250	0.009	1000	0.014
6000	0.010	100	0.025	500	0.014	2000	0.038
10000	0.015	300	0.040	1200	0.019	3000	0.067
15000	0.025	400	0.079	2500	0.042	4000	0.096
20000	0.030	500	0.148	6000	0.051	5000	0.130
25000	0.080	550	0.168	10000	0.051	6000	0.159
27000	0.140	600	0.188	15000	0.056	8000	0.202
30000	0.299	800	0.222	18000	0.093	10000	0.236
33000	0.399	1200	0.247	20000	0.159	13000	0.279
36000	0.454	2500	0.282	22000	0.257	15000	0.308
40000	0.489	5000	0.306	25000	0.378	18000	0.356
50000	0.503	10000	0.361	28000	0.457	20000	0.390
60000	0.503	15000	0.450	32000	0.513	23000	0.452
		20000	0.593	40000	0.541	25000	0.500
		25000	0.751	50000	0.551	28000	0.553
		30000	0.791	60000	0.551	30000	0.577
		40000	0.805			35000	0.611
		60000	0.810			40000	0.625
						50000	0.625
						60000	0.625

TABLE XLVI (continued)

| Catalyst Used in: | | | | | | | |
| KER Series | | KDC Series | | KDT Series | | KDP Series | |
Absolute Pressure, psia	Intrusion, cc/gm	Absolute Pressure, psia	Intrusion, cc/gm	Absolute Pressure, psia	Intrusion, cc/gm	Absolute Pressure, psia	Intrusion, cc/gm
1.8	0.000	1.8	0.000	1.8	0.000	1.8	0.000
9.8	0.006	9.8	0.000	9.8	0.005	9.8	0.014
149.8	0.012	250	0.008	1000	0.005	250	0.019
1000	0.012	2000	0.008	3000	0.010	1000	0.024
4000	0.015	5000	0.008	6000	0.015	2000	0.048
8000	0.021	6000	0.015	9000	0.020	3000	0.077
15000	0.030	10000	0.023	10000	0.030	4000	0.106
20000	0.045	17000	0.030	15000	0.059	6000	0.159
22000	0.060	21000	0.038	18000	0.093	10000	0.207
24000	0.096	24000	0.053	20000	0.137	15000	0.250
25000	0.129	26000	0.083	21000	0.171	20000	0.299
26000	0.168	28000	0.166	22000	0.215	25000	0.371
27000	0.211	29000	0.226	23000	0.259	30000	0.424
28000	0.250	30000	0.271	25000	0.333	35000	0.443
30000	0.316	32000	0.339	27000	0.391	40000	0.448
32000	0.364	35000	0.407	30000	0.450	60000	0.448
35000	0.409	40000	0.452	35000	0.489		
40000	0.439	45000	0.460	40000	0.499		
45000	0.446	50000	0.467	60000	0.499		
50000	0.449	60000	0.467				
60000	0.452						

APPENDIX C

DISTILLATION DATA

A total of twelve samples were fractionated using an ASTM vacuum distillation technique. Table XLVII presents the operating conditions of these samples.

TABLE XLVII

OPERATING CONDITIONS FOR THE DISTILLED SAMPLES

Sample No.	Run Series	Temperature °F	Volume Hourly Space Time, hour	Weight Percent Nitrogen in product oil
KDC #8	KDC	700	1.84	0.626
KDC #11	KDC	700	0.92	0.910
KDC #13	KDC	700	0.46	1.187
KDT #8	KDT	700	1.84	0.917
KDT #11	KDT	700	0.92	1.162
KDT #13	KDT	700	0.46	1.468
KDP #8	KDP	700	1.84	0.737
KDP #11	KDP	700	0.92	0.998
KDP #13	KDP	700	0.46	1.257
Mixture of KEC 29 & 30	KEC	700	0.46	0.510
Mixture of KET 28 & 30	KET	700	0.46	0.752
Mixture of KEP 29 & 30	KEP	700	0.46	0.598

Table XLVIII presents the results from the distilled samples.

TABLE XLVIII

RAW DATA FROM DISTILLATION

FD - First Drop   RAO - Raw Anthracene Oil

DRAO - Doctored Raw Anthracene Oil

Sample No.	Fraction No.	Pot Temperature °F	Vapor Temperature °F	Volume Distilled cc	Weight of Fraction gm x 10^2	Weight % Nitrogen
RAO	FD	376	247			
	1	394	291	4.5		0.741
	2	429	327	11		1.209
	3	470	370	16		0.805
	4	485	399	9		0.878
	5	507	427	11		0.961
	6	548	474	16		1.013
	7	608	531	11		1.13
	8	660		3.5		1.490
DRAO	FD	336	232			
	1	360	249	9	9.28	3.205
	2	394	272	9	9.43	3.943
	3	429	330	9	9.57	3.29
	4	472	390	13	14.02	1.140
	5	485	410	6	6.55	0.861
	6	507	428	10	11.04	0.959
	7	548	477	15	16.79	1.077
	8	608	532	9.5	10.77	1.154
	9	660	592	3.5	3.62	1.570
KDC #8	FD	196	86			
	1	310	214	8	6.72	1.537
	2	360	270	11	10.40	2.318
	3	394	300	7.5	7.20	1.500
	4	429	369	15	14.70	1.057
	5	460	402	14	14.16	0.443
	6	485	429	8.5	8.92	0.433
	7	507	450	5.5	5.94	0.565
	8	548	489	6.5	7.06	0.620
	9	608	522	5	5.43	0.689

TABLE XLVIII (continued)

Sample No.	Fraction No.	Pot Temperature °F	Vapor Temperature °F	Volume Distilled cc	Weight of Fraction gm x 10^2	Weight % Nitrogen
KDC #11	FD	160	91			
	1	310	218	6.5	5.14	1.24
	2	360	276	10	9.41	1.766
	3	394	310	8	7.76	1.943
	4	429	365	12	12.01	1.101
	5	460	399	13	13.60	0.468
	6	485	429	10	10.64	0.497
	7	507	452	7	7.49	0.585
	8	548	499	8.5	9.22	0.670
	9	602	557	6	6.51	0.904
KDC #13	FD	242	164			
	1	310	212	4.5	3.89	1.225
	2	360	266	10	9.62	2.330
	3	394	297	9	8.99	2.442
	4	429	358	11.5	11.93	1.473
	5	460	390	11	11.75	0.673
	6	485	425	11	11.86	0.675
	7	507	445	7.5	8.17	0.736
	8	548	482	9	10.00	0.831
	9	608	529	6	6.66	0.989
KDT #8	FD	152	85			
	1	310	197	7	6.00	1.625
	2	360	253	10	9.69	1.639
	3	394	287	8	8.00	2.021
	4	429	359	11.5	11.95	1.067
	5	460	385	12	12.77	0.592
	6	485	422	10	10.79	0.572
	7	507	442	6.5	7.10	0.657
	8	548	477	8.5	9.44	0.891
	9	608	512	6	6.44	0.923
KDT #11	FD	182	93			
	1	310	186	5	4.46	2.632
	2	360	251	10	9.07	2.217
	3	394	285	8	7.24	2.333
	4	429	351	11	10.08	1.787
	5	460	383	11.5	11.86	0.780
	6	485	422	11	11.96	0.778
	7	507	439	8	8.70	0.769
	8	548	480	10	11.10	0.863
	9	608	510	7	7.78	1.073

TABLE XLVIII (continued)

Sample No.	Fraction No.	Pot Temperature °F	Vapor Temperature °F	Volume Distilled cc	Weight of Fraction gm x 10^2	Weight % Nitrogen
KDT #13	FD	292	167			
	1	310	192	3	2.68	3.664
	2	360	260	10	9.52	3.145
	3	394	290	9	8.88	3.289
	4	429	352	11	10.98	2.151
	5	460	385	11	11.00	0.792
	6	485	422	11	11.47	0.692
	7	507	442	9	9.73	0.770
	8	548	482	10	10.73	0.919
	9	608	515	7.5	8.63	1.077
KDP #8	FD	170	81			
	1	310	199	8.5	6.93	4.089
	2	360	255	11	9.70	2.009
	3	394	292	8	7.81	1.676
	4	429	357	13	12.40	0.600
	5	460	388	13	12.72	0.468
	6	485	405	9	9.30	0.528
	7	507	426	7.5	7.59	0.547
	8	542	468	7	7.68	0.644
	9	608	479	5	5.57	0.775
KDP #11	FD	268	155			
	1	310	192	5.5	4.80	1.060
	2	360	253	10.5	10.05	2.028
	3	394	283	8	7.85	1.982
	4	429	354	12	12.38	0.956
	5	460	385	12	12.60	0.455
	6	485	419	11	12.05	0.551
	7	507	433	6.5	7.23	0.662
	8	548	471	9	10.06	0.773
	9	608	492	6	6.78	0.910
KDP #13	FD	284	152			
	1	310	177	3.5	3.18	1.478
	2	360	251	10	9.57	2.180
	3	394	277	8	7.92	2.615
	4	429	340	11.5	11.53	1.620
	5	460	366	11.5	12.11	0.682
	6	485	410	11	12.07	0.635
	7	507	426	8	8.83	0.709
	8	548	460	9	10.06	0.825
	9	608	477	7	7.88	1.096

TABLE XLVIII (continued)

Sample No.	Fraction No.	Pot Temperature °F	Vapor Temperature °F	Volume Distilled cc	Weight of Fraction gm x 10^2	Weight % Nitrogen
KEC 29	FD	288	132			
& 30	1	310	194	2		0.592
	2	360	244	9.5		0.697
	3	394	285	8		0.550
	4	429	353	14		0.584
	5	460	382	14		0.541
	6	485	418	13		0.613
	7	507	434	7		0.693
	8	548	471	9.5		0.730
	9	608	483	6		0.826
KET 28	FD	300	123			
& 30	1	310	173	1		0.337
	2	360	246	9.5		0.486
	3	394	272	7		0.567
	4	429	349	14		0.484
	5	460	379	13		0.436
	6	485	415	11		0.576
	7	507	429	8		0.580
	8	548	464	10		0.707
	9	608	491	7		0.984
KEP 29	FD	306	150			
& 30	1	310	170	0.5		0.528
	2	360	244	9		0.607
	3	394	260	7.5		0.605
	4	429	341	13.5		0.629
	5	460	372	13.5		0.501
	6	485	413	13		0.494
	7	507	424	8		0.592
	8	548	470	10		0.632
	9	608	480	6		0.781

The discussion section pointed out that material balances on the amount of nitrogen present in the sample were not satisfactory for two of the samples distilled. Table XLIX presents a comparison of the total mass of nitrogen present in the samples against the total mass of nitrogen found in the individual fractions excluding the residue left in the distillation flask.

TABLE XLIX

AMOUNT OF NITROGEN IN DISTILLED SAMPLES

Sample No.	Total Mass of Nitrogen in the Distilled Sample gms x 10^2	Cumulative Mass of Nitrogen in the Distilled Fractions Excluding the Residue gms x 10^2
KDC 8	63.6	91.7
KDC 11	95.3	78.7
KDC 13	125.4	103.6
KDT 8	92.3	87.5
KDT 11	119.6	110.0
KDT 13	153.0	136.3
KDP 8	74.3	84.6
KDP 11	102.7	84.0
KDP 13	127.6	104.11

The second column in the Table XLIX should be less than the first column, since the amount of nitrogen in the residue is not represented in the numbers presented. However, as can be seen from the table, for the samples KDC 8 and KDP 8 the material balance was not satisfactory.

APPENDIX D

DATA USED IN DIFFERENTIAL METHOD OF

ESTIMATING ORDER OF REACTION

The data used to determine the polynomial equations along with the dC_A/d_t values and the polynomial equations are presented in this Appendix for the KEC and KET series.

TABLE L

POLYNOMIAL EQUATIONS

Series	Temperature ^oF	Polynomial Equation
KEC	650	$C_A = 0.7418 - 0.252t + 0.0479t^2$
KEC	700	$C_A = 0.6408 - 0.2929t + 0.04615t^2$
KEC	750	$C_A = 0.4929 - 0.3803t + 0.1035t^2$
KET	650	$C_A = 1.01 - 0.498t + 0.116t^2$
KET	700	$C_A = 0.917 - 0.424t + 0.053t^2$
KET	750	$C_A = 0.602 - 0.219t + 0.0029t^2$

TABLE LI

DATA USED FOR DETERMINING POLYNOMIAL EQUATION

Series	Temperature °F	Space Time, hr^t	% Nitrogen in Product Oil	dC_A/dt
KEC	650	0.5	0.630	-0.2041
		0.6	0.617	-0.1945
		0.7	0.582	-0.1845
		0.8	0.565	-0.1754
		0.9	0.550	-0.1658
		1.0	0.535	-0.1562
		1.1	0.520	-0.1466
		1.2	0.510	-0.1370
		1.3	0.500	-0.1275
		1.4	0.490	-0.1178
		1.5	0.475	-0.1083
		1.6	0.460	-0.0987
		1.7	0.450	-0.0891
		1.8	0.440	-0.0795
KEC	700	0.5	0.515	-0.2467
		0.6	0.480	-0.2375
		0.7	0.455	-0.2283
		0.8	0.430	-0.2191
		0.9	0.410	-0.2098
		1.0	0.390	-0.2006
		1.1	0.375	-0.1914
		1.2	0.360	-0.1821
		1.3	0.342	-0.1729
		1.4	0.326	-0.1637
		1.5	0.310	-0.1545
		1.6	0.290	-0.1452
		1.7	0.273	-0.1359
		1.8	0.260	-0.1267
KEC	750	0.5	0.337	-0.2768
		0.6	0.302	-0.2561
		0.7	0.274	-0.2354
		0.8	0.250	-0.2147
		0.9	0.230	-0.1940
		1.0	0.210	-0.1733
		1.1	0.198	-0.1526
		1.2	0.187	-0.1319
		1.3	0.179	-0.1112
		1.4	0.170	-0.0905
		1.5	0.162	-0.0698
		1.6	0.152	-0.0491
		1.7	0.142	-0.0289
		1.8	0.138	-0.0077

TABLE LI (continued)

Series	Temperature °F	Space Time, t	% Nitrogen in Product Oil	dC_A/dt
KET	650	0.5	0.798	-0.382
		0.6	0.756	-0.358
		0.7	0.720	-0.336
		0.8	0.680	-0.312
		0.9	0.650	-0.289
		1.0	0.625	-0.266
		1.1	0.600	-0.243
		1.2	0.580	-0.219
		1.3	0.567	-0.196
		1.4	0.550	-0.173
		1.5	0.535	-0.150
		1.6	0.520	-0.127
		1.7	0.500	-0.104
		1.8	0.482	-0.0804
KET	700	0.5	0.724	-0.371
		0.6	0.680	-0.260
		0.7	0.645	-0.349
		0.8	0.610	-0.339
		0.9	0.579	-0.329
		1.0	0.545	-0.318
		1.1	0.515	-0.307
		1.2	0.485	-0.297
		1.3	0.458	-0.286
		1.4	0.430	-0.276
		1.5	0.408	-0.265
		1.6	0.380	-0.254
		1.7	0.350	-0.244
		1.8	0.324	-0.233
KET	750	0.5	0.496	-0.2161
		0.6	0.470	-0.2155
		0.7	0.450	-0.2149
		0.8	0.430	-0.2143
		0.9	0.410	-0.2137
		1.0	0.388	-0.2132
		1.1	0.367	-0.2126
		1.2	0.345	-0.2120
		1.3	0.324	-0.2114
		1.4	0.301	-0.2108
		1.5	0.280	-0.2103
		1.6	0.260	-0.2097
		1.7	0.240	-0.2091
		1.8	0.220	-0.2085

APPENDIX E

ACTUAL AMOUNT OF CHEMICALS USED IN

THE PREPARATION OF CATALYSTS

Table LII presents the actual amounts of the molybdenum

oxide and cobaltous nitrate used in preparing the catalysts that were

used in this study, for each series and the amount of catalyst used

in each series.

TABLE LII

ACTUAL AMOUNT OF CHEMICALS USED IN THE
PREPARATION OF CATALYSTS

Run Series	Weight of Alumina gms	Weight of MoO_3 gms	Weight of $Co(NO_3)_2 6H_2O$ gms	Weight of Catalyst packed in the Reactor, gms
CAT	25.007	3.7258	4.0548	21.373*
KEC	25.0061	3.7589	4.0692	25.614*
KET	25.0068	3.7204	4.0618	22.568*
KEP	25.0156	3.7376	4.0755	21.441
KER	25.0125	3.7669	4.0708	26.052
KDC	25.0060	3.7321	4.0664	25.181
KDT	25.0047	3.7302	4.0505	22.570
KDP	25.0053	3.7262	4.0087	20.783

*estimated numbers

264

APPENDIX F

CALCULATION OF MEARS' CRITERIA FOR

AXIAL DISPERSION EFFECTS

Mears (13) presented the following criterion for the minimum h/d_p ratio required to hold the reactor length within 5% of that needed for plug flow.

$$\frac{h}{d_p} > \frac{20m}{B_o} \ell n \frac{C_{in}}{C_{out}}$$

where

h = height of catalyst bed, cm

d_p = diameter of the catalyst particle, cm

n = order of reaction

B_o = Bodenstein number, $d_p\bar{V}/D_a$

C_{in} = concentration of reactant in the feedstock, moles/cm^3

C_{out} = concentration of reactant in the product, moles/cm^3

D_a = axial eddy diffusivity, cm^2/hr

$\bar{V}$ = superficial velocity, cm/hr.

The length of catalyst bed used in this study varied from 49.86 to 50.50 cm. However, the catalyst bed was preceded and succeeded by inert packings to serve as pre- and post-heat zones. The total length of the packed bed including inerts and catalysts was the same for all runs. Since some thermal denitrogenation occurs over the inerts (6),

the quantity h in the above equation is used as the total bed length
of the reactor (83.82 cm). In order to be conservative, the following
calculations were done at the highest conversion achieved in this study.

First h/d_p is calculated.

$$h = 83.82 \text{ cm}$$

$$d_p = 0.219 \text{ cm}$$

$$h/d_p = 382.74.$$

Hochman, et al. (15) presented a plot from which B_o can be obtained.
However, this requires the calculation of a liquid Peclet number
defined as $d_p \bar{V}/\mu_L$ where μ_L is the viscosity of the liquid. The
viscosity of raw anthracene oil is taken to be 3.8 gm/cmhr (7).

$$\text{Liquid Peclet Number} = d_p \bar{V}/\mu_L$$

$$= \frac{0.219 \text{ cm} \times 20 \text{ cc} \times 1.02 \text{ gm}}{3.8 \frac{\text{gm}}{\text{cmhr}} \quad \text{hr} \quad \text{cc} \quad 0.295 \text{ cm}^2}$$

$$= 4.0.$$

From the plot of Hochman, et al. (15)

$$B_o = 0.15 \quad \text{at liquid peclet number of } 4.0.$$

At the reactor operating condition of 750F, 1500 psig and 1.84
hours, the average weight percent nitrogen in the product oil from the
KEC series was 0.135, which represents the highest conversion achieved
in this study.

$$\ln \frac{C_{in}}{C_{out}} \;=\; \ln \frac{1.06}{0.135} \;=\; 2.06$$

$$\frac{20\ m}{B_o} \ln \frac{C_{in}}{C_{out}} \;=\; \frac{20}{0.15} \times 1 \times 2.06$$

$$=\; 275 \;(\text{for a 1st order reaction})$$

Hence,

$$h/d_p \;>\; \frac{20\ m}{B_o} \ln \frac{C_{in}}{C_{out}} \qquad .$$

APPENDIX G

TEMPERATURE PROFILES FOR STEAM TREATING

Table LIII presents the temperature readings obtained during
the 10 hour steam treating of the Ketjen 007-1.5E support material.
Similar profiles were obtained during the one hour steam treating.
1200 ml of water were used during 10 hour steam treating. A 12 inch
catalyst bed followed and preceded by an inert bed was maintained
within the tube and only the temperatures in the catalyst bed are
presented below.

TABLE LIII

TEMPERATURE PROFILES DURING STEAM TREATING

Steam Contact Time	Temperature, °F				
Length of Catalyst Bed, inches	2 hours	4 hours	6 hours	8 hours	10 hours
1	1026	1064	1079	1093	1091
2	1048	1079	1096	1106	1107
3	1057	1090	1104	1115	1114
4	1070	1095	1111	1120	1123
5	1083	1098	1114	1121	1126
6	1088	1098	1114	1119	1125
7	1092	1091	1111	1112	1110
8	1095	1071	1102	1093	1082
9	1045	1042	1076	1063	1053
10	1028	1024	1040	1033	1037
11	1032	1022	1038	1043	1046
12	1065	1047	1060	1065	1066

APPENDIX H

APPLICATION OF SATHCELL'S (6) MODEL TO THE

DATA FROM THIS STUDY

Satchell (6) developed a model to predict the nitrogen content of the product oil from the trickle bed reactor assuming that the rate of denitrogenation is a linear function of the boilingpoint of the individual fractions of the feed. Satchell defined the rate constants as

$$k_i = \ln (N_{fi}/N_{pi})/t \tag{1}$$

for a first order reaction.

k_i = pseudo first order rate constant for boiling range i, $(hr)^{-1}$

N_{fi} = weight percent nitrogen in the feed in boiling range i

N_{pi} = weight percent nitrogen in product in boiling range i

t = volume hourly space time, hr.

For reaction orders greater than one, the following equation was used.

$$k_i = \frac{1}{(n-1)} \left[(1/N_{pi})^{n-1} - (1/N_{fi})^{n-1} \right] 1/t \tag{2}$$

Satchell then defines an activity ratio as

$$r_i = k_i/k_8$$

where

r_i = activity ratio

k_i = rate constant for the boiling range i

k_8 = rate constant for the eighth, the highest boiling range.

Assuming that the activity ratios are independent of reactor temperature and pressure, Satchell arrived at the following two equations, one for the first order and the other for reaction orders greater than one.

$$N_p = \sum_i w_i N_{fi} \, e^{-(r_i k_8 t)} \tag{3}$$

$$N_p = \sum \frac{w_i}{\left[k_8 r_i (n-1) t + (1/N_{fi})^{n-1}\right]^{1/n-1}} \tag{4}$$

where

N_p = weight percent nitrogen in product oil

w_i = weight of nitrogen in boiling range i in the feedstock

k_8 = rate constant for the highest boiling range

r_i = activity ratio

N_{fi} = weight percent nitrogen in product fraction boiling range i

t = volume hourly space time, hr.

Equation (3) was used for first order reaction and equation (4) was used for higher order reactions. Satchell found that a second order reaction fitted his data extremely well.

Since Satchell used the same feedstock that was used in this study, a fit of his model to the data of this study would be interesting; however, applying his model is not possible in the light of

information gathered from this study. Satchell's model is an extremely
interesting one in that sense that it takes into account the variations
in the reactivities of the different organonitrogen species present
in the feedstock. However, there were two major assumptions built
into the model that are questionable. The assumptions were:

1. All species remain in the same boiling range in the product
   as they occupied in the feed oil.

2. The activity ratios as defined are independent of the reactor
   operating temperature and pressure.

Satchell himself observed a substantial amount of cracking, reduction of
the molecular weights and boiling point of the oil in his reactor
products (Table XXI in Satchell's thesis (6)). However, he found that
the reaction rate constants did follow a linear relationship with the
boiling point of the fraction except for the lowest boiling range. He
explained the results for the lowest boiling range as due to cracking
of organonitrogen species into the lowest boiling range before hydro-
denitrogenation occurred. Satchell excluded the results from the
lowest boiling range and assumed that the pseudo rate constant of any
order is actually a function of the boiling point.

Satchell's data do show that the rate constants are roughly a
linear function of boiling point if the lowest boiling range is
excluded. However, his reaction rate constants were calculated from
data at a single space time, since he did not have sufficient data at
other space times. Results from the present study showed that Satchell's
method does not give the true value of the reaction rate constants.

Selected reactor samples were fractionated into several cuts using
an ASTM vacuum distillation technique, for this study and the nitrogen

TABLE LIV

REACTION RATE CONSTANTS FOR DIFFERENT BOILING
RANGE FRACTIONS FOR THE KDC SERIES

Operating Conditions: 1500 psig, 371C (700F), 0.46, 0.92 and 1.84 hours

Fraction Number	1	2	3	4	5	6	7	8
k_1, 1.84	0.432	0.525	0.618	0.513	0.373	0.287	0.300	0.280
k_1, 0.92	0.647	0.769	1.192	0.967	0.597	0.528	0.515	0.265
k_1, 0.46	0.693	1.041	1.752	1.145	0.528	0.556	0.563	0.335
k_1, LR	0.327	0.343	0.212	0.268	0.297	0.170	0.194	0.267
k_2, 1.84	0.206	0.224	0.349	0.751	0.623	0.395	0.371	0.317
k_2, 0.92	0.276	0.284	0.657	1.368	0.924	0.715	0.613	0.259
k_2, 0.46	0.254	0.339	0.815	1.321	0.695	0.667	0.596	0.315
k_2, LR	0.182	0.183	0.172	0.498	0.561	0.265	0.273	0.326

k_i, t_i = ith order rate constant calculated at space time t_i using equation (1) or (2).

k_i, LR = ith order rate constant calculated using integrated form of equation (5).

content of these fractions were analyzed. Unlike Satchell's study, the

nitrogen content in the product oil boiling at a certain range was

available as a function of space time for the doctored raw anthracene

oil used in this study. Hence, first and second order reaction rate

constants were calculated at each space time using equations 1 and 2.

Using the data available at three space times, reaction rate constants

were also calculated, after assuming a reaction order by curve fitting

the integrated form of the following equation

$$-dC_A/d_t = kC_A^n \qquad\qquad (5)$$

Table LIV presents the results obtained for the KDC series. The

fraction numbers in this table corresponds to 1 for the lowest boiling

range and increases to 8 for the highest boiling range.

The data in Table LIV were obtained from the doctored raw

anthracene oil whereas Satchell's data were obtained for the undoctored

raw anthracene oil. However, as shown in Figure 25, there was

essentially no difference between the two feedstocks in the higher

boiling ranges. Hence the results from the higher fractions (above

fraction 4) of this data can be considered as those that would have

been obtained if raw anthracene oil had been used as the feedstock.

Note that, the reaction rate constants in Table LIV tend to increase

through fraction 3 and thereafter do show a tendency to decrease with

increase in the boiling temperature. However, the Table LIV also

reveals that the reaction rate constants tend to change with space

time. Also the rate constants calculated using the data from all three

space times used in this study do not show a definite trend with increase

in boiling range temperature. Similar results were obtained for the KDT

and KDP series. This is true for both first and second order models tested. This leads one to believe that calculating reaction rate constants based on data from one space time alone as Satchell had done could lead to erroneous results. The differences in reactivities could be due to a coupled effect of hydrodenitrogenation and hydro-cracking.

Satchell's second assumption that activity ratios are independent of reactor temperature and pressure is yet to be proven. Neither Satchell's study nor this study have the necessary data to disprove or prove the assumption. However, since the present study showed that reaction rate constants calculated using data obtained from different space times do not follow a definite trend with boiling points of the individual fractions, Satchell's model could not be used to test the data from the present study.

APPENDIX I

UNCERTAINTY ANALYSIS

Kline and McClintock (113) presented a method of estimating uncertainty in experimental results. The method is based on a careful specification of the undertainties in the various primary experimental measurements. This method was used in this study to calculate the uncertainties in the k_s values. An explanation of the method is presented here.

Suppose a set of measurements is made and the uncertainty in each measurement may be expressed with the same odds. These measurements are then used to calculate some desired result of the experiments. The uncertainty in the calculated result on the basis of the uncertainties in the primary measurements is often necessary to interpret the experimental results properly.

Let R be a function of the independent variables x_1, x_2, x_3, ..., x_n.

$$R = R(x_1, x_2, x_3, ..., x_n)$$

Let w_r be the uncertainty in the result and w_1, w_2, ..., w_n be the uncertainties in the independent variables. Then the uncertainty in the result is given by

$$w_R = \left[\left(\frac{\partial R}{\partial x_1} w_1\right)^2 + \left(\frac{\partial R}{\partial x_2} w_2\right)^2 + ... \left(\frac{\partial R}{\partial x_n} w_n\right)^2 \right]^{\frac{1}{2}}$$

276

Note that the uncertainty propagation in the result w_R predicted by the above equation depends on the square of the uncertainties of the independent variables. This means that if the uncertainty in one variable is significantly larger than the uncertainties in the other variables, then it is the largest uncertainty that predominates and the others may probably be neglected.

APPENDIX J

CALCULATIONS FOR DEFINING THE QUINOLINE ZONE

Figure 25 showed that there was no difference between the two
feedstocks in the higher boiling ranges (> 400F). Hence, a conclusion
was drawn that all the quinoline added to the feedstock boils at or
below 400F. The following calculations confirm that conclusion.

Total weight of nitrogen boiling up to

400F at 50 mm Hg pressure from

100 gm of raw anthracene oil = 0.1764 gms (from Satchell's

data (6)).

Weight of nitrogen due to quinoline

added to the feedstock = $\frac{100(1.887 - 1.06)}{100}$ = 0.827

Total weight of nitrogen = 1.0034 gms.

Weight of nitrogen boiling up to

400F at 50 mm Hg pressure from

100 gm of doctored raw anthracene oil = 1.14 gms.

Since the weight of nitrogen that boils up to 400F from 100 gm of
doctored raw anthracene oil exceeds 1.0034 gms, the conclusion that all
the quinoline added to the feedstock boils below 400F is valid.

APPENDIX K

CALCULATION OF AVERAGE MOLECULAR WEIGHT AND

SURFACE TENSION OF RAW ANTHRACENE OIL

The average molecular weight and surface tension of raw anthracene oil were estimated using a method presented in Engineering Data Book (116). The following distillation data were used to calculate average molecular weight.

% Over	Temp., ^{o}F
Initial	380
10	450
30	570
50	650
70	700
90	815

$$S = \frac{t_{70} - t_{10}}{60} = \frac{700 - 450}{60} = 4.166$$

$$\text{Volume average boiling point} = \frac{t_{10} + 2t_{50} + t_{90}}{4}$$

$$= \frac{450 + 2(650) + 815}{4}$$

$$= 641.25F$$

Referring to Figure 16-18 from Engineering Data Book

Corrected Volume Average Boiling Point = 651.25F

From Figure 16-18 at average boiling point = 651F and ^{o}API = -7,

Molecular Weight = 208.

The surface tension is estimated using the following empirical equation (116)

$$\sigma^{\frac{1}{4}} = \frac{P}{M} (d_L - d_V)$$

where $\quad \sigma$ = surface tension, dynes/cm

$\quad M$ = molecular weight

$\quad d_L$ = liquid density, gm/cc

$\quad d_V$ = vapor density, gm/cc

$\quad P$ = Parachor given by 40 + 2.38 (molecular weight).

Assume $\quad d_V \ll d_L$

$\quad d_L$ = 1.136 gm/cc

$\quad P$ = 40 + 2.38(208) = 535

$\quad \sigma^{\frac{1}{4}} = \frac{535}{208} (1.136) = 2.92$

$\quad \sigma$ = 73 dynes/cm.

APPENDIX L

KELVIN EQUATION

The Kelvin equation (111) for capillary condensation can be written as

$$r - t = \frac{-2\sigma V_e}{RT \, \ell n(p/p_0)}$$

where

r = pore radius, Å

t = thickness of the adsorbed layer, Å

σ = surface tension of the liquid, dynes/cm

V_e = molar volume of the condensed liquid, cm^3/mole

p_0 = vapor pressure, psi

p = normal pressure, psi

The equation indicates that all pores below a radius of r will be filled by capillary condensation at pressure p with a liquid of surface tension σ and vapor pressure p_0.

Raw anthracene oil has a boiling range of 380 to 815F at atmospheric pressure. Hence, the fraction boiling at 700F will have a vapor pressure of 14.7 psi at 700F and fractions boiling above will have vapor pressures smaller than 14.7 psi. Hence, at a reaction pressure of 1500 psig, a value of 0.01 for p_0/p will probably represent the best approximation. Using a value of 0.01 for p_0/p the Kelvin equation predicts a value of 13 Å for $r - t$, at a temperature of 700F and a pressure of 1500 psig. However, in this calculation the surface tension

calculated at room temperature was used. Surface tension decreases

with increasing temperature. This could mean that raw anthracene oil

will fill all the pores at reaction conditions.

APPENDIX M

DETERMINATION OF PORE DISTRIBUTION

PARAMETERS

Pore distribution factor (PD) is defined in the patent (118) as follows:

$$PD = \frac{(D_f)^2 \times \Delta D_r}{10^4}$$

where

D_f = most frequent pore diameter

ΔD_r = range of the more frequent pore diameters.

The above parameters are determined from pore distribution curves ($\Delta V/\Delta \ln r$ vs. r) as follows:

1. Draw a base line from the lower extremities of the pore distribution curve.

2. Draw a vertical line from this base line to the apex of the pore distribution curve.

3. Draw a line half way up the vertical line parallel to the base line.

4. The points at which the parallel line crosses the two branches of the distribution curve defines the range of the more frequent pore diameters.

5. The pore diameter corresponding to the apex of the distribution curve is the most frequent pore diameter.

VITA

RAJASUNDARAM SIVASUBRAMANIAN

Candidate for the Degree of

Doctor of Philosophy

Thesis: EFFECT OF CATALYST SUPPORT PROPERTIES ON HYDRODENITROGENATION
OF A COAL LIQUID

Major Field: Chemical Engineering

Biographical:

Personal Data: Born in Punalur, India, February 24, 1948, the
son of Mr. and Mrs. T. S. Rajasundaram; married to
Anantharani Sivasankaran, July 1, 1974.

Education: Attended Little Flower High School, Salem, India;
received the degree of Bachelor of Technology in Chemical
Engineering from University of Madras, India, in 1969;
received the degree of Master of Technology in Chemical
Engineering from University of Madras, India, in 1971;
completed requirements for the Doctor of Philosophy degree
at Oklahoma State University in May, 1977.

Professional Experience: Junior Research Fellow, University of
Madras, India, October 1969 to September 1971; Graduate
Teaching Assistant, Oklahoma State Univeristy, Stillwater,
Oklahoma, September 1972 to May 1974; Graduate Research
Assistant, Oklahoma State University, Stillwater, Oklahoma,
September 1974 to December 1976.

Membership in Scholarly or Professional Societies: Omega Chi
Epsilon, Sigma Xi, American Institute of Chemical Engineers.